

F

N73-11915

NASA CR 120873



# **APPLICATIONS TECHNOLOGY SATELLITE ADVANCED MISSIONS STUDY**

**CASE FILE**  
**FINAL REPORT COPY**  
**VOLUME II OF II**



**FAIRCHILD**  
SPACE & ELECTRONICS DIVISION

prepared for

**NATIONAL AERONAUTICS AND SPACE ADMINISTRATION**

**NASA Lewis Research Center**

**Contract NAS 3-14360**



# **APPLICATIONS TECHNOLOGY SATELLITE ADVANCED MISSIONS STUDY**

**FINAL REPORT  
VOLUME II OF II**

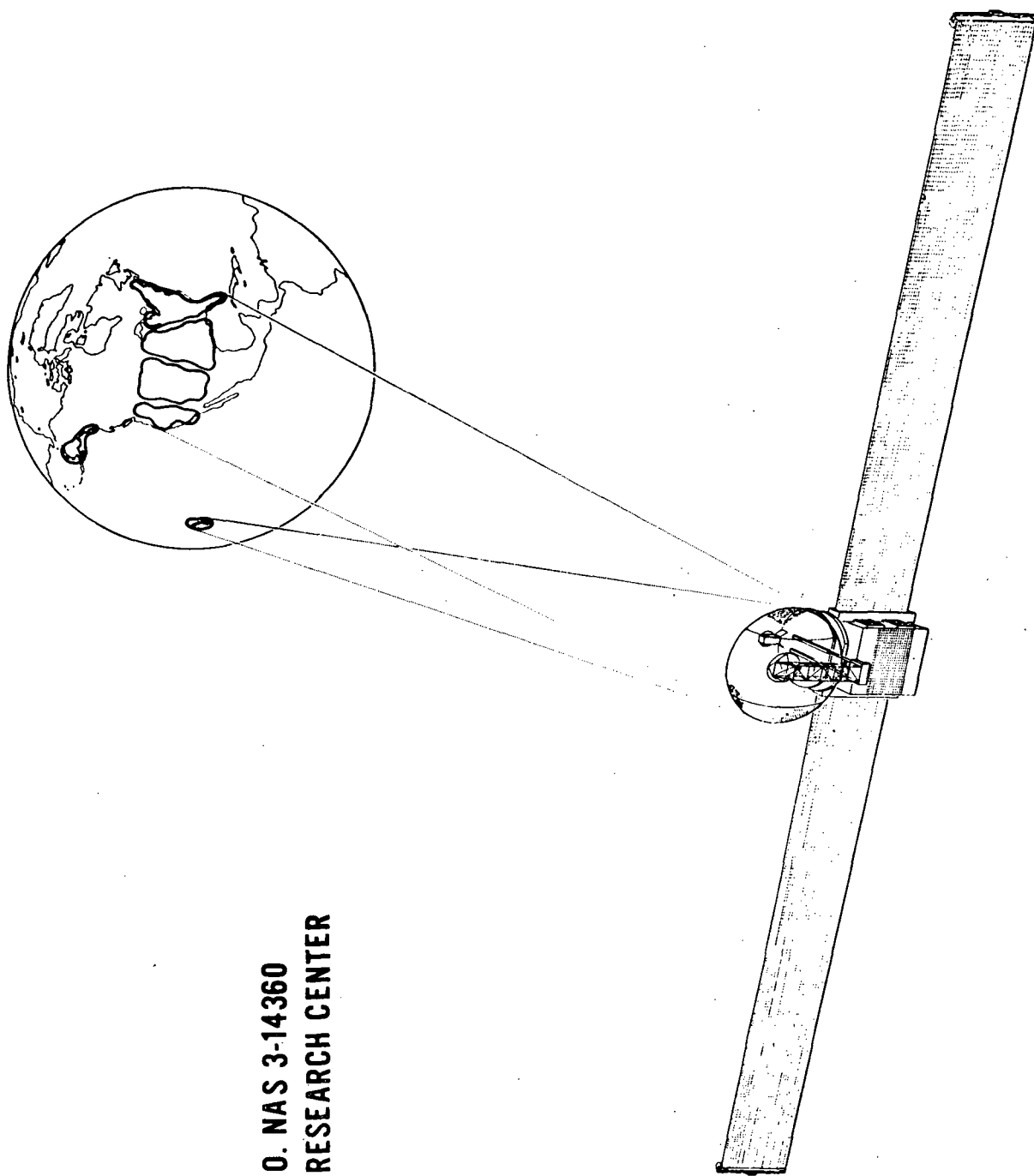


prepared for  
**NATIONAL AERONAUTICS AND SPACE ADMINISTRATION**

**NASA Lewis Research Center  
Contract NAS 3-14360**

# APPLICATIONS TECHNOLOGY SATELLITE ADVANCED MISSIONS STUDY

CONTRACT NO. NAS 3-14360  
NASA LEWIS RESEARCH CENTER



1. Report No. NASA CR 120873		2. Government Accession No.		3. Recipient's Catalog No.	
4. Title and Subtitle Applications Technology Satellites Advanced Mission Study		5. Report Date		6. Performing Organization Code	
7. Author(s) D. L. Robinson et. al.		8. Performing Organization Report No.		10. Work Unit No.	
9. Performing Organization Name and Address Fairchild Industries Space and Electronics Division Germantown, Maryland 20767		11. Contract or Grant No. NAS 3-14360		13. Type of Report and Period Covered	
12. Sponsoring Agency Name and Address National Aeronautics and Space Administration Washington, D. C. 20546		14. Sponsoring Agency Code		15. Supplementary Notes Project Manager, Robert E. Alexovich, NASA Lewis Research Center, Cleveland, Ohio Division,	
16. Abstract Four different spacecraft configurations were developed for geostationary service as a high power communications satellite. The first configuration is a Thor-Delta launch into a low orbit with a spiral ascent to synchronous altitude by ion engine propulsion. The spacecraft is earth oriented with rotating solar arrays. Configuration #2 is a direct injection Atlas/Centaur/Burner II vehicle which when in orbit is sun-oriented with a rotating transponder tower. Configurations #3 and #4 are Titan IIC launches, and are therefore larger and heavier than Configuration #2. They are both sun-oriented, with rotating transponder towers and are directly injected into orbit. Technology discussed in this report includes high power (up to 2 kW) transmitters with collectors radiating heat directly into space, and contoured antenna patterns designed to illuminate particular earth regions. There is also a review of potential users of the services which can be performed by this type satellite in such areas as information networking, Public Broadcasting and Educational Television.					
17. Key Words (Suggested by Author(s)) Communication Satellite Contoured Antenna Patterns High Power Transmitters		18. Distribution Statement Unclassified - Unlimited			
19. Security Classif. (of this report) Unclassified		20. Security Classif. (of this page) Unclassified		21. No. of Pages	
				22. Price*	



## TABLE OF CONTENTS

<u>Section</u>	<u>Subject</u>	<u>Page</u>
	Summary	
1	Introduction	1-1
	1.1 Mission Objectives	1-1
	1.2 Study Objectives	1-1
	1.3 Constraints	1-2
	1.4 Reactor-Thermoelectric Power Systems	1-7
2	High Power Communication Satellite Missions	2-1
	2.1 Missions and Requirements	2-1
	2.2 Baseline Information Networking Experiments	2-3
3	Ascent Trajectories and Launch Sequences	3-1
	3.1 Titan IIC Trajectory and Launch Sequence	3-1
	3.2 Atlas/Centaur/Burner II Trajectory and Launch Sequences	3-10
	3.3 Delta/Ion Engine Launch and Injection Sequences	3-18
4	Spacecraft Description	4-1
	4.1 Summary of Spacecraft Characteristics	4-1
	4.2 Spacecraft Configuration	4-16
	4.3 Antennas and Feeds	4-35
	4.4 Communications Transponder Subsystem	4-52
	4.5 Power Supply Subsystem	4-66
	4.6 Attitude Control Subsystem	4-90
	4.7 Orbit Control Subsystem	4-118
	4.8 Thermal Control Subsystem	4-122
	4.9 Telemetry and Command Subsystem	4-133

## TABLE OF CONTENTS (Cont'd.)

<u>Section</u>	<u>Subject</u>	<u>Page</u>
	4.10 Structures	4-138
5	Tradeoffs and Analysis	5-1
	5.1 Spacecraft - Ground Station	5-1
	5.2 Spacecraft System and Subsystem Interrelation Tradeoffs	5-24
	5.3 Antenna and Feeds	5-29
	5.4 Communications Subsystem Analysis and Tradeoffs	5-97
	5.5 Power Supply Subsystem	5-107
	5.6 Attitude Control	5-121
	5.7 Orbit Control	5-143
	5.8 Thermal Control Analysis	5-145
	5.9 Telemetry and Command System Tradeoffs	5-161
	5.10 Structural Analysis	5-162
6	Critical Research and Development	6-1
	6.1 Spacecraft Technology Critical R & D	6-1
	6.2 Earth Terminal Technology Critical R & D	6-5
	6.3 Communication System Technology Required R & D	6-5
	6.4 Recommended Future Studies	6-9
7	Additional Experiments	7-1/7-2
	7.1 Operational Experiments	7-1/7-2
	7.2 Technology Experiments	7-25
8	Manufacturing, Testing and Support	8-1
	8.1 Manufacturing and Assembly	8-1
	8.2 Testing and Support	8-2

TABLE OF CONTENTS (Cont'd.)

<u>Section</u>	<u>Subject</u>	<u>Page</u>
9	Ground Support System	9-1
	9.1 Earth Terminals	9-1
	9.2 Spacecraft Performance Evaluation	9-9
10	Launch Through Orbit Injection	10-1
	10.1 Ground Support Equipment	10-1
	10.2 Launch Site Support	10-1
11	Implementation Schedule and Requirements	11-1
	11.1 Work Breakdown Structure (WBS)	11-1
	11.2 Gross Resources Required	11-1
	11.3 Implementation Schedule	11-1
12	Conclusions and Recommendations	12-1
	12.1 Small Terminal Information Networking Systems	12-1
	12.2 Demonstration of High Power Satcom Technology	12-2
	12.3 Assessment of Technical Feasibility	12-2
	12.4 Selection of Spacecraft Approach	12-3
	12.5 Recommended Additional Experiments	12-4
	12.6 Recommended Research and Development	12-4
	12.7 Recommended Future Studies	12-5

## LIST OF ILLUSTRATIONS

<u>Figure</u>	<u>Title</u>	<u>Page</u>
1.3.2-1	ATS-Advanced Mission Spacecraft III (Direct Ascent-Titan IIIC Launch)	1-3
1.3.2-2	ATS-Advanced Mission Spacecraft II (Direct Ascent-SLV3D/Centaur D-1A/Burner II Launched)	1-4
1.3.2-3	ATS-Advanced Mission Spacecraft I (Spiral Ascent-Delta 2910/30 Cm Ion Engine Launched)	1-5
2.2-1	ATS-AMS III Baseline PBS Information Networking Experiment	2-4
2.2-2	ATS-AMS III Baseline Special Interest Areas Information Networking Experiment	2-6
2.2-3	ATS-AMS Baseline Rainfall Attenuation Information Networking Experiment	2-7
2.2-4	ATS-AMS III Baseline of Regional Interactive TV Information Networking Experiment	2-9
3.1-1	Titan IIIC (T IIIC-26), Payload Weight vs. Characteristic Velocity, ETR	3-3
3.1-2	Titan IIIC Payload Fairing	3-4
3.1-3	Titan IIIC Profile	3-5
3.1-4	Titan IIIC Ascent Trajectory Ground Trace	3-6
3.1-5	Positioning of S/C Over USA Obtained by Eastward Drift After Injection into Orbit	3-9
3.2-1	Atlas/Centaur Configuration	3-11
3.2-2	Spacecraft Envelope for Centaur D-1A	3-12
3.2-3	Burner II/Centaur Physical Interface	3-13
3.2-4	Synchronous Transfer Orbit Payload Capability	3-15
3.2-5	Spacecraft Positioning Over Final Station Will be Obtained by a Combination of Multiple Equatorial Crossings in either the Parking Orbit or the Transfer Orbit and Eastward Drift	3-17

## LIST OF ILLUSTRATIONS (Cont'd.)

<u>Figure</u>	<u>Title</u>	<u>Page</u>
3.3-1	Delta Outboard Profile	3-20
3.3-2	Payload Envelope, Two Stage, 5414 Attach Fitting	3-21
3.3-3	5414 Conical Attach Fitting Detailed Dimensions	3-22
3.3-4	Delta 2910 Capabilities	3-23
3.3-5	Delta 2910 Load vs. Altitude	3-24
3.3-6	During the Final Stage of the Spiral Ascent, the Necessary Adjustment to Obtain Final Orbit Position will be made	3-29
3.3-7	Typical Orbit Radius vs. Time	3-30
3.3-8	Typical Thrust Profile	3-32
4.2-1	ATS-AMS IIIA Sun Oriented Spacecraft 25 ft. Fairing Titan Booster	4-17/4-18
4.2-2	Equipment Module Structure ATS-AMS III	4-21/4-22
4.2-3	ATS-AMS IIIA Sun Oriented Spacecraft Equipment Layout	4-25/4-26
4.2-4	Layout of ATS-AMS II	4-29/4-30
4.2-5	Earth Oriented Spacecraft Rotating Arrays Delta Booster 2910	4-33/4-34
4.3.1-1	ATS-AMS IIIA Multibeam Contoured Coverage for PBS Experiment	4-36
4.3.1-2	ATS-AMS III Alaska Coverage from Two Satellite Locations	4-37
4.3.1-3	ATS-AMS III Multibeam Contoured Coverage for ITV Experiment	4-39
4.3.1-4	ATS-AMS III Antennas	4-40
4.3.1-5	ATS-AMS III Conceptual Feed Layout	4-43
4.3.2-1	Small Antenna Dimensions	4-47
4.3.2-2	Large Antenna Dimensions	4-50
4.4.1.3-1	Typical Frequency Plan (ATS-AMS IIIA)	4-53

## LIST OF ILLUSTRATIONS (Cont'd.)

<u>Figure</u>	<u>Title</u>	<u>Page</u>
4.4.2-1	ATS-AMS III Communications Transponder	4-55/4-56
4.4.3.1-1	Satellite Repeater Block Diagram ATS-AMS I/II	4-63
4.5-1	ATS-AMS III Power Subsystem Block Diagram	4-70
4.5-2	Low Voltage Power Subsystem Block Diagram-AMS-II	4-74
4.5-3	High Voltage Solar Array - Power Supply Subsystem Functional Block Diagram ATS-AMS-I	4-77
4.5-4	Solar Array Design ATS-AMS I and II	4-81/4-82
4.5-5	Simplified Schematic High Voltage Power Supplies	4-86
4.5-6	Typical TWT Load Interface Circuit	4-89
4.6.1-1	Reference Frames for the ATS-AMS III and II Configurations	4-92
4.6.1-2	Reference Frames for the ATS-AMS I Configuration	4-93
4.6.2-1	Back-Up Hydrazine Thruster Matrix	4-97
4.6.2-2	ACS Configuration, ATS-AMS II and AMS III	4-98
4.6.4-1	ACS Configuration, ATS-AMS I	4-111
4.8.1-1	ATS-AMS III Thermal Configuration	4-124
4.8.1-2	Power Amplifier Tube Insulation Support Design	4-126
4.8.2-1	Thermal Control Sun Oriented S/C	4-129/4-130
4.8.2-2	Thermal Control System Delta Launched Earth Oriented Spacecraft	4-131/4-132
4.9-1	T&C Subsystem Block Diagram	4-134
5.1-1	Downlink TV Performance with Area Coverage	5-2
5.1-2	Distribution of Rainfall Attenuation, New Jersey	5-4
5.1-3	Earth Station Antenna Size vs. Satellite Transmitter Power	5-5
5.1-4	FM Subcarrier Performance - Program Audio	5-8
5.1-5	Downlink Performance - Interactive Audio Using Spot Beam Coverage	5-10

## LIST OF ILLUSTRATIONS (Cont'd.)

<u>Figure</u>	<u>Title</u>	<u>Page</u>
5.1.3.1-1	Comparison of Performance of Predistorted TWT with Standard TWT	5-14
5.2.5-1	Coverage Limitations (Satellite at 110°W)	5-28
5.3.3-1	Coordinate System Geometry	5-39
5.3.3-2	Geometry for Secondary Pattern Addition	5-42
5.3.4-1	Two-Beam Pattern for Various Cross-Over Levels	5-46
5.3.4-2	Comparison of Multibeam and Single-Beam Patterns	5-47
5.3.4-3	Principal Plane Cuts of Four-Feed Pattern (x=-7dB)	5-48
5.3.4-4	Principal Plane Cuts of Four Feed Pattern (x=-5.6dB)	5-49
5.3.4-5	Four-Feed Pattern - x, y plot	5-50
5.3.4-6	Principal Plane Cuts of Six-Feed Pattern	5-52
5.3.4-7	Six-Feed Pattern - x, y plot	5-53
5.3.5-1	Parabola Geometry	5-55
5.3.6-1	Typical Feed Interconnection for ATS-AMS IIIA	5-59
5.3.6-2	ATS-AMS IIIA Switching Diagram	5-61
5.3.6-3	ATS-AMS IIIA PBS Information Networking Experiment Video Signal Flow Chart	5-62
5.3.6-4	ATS-AMS IIIA Interactive TV Experiment Video Signal Flow Chart	5-63
5.3.6-5	Switching Diagram	5-64
5.3.6-6	ATS-AMS IIIB PBS Information Networking Experiment Video Signal Flow Chart	5-65
5.3.6-7	ATS-AMS IIIB Interactive TV Experiment Video Flow Chart	5-66
5.3.7-1	Cassegrain Reflector Geometry	5-70
5.3.7-2	Equivalent Parabola	5-72
5.3.7-3	Large Reflector Feed Cluster	5-73
5.3.7-4	Large Antenna Dimensions	5-79
5.3.7-5	ATS-AMS I & II Small Reflector Feed Cluster	5-80

## LIST OF ILLUSTRATIONS (Cont'd.)

<u>Figure</u>	<u>Title</u>	<u>Page</u>
5.3.7-6	Small Antenna Dimensions	5-83
5.3.8-1	Small Reflector Beam Forming Matrix	5-85
5.3.8-2	Spot Beam Switching Matrix	5-87
5.3.8-3	Solid State Switches Matrix Configuration	5-90
5.3.8-4	Alternate Transponder Front End	5-91
5.3.8-5	Beam Assignment	5-95
5.3.8-6	Channel Routing	5-95
5.4.3-1	Simplified Transmitter/Receiver Isolation Network	5-102
5.4.3-2	Waveguide Strip Isolation & Loss vs. Cut-Off Frequency	5-105
5.4.3-3	Waveguide Strip Insertion Loss vs. Cut Off Frequency (for 100 dB Isolation)	5-106
5.5.1-1	ATS-AMS IIIB Daily Power Budget Distribution During Equinox (EOL)	5-108
5.6.1-1	Polaris Yaw Sensing in Equatorial Orbit	5-124
5.6.2.1-1	Spacecraft Configuration at 0° and 180°	5-126
5.6.2.1-2	Spacecraft Configuration at 90° Point in Orbit	5-127
5.6.2.1-3	Spacecraft Configuration at 270° Point in Orbit	5-128
5.6.2.1-4	Solar Torques and Resulting Momentum Requirements	5-129
5.6.2.1-5	Solar Torques and Resulting Momentum Requirements	5-130
5.6.2.2-1	Gravity Gradient Torque and Resulting Momentum Requirements	5-132
5.6.2.2-2	Geometry for Gravity Gradient Torques	5-133
5.6.2.2-3	Euler Angles	5-134
5.6.2.3-1	Momentum Storage Requirements	5-140
5.6.2.3-2	Momentum Storage Requirements	5-141
5.8.1.3-1	Louver Control Characteristics	5-148



## LIST OF ILLUSTRATIONS (Cont'd.)

<u>Figure</u>	<u>Title</u>	<u>Page</u>
5.8.1.4-1	Temperature of High Voltage Solar Array Experiment as a Function of Percent Ratio of Optical Solar Reflection	5-149
5.8.4-1	Ion Engine Cluster Node	5-152
5.8.5-1	Maximum Temperatures of Flexible Solar Arrays	5-155
5.8.5-2	Array Transient Warm-Up	5-156
5.8.7-1	Performance of Grooved Ammonia Heat Pipes	5-159
5.8.8-1	Heater Power Required for Passive Radiator	5-160
5.10.2-1	ATS-AMS III Mass Properties Launch Configuration	5-169
5.10.2-2	ATS-AMS III Mass Properties Deployed Configuration	5-170
9.1-1	Block Diagram of Major Stations	9-3
9.1-2	Block Diagram of Receive Only Stations	9-6
9.1-3	Transportable Station	9-8
11.1-1	ATS-AMS Work Breakdown Structure	11-2
11.2-1	Manpower Projection	11-4
11.3-1	ATS-AMS Program Plan	11-5

## LIST OF TABLES

<u>Table No.</u>	<u>Title</u>	<u>Page</u>
3.1-1	Titan III Typical Flight Sequence	3-8
3.2-1	Typical Synchronous Equatorial Mission, Atlas/Centaur Sequence of Events	3-16
3.3-1	Low Altitude Ascent Trajectory Summary	3-26
3.3-2	Typical Sequences of Events for Two Stage Missions	3-28
4.1-1	ATS-AMS III B Spacecraft Characteristics	4-3
4.1-2	ATS-AMS III A Spacecraft Characteristics	4-6
4.1-3	ATS-AMS II Spacecraft Characteristics	4-9
4.1-4	ATS-AMS I Spacecraft Characteristics	4-12
4.1-5	Weight Budget Summary kg (lbs)	4-15
4.3.1-1	ATS-AMS III Feed Assignment	4-42
4.3.1-2	ATS-AMS III Antenna and Feed Subsystem Equipment List	4-44
4.3.2-1	ATS-AMS I & II Beam Formation Summary	4-49
4.4.2.5-1	Transponder Input/Output Levels	4-60
4.4.2.5-2	ATS-AMS II Communication Subsystem Equipment List	4-61
4.4.3.2-1	Communication Subsystem Equipment List ATS AMS I & II	4-65
4.5-1	ATS-AMS-III Power Subsystem Load Requirements (EOL)	4-68
4.5-2	AMS-III 30.5 VDC Power Requirements	4-69
4.5-3	Summary of Power Subsystem Characteristics for ATS-AMS III Spacecraft	4-73
4.5-4	Summary of Power Subsystem Characteristics for ATS-AMS I and II	4-79
4.6.2-1	ACS Components for ATS-AMS II & III	4-99
4.6.3-1	Digital Solar Aspect Sun Sensor Characteristics	4-101
4.6.3-2	Earth Sensor Characteristics	4-103

## LIST OF TABLES (Cont'd.)

<u>Table No.</u>	<u>Title</u>	<u>Page</u>
4.6.3-3	Polaris Sensor Characteristics	4-105
4.6.3-4	Attitude Control Computer	4-106
4.6.4-1	Attitude Control Requirements - Configuration 1	4-109
4.6.4-2	ACS Components for ATS-AMS I	4-117
4.7.2-1	Weight and Power Summary for ATS-AMS II and III	4-119
4.7.4-1	Orbit Control Weight and Power Summary for ATS-AMS I	4-120
4.8-1	Thermal Control Weight Estimates	4-123
4.9-1	T&C Message Characteristics	4-135
4.9.3-1	T&C Subsystem Equipment List	4-137
5.1.4-1	Uplink Performance - Video (14 GHz)	5-16
5.1.4-2	Uplink Performance of Transportable Station Video (14 GHz)	5-18
5.1.5-1	Combined Uplink and Downlink Performance - Video	5-19
5.1.5-2	Transportable Station - Combined Uplink and Downlink - Video	5-20
5.1.6-1	Uplink Performance - Interactive Audio	5-22
5.1.7-1	Combine Uplink and Downlink Performance-Interactive Audio	5-23
5.3.2-1	ATS-AMS III Candidate Antenna Matrix	5-36
5.3.6-1	ATS-AMS III Feed Assignment	5-58
5.3.6-2	ATS-AMS III A Feeds and Switching Weight Tabulation	5-67
5.3.7-1	ATS-AMS I and II Large Reflector Design Summary	5-77
5.3.7-2	Beam Formation Summary	5-82
5.3.8-1	Transmit Hardware Weight Characteristics	5-88
5.3.8-2	Transmit and Receive Hardware Weight Characteristics	5-88
5.3.8-3	System Comparison Table	5-93
5.3.8-4	Weight Breakdown for System 1, 2 and 3 Front End	5-94

## LIST OF TABLES (Cont'd.)

<u>Table No.</u>	<u>Title</u>	<u>Page</u>
5.3.8-5	Weight Breakdown for System 4 Front End	5-94
5.5.1.2-1	ATS-AMS-III A Power Budget, Primary Communication Mode	5-110
5.5.1.4-1	ATS-AMS-III B Power Budget, Primary Communication Mode	5-118
5.8.1.1-1	Power/Heat Distribution Watts	5-146
5.8.4-1	Ion Engine Cluster Thermal Analyses Steady State Node Temperatures - °K	5-153
5.10.1-1	Structural System Weight Summary	5-162
5.10.1-2	Equipment Module Weight Summary	5-163
5.10.1-3	Rotating Platform Weight Summary	5-164
5.10.1-4	Reflector Deployment System Weight Summary	5-165
5.10.1-5	Solar Array Weight Summary	5-166
5.10.1-6	Parabolic Reflector Weight Summary	5-167
5.10.1-7	Adapter Assembly Weight Summary	5-167
5.10.3-1	Design Criteria Summary	5-172
7.1.1-1	Application Matrix	7-3/7-4
7.1.1-2	Key Index for References Used in the Preparation of the Application Matrix for the Study	7-9
7.1.1-3	Requirements Matrix	7-15/7-16
7.1.1-4	ATS-AMS Simplified Service Matrix	7-18
7.1.2-1A	ATS-AMS Communication System Requirements	7-19
7.1.2-1B	ATS-H Advanced Mission Study Communication System Requirements	7-20
7.1.2-2	Communications Experiments	7-21
9.1-1	Types of Earth Stations	9-2
9.1-2	Major Station Characteristics	9-4

LIST OF TABLES (Cont'd.)

<u>Table No.</u>	<u>Title</u>	<u>Page</u>
9.1-3	Receive Only Station Characteristics	9-7
10.2-1	Preliminary Spacecraft Operations Building Requirements	10-3
10.2-2	Spacecraft Launch Complex Support Requirements	10-4
11.2-1	Gross Cost Matrix	11-3

## SUMMARY

The objective of the Applications Technology Satellite Advanced Mission Study was to develop several approaches to the design of a spacecraft capable of demonstrating the feasibility of high power microwave communication satellites which produce shaped multi-beams to illuminate desired areas of the earth. Additionally, the satellites are suitable for use in the demonstration of information networks comprised of small user terminals.

Included in the scope of the work accomplished was the preliminary design of several possible spacecraft approaches and the associated prime experiments together with supporting analysis and tradeoff studies. Additional experiments compatible with the capabilities of the spacecraft were defined. The program implications, such as gross implementation schedules and resources; manufacturing, test and support; and critical research and development requirements were identified.

This report identifies potential users of wideband information networking systems whose operations would be enhanced by the use of a high power microwave communication satellite in geostationary orbit operating into small earth terminals. These potential users require technical data, operational experience, and hardware prove-out before committing their resources. An Applications Technology Satellite designed to meet this requirement is the ideal response to the requirement for the experimental data, experience and hardware that is essential for system specification.

The Titan III C launched spacecraft versions were found to be the most suitable for meeting the objectives.

## SECTION 5

### TRADEOFFS AND ANALYSIS

#### 5.1 SPACECRAFT - GROUND STATION

##### 5.1.1 VIDEO DISTRIBUTION (DOWN LINK)

The experiments for ATS-AMS III will demonstrate the feasibility of multi-service systems which will serve the needs of the public for both network distribution and community service. The video signal to noise for television distribution has been specified by CCIR Recommendations 421-1 at greater than 56 dB peak to peak to rms weighted noise for 99% of any month. This value allows for degradation due to subsequent re-distribution by terrestrial interconnection and broadcast stations. A value of 46 dB signal to noise ratio has been chosen for community service direct to community centers such as schools, hospitals, and similar facilities. This service will involve direct translation for connection to commercial TV receivers and thus need not be CCIR relay quality.

A parametric analysis has been made of the RF bandwidth requirements for FM television transmission as a function of satellite EIRP and earth station G/T for values of predetection C/N and output S/N. The results are shown in Figure 5.1-1. This chart serves as a useful tool for determining the operating conditions for the system. Point A defines the operating conditions for network distribution service. An RF bandwidth of approximately 23 MHz will provide a  $C/N = 23$  dB and an output  $S/N = 56$  dB at an  $EIRP + G/T$  value of 74 dBW/°K. Point B defines the operating conditions for community service. Since a multi-service is desired, the RF bandwidth will remain constant. The  $C/N = 13$  dB and an output

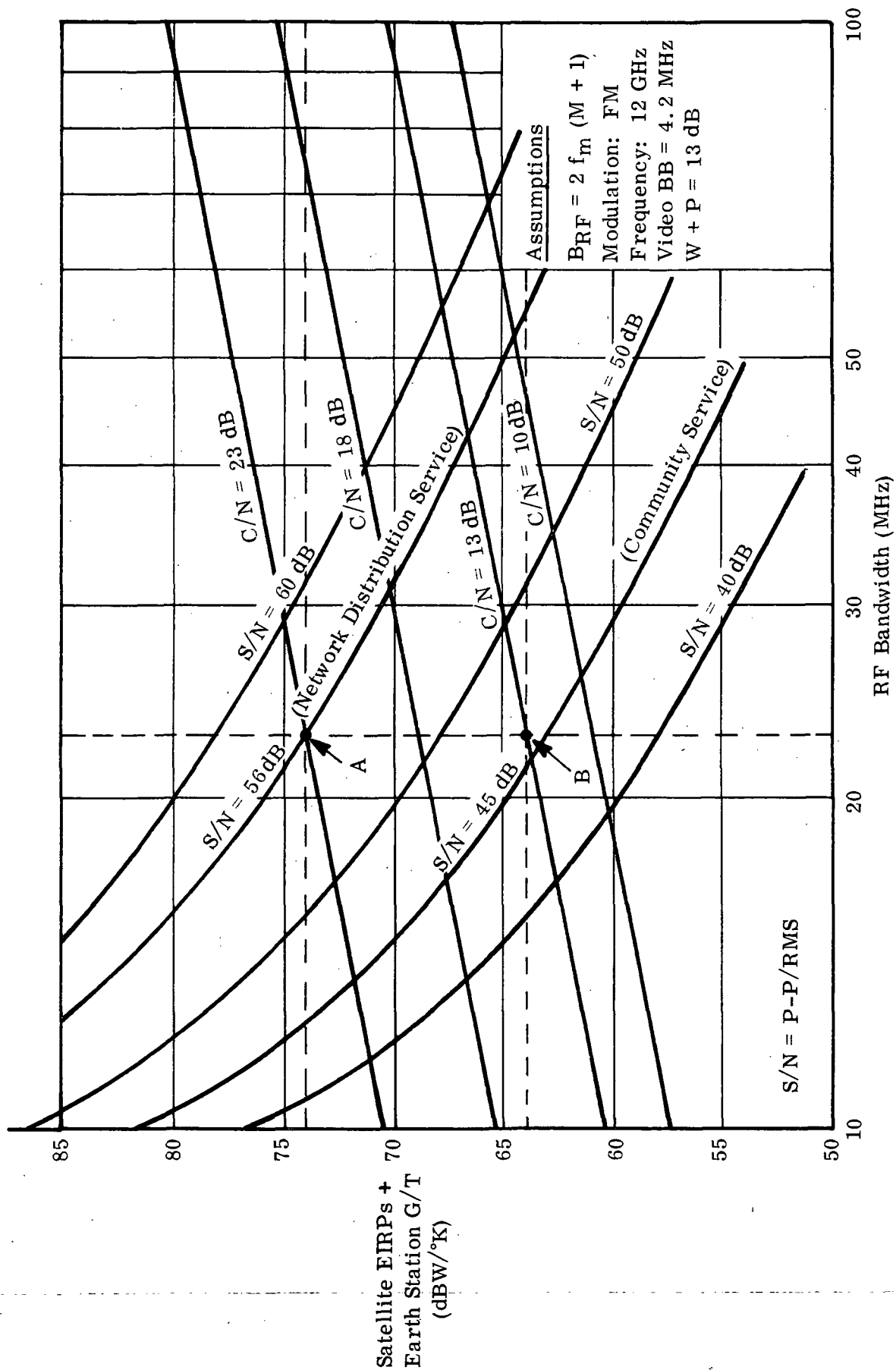


Figure 5.1-1. Downlink TV Performance with Area Coverage



$S/N = 46$  dB will result in an EIRP + G/T value of 64 dBW/°K for this service.

The values of predetection C/N have been established by the reliability of service required. Network distribution service has been assumed to require C/N margins for rainfall attenuation not exceeded 99.99% of any month and community service 99.9% of any month. The value of 99.9% of any month has been specified by the major TV networks as the percentage of the time that the peak to peak video to rms weighted noise ratio (S/N) must exceed the minimum useable quality level.

The C/N margin provided for this type of service meets that requirement. The value of 99.9% for community service is based upon the fact that reduced reliability of service is acceptable for a service used less frequently. The outage represented by 99.9% corresponds to 1 minute per month assuming an 8 hour day and a 5 day week useage schedule. Rainfall attenuation at 12 GHz for these values of service reliability then establishes the operating margins above threshold (10 dB). Rainfall attenuation at various frequencies above 10 GHz has been extrapolated based upon work at BTL\* with the results shown in Figure 5.1-2 for New Jersey climate. An antenuation value of 13 dB for 99.99% and 3 dB for 99.9% is used in this analysis. These values yield a carrier to noise (C/N) of 23 dB for network distribution service and 13 dB for community service.

The normalization of satellite EIRP and earth station G/T permits trade-offs to be made between satellite transmitter power and earth station antenna size. These tradeoffs have been plotted in Figure 5.1-3. The concept of a multi-service system provides the opportunity to reduce the cost of the earth station for community service while maintaining the satellite power and bandwidth constant. The result using this assumption

---

\* H. W. Evans, Attenuation on Earth Space Paths at Frequencies Up to 30 GHz, ICC 1971.

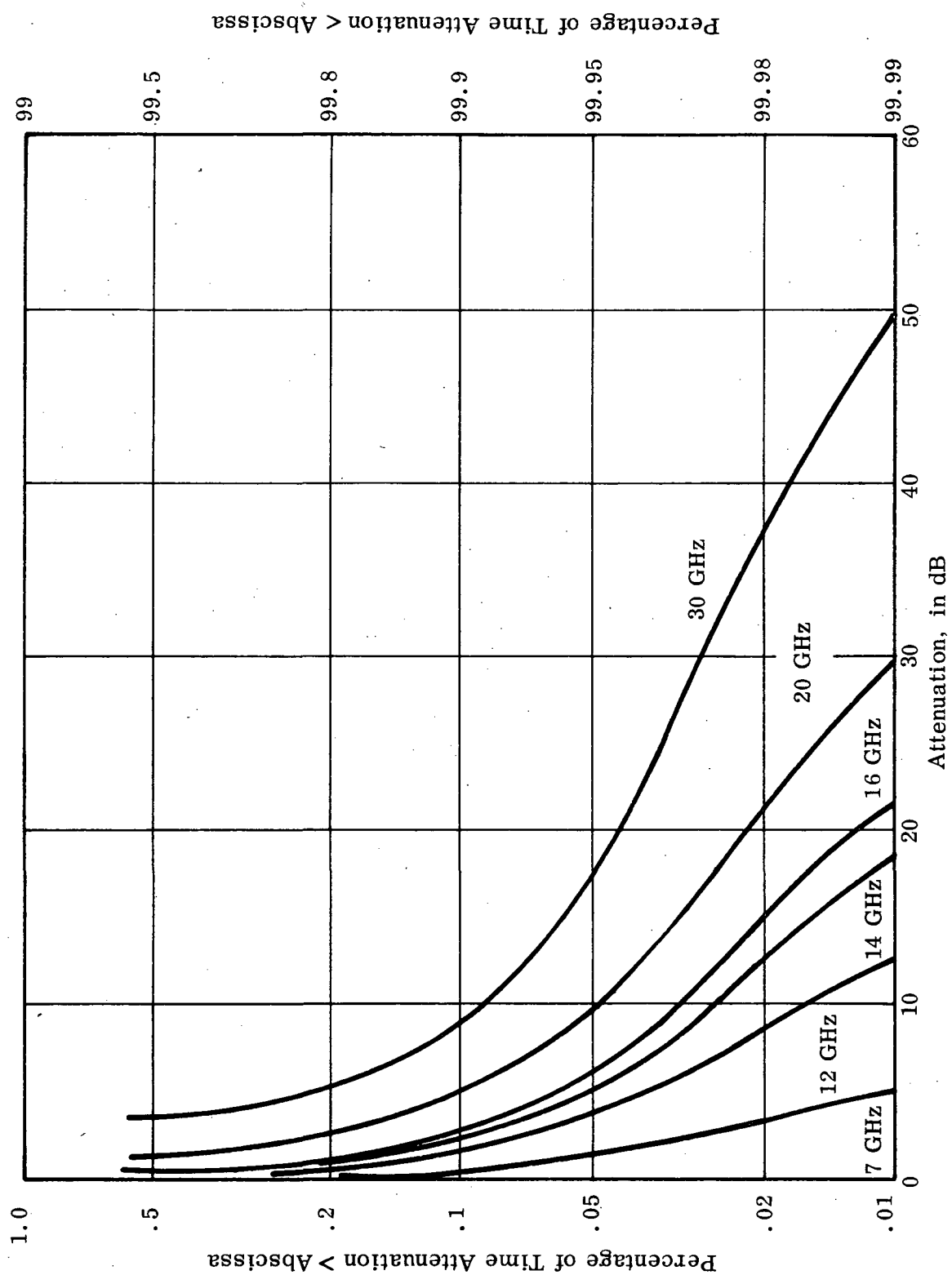


Figure 5.1-2. Distribution of Rainfall Attenuation, New Jersey

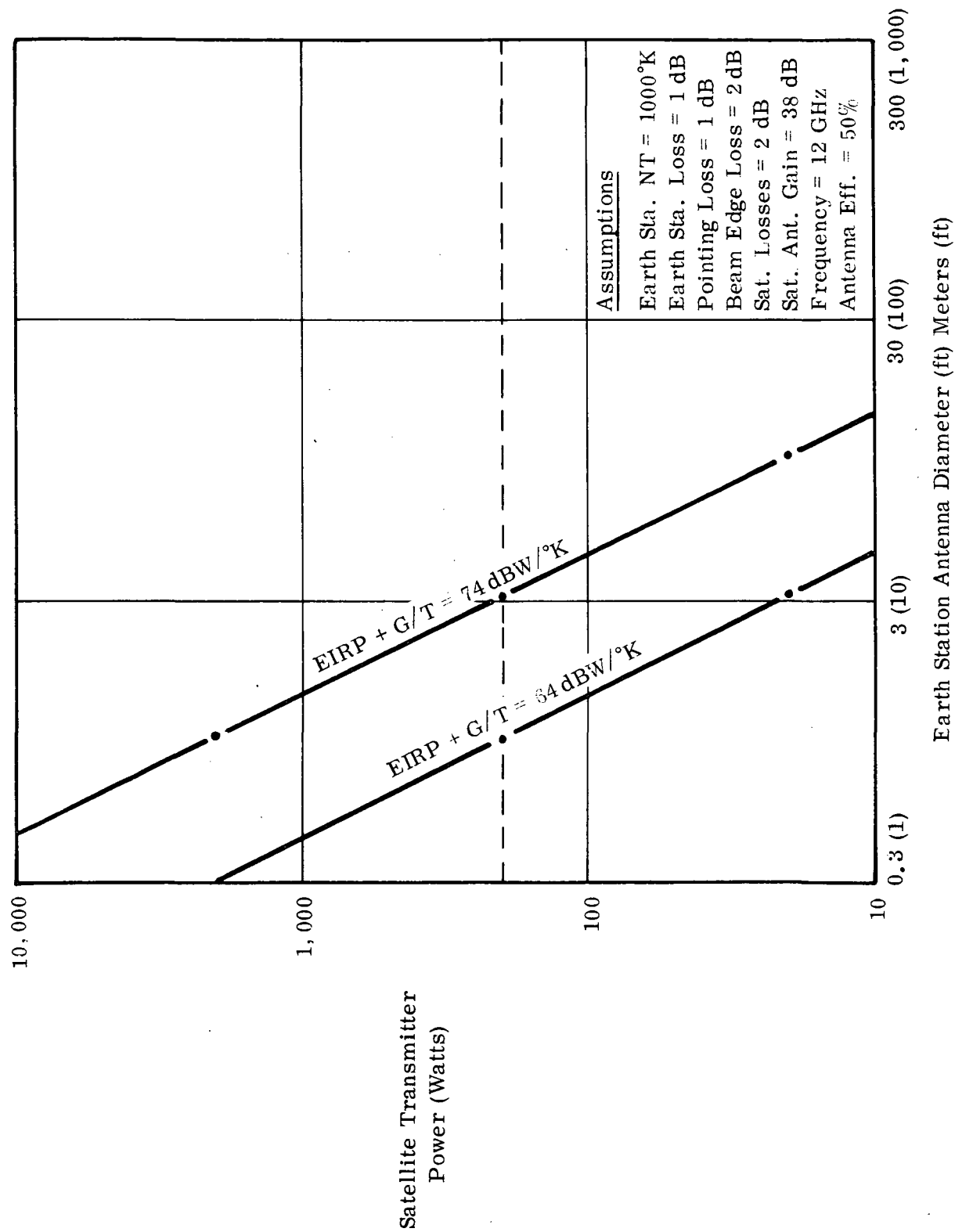


Figure 5.1-3. Earth Station Antenna Size Vs. Satellite Transmitter Power

and a satellite transmitter power of 200 watts yields earth station antenna diameters of approximately 3.3 m (11 ft) for network distribution service and 1 m (3.3 ft) for community service. These antenna sizes are very realistic from the standpoint of minimum cost for both services.

The satellite EIRP assumed for video distribution is based upon use of an area coverage antenna beam with a gain of 38 dB. In order to maintain a given size earth station antenna for all coverage areas the satellite transmitter power will be varied about the value of 200 watts to compensate for variations in satellite antenna gain and to maintain a constant satellite EIRP = 49 dBW at beam center. The satellite antenna gain will vary from approximately 36 dB for the largest coverage area to approximately 40 dB for the smallest area. This corresponds to a range of transmitter power of 125 to 320 watts.

The margins for rainfall mentioned above are adequate for most of the United States. However, for the extreme rainfall areas such as southeastern U.S. and Hawaii special consideration will be given to the values of rainfall attenuation exceeding the margin provided. This extra margin may be obtained either in the spacecraft with reserve power concentrated in a small area or on the ground by geographical separation of earth station antennas.

#### 5.1.2 PROGRAM AUDIO (DOWNLINK)

The video associated audio (program audio) together with cue/control, order wire, and interactive return audio will be carried together with the video on FM subcarriers. This method simplifies the receiving earth station equipment by the transmission of a single composite baseband signal to all stations. The program audio is a high quality channel with a baseband frequency response of 15 kHz and with signal to weighted noise ratio of 55 dB (EIA Standard RS-250-A Para. 5.7) with margin for 99.99% of any month for network distribution service. The signal to noise ratio for community service then becomes 45 dB with margin for 99.9% of any month.

A parametric analysis was made of the RF channel bandwidth  $BW_{ch}$  requirements of FM subcarrier audio as a function of total system carrier to noise  $(C/N)_T$  for values of weighted signal to noise ratio  $(S/N)_{SC}$  and carrier to noise ratio  $(C/N)_{SC}$  of the subcarrier. The results are shown in Figure 5.1-4. From this curve an operating point for the subcarrier audio can be established. For proper subcarrier operation the  $(C/N)_{SC}$  must be equal to or greater than the total system  $(C/N)_T$ . Point A defines the operating conditions for network service and Point B for community service. The RF channel bandwidth remains constant for the two services. The total RF bandwidth ( $B_T$ ) is given by Carson's rule as follows:

$$B_T = 2 (\Delta f_v + \Delta f_a + f_m)$$

where:  $\Delta f_v$  = peak deviation due to video

$\Delta f_a$  = peak deviation due to audio subcarrier =  
0.750 MHz

$f_m$  = video baseband = 4.2 MHz

The RF bandwidth required by video has been established previously at  $B_v = 23$  MHz. Therefore, the peak deviation of the video is given as follows:

$$(\Delta f_v) = \frac{B_v}{2} - f_m$$

$$= 11.5 - 4.2$$

$$= 7.3 \text{ MHz}$$

From the first equation, then, the total RF bandwidth including the subcarrier is given as follows:

$$\begin{aligned} B_T &= 2 (7.3 + 0.75 + 4.2) \\ &= 24.5 \text{ MHz} \end{aligned}$$

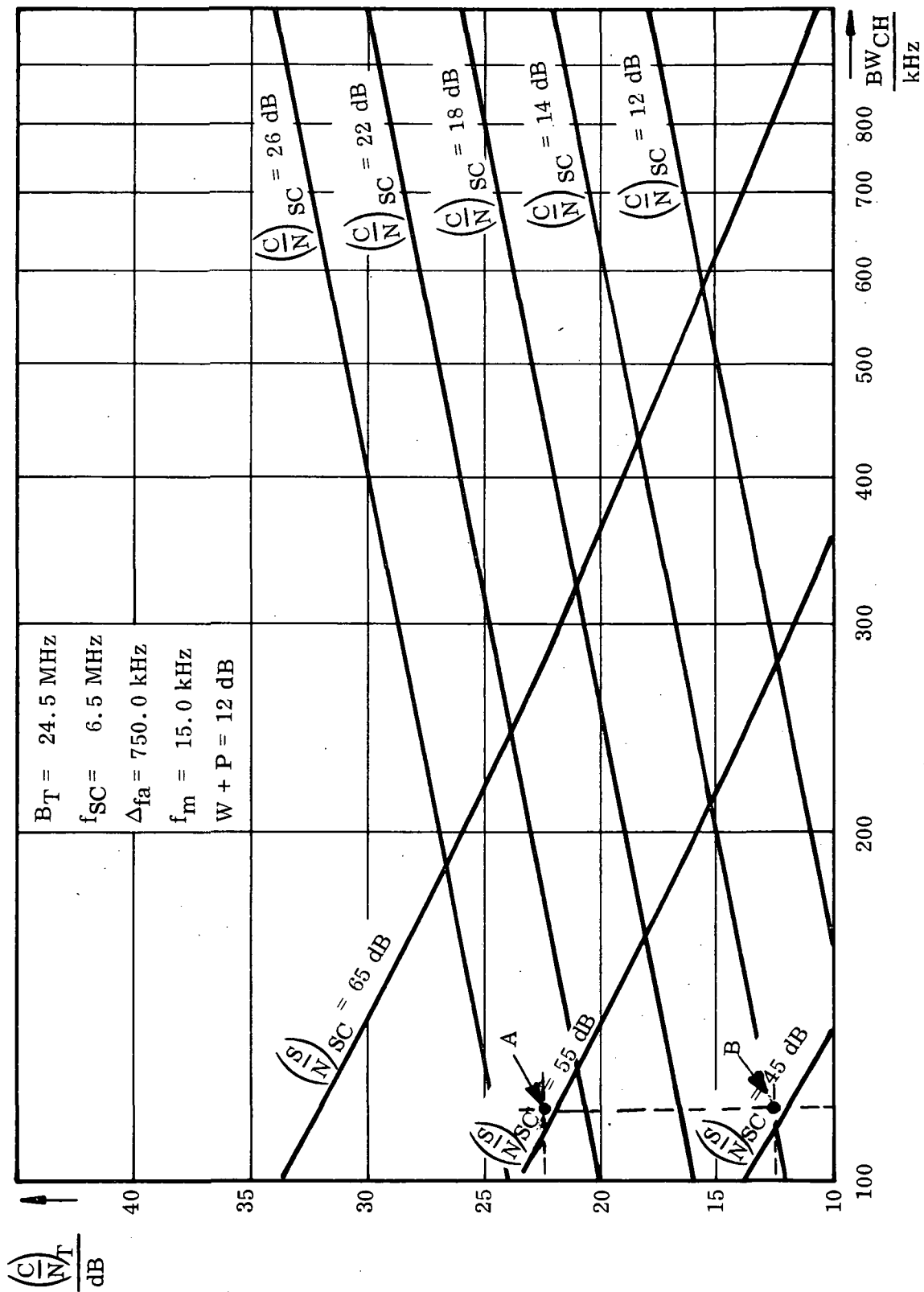


Figure 5.1-4. FM Subcarrier Performance - Program Audio

## INTERACTIVE AUDIO (DOWNLINK)

The experiment involving interactive instructional television to cultural regions will require an interactive communication link originating at community size earth stations (1 m). The type of interactive communications required depends on the type of service, i.e., computer aided instruction, medical information or diagnosis. In order to provide maximum flexibility the interactive channel will be analyzed on the basis of a single 5 kHz audio channel per RF carrier utilizing FM. These channels will be transmitted through a common amplifier in the satellite properly backed off to reduce inter-modulation products. The spot beam generated by a single antenna feed is used for the downlink.

A parametric analysis has been conducted of the RF bandwidth of this single carrier as a function of satellite EIRP and earth station G/T for values of predetection C/N and output weighted S/N. The results are shown in Figure 5.1-5. The operating point has been established at a C/N = 20 dB or 13 dB above threshold (assuming threshold extension) and an output weighted S/N = 50 dB. The RF bandwidth then is 44 kHz and the EIRP + G/T value is 43.8 dB W/°K. The resulting satellite transmitter power required using the spot beam and an earth station antenna of 3.3 m is 25.0 milliwatts per channel. The carrier to noise margin has been chosen such as to insure adequate audio performance during rainfall not exceeded 99.99% of any month while receiving at the major station.

The number of interactive audio channels required for each zone will depend upon the number of receiving earth stations and the population being served. A bandwidth of 1 MHz has been tentatively assigned as the interactive audio bandwidth for each zone. The number of audio

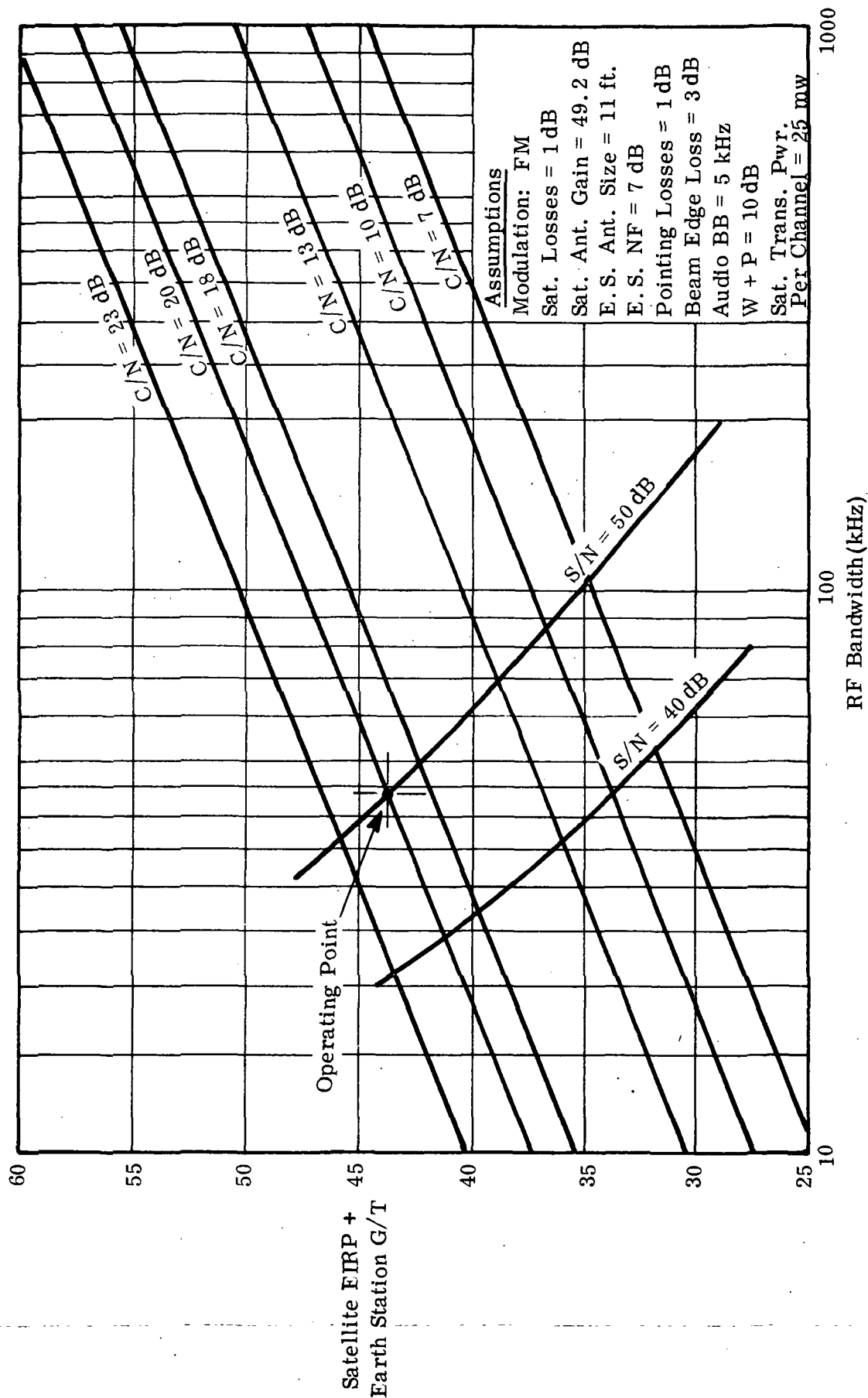


Figure 5.1-5. Downlink Performance - Interactive Audio Using Spot Beam Coverage



channels which can be transmitted within a transponder of this bandwidth will depend upon the output backoff required for acceptable intermodulation + AM-PM conversion. There will exist an optimum backoff for each value of C/N and RF bandwidth. An analysis of these factors which illustrates the maximum number of channels available as a function of backoff below single carrier saturation using a typical satellite TWT amplifier is included in the following section.

The interactive audio requirements have been analyzed on the basis of frequency division multiple access (FDMA) primarily because of its simplicity and low cost. A substantial loss in channel capacity is experienced with FDMA due to the necessity of backing off the output power of the satellite transponder. An alternate means of avoiding the backoff problem is to transmit only one carrier through the transponder at a time, which is accomplished by each earth station transmitting information in bursts. These bursts are synchronized so that they enter the transponder in non-overlapping sequences. This alternate approach is called time division multiple access (TDMA). Because of the store and forward features of the system, it is usually implemented using digital techniques. One disadvantage of the TDMA system is the complete reliance on the system clock. Further, the inadequate attention to precise timing on the part of any user immediately causes interference to other users.

The FDMA system also has the lesser disadvantage of requiring rather precise frequency and power management among all users. However, this disadvantage may be overcome by discrete channel frequency assignments and monitoring of relative carrier power of all channels by a central monitoring station. An additional feature could be added which makes use of coded addresses. Users then could make use of

any available frequency channel by an automatic channel selector which hunts for and selects the first idle channel. A similar system is now in operation in the AT&T land mobile radio telephone system. Further study is needed in this area to determine the optimum modulation and multiple access method for interactive audio. The final conclusion must be based upon the many usage factors as well as equipment complexity and cost.

The use of the interactive audio for computer aided instruction (CAI) will involve conceivably the assignment of a voice channel to a school district. Since the data rate required for each user in this application is of the teletype (TTY) speed (100 bps), many TTY channels could be multiplexed on to one audio channel. In the applications such as medical diagnosis and two way lectures, the complete audio channel could be used for voice communications. Thus, the advantages of flexibility of the interactive FM audio channel becomes evident.

Other more elaborate multiple access schemes for interactive audio can be devised. An example is the PCM-PSK-FDMA system known as SPADE. In this system each channel accesses the satellite by FDMA as described above. However, greater flexibility and versatility is achieved by use of digital modulation techniques for channel assignment and communications. The SPADE system features self assignment of channels via a common signalling channel and voice activation of the carrier.

#### 5.1.3.1

##### Optimum Backoff in Multichannel Transmission

The use of frequency division multiple access (FDMA) for interactive audio requires backing off the output power of the satellite transponder in order to reduce intermodulation. The proper output power level

of a TWT is that which provides sufficiently low intermodulation with minimum power loss. In the light of system performance, the optimum backoff for a TWT is that output power level which permits transmission of the maximum number of a given quality channels.

It was explained in the previous subsection that interactive audio is to be carried out with a number of 44 kHz FM channels. Theoretically, 20 of these channels can be transmitted within the 1 MHz band allotted to each cultural region. As shown in Figure 5.1.3.1-1, for a channel quality of 20 dB carrier to noise, a 5 watt TWT can transmit a maximum of 15 channels when optimized to an input backoff of 18 dB (10.8 dB output back off). It is obvious from the figure that if more than 15 channels are transmitted by a 5 watt TWT, system carrier to noise (or channel quality) will be lower than the required 20 dB.

A recent publication by A. F. Standing\* on multichannel transmission describes a technique which permits intermodulation reduction of up to 10 dB. The technique is basically to compensate for the amplitude and phase non-linearities of a traveling wave tube. With 10 dB reduction in intermodulation, a 1.5 watt TWT can transmit 18 channels and still maintain a carrier to noise of 20 dB. This is shown in dashed lines in Figure 5.1.3.1-1. The optimum input backoff with compensation is expected to be only 12 dB (5.6 dB output backoff), allowing a 1.5 watt TWT to replace the 5 watt tube.

It is recommended that additional consideration be given to phase and amplitude compensation techniques, which might permit a more efficient system that utilizes the smaller 1.5 watt TWT's.

---

\* Standing, A. F. (Comsat Laboratories) "Predistorter Trims Tube Intermodulation Distortion in FM Multicarrier Designs", Communications Designer's Digest, January-February 1971.

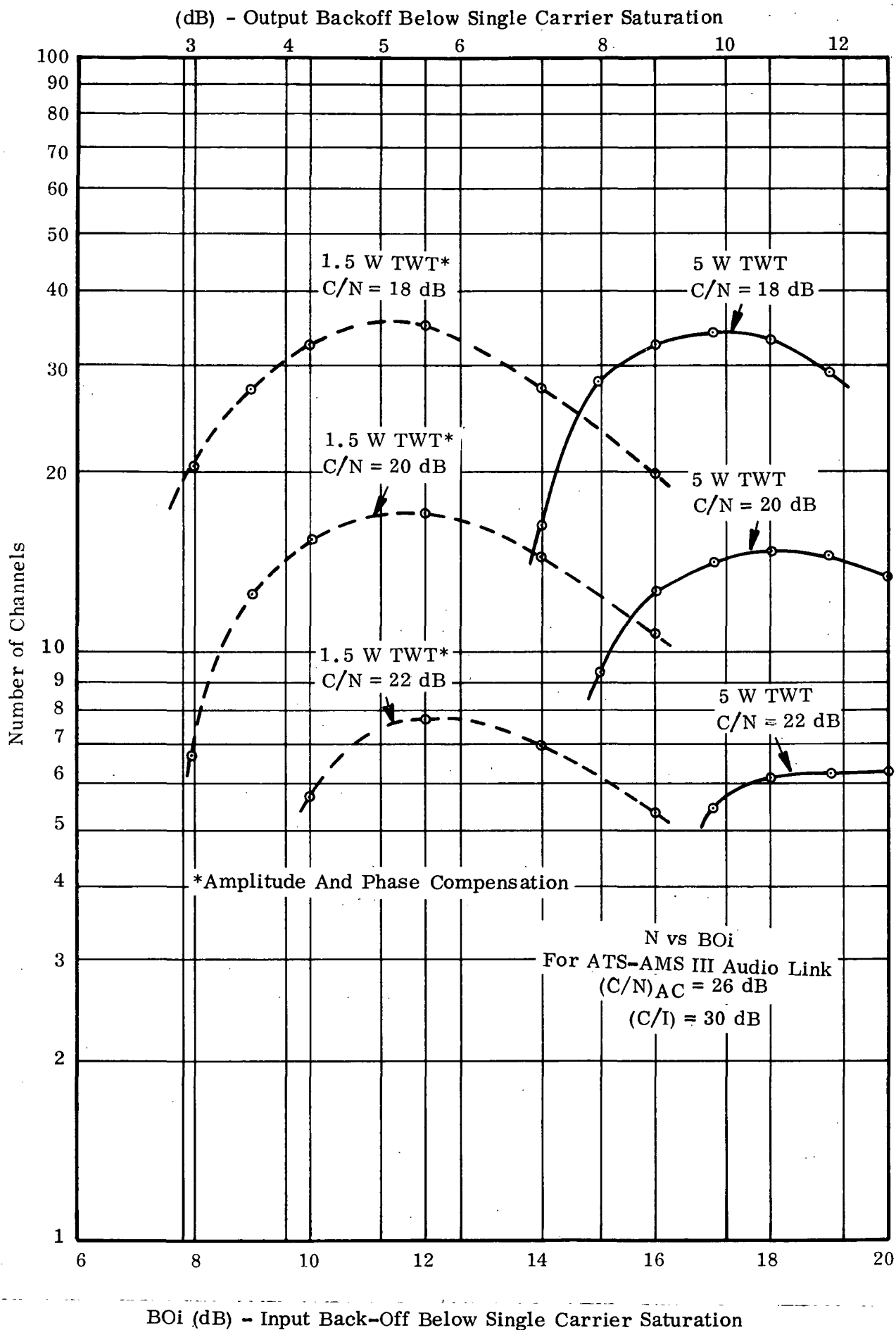


Figure 5.1.3.1-1. Comparison of Performance of Predistorted TWT with Standard TWT

#### 5.1.4

#### VIDEO ORIGINATION (UPLINK)

Two types of major origination stations are proposed for the ATS-AMS III experiment. The first type will be used by the Public Broadcasting Service (PBS) for origination of television programs to both the 3.3 m (11 ft) network distribution receiving earth stations and the 1 m (3.3 ft) community service earth stations, and for storage and delayed origination of programs. In order to compensate for the degradation attendant with retransmission of program material, the major station antennas will be larger than the 3.3 m (11 ft) receiving station antennas. Other considerations such as interference coordination and transmitting equipment power and complexity may also dictate large earth antenna sizes for these stations. Therefore, the antenna size selected will be the maximum considered feasible without unreasonable costs attendant with the difficulty of achieving the required dish surface tolerance and mechanical stability of the antenna mount. The antenna size selected for the major origination station for PBS is 7.6 m (25 ft). This antenna receives video transmissions from the adjacent time zone and retransmits to receiving stations in its own zone plus retransmitting to a receiving station in the adjacent time zone.

The second type of major origination station will be used by the Office of Education and Alaska Medical Network for transmission of television program material to 1 m (3.3 ft) community service earth stations within individual cultural zones. Transmission outside zones or delay-record and retransmission is not required. As a result, the size of this station antenna is determined solely by the required transmitter power. The size antenna selected is 3.3 m (11 ft). A tabulation of up-link performance parameters for both video services is given in Table 5.1.4-1.

Table 5.1.4-1. Uplink Performance - Video (14 GHz)

Earth Station	7.6 m (25 ft) Major Station		3.3 m (11 ft) Major Station	
E. S. Trans. Pwr (W)	60		380	
(dBW)	17.7		25.8	
E. S. Ant. Gain(dB)	57.9		50.8	
@ 50%				
E. S. Losses(dB)	3.0		3.0	
E. S. EIRP (dBW)	72.6		73.6	
Path Loss (dB)	207.0		207.0	
Pointing Loss(dB)			1.0	
* Rainfall Distribution (%)	0.1	0.01	0.1	0.01
Rain Attenuation (dB)	3.0	18.0	3.0	18.0
Beam Edge Loss (dB)	3.0	3.0	3.0	3.0
Sat. Ant. Gain(dB)	50.8	50.8	50.8	50.8
3.44 m at 48%				
Sat. Ant. Losses(dB)	1.0	1.0	1.0	1.0
Sat. Sys. NT (dB/°K)	30.8	30.8	30.8	30.8
Sat G/T(dB/°K)	19.0	19.0	19.0	19.0
Uplink C/T(dBW/°K)	-121.4	-136.4	-121.4	-136.4
10 log KB(dBN/°K)	-155.0	-155.0	-155.0	-155.0
Uplink C/N(dB)	33.6	18.6	33.6	18.6

\*Percentage of time rain attenuation value is exceeded (see Figure 5.1-2)

#### 5.1.4.1

#### Transportable Station (Uplink)

A transportable station for remote origination of TV program material is proposed for use by PBS for program assembly and for live distribution to community stations. A 3.3 m (11 ft) earth station antenna is utilized together with a wide coverage satellite antenna to enable access to the system from any CONUS location. Since this facility will be used only occasionally the link analysis will be based upon rainfall in the uplink exceeded 0.1% of any month. A tabulation of uplink performance of the transportable station is given in Table 5.1.4-2.

#### 5.1.5

#### COMBINED VIDEO PERFORMANCE (UPLINK AND DOWNLINK)

The combined video performance of the various experiments will be determined primarily by the uplink and downlink C/N and rainfall conditions at the origination station and the receiving station. For the purposes of this analysis, it will be assumed that maximum rainfall conditions do not exist simultaneously in the uplink and downlink. This is a reasonable assumption for the majority of the links, however, as the coverage area decreases the probability of simultaneous intense rainfall does increase. Secondary factors such as adjacent satellite and terrestrial interference have been omitted in the analysis. A tabulation of combined uplink and downlink performance for both video services is given in Table 5.1.5-1.

Table 5.1.4-2. Uplink Performance of Transportable Station Video (14 GHz)

E.S. Transmitter Power (N)	1000
(dBW)	30
E.S. Losses (dB)	1.0
E.S. Antenna Gain @ 50% (dB)	50.8
E.S. EIRP (dBW)	79.8
Path Loss (dB)	207.0
Pointing Loss (dB)	1.0
* Rainfall Attenuation @ 0.0/0.1% (dB)	0.0/3.0
Beam Edge Loss (dB)	3.0
Satellite Antenna Gain @ 55% (dB)	31.4
Satellite Antenna Losses (dB)	1.0
Satellite System NT (dB/°K)	30.8
Satellite C/T (dBW/°K)	-0.4
Uplink G°T (dBW/°K)	-131.6/-134.6
10 log KB (dBW/°K)	-155.0
Uplink C/N (dB)	23.4/20.4

\*Percentage refers to percentage of time rain attenuation value is exceeded (see Figure 5.1-2)



Table 5.1.5-1. Combined Uplink and Downlink Performance - Video

Earth Stations	7.6 m MS to 3.3 m RO			7.6 m MS or 3.3 m MS or to 1 m RO		
* Rainfall Dist. (%)	0.0	0.1	0.01	0.0	0.1	0.01
Rain Attenuation (dB)						
Downlink 12 GHz	0.0	2.0	13.0	0.0	2.0	---
Uplink 14 GHz	0.0	3.0	18.0	0.0	3.0	18.0
Downlink C/N (dB)	23.5	21.5	10.5	13.0	11.0	---
Uplink C/N (dB)	36.6	33.6	18.6	36.6	33.6	18.6
Total C/N (dB)						
Up/Dn (0.0/0.0)		23.3			13.0	
Up/Dn (0.1/0.01)		10.5			---	
Up/Dn (0.01/0.1)		16.9			10.3	

MS - Major Station

RO - Receive Only Station

\* Percentage of the time the rain attenuation value is exceeded (Figure 5.1-2)

#### 5.1.5.1 Transportable Station (Uplink and Downlink)

The combined video performance using the mobile station will be determined again by the uplink and downlink C/N together with rainfall conditions existing at the portable station and at the receiving station. For the purposes of this analysis it will be assumed that worse case conditions are when the uplink is experiencing moderate rainfall (0.1%) and the downlink is experiencing heavy rainfall (0.01%) at the major station or the community station is experiencing moderate rainfall (0.1%). A tabulation of the combined performance using the transportable terminal is given in Table 5.1.5-2.

Table 5.1.5-2. Transportable Station - Combined Uplink and Downlink - Video

Earth Stations	3.3 m TR to 7.6 m MS			3.3 m TR to 1 m RO	
* Rainfall Distribution (%)	0.0	0.1	0.01	0.0	0.1
Rainfall Attenuation (dB)					
Downlink (12 GHz)	0.0	2.0	13.0	0.0	2.0
Uplink (14 GHz)	0.0	3.0	-	0.0	3.0
Downlink C/N (dB)	30.0	28.0	17.0	13.0	11.0
Uplink C/N (dB)	23.4	20.4	-	23.4	20.4
Total C/N (dB)					
Up/Down (0.0/0.0)		22.5		12.7	
Up/Down (0.1/0.1)		19.7		10.6	
Up/Down (0.1/0.01)		15.3		-	

\* Percentage of the time the rain attenuation values are exceeded (See Figure 5.1-2)

## 5.1.6

## INTERACTIVE AUDIO (UPLINK)

The interactive audio link is that established as response from the school house or the medical center to the generating station, in order to implement two-way medical and educational programs. Although this link may well be data transmission a 44 kHz FM channel is used in determining the power requirements at the school house. Over 200 data channels can be transmitted in place of this 44 kHz FM channel if response is to be carried out through teletypes rather than audio.

In order to minimize degradation of the total link and maintain a high C/N level at the satellite transponder, the power required at the school house or medical school is 38 watts per 44 kHz channel, using the 1 meter antenna described previously for video reception. This uplink tabulation is shown in Table 5.1.6-1.

## 5.1.7

## COMBINED INTERACTIVE AUDIO PERFORMANCE (UPLINK AND DOWNLINK)

The combined performance of the replay link for the ITV experiment, is shown in Table 5.1.7-1. Worst-case rain conditions have been assumed to be 0.01% rainfall rate in the downlink (to the master station) and 0.1% in the uplink (from the school house.) Although 0.1% service is all that is desired, the master station has been given additional margin (0.01%) as failure of this link implies failures of all replies. Threshold extension receivers have been assumed for use in the major station with a threshold  $C/N = 7$  dB.

Table 5.1.6-1. Uplink Performance - Interactive Audio

Location Earth Station	School or Medical Center 1 m (3.3 ft) Antenna	
E. S. Power/Channel (W)	38	38
(dBW)	15.8	15.8
E. S. Ant. Gain (dB) @55%	40.7	40.7
E. S. Losses (dB)	2.0	2.0
E. S. EIRP/Channel (dBW)	54.5	54.5
Path Loss (dB)	207.0	207.0
Pointing Loss (dB)	0.2	0.2
*Rainfall Distribution (%)	0.0	0.1
Rainfall Attenuation (dB)	0.0	3.0
Edge loss (dB)	3.0	3.0
Sat. Ant. Gain (dB) CONUS @ 55%	31.4	31.4
Sat. Ant. losses (dB)	1.0	1.0
Sat. Sys. NT (dB-°K)	30.8	30.8
Sat. G/T (dB/°K)	-0.4	-0.4
Uplink C/T (dBW/°K)	-156.1	-159.1
10 log KB (dBN/°K)	-182.1	-182.1
Uplink C/N (dB)	26	23

\* Percentage of the time the rain attenuation values are exceeded (Figure 5.1-2)

Table 5.1.7-1. Combine Uplink and Downlink Performance-Interactive Audio

Earth Station	1 m to 3.3 m MS		
Rainfall Dist. %	0.0	0.1	0.01
*Rain Attenuation (dB)			
Downlink 12 GHz	0.0	2.0	13.0
Uplink 14 GHz	0.0	3.0	-
Downlink C/N (dB)	21.3	19.3	8.2
Uplink C/N (dB)	26	23	-
Total C/N (dB)			
Up/Dn (0.0/0.0)		20	
Up/Dn (0.1/0.1)		17.7	
Up/Dn (0.01/0.1)		8.1	

\* Percentage of the time the rain attenuation values are exceeded  
(See Figure 5.1-2)

## 5.2

### SPACECRAFT SYSTEM AND SUBSYSTEM INTERRELATION TRADEOFFS

#### 5.2.1

#### SELECTION OF SHAPED MULTIBEAM CONTOURED ANTENNA PATTERN COVERAGE

Amendment Number 1 of the Statement of Work set forth as a mission objective for the ATS-AMS III considered in the study:

"Paragraph 2.1.2 To develop the technology for the controlled illumination of desired areas of the earth with shaped multibeam transmission, using antennas producing contoured beam patterns having maximum contour curvature of 0.1 radian and minimum contour curvature of 0.004 radian."

Also the mission constraints were amended to require that the spacecraft incorporate as an experiment:

"Paragraph 3.15.1 (2) Contoured illumination of desired areas on earth by spaceborne antennas having multibeam contoured patterns. The contoured patterns shall be other than circular or elliptical and have contour curvature not greater than 0.1 radian and a minimum contour curvature of 0.008 radian\*. Contour curvature shall be defined as  $\frac{r}{d}$  where r is the radius of curvature of the half power contour measured in a plane normal to the direction of propagation and located at a distance d from the source."

These contour curvatures of 0.1 and 0.004 radians correspond to beam widths of 11 degrees and .5 degree respectively. The smaller beam (.5 degree) sizes the aperture of the antenna, which at 12 GHz requires a 3.44 m (11.3 feet) reflector. Contoured antenna patterns fitting the desired coverage area can be produced by combining a number of .5 degree beams.

\* It was understood that the experiment requirement should be the same as the mission objective requirement; i.e., 0.004 radian.

### 5.2.2

#### SELECTION OF NUMBER OF CHANNELS

The ATS-AMS III was sized at ten video channels for striking a reasonable balance between the PBS Networking Experiment and the regional Interactive TV Experiment. For the latter, one video/voice/data channel per each of the ten originating stations was selected. Allocating these ten channels to the other experiment results in two channels per time zone.

For the interactive experiment, one talk-back transponder was assigned for usage with each regional originating station. Limitation on solid-state 12 GHz devices sized each transponder to 25 voice circuits or 6,250 data circuits. This was judged to be satisfactory as a starting point for designing the experiment.

### 5.2.3

#### EARTH ORIENTED VS. SUN ORIENTED SPACECRAFT

Functionally it makes little difference whether the ATS-AMS is oriented tangent to the orbit with the antennas continuously looking at the earth and the solar arrays rotated once per orbit, or whether the ATS-AMS is oriented perpendicular to the orbit plane with the solar array continuously pointed along the projection of the sun line in the orbit plane and the antennas rotated once per orbit. The large antenna is mounted on a tower structure in either case and the mechanism required to rotate the tower appears to be about the same in complexity as that required to rotate the solar array, provided that the RF and high voltage conditioning components are mounted on the tower and do not appear across the rotating joint.

The constant solar orientation of the sun-oriented ATS-AMS reduces the thermal control problem and saves weight in thermal control equipment. A convenience advantage with the sun oriented approach is that the 30 cm ion ascent engines are in the attitude required for N-S station keeping and maneuvering of the spacecraft would not be necessary. E-W station keeping could be accomplished with the 5 cm attitude control ion engines.

An examination of the weight differential associated with the deployable solar arrays was made during the preliminary design of ATS-AMS I and II:

ATS Number	Array Area	Type Design	Aspect Ratio	Orientation	Array Weight Estimate
	m <sup>2</sup> (sq ft)				kg (lb)
AMS I	107 (1150)	2 arrays per side	3.5 to 1	Earth	220 (484)
AMS II	65.5 (705)	1 array per side	4.5 to 1	Sun	107.4 (236)

Earth orientation for the ATS-AMS I was dictated by the maneuvering requirements during the spiral-out transfer orbit. Unfortunately, it was impossible to achieve the minimum system weight predicted for an array with aspect ratio of 3.5:1 due to rotation provisions and clearance from ion engine effluents. Allowing for slip rings and drive mechanisms, the specific weight is 18.8 kilograms (41.4 lb) per kilowatt.

Sun orientation was selected for the ATS-AMS II to provide a comparison and to gain the lower specific weight advantage of 15.5 kilograms (34.1 lb) per kilowatt. Additionally, the sun side of the equipment module could be used for sun-oriented experiments or additional array area. For these reasons, and the thermal control consideration, sun orientation was also selected for the ATS-AMS III.

#### 5.2.4 DIRECT VS. SPIRAL ASCENT

A spiral out ascent was selected for ATS-AMS I to provide a preliminary design definition for this approach while the ATS-AMS II provided the definition for the direct ascent approach. The Delta 2910 was deemed to be most suitable for the spiral out approach since it has the smaller direct ascent payload capability.



Direct ascent was chosen for the ATS-AMS III because the payload capability of the improved Titan III C should be quite adequate for any proposed ATS experiment.

#### 5.2.5

#### ORBIT STATION SELECTION

Selection of the orbit station is determined primarily by the coverage desired and the station locations. Experience gained on the AAFE Program at FII has been utilized to help select the orbit station. The satellite position for a given station location must be such that transmission to the station is above the local station horizon. A minimum angle of arrival of five degrees (the satellite is at least 5° above the local station horizon) has been selected. For this angle of arrival, the relationship between latitude and differential longitude is given by:

$$\cos T \cos D = 0.2363$$

where T is the latitude of the earth station and D is the difference in longitude between the earth station and the satellite.

Orbit station will be dictated by coverage requirements for Hawaii, the northwest section of Alaska, and the northeast section of CONUS. Using these extreme points and the above equation, the allowable satellite positions are:

Alaska	greater than 122° W
CONUS	less than 136° W
Hawaii	greater than 85° W

Thus the allowable spread for the satellite position is governed by Alaska and the northeast section of CONUS, and is only 14 degrees. A compromise location of 129° W could be chosen; however, for this application coverage of CONUS is emphasized. Therefore, a more optimum position of 110° W has been selected for the satellite. For this position, the 5 degree minimum elevation locus crosses Alaska just north of Nome at the western edge and in the vicinity of Point

Barrow at the northern edge. This is shown in Figure 5.2.5-1 which illustrates the coverage limitation for a satellite orbit station of  $110^{\circ}$  W, using a 5 degree minimum angle of arrival as a criteria. As can be seen this orbit station favors CONUS; however, the only coverage sacrifice is just the northwestern tip of Alaska.

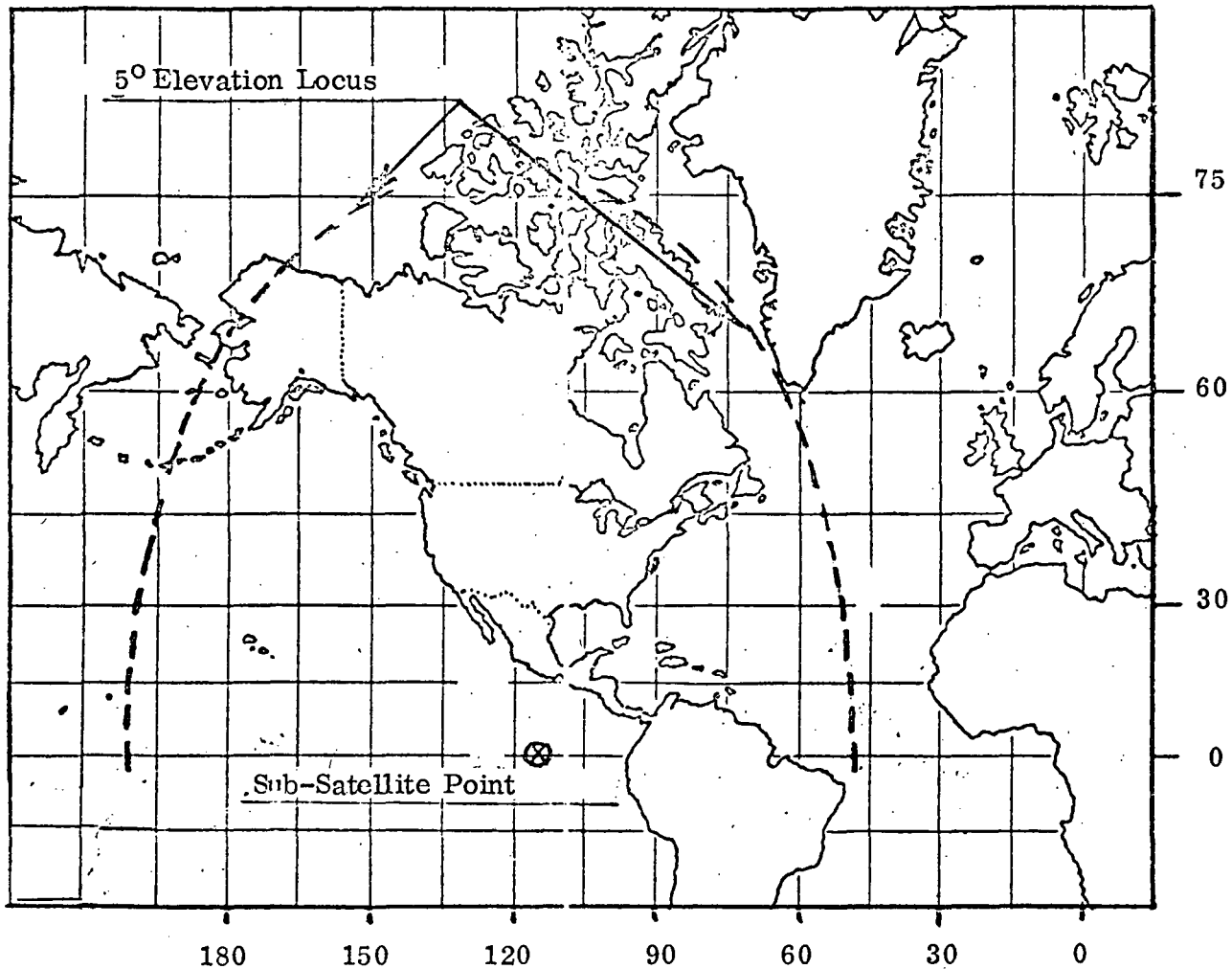


Figure 5.2.5-1. Coverage Limitations (Satellite at  $110^{\circ}$ W)

### 5.3

### ANTENNAS AND FEEDS

#### 5.3.1

#### ANTENNA CANDIDATES FOR CONTOURED PATTERNS

Candidate antennas considered for the ATS-AMS III were arranged into three general categories:

Reflector Antennas

Lens Systems

Phased Arrays

There is obviously a degree of overlap in such a classification, e.g., an active lens system is clearly akin to a phased array, reflector antennas may have phased array feeds, etc. A degree of flexibility is therefore necessary in classifying the candidate antennas in their closest to generic senses. The following discussion is limited to the identification of those particular features of the antenna under consideration which add or detract from its potential applicability in the beamshaping/multibeam area.

##### 5.3.1.1

##### Reflector Antennas

##### 5.3.1.1.1

##### Spherical Reflectors (Prime Focus, Cassegrain-Gregorian)

Spherical reflector antennas are generally designed using one of the following feed assemblies:

Single Element Feed

Line Source Feed

Phased Array Feed

Properly designed primary feeds for spherical reflectors that minimize or correct for spherical aberration permit the secondary pattern of the reflector to be scanned over a relatively large number of half-power beamwidths with minimum beam deterioration. The presence of spherical aberration in an antenna system produces a loss of gain and an increase in the secondary pattern sidelobe levels.

The single element feed requires the usage of a relatively large  $f/D$  ratio to minimize these aberration effects. The line source and phased array (transverse or other) feeds correct for spherical aberration. The correction techniques, in whichever manner implemented, are never perfect so that spherical reflector antennas with sidelobe levels less than -20 dB are quite uncommon. Furthermore, it is not possible to offset the primary feed and/or subreflector in a spherical antenna system. Thus aperture blockage is always a contributor to the secondary pattern sidelobes. In this respect, the utilization of relatively large phased array feeds for beamshaping requirements would result in major sidelobe control problems.

#### 5.3.1.1.2 Paraboloid Reflectors (Prime Focus, Cassegrain)

The large usage of the paraboloid reflector antenna has resulted in a multitude of various feed designs. These designs may generally, be classified as follows:

Single Element Feed

Phased Array Feed

Near Field Feed

The principal source of aberration in a paraboloid antenna system is comatic aberration which occurs when a single radiating feed element is laterally displaced from the paraboloid focal point. This effect is most prevalent in prime focus antenna systems, i.e., relatively small  $f/D$  ratios. In Cassegrain antenna systems designed with relatively large effective  $f/D$  ratios astigmatism becomes the principal source of aberration. The effects of comatic aberration as well as corrective techniques have been investigated more so than astigmatism in the microwave antenna region.

Single element feeds have found great usage in both prime focus and Cassegrain antenna systems. Because of the magnification effects in Cassegrain antennas, a lesser amount of beam deterioration with

scan prior to the onset of astigmatism can be expected. Thus phased array feeds, which have been utilized to correct for comatic aberration in prime focus systems, would seem to possess desirable characteristics when placed in dual reflector Cassegrain systems. In a Cassegrain system, a relatively large phased array would most likely operate as a near field feed, i.e., the subreflector is illuminated by a sector beam.

A prior requirement for sidelobe control in paraboloid antenna systems is elimination of aperture blockage. Thus, prime focus or Cassegrain antenna systems possessing complex phased array feeds would require offset feed/subreflector geometrics for sidelobe control.

#### 5.3.1.1.3 Cylindrical Parabola Reflectors

The singly curved cylindrical parabola antenna generally possesses a line source feed or an array of such. The principal reason for its inclusion here as an AMS candidate is to point out its historical importance. Aperture distributions that are separable in orthogonal planes have played an important part in the aperture analysis antenna area. The cylindrical parabola falls into this category by virtue of the means utilized in obtaining its aperture distribution, i.e., line sources. An expected consequence of separable aperture distributions is that since the half-power beamwidths in orthogonal planes are independent, the half-power beamwidth contour will be circular or elliptical, which is not one of the goals of this program. Furthermore, increasing the complexity of the primary feed system for this configuration to produce contoured patterns as required appears a more formidable task than that associated with the doubly curved paraboloid.

#### 5.3.1.1.4 Specially Shaped Reflectors

Particular beamshaping needs of airborne and ground search radars as well as communications systems have resulted in a relatively

large class of shaped beam antennas that have been largely derived from sections of or deformations to the circularly symmetrical paraboloid. The beam shapes have been coined in various ways, e.g., csc, sector, fan, etc. The majority of this particular class of antennas were developed prior to the time that analytical techniques existed for the complex analyses of the resulting secondary patterns so that these varieties of antennas may truly be regarded as having been developed in the antenna art sense. Furthermore, the various deformations made to the reflecting surface to effect particular antenna pattern shapes appear to defy the desires of pattern shaping in the contoured sense since extremely accurate amplitude and phase control appears as a prior requirement in complex contoured beam shaping.

In recent years, a number of other antenna beam shaping techniques (in the most unrestricted sense) have been introduced and subjected to much more rigorous analyses. The multiplate antenna developed primarily for low frequency operation, for example, permits individual sections of the reflecting surface to be mechanically adjusted for minimization of r.m.s. surface errors. The doubly shaped symmetric Cassegrain antenna approaches the goal of the ideal aperture antenna, i.e., uniform amplitude and phase distribution. Zoned reflector antennas strive to achieve amplitude and phase aperture distributions that are compatible with particularly shaped symmetrical antenna patterns.

In attempting to evaluate specially shaped reflectors in the context of contoured, multibeam antennas, one facet appears to be clear. If indeed a particular contoured beam were achievable with a specially shaped reflector, which is in itself a questionable hypothesis, it appears highly improbable that the synthesized surface would permit generation of a different contoured antenna pattern without a complex feed system. The multiplate antenna, in concept, would appear to

possess the ability to alter the pattern shaped by mechanical adjustments of the reflector surface. However, sidelobe control difficulties resulting from shadowing, r.m.s. surface errors, and amplitude distribution variations make even this technique highly speculative for contoured, multibeam antenna patterns.

#### 5.3.1.2 Lens Antennas

##### 5.3.1.2.1 Passive Lens

Viewed in the context of an optic system, a lens antenna system performs the identical function of a paraboloid antenna. Both antenna systems have the ability to collimate a system of parallel rays into a virtual point focus. In this respect, the single element and phased array feeds discussed under paraboloid antennas carry over directly to lens systems. As with the offset versions of the paraboloid family, the lens antenna system has no aperture blockage. Furthermore, with proper lens design, it is possible to minimize or virtually eliminate aberrations. Thus the lens antenna system must be regarded in a favorable light when contoured beam antenna patterns are required. One seeming disadvantage in a lens system resides in the relative difficulty of obtaining a light weight lens structure which does not in itself introduce r.m.s. phase and amplitude errors into the lens aperture distribution. Another disadvantage with a lens system is the relatively small bandwidth obtainable.

##### 5.3.1.2.2 Active Lens (Distributed Amplifiers)

Active lens antenna systems, most commonly considered for or utilized in Bootlace antenna designs, are characterized by the fact that active amplifiers are associated with single elements or subarrays of elements on the lens output surface. An apparent advantage exists here in that an additional degree of freedom is available to the antenna designer in controlling the amplitude and phase of the

aperture distribution. It is, however, true that the physical difficulties of implementing coherent amplifiers is a non-trivial task. Furthermore, when it is recognized that the price for contoured antenna patterns will be paid ultimately in aperture size; i.e., low aperture efficiency, the weight penalty and complexity required for the active lens antenna system would be enormous.

### 5.3.1.3 Full Phased Arrays

#### 5.3.1.3.1 Distributed Amplifier Array

The phased arrays considered for contoured, multibeam antenna patterns will be assumed non-steerable; i.e., fixed beam variety. Any full phased array has the advantage of not being afflicted with the classical optical aberrations. Grating lobes, which are one of the problems associated with scanning arrays, can be minimized for fixed beam arrays by proper element/spacing choice. Neglecting for a moment the manner in which the inputs to the distributed amplifiers are obtained, it is recognized that the full phased array is almost exactly equivalent to the active lens antenna system. Therefore, the previously mentioned weight penalty and complexity associated with implementing the active lens antenna would carry over directly to the distributed amplifier phased array system.

#### 5.3.1.3.2 Passive Network Fed Phased Arrays

The term passive is to be interpreted in the network sense and does not exclude variable power divider, variable phase shifter components which would normally be associated with aperture amplitude and phase control. In this particular form of fixed beam array, controlled amplitude and phase aperture distributions associated with particular contoured patterns would be created by a complex feed network interfaced with the radiating elements. For relatively large aperture arrays, which are envisioned as required for contoured patterns, severe weight and complexity penalties are



anticipated. In addition, insertion losses and aperture amplitude and phase control are expected to make this approach somewhat questionable.

### 5.3.2

#### SELECTION OF CANDIDATE ANTENNAS

The basic properties of the most promising antenna types for pattern contouring are shown in Table 5.3.2-1.

The type of antenna that appears least applicable for contouring of patterns to the degree of complexity desired, is the phased array. For other than simple patterns, the complexity of the array appears to make this approach impractical because of hardware requirements and its associated weight. Moreover, changes in the pattern require a complete synthesis because of the strong interdependency of the array elements. This lack of flexibility is a serious drawback.

Of the various types of reflectors under consideration, the paraboloid reflector with multiple feeds appears best suited for beam contouring. Blockage can be overcome with offset feeds, and for small scan angles little aberration is introduced. Further analysis is necessary on the multiple feed system, and some effort will be necessary in analyzing techniques to reduce the aberrations inherent in scanning with this type of antenna. The paraboloid reflector is the most attractive type of antenna for the ATS-AMS III application.

Passive lenses present properties similar to those of the paraboloid reflector. The desired contouring can be achieved with multiple feeds, and blockage is of no concern with this type of antenna system. However, the bandwidth required for the ATS-AMS III application is not achieved with lenses at the present time. Furthermore, additional R & D is required for deployable lightweight lenses of high efficiency and large aperture for frequencies above S-band. This type of antenna appears extremely attractive and should be given further consideration.

Table 5.3.2-1. ATS-AMS III Candidate Antenna Matrix

CHARACTERISTICS	REFLECTORS			LENSES		PHASED ARRAYS	
	SPHERICAL REFLECTORS	PARABOLOID REFLECTORS	SPECIAL SHAPES & REFLECTOR PERTURBATION	PASSIVE LENSES	ACTIVE LENSES	DISTRIBUTED AMPLIFIERS	PASSIVELY FED ARRAY
PATTERN VERSATILITY	Spherical aberration corrections required. Poor skirts.	Multiple feeds allows pattern contouring. Some aberrations.	Difficult to phase properly. Not versatile. Little contouring.	Similar to reflectors. Multiple beams appear attractive.	Steering and analysis is complex.	Complex analysis and interdependency of all elements.	Not versatile. Interdependency of all elements.
FLATNESS	Good flatness of patterns is possible with multiple feeds. Ripple.	Multiple feeds allows flatter beams. Some ripple.	Sometimes achievable at cost of heavy losses.	Similar to reflectors.	Amplitude control allows more versatility. Good patterns possible.	Flat patterns can be obtained from complex arrays.	Same as distributed amplifiers.
SIDELOBE	Poor sidelobes, specially for medium scan angles.	Relatively good. Coma lobe of concern for large scan angles.	Certain shapes improve sidelobe rejection, which are applicable to all reflectors.	Coma lobe not of concern. Most aberrations can be reduced.	Difficult phasing in order to achieve acceptable sidelobes.	Fairly good sidelobe levels can be obtained in conjunction with flat patterns.	Difficult amplitude and phase adjustment between elements. Poor.
LOSSES	Medium losses for multiple feeds. Blockage is of concern.	Medium losses for multiple feeds. Blockage, unless offset feeds used.	Most shaping and perturbing is very lossy.	No blockage. Some difficulty (at high freq.) with surface errors.	Poor aperture efficiency.	No blockage, not much aberration. Difficult to reduce phasing errors.	Insertion losses. Phase and amplitude control.
HARDWARE	Light to medium additional hardware, depends on feed complexity.	Medium. Some hardware in multiple feed systems.	Very light.	Same as reflectors.	For complex contouring it gets extremely large.	Very complex. Similar to active lenses.	Complex. Phase and amplitude control.
WEIGHT & SIZE	Medium to large for Gregorian systems.	Medium to large to Cassegrain systems.	Better than average.	Higher than reflectors.	Very large.	Very large.	Large.
COMMENTS	Main drawback is the spherical aberrations and poor sidelobes.	Attractive. Some R&D on feed system, hardware. Probable offset feeds to avoid blockage. No increase in aberrations with frequency changes.	Some special shapes are helpful, and can be used with other feeds to avoid blockage. Not sufficient by itself.	The lens has several advantages over equivalent reflectors. However, it appears to require additional R&D at high frequencies for large apertures. Bandwidth limitations are also of concern.	Physical qualities such as size, weight and fold-ability makes this antenna type undesirable. Bandwidth limited.	This is similar to the active lens. Unattractive for size, weight and hardware complexity. Also bandwidth is of concern.	This is similar to active lenses. Also has bandwidth limitation (questionable for 12 to 14 GHz)

Specially shaped reflectors and other perturbation techniques are often lossy and/or heavyweight, as well as inflexible. Such techniques are useful in conjunction with other types of antennas, but do not represent an attractive solution by themselves.

### MULTIPLE FEEDS IN A PRIME FOCUS PARABOLOID ANTENNA SYSTEM

A description of the method of adding secondary patterns of individual feed elements in a prime focus paraboloid antenna will be given. In order to accomplish this, a brief summary follows of the pertinent equations required to describe the pattern characteristics of a paraboloid antenna with a single element feed scanned-off axis. The beam addition method may be generally regarded as an extension of the fundamental work in this area by J. Ruze. \*

Figure 5.3.3-1 shows the germane coordinate system and geometry for the single element feed case. The far field pattern for an element displaced from the focal axis as shown is given by the scalar diffraction integral

$$\bar{E}(\theta, \phi) = \int_0^{2\pi} \int_0^a f(r, \phi') e^{ik(\mathbf{p}' - \bar{\mathbf{p}}' \cdot \hat{\mathbf{R}}_0)} r dr d\theta' \quad (1)$$

With the assumption that the aperture illumination function  $f(r, \phi') = f(r)$  plus a number of simplifications to the phase function in equation (1),  $\bar{E}(\theta, \phi)$  becomes after integration with respect to  $\phi'$ ,

$$\bar{E}(\theta, \phi) = e^{i\beta(\theta, \phi)} E(\theta, \phi) \quad (2)$$

where,

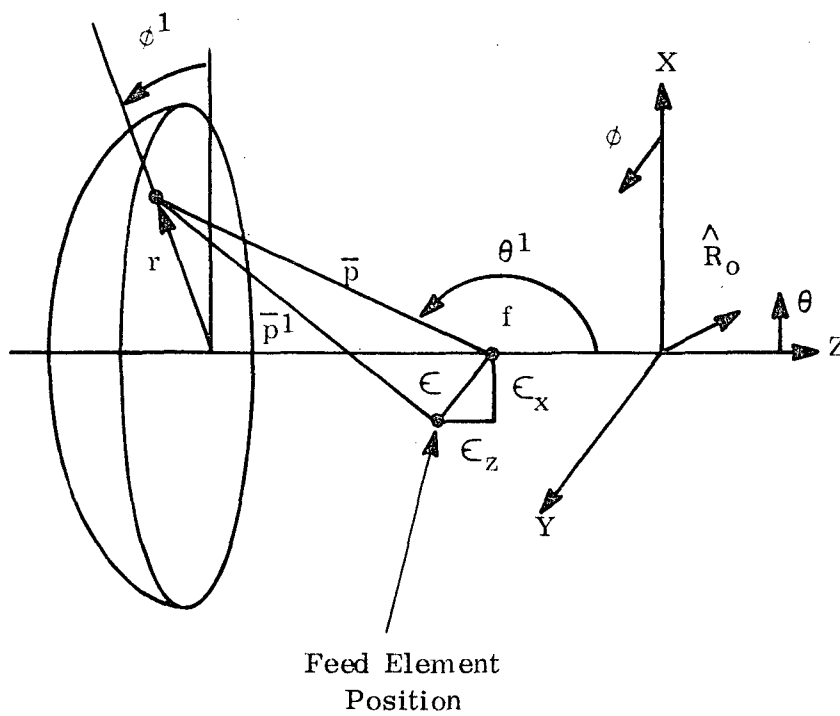
$$\beta(\theta, \phi) = k(2f - \epsilon_x \sin\theta \cos\phi - \epsilon_z (\cos\theta)) \quad (3)$$

$$E(\theta, \phi) = 2\pi a \int_0^1 f(\rho) J_0(ka C \rho) \rho d\rho \quad (4)$$

$$\text{and, } C^2 = \mu^2 - \frac{2\mu\mu_s \cos\phi}{M(\rho)} + \frac{\mu_s^2}{M^2(\rho)} \quad (5)$$

$$\mu = \sin\theta ; \mu_s = \tan \phi_s = \frac{\epsilon_x}{f}$$

\* Ruze, John, "Lateral feed displacement in a paraboloid," IEEE Transactions on Antenna and Propagation, Vol. AP-13, Sept. 65.



$\hat{R}_0$  = Unit Vector to Field Point Position

Figure 5.3.3-1. Coordinate System Geometry

$$M(\rho) = 1 + \frac{\rho^2}{(4f/D)^2} ; \quad \epsilon_z = \frac{\epsilon_x^2}{2f} \quad (6)$$

The definition of  $\epsilon_z$  in terms of  $\epsilon_x$  is actually the condition required to render  $E(\theta, \phi)$  a real function, i.e., the Petzval surface condition. A blockage function would normally be included in equation (4); however, the utilization of offset geometry will obviate this need here. The aperture illumination function will be assumed of the form,

$$f(\rho) = \frac{A + B(1 - \rho^2)\rho}{A + B} \quad (7)$$

Inserting (7) into (4) and normalizing so that  $E(\theta, \phi) = \text{unity}$  enables  $E(\theta, \phi)$  to be written as,

$$E(\theta, \phi) = \frac{2(p+1)}{A p + 1} \int_0^1 (A + B(1 - \rho^2)\rho) J_0(kaC) \rho d\rho \quad (8)$$

The evaluation of (8) by computer enables  $E(\theta, \phi)$  to be specified at any far field position for any fixed scan angle  $\theta_s$ . Implicit in equation (8) is the fact that the gain loss due to beam scan is included.

Now it may be noted that while  $\bar{E}(\theta, \phi)$  is in general complex, there are conditions under which the variable portion of the phase function in (2) will be essentially unity. This occurs when,

$$k(\epsilon_x \sin \theta \cos \phi - \epsilon_z \cos \theta) \ll 1 \quad (9)$$

so that under condition (9),

$$\bar{E}(\theta, \phi) \simeq e^{i2kf} E(\theta, \phi) \quad (10)$$

Equation (9) will not be satisfied for arbitrary  $\theta$  when  $\epsilon_x$  is a number of wavelengths. However, near boresight, i.e.,  $\theta = 0^+$ , (9) and hence (10) will always be true.

The complex nature of equation (2) must be considered when far field pattern addition of a number of antenna beams is done. If equation (9) does hold, however, for a number of feed elements displaced from the focal axis of a paraboloid and oriented so that the resultant polarizations are parallel, beam addition with proper regard to focal plane feed placement is possible without resorting to complex number addition. When beam addition is done in this or any other sense considered here, however, the restriction that all  $f(\rho)$ 's are identical will be made, i.e., the feed elements are all identical. The reason for this is that equation (8) does not give the absolute value of the field intensity and were  $f(\rho)$  different for each feed element, the gain function for each feed element would need explicit inclusion.

The problem of proper addition of secondary antenna patterns from paraboloid antennas will now be further discussed. Consider Figure 5.3.3-2 where a coordinate system designed by  $X^n$ ,  $Y^n$  which has been rotated about a common Z-axis is shown. With the simple<sup>n</sup> rotation shown, the pattern of the  $m^{\text{th}}$  element placed on the  $X_m^{\text{nth}}$  axis will be,

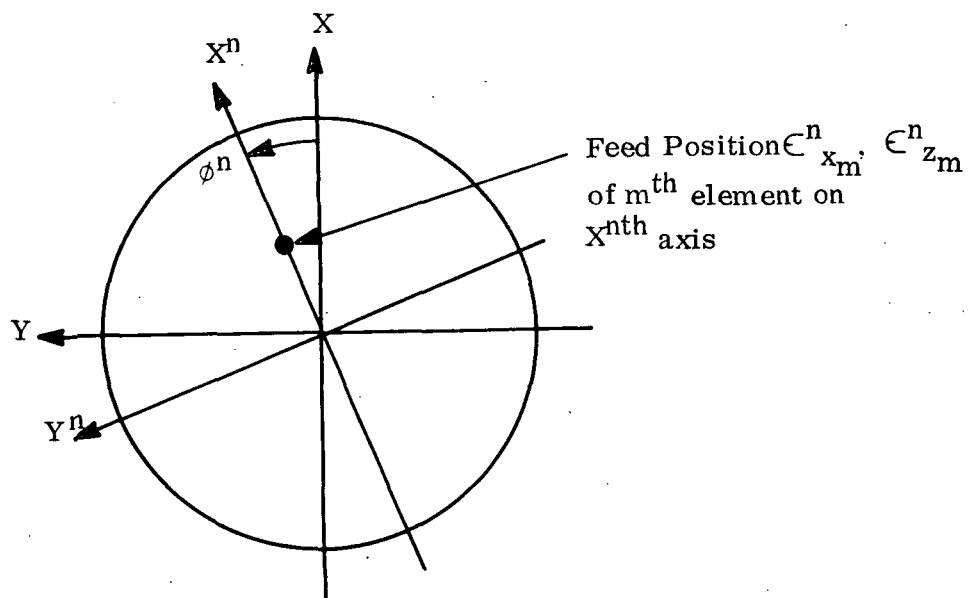
$$\bar{E}_m^n = e^{i \beta_m^n(\theta, \phi)} E_m^n(\theta, \phi) \quad (11)$$

where,

$$\beta_m^n = k(2f - \epsilon_{X_m}^n \sin \cos \theta (\phi - \phi_m^n) - \epsilon_{Z_m}^n \cos \theta) \quad (12)$$

$$E_m^n(\theta, \phi) = \frac{2(p+1)}{Ap+1} \int_0^1 f(\rho) J_0(ka C_m^n \rho) \rho d\rho \quad (13)$$

$$(C_m^n)^2 = \mu^2 - \frac{2\mu \mu_{s_m}^n \cos(\phi - \phi_m^n)}{M(\rho)} + \frac{(\mu_{s_m}^n)^2}{M^2(\rho)} \quad (14)$$



$m = 1, 2 \dots M_n$ ;  $M_n = \#$  of Elements on  $X^{\text{nth}}$  Axis

$n = 1, 2 \dots N$ ;  $N = \#$  of Coordinate Systems Rotated about Z-Axis

Figure 5.3.3-2. Geometry for Secondary Pattern Addition



$$\mu_{s_m}^n = \frac{\epsilon_{x_m}^n}{f} ; \quad \epsilon_{z_m}^n = \frac{(\epsilon_{x_m}^n)^2}{2f} \quad (15)$$

Now, if  $M_n$  elements exist on the  $X^{nth}$  axis where the  $\epsilon_{x_m}^n$ 's may be positive or negative, the far field pattern will be given by

$$\bar{E}_{M_n}^n = \sum_{m=1}^{M_n} \bar{E}_m^n = \sum_{m=1}^{M_n} e^{i\beta_m^n(\theta, \phi)} E_m^n(\theta, \phi) \quad (16)$$

Equation (16) in essence gives the antenna pattern of a linear array of  $M_n$  elements displaced by the angle  $\phi^n$  in the coordinate system shown in Figures 5.3.3-1 and 5.3.3-2.

Now, there may be  $N$  linear arrays which each possess patterns of the form of equation (16) so that the composite pattern for this case would be,

$$\begin{aligned} \bar{E}_M^N &= \sum_{n=1}^N \bar{E}_{M_n}^n = \sum_{n=1}^N \left( \sum_{m=1}^{M_n} \bar{E}_m^n \right) \\ &= \sum_{n=1}^N \sum_{m=1}^{M_n} e^{i\beta_m^n(\theta, \phi)} E_m^n(\theta, \phi) \end{aligned} \quad (17)$$

Equation (17) is the desired result for proper secondary pattern addition from feed elements placed about the focal plane of a prime focus paraboloid system.

The contoured non-circular and non-elliptical antenna patterns that are recommended in this study are based on the apparent validity of equation (17). It is proper at this time to mention a seeming paradox that results from the inclusion of the phase function defined by equation (3) in the pattern addition technique. It is well known that scanned paraboloid antenna systems that possess relatively large  $f/D$  ratios are afflicted to a much lesser degree with the pattern

distortions resulting from comatic aberration. This may be readily deduced upon inspection of  $M(\rho)$  defined in equation (6), and the impact of  $M(\rho)$  on  $C^2$  defined by equation (5). It can thus be observed that for  $(f/D) \gg 1$ ,  $M(\rho)$  approaches unity, consequently  $C$  in (5) becomes virtually independent of  $\rho$  which in turn negates the effects of coma, i.e., beam shift without aberration. (The effects of astigmatism enter into the analysis of antennas that possess large  $f/D$  ratios; however, this pattern distortion is neglected in the work of J. Ruze.) The paradox occurs when the phase addition technique required by equation (17) for multiple pattern addition is interpreted in the context of the phase function defined by equation (3). The phase function may be regarded as being directly proportional to  $\epsilon_x$ , i.e., the amount of feed displacement required to produce a given secondary pattern squint. For a fixed squint angle,  $\epsilon_x$  will be proportional to  $f$ ; consequently the complex pattern addition required by equation (17) will manifest much more in paraboloid antennas with large  $f/D$  ratios, and this effect will tend to occur nearer to the boresight axis, i.e., in the vicinity of the contoured shaped beam. It can further be inferred that complex pattern addition in the main beam area will be derogatory since arithmetic addition produces near optimum contours in the main beam area.

At the present time, it is believed that a choice of an  $f/D$  ratio slightly less than unity is the proper compromise between the known effects of coma and the unknown effects of astigmatism. The  $f/D$  ratio utilized in performing the pattern additions required to produce the shaped beams presented in this study was chosen on this premise. Further analysis is recommended to determine if a slightly different  $f/D$  ratio is justified. Consideration must be given to sidelobe levels, flatness of the main beam, other aberrations and even displacement distances, in order to have assurance that an optimization of the focal length has been carried out.

A computer analysis was made of the pattern produced by two feeds with illumination taper of -14 dB on a paraboloid reflector with  $f/D = 0.9$ . As shown in Figure 5.3.4-1, a cross-over of about 7 dB between beams allows for the largest coverage without significant ripple in the main pattern. Although it is not shown in the figure, the sidelobe levels for this case are better than -30 dB. Subsequently, the plot of this pattern was superimposed on the plot of a pencil-beam pattern of equivalent coverage at the -3 dB level, and same illumination as the two individual feeds. This is shown in Figure 5.3.4-2. It is clear from this comparison that the pattern achieved with the pair of feeds has a flatter "top" and sharper "skirts" than the pencil-beam of equivalent coverage. This would be more apparent if a 2 dB coverage was desired.

The case of four equal feeds placed at  $90^\circ$  from each other so as to form a box about the boresight, was considered next. If the cross-over level of -7 dB is maintained, the center of the pattern will have a dip in signal strength of 3.8 dB below the maximum value, which is not acceptable. This is shown in Figure 5.3.4-3. However, if the crossover level is modified to 5.6 dB, a ripple of -0.7 dB is achieved. The sidelobe level for this case was found to be below -24 dB. Figure 5.3.4-4 shows the two principal plane cuts of this pattern, and Figure 5.3.4-5 shows an X-Y plot of the same.

The square beam described above is a good example of contoured patterns from block-building multibeam. However, further analysis is desirable for more complex patterns. An additional two feeds placed next to the first four was also studied, and because of additional phase error and aberrations introduced with scanning, the ripple in this new pattern (-1.6 dB) is greater than with the

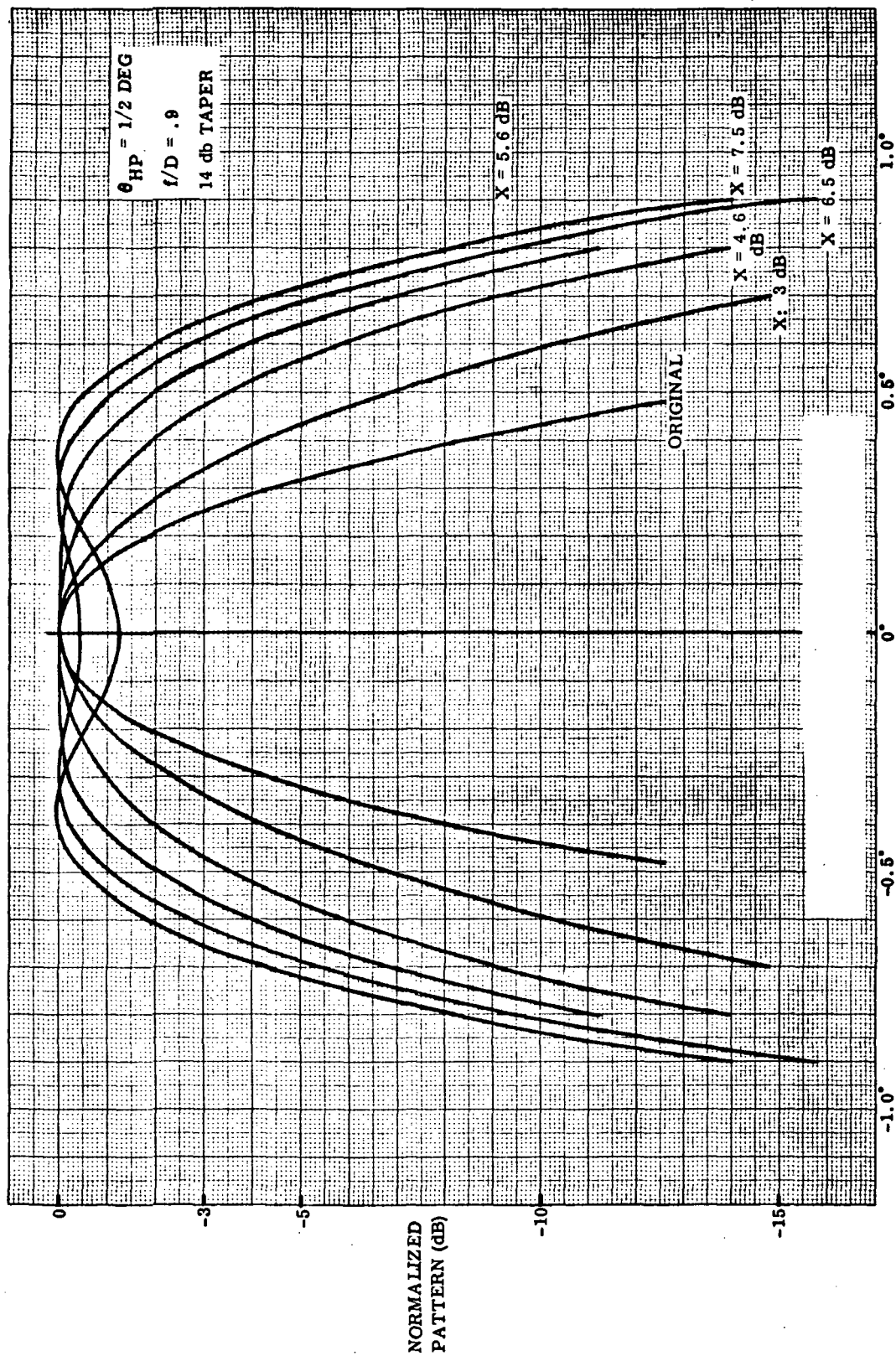


Figure 5.3.4-1. Two-Beam Pattern for Various Cross-Over Levels

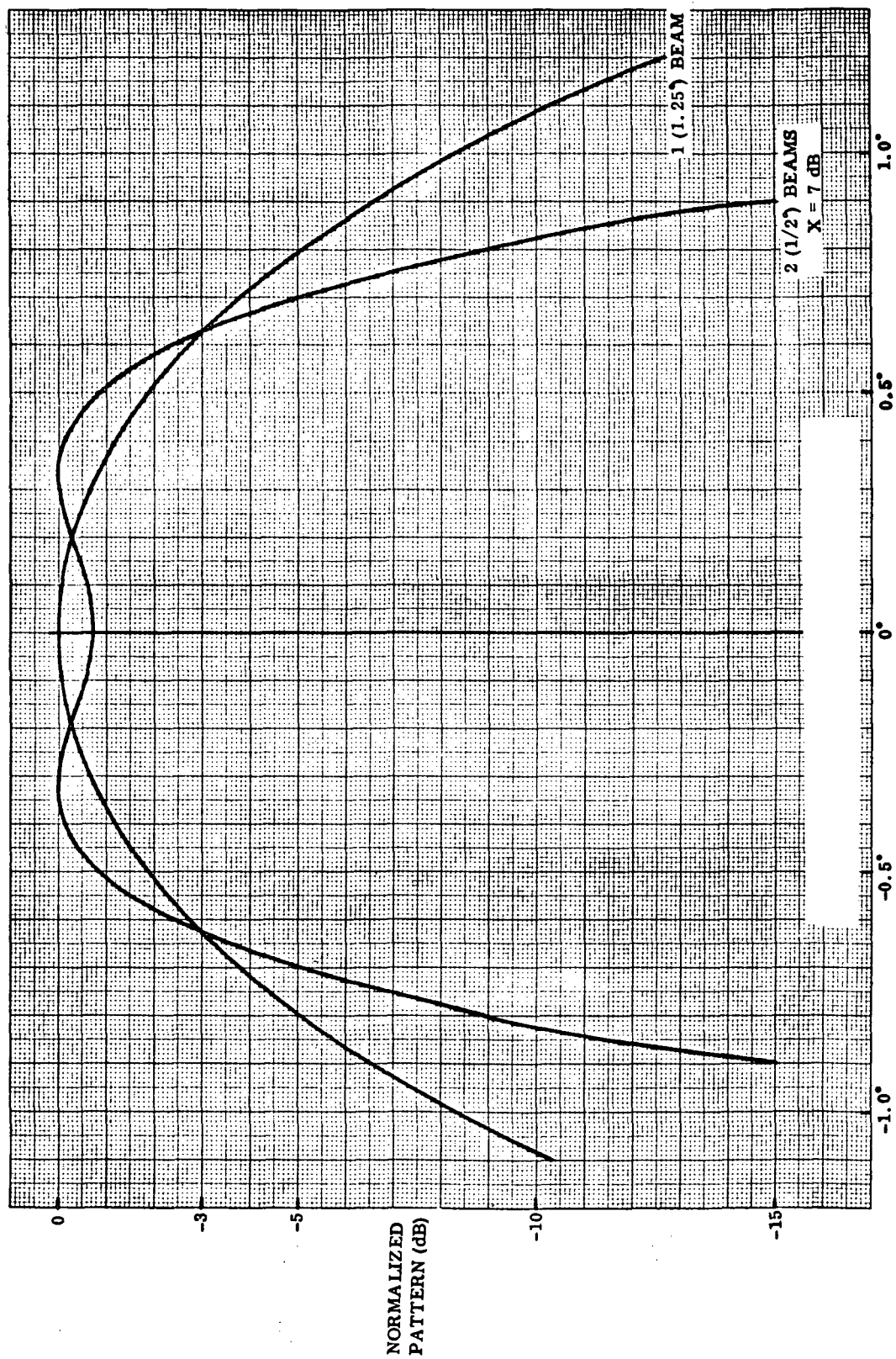


Figure 5.3.4-2. Comparison of Multibeam and Single-Beam Patterns

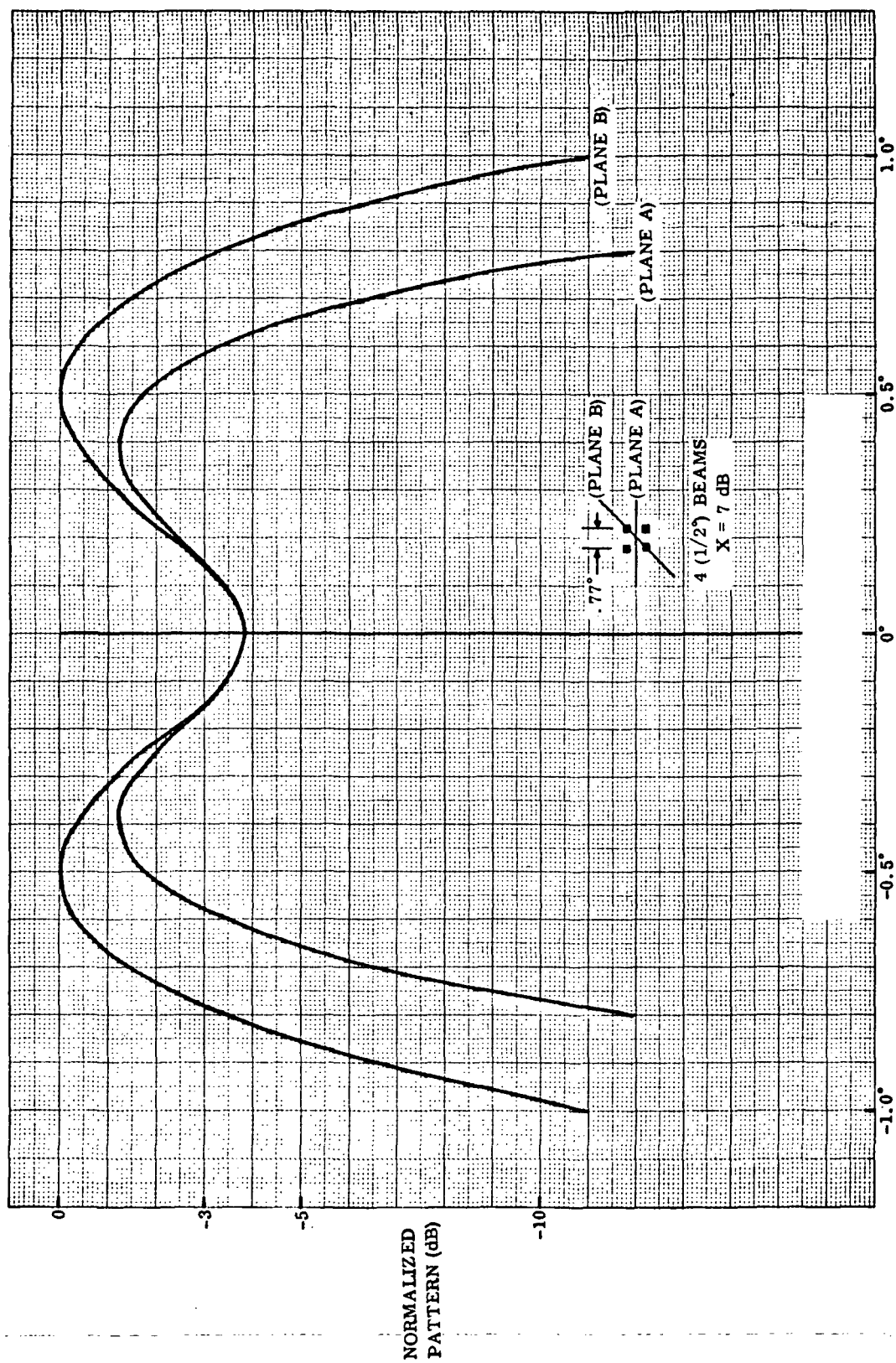


Figure 5.3.4-3. Principal Plane Cuts of Four-Feed Pattern ( $x = -7$  dB)

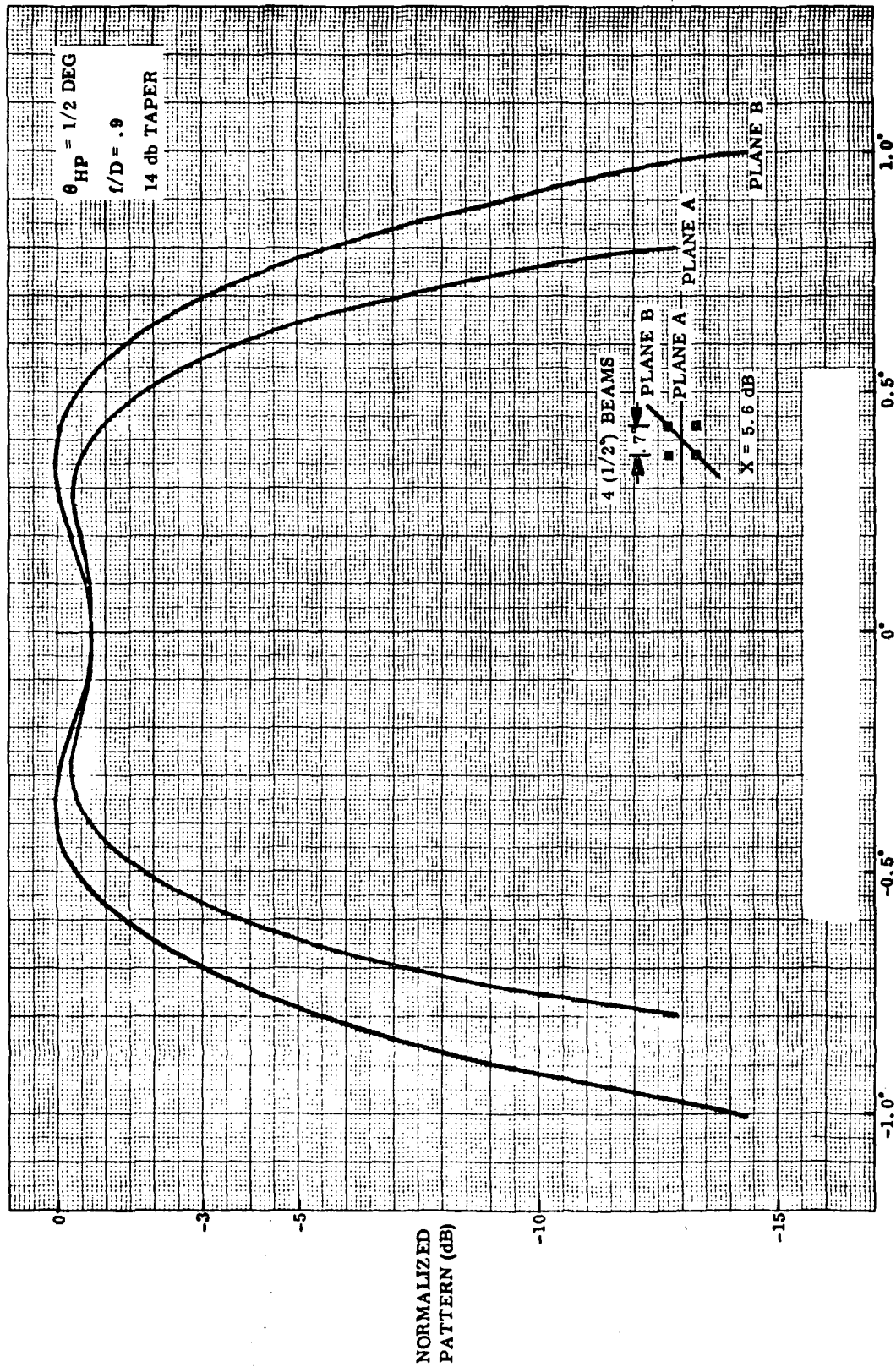


Figure 5.3.4-4. Principal Plane Cuts of Four Feed Pattern ( $x = -5.6 \text{ dB}$ )

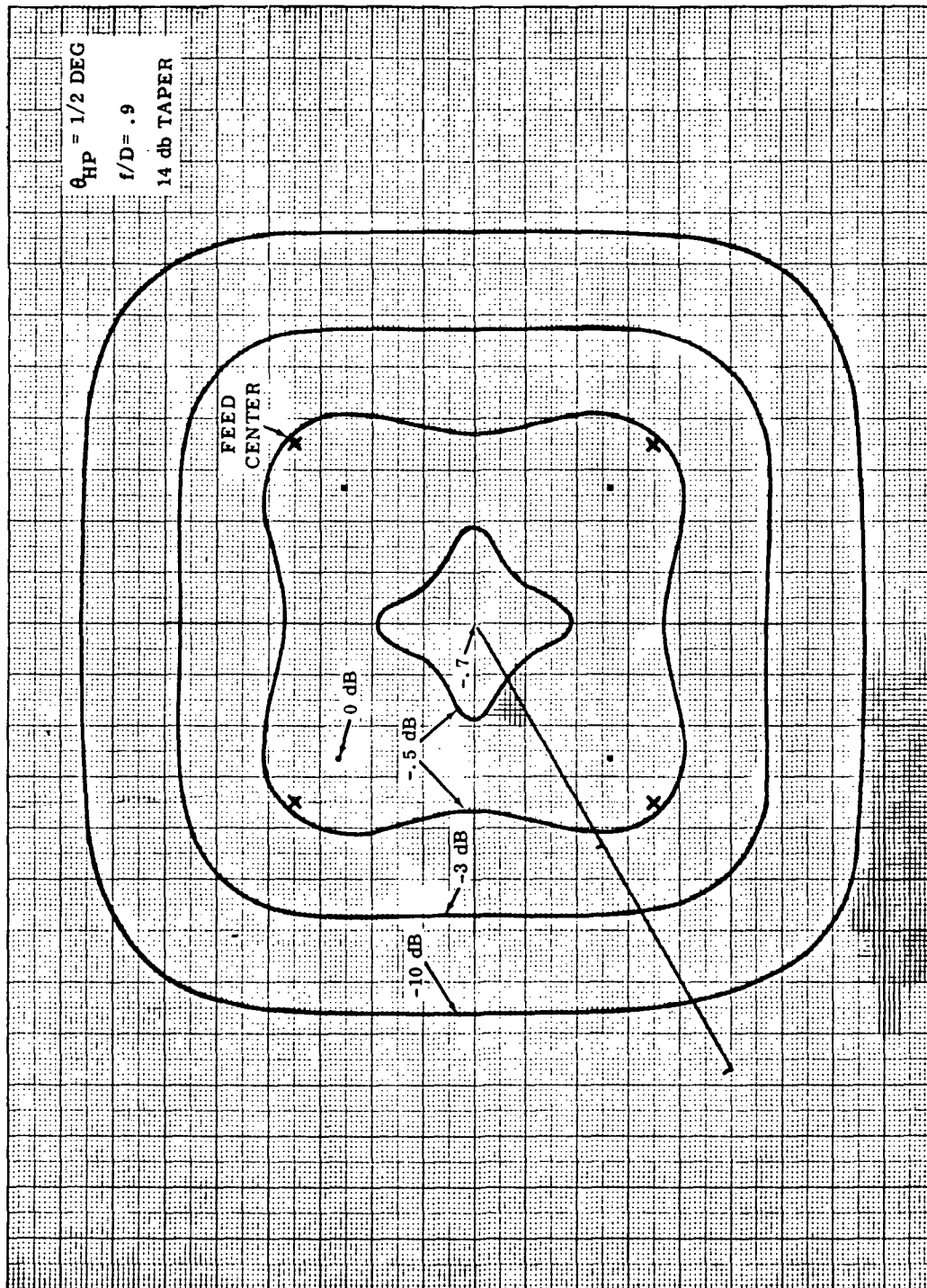


Figure 5.3.4-5. Four-Feed Pattern - x, y plot



original four feeds symmetrically displaced about the focal point. This is shown in Figure 5.3.4-6 and 5.3.4-7. The sidelobe level for this pattern was calculated at -25 dB.

It is obvious at this point that a fixed cross-over level for all pattern contours is not the best answer. By starting with  $1/2^\circ$  beam-width beams, contouring can be achieved within the given minimum and maximum curvature specifications. However, each individual pattern will require a slightly different feed separation, so as to achieve the best contouring and reasonably flat patterns.

The patterns shown in this section are typical of what is expected of multiple beams from a parabolic reflector. The computer software available up to now did not consider offset reflectors, and thus did not permit accurate description of the aberrations and sidelobe levels that can be obtained with the recommended offset-fed paraboloid. It is expected that the final cross-over levels will be somewhat different from what was used in the generation of these patterns, and that sidelobes several dB higher will be obtained when the additional coma and phase effects of an offset paraboloid are taken into account. It is also necessary to recognize that, as shown in paragraph 5.3.3, phase effects between beams become severe as the scan angle increases, and as the feeds separate from each other. Therefore, the patterns shown in this section are only representative of the performance that a multibeam antenna system can achieve.

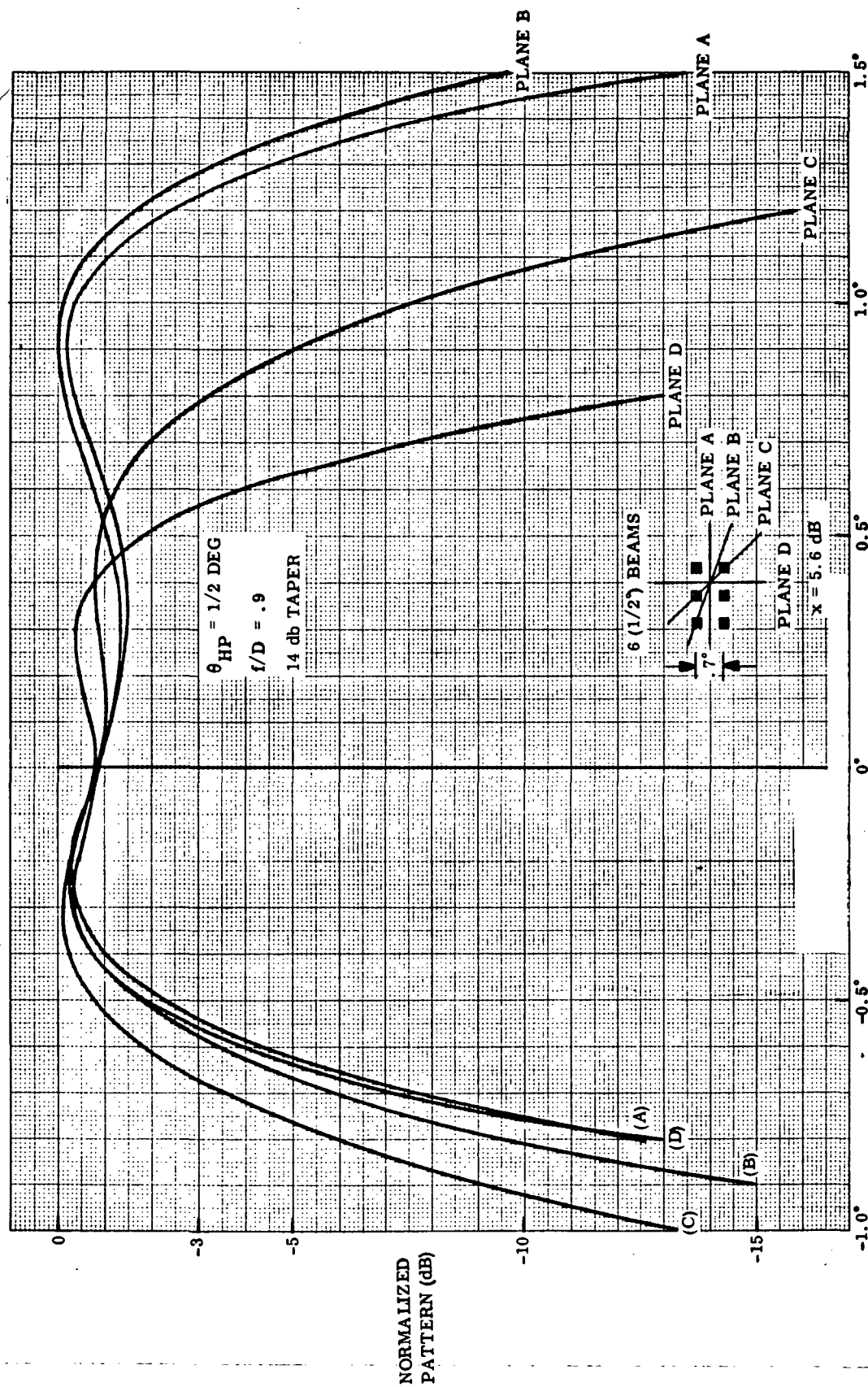


Figure 5.3.4-6. Principal Plane Cuts of Six-Feed Pattern

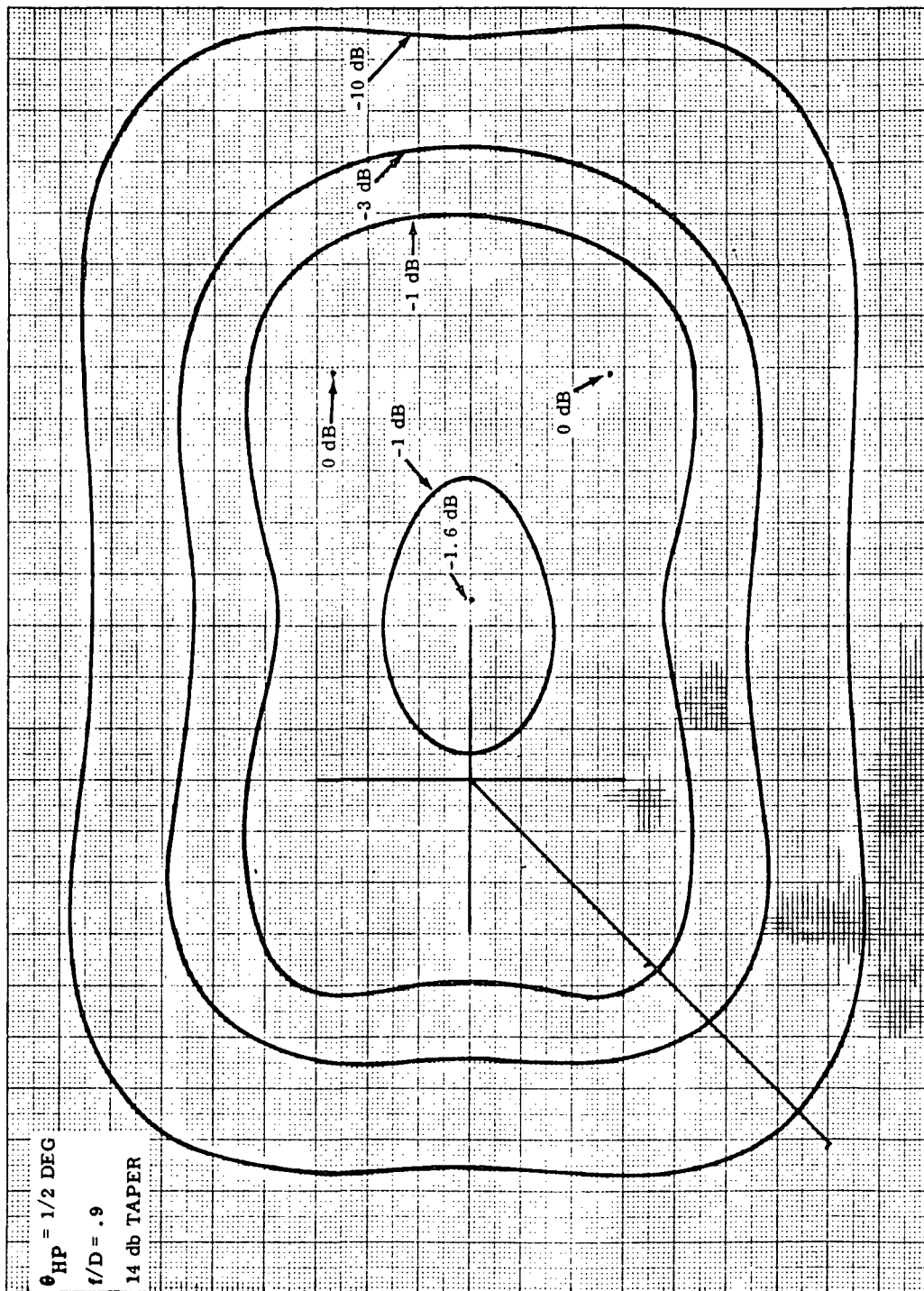


Figure 5.3.4-7. Six-Feed Pattern - x, y plot

### 5.3.5

### AMS III REFLECTORS

#### 5.3.5.1

#### Large Reflector

As detailed in paragraphs 5.3.1 and 5.3.2, a parabolic reflector was chosen for the shaped multibeam required for the baseline experiments. Since the matrix of feeds was anticipated to be relatively large, an offset reflector was believed necessary to avoid severe blockage effects.

Figure 5.3.5-1 shows a paraboloid and its basic parameters. The subtended angle from the focal point is described by

$$\tan (1/2 \phi_M) = (1/4) \frac{D_M}{f}$$

and the surface of the reflector is defined by

$$X = \frac{Z^2}{4f}$$

$$Y = \frac{Z^2}{4f}$$

where  $D_M$  = Diameter of full reflector

$f$  = Focal length

$\phi_M$  = Subtended angle of full reflector

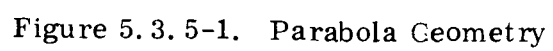
This figure also shows an offset section of the reflector, diameter  $D_O$  and subtended angle  $\phi_O$ . It is this section of the full reflector that will be utilized, with

$$D_O = 3.44 \text{ m}$$

$$f = 3.1 \text{ m}$$

such that

$$f/D_O = 0.9$$



It is obvious from this figure that, for the full reflector,

$$f/D_M \lesssim (1/2) f/D_O = 0.45$$

Therefore, the reflector to be utilized has coma effects equivalent to an  $f/D$  of 0.45, and it is this ratio which must be taken into account if an adjustment of the focal length is to be considered, as suggested in paragraph 5.3.3.

In order to carry out beam scanning, displacement of the feeds by an angle  $\theta_d$  is required. However, due to a beam deviation factor (BDF) somewhat less than unity, it is necessary that the feed displacement be larger than the required beam scan. The reflector boresight location is assumed to be 38° North latitude, 102° West longitude, in order to minimize scanning angles.

$$\frac{\theta_s}{\theta_d} = \text{BDF}$$

Further description on the feeds is found in paragraph 5.3.6.

#### 5.3.5.2

##### Small Reflector

CONUS coverage at 14 GHz is obtained by means of a small parabolic dish with a single feed. For a 3° x 7° beam, a dish with dimensions 51.8 cm vertical by 22.8 cm horizontal (20.4 x 9 inches) is used. The boresight location for proper CONUS coverage is 38° North latitude and 97° West longitude.

The antenna parameters that describe this reflector have been presented in the previous section, and will not be repeated here.

To generate the contoured beams described in paragraph 4.3.1, a matrix of 39 waveguide-fed horns is used to illuminate the large reflector. To obtain the reduced coverage of AMS III B, 36 feeds suffice. Each of the regions to be covered requires several feeds radiating simultaneously, the exact number varying from region to region, as shown in Table 5.3.6-1. The feeds themselves consist of horns with tapering in both planes to a mension of 3.64 cm.

The estimated illumination taper on the edge of the reflector is -14 dB in the E-plane and -8 dB in the H-plane, but more tapering in the H-plane is recommended by means of any of the known techniques, such as dielectric loading, to improve sidelobe performance of the reflector antenna. Separation between feeds is estimated as  $0.70^\circ$  (3.7 cm) minimum, and varies depending on the coverage region, as previously indicated.

The feeds of any one region are interconnected and phased so as to radiate with equal amplitude and phase from each of the feeds. A typical interconnection is shown in Figure 5.3.6-1, where feed No. 1 is shown to be connected to a circulator and to the front end of a receiver - a TDA. The circulator allows the combination of audio with video power out on feed No. 1. This power does not enter the receiver waveguide because of cross-polarization, and additional isolation is obtained from a strip of beyond-cut-off waveguide at the receiver input. The hybrids and couplers shown distribute the power evenly to all feeds. Not shown are possible phase shifters in certain branches, to equalize the output phase of all the feeds in a region. The amount of phase correction required depends on the length of waveguide and the devices present in each branch.

Table 5.3.6-1. ATS-AMS III Feed Assignment

PBS EXPERIMENT		
<u>TIME ZONE</u>	<u>AMS III A</u>	<u>AMS III B</u>
	<u>NO. OF FEEDS</u>	
EASTERN	8	6
CENTRAL	12	8
MOUNTAIN	8	8
PACIFIC	4	} 8
ALASKA	4	
HAWAII	1	

ITV EXPERIMENT		
<u>CULTURAL REGION</u>	<u>AMS III A</u>	<u>AMS III B</u>
	<u>NO. OF FEEDS</u>	
NORTHEAST	4	(2)
SOUTH	8	6
MID-WEST	6	6
SOUTHWEST	6	6
FAR-WEST	6	6
PACIFIC	4	} 6
ALASKA	0	



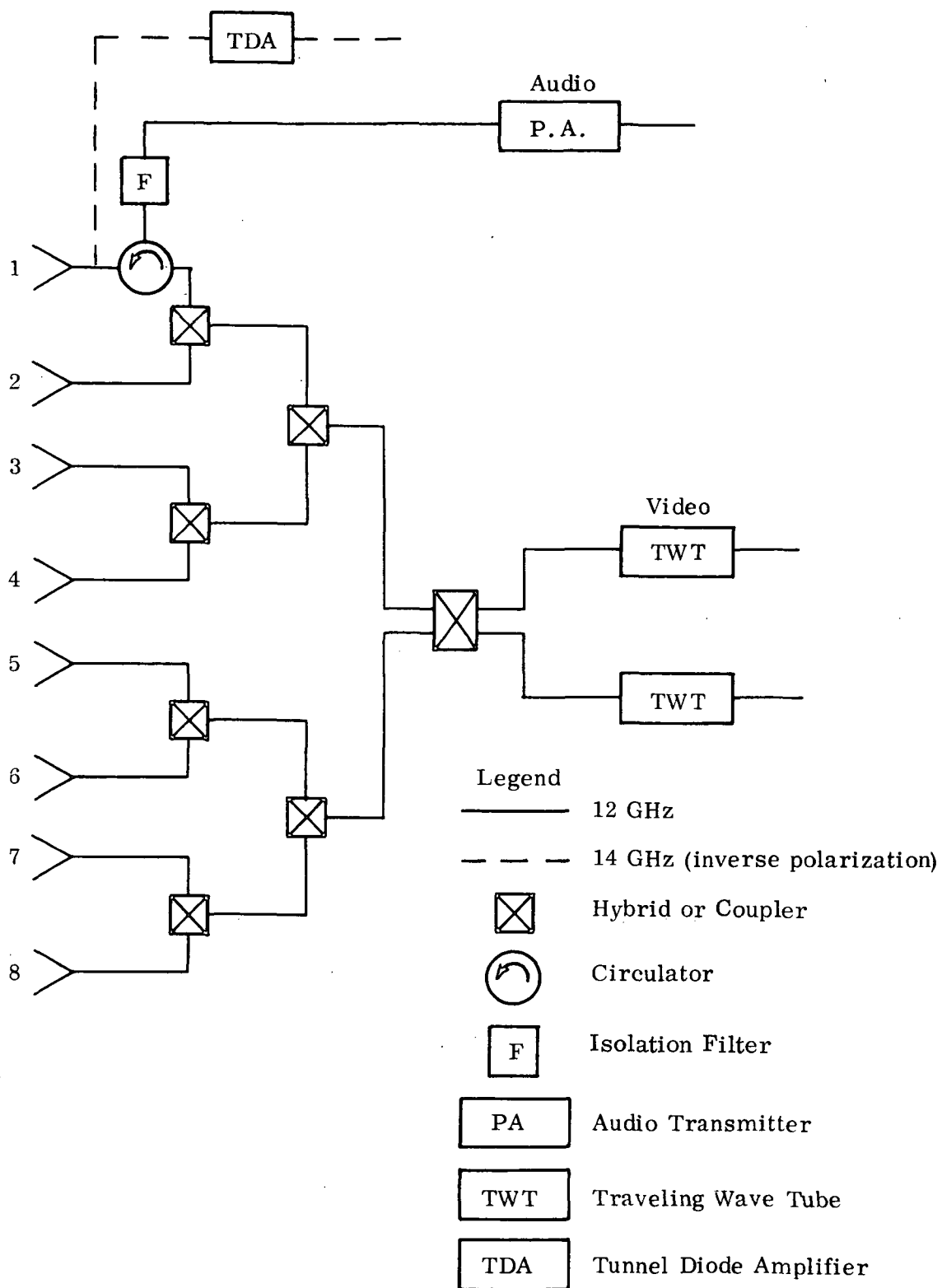


Figure 5.3.6-1. Typical Feed Interconnection For ATS-AMS III A

The assignment of feeds is different for the PBS experiment and the ITV experiment. The transmitters and feeds can be efficiently switched by means of electromechanical switches, which are available at the frequencies in question with very low insertion losses (0.1 - 0.2 dB). Figure 5.3.6-2 shows the complete interconnection required to carry out the baseline experiments for ATS-AMS III A. (The frequency of each receiver is labeled  $f_A$ ,  $f_B$ , etc. corresponding to the sequence of bands as described throughout this report.) A signal flow diagram for the ATS-AMS III A PBS and the ITV experiments is shown in Figures 5.3.6-3 and 5.3.6-4, which describe the operation of the system in each instance. No switches are shown in the latter figures for the sake of clarity.

Figure 5.3.6-5 shows the complete interconnection of ATS-AMS III B, and Figure 5.3.6-6 and 5.3.6-7 show the corresponding signal flow diagrams for the PBS and ITV experiments. In version AMS III B, coverage is not as complete as in version III A, but more versatile switching is provided for medical communications with Alaska.

The switching insertion loss from transmitter to feed varies between 0.5 dB and 1.4 dB, depending on the number and type of devices present in a particular branch.

The weight tabulation for the feeds and RF switching is shown in Table 5.3.6-2. It should be noted that, although Figures 5.3.6-2 and 5.3.6-5 show both RF and IF switches and interconnections, only the weight of the RF switching sections is included in the antenna subsystem weight and power budget. IF switches are part of the communications subsystem, which is described in paragraph 4.4.2. The isolation filters are also part of the communications subsystem of paragraph 4.4.2, and are thus not included in Table 5.3.6-2.

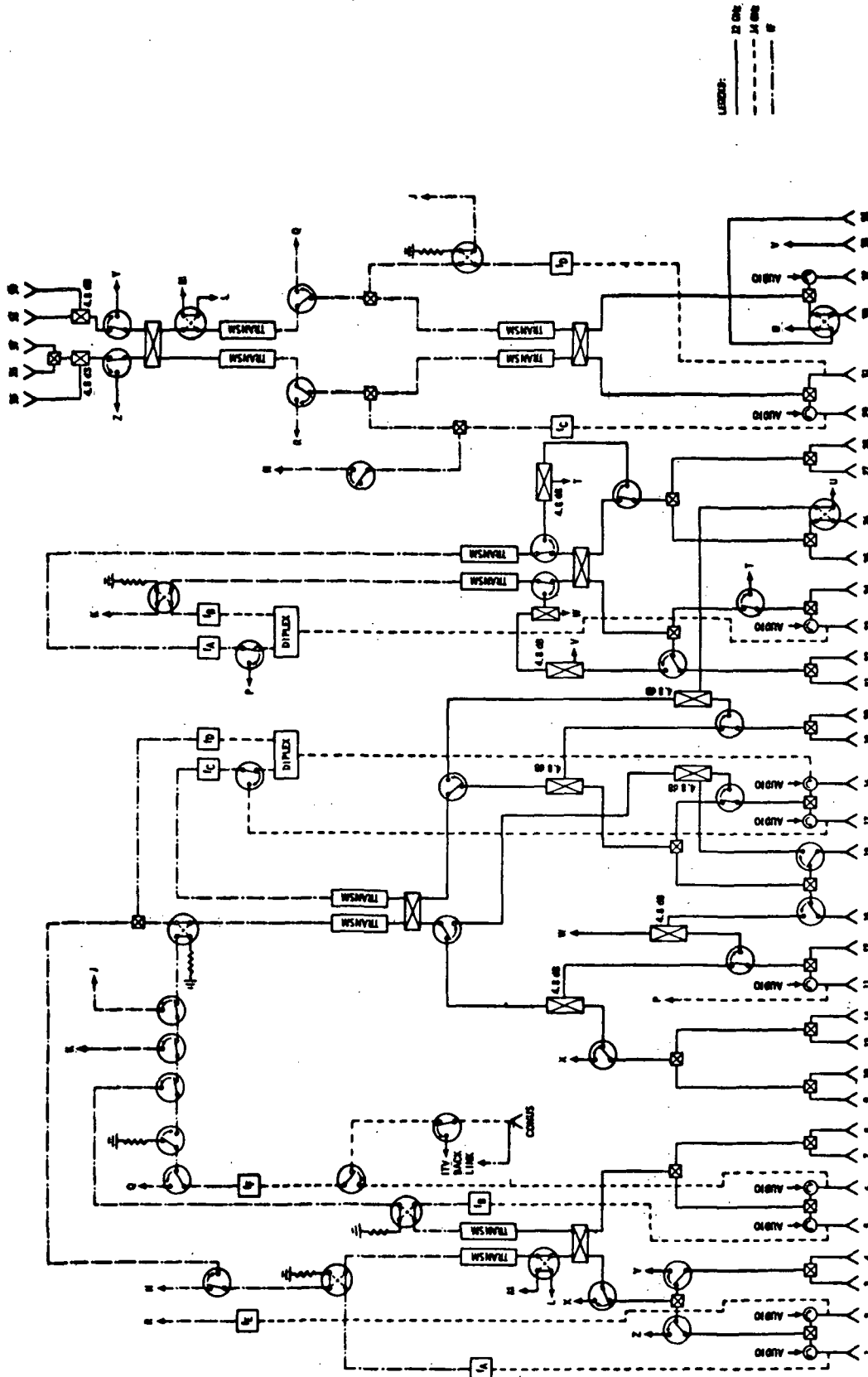


Figure 5.3.6-2. ATS-AMS III A Switching Diagram

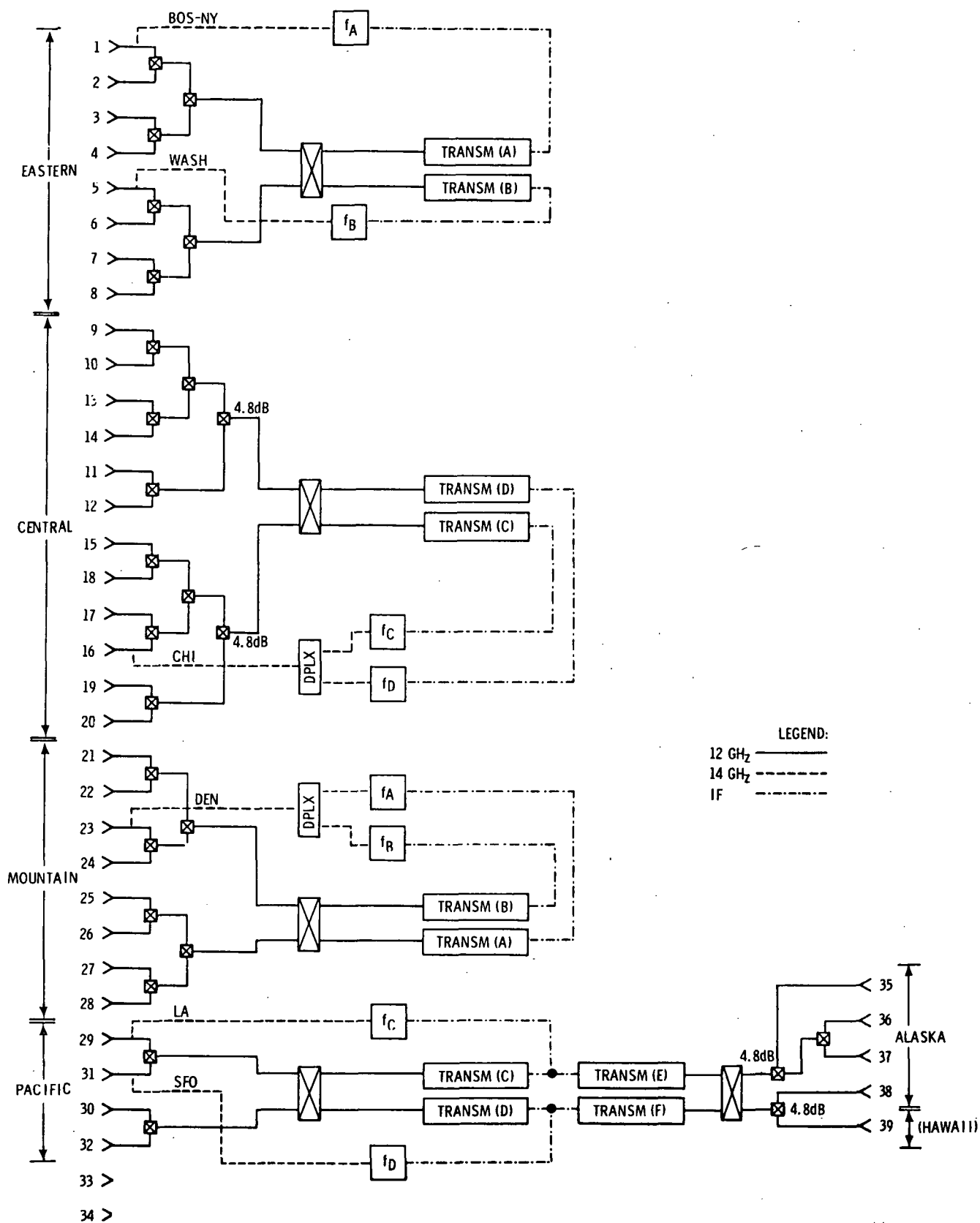


Figure 5.3.6-3. ATS-AMS III A PBS Information Networking  
Experiment Video Signal Flow Chart

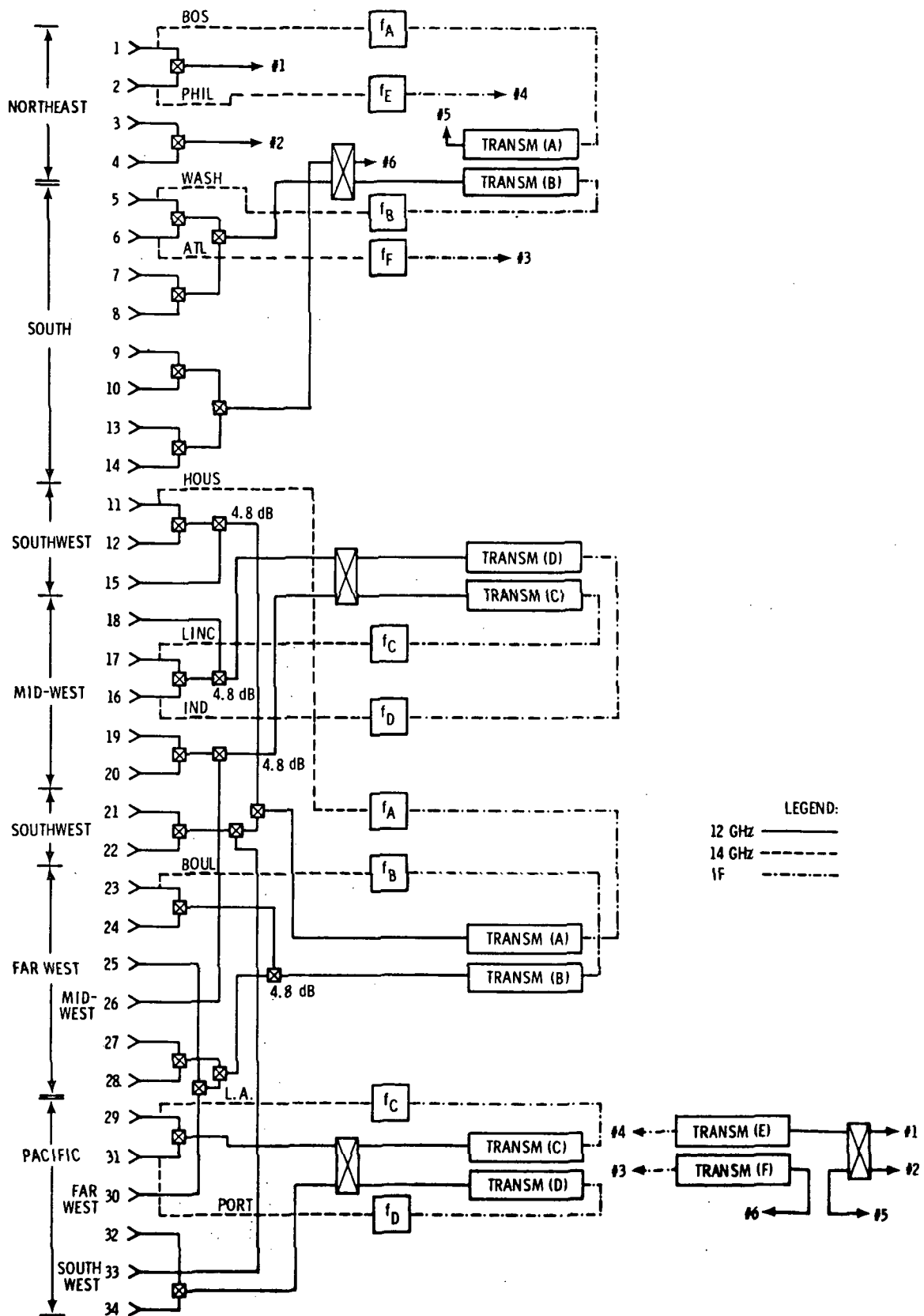


Figure 5.3.6-4. ATS-AMS III A Interactive TV Experiment  
Video Signal Flow Chart

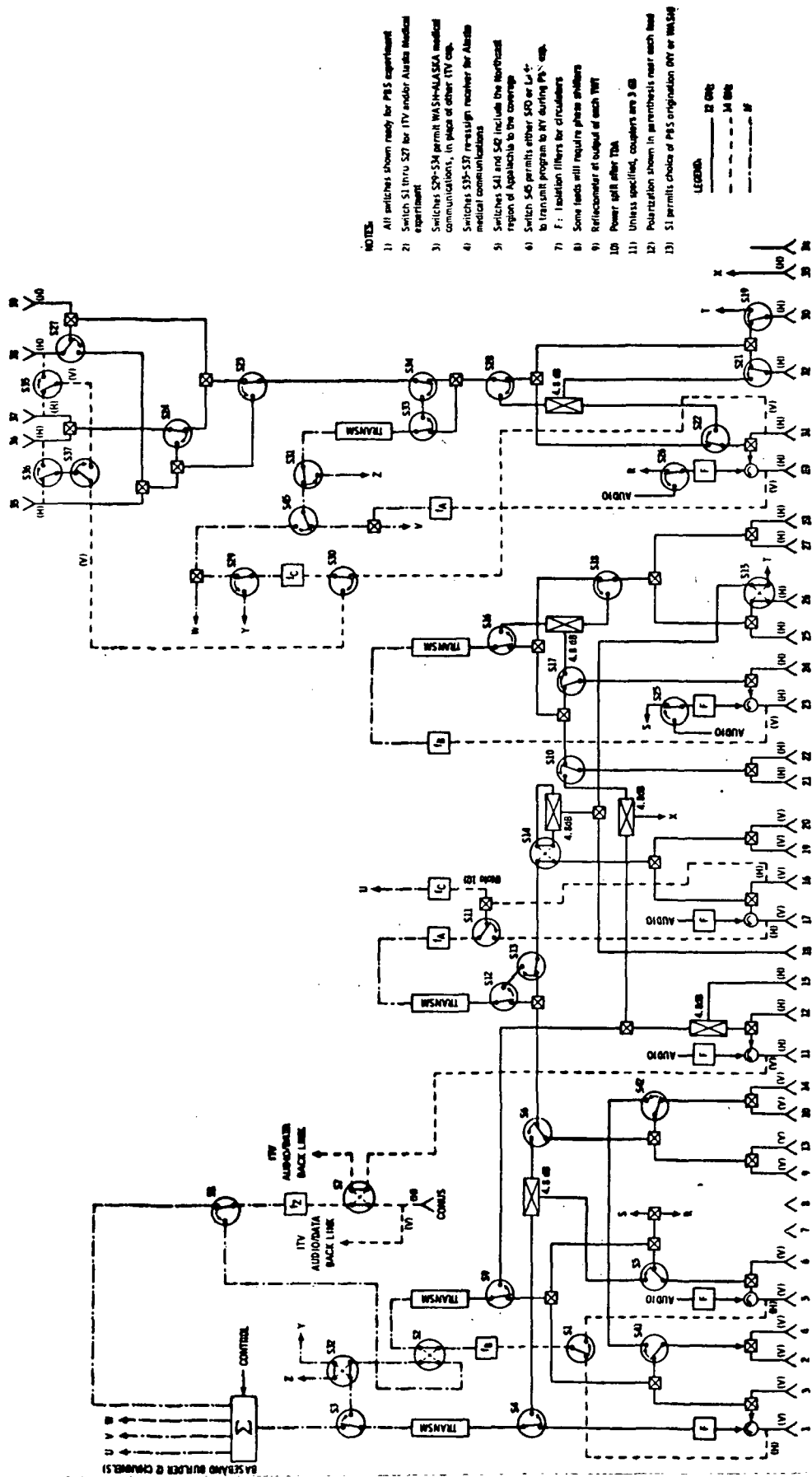
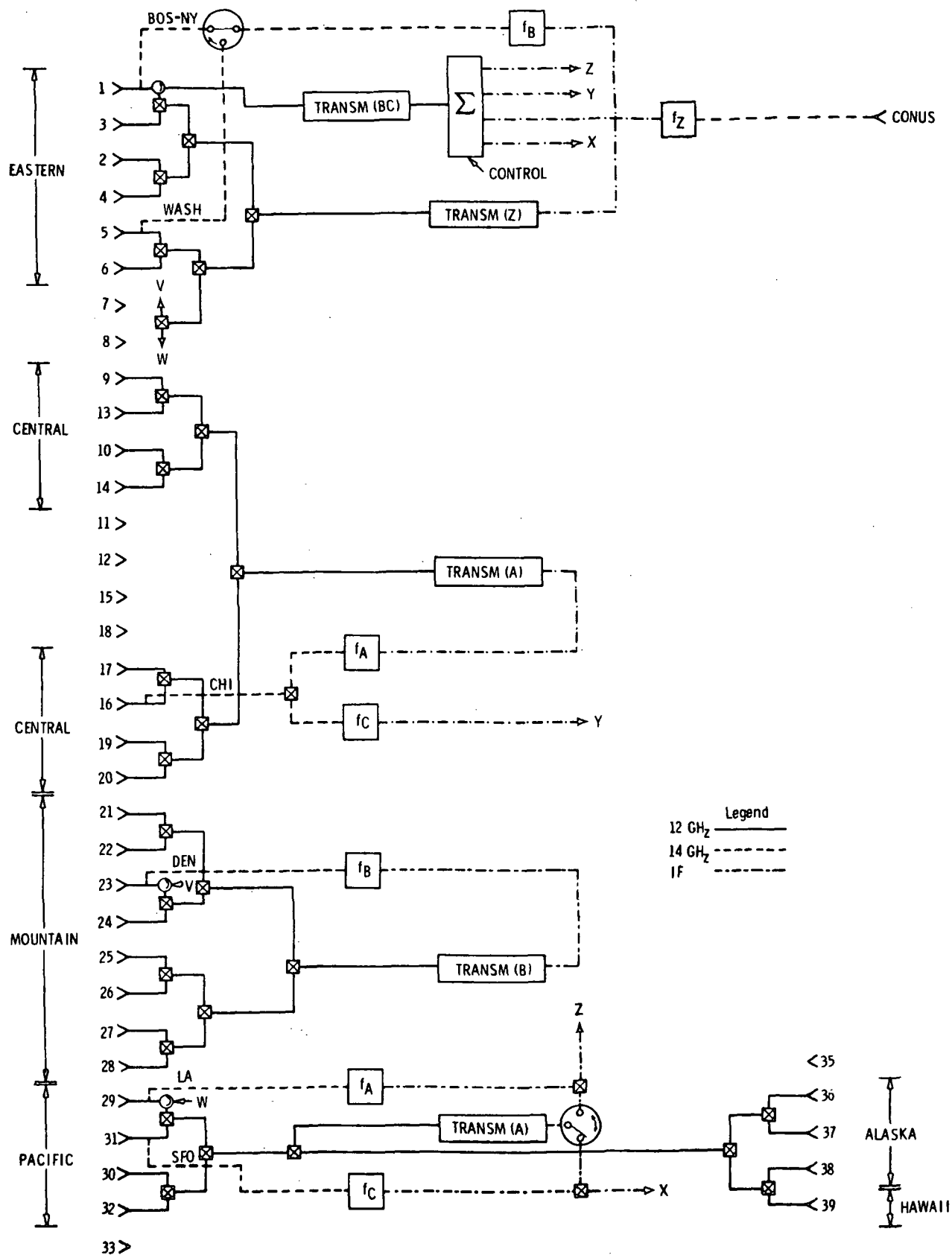


Figure 5.3.6-5. Switching Diagram



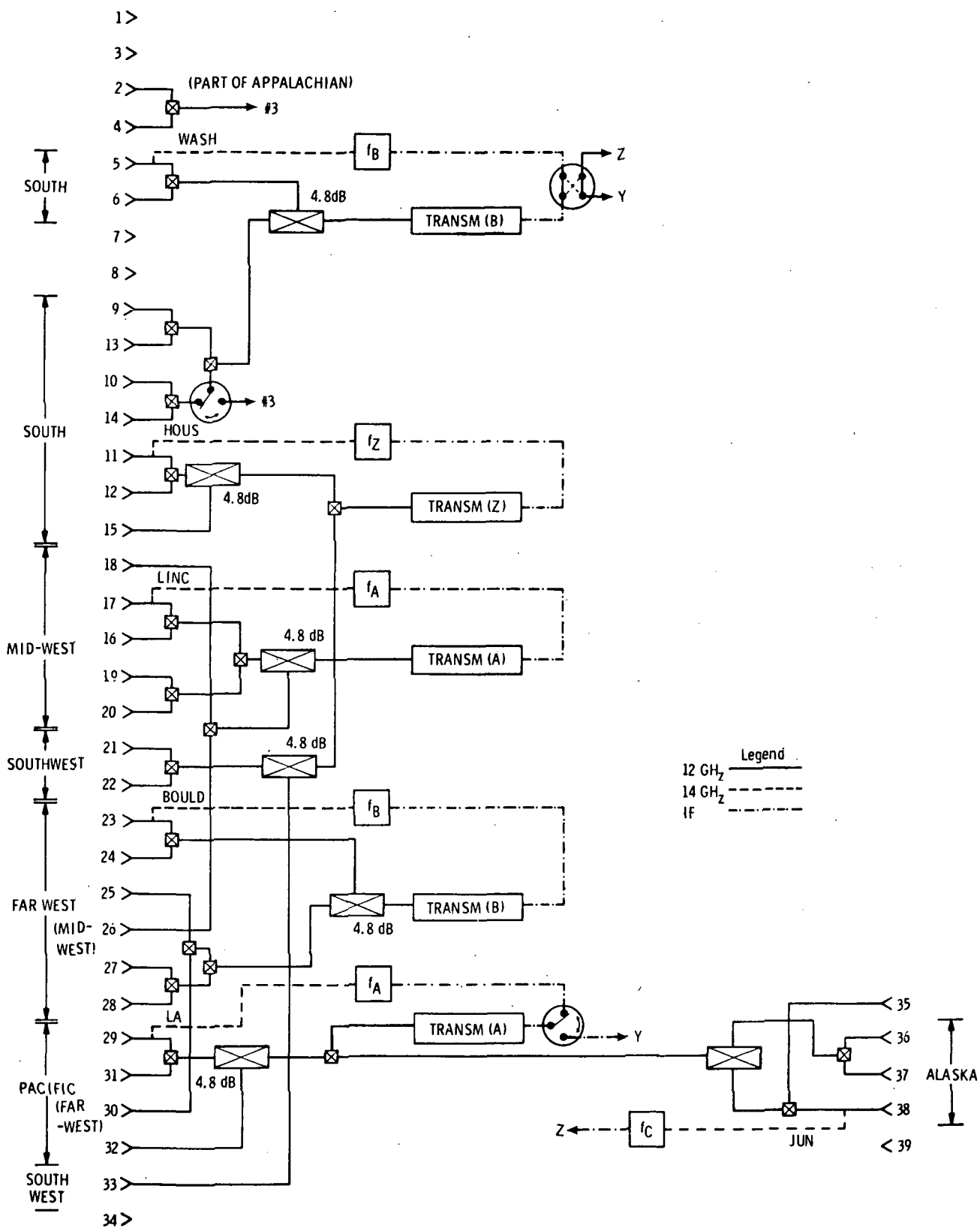


Figure 5.3.6-7. ATS-AMS III-B Interactive TV Experiment Video-Flow Chart



Table 5.3.6-2. ATS-AMS III A Feeds and Switching Weight Tabulation

Item	Quantity		AMS IIIA kg (lb)	AMS IIIB kg (lb)
	AMS IIIA m ( ft )	AMS IIIB m ( ft )		
Horns	39	36	7	AMS IIIB kg (lb) 6.3 (14)
Waveguide For:				
Switches	9.2 30.3	13.3 44		
Feeds	10.1 33.3	9.3 31		
Couplers 2 Hybrids	10.0 33	10.0 33		
TWT's	6.1 20	3.0 10		
CONUS Feed	0.9 3	0.9 3		
Audio P.A.'s	6.1 20	3.0 10		
Circulators	1.5 5	0.9 3		
Waveguide (TOTAL)	43.9 (144.6)	40.4 (134)	23.5 (51)*	21.2 (47)*
Flanges	300		4.5 (10)	4.5 (10)
TOTAL FEEDS AND WAVEGUIDES			35 (77)	32 (71)
Switches	22	32	10 (22)	14.5 (32)
Couplers 2 Hybrids	38	39	9.5 (21)	9.1 (20)
Circulators	10		4.5 (10)	2.7 ( 6)
TOTAL			59 (130)	
* includes 20 per cent margin				

Based on the coverage described in paragraph 4.3.1, the layout of the ATS-AMS III feed cluster has been calculated assuming a beam deviation factor of 0.90, which corresponds to an effective  $f/D$  of 0.45 for a full reflector, or approximately 0.90 for the offset sector. The center of each feed was computed vectorially with reference to the boresight vector of the reflector, which involves transformation from an earth-centered spherical coordinate system to a rectangular coordinate system at the focal point of the reflector.

Large Reflector

During the initial stage of the program, a decision was made to use a Cassegrain reflector system for two reasons: to obtain a more compact package and to achieve a compromise on aperture blockage. Because of the scan characteristics desired, a long focal length was anticipated. The Cassegrain technique allows folding of optics and thereby provides a compact reflector system. Although the subreflector produces aperture blockage itself, it was felt that the blockage may not be as much as that produced by the anticipated feed and switching matrix.

The most convenient analysis of a Cassegrain system is provided by the concept of an equivalent parabola.<sup>1</sup> As shown in Figure 5.3.7-1 the combination of main reflector and subreflector is considered as being replaced by an equivalent parabola with focal length,  $f_e$ . The following equations provide the relationship between the equivalent parabola and the antenna parameters shown in Figure 5.3.7-1.

$$\tan 1/2 \phi_r = 1/4 \frac{D_m}{f_e}, \quad (1)$$

$$\tan 1/2 \phi_v = 1/4 \frac{D_m}{f_e}, \quad (2)$$

$$\frac{f_e}{f_m} = \frac{\tan 1/2 \phi_v}{\tan 1/2 \phi_r} = \frac{L_r}{L_v} = \frac{e+1}{e-1}, \quad (3)$$

$$2 \frac{f_c}{D_s} = \frac{1}{\tan \phi_v} + \frac{1}{\tan \phi_r}, \quad (4)$$

1. P.W. Hannon, "Microwave Antennas Derived from the Cassegrain Telescope", IRE Trans. on Antennas and Propagation, pp. 140-153, March 1961

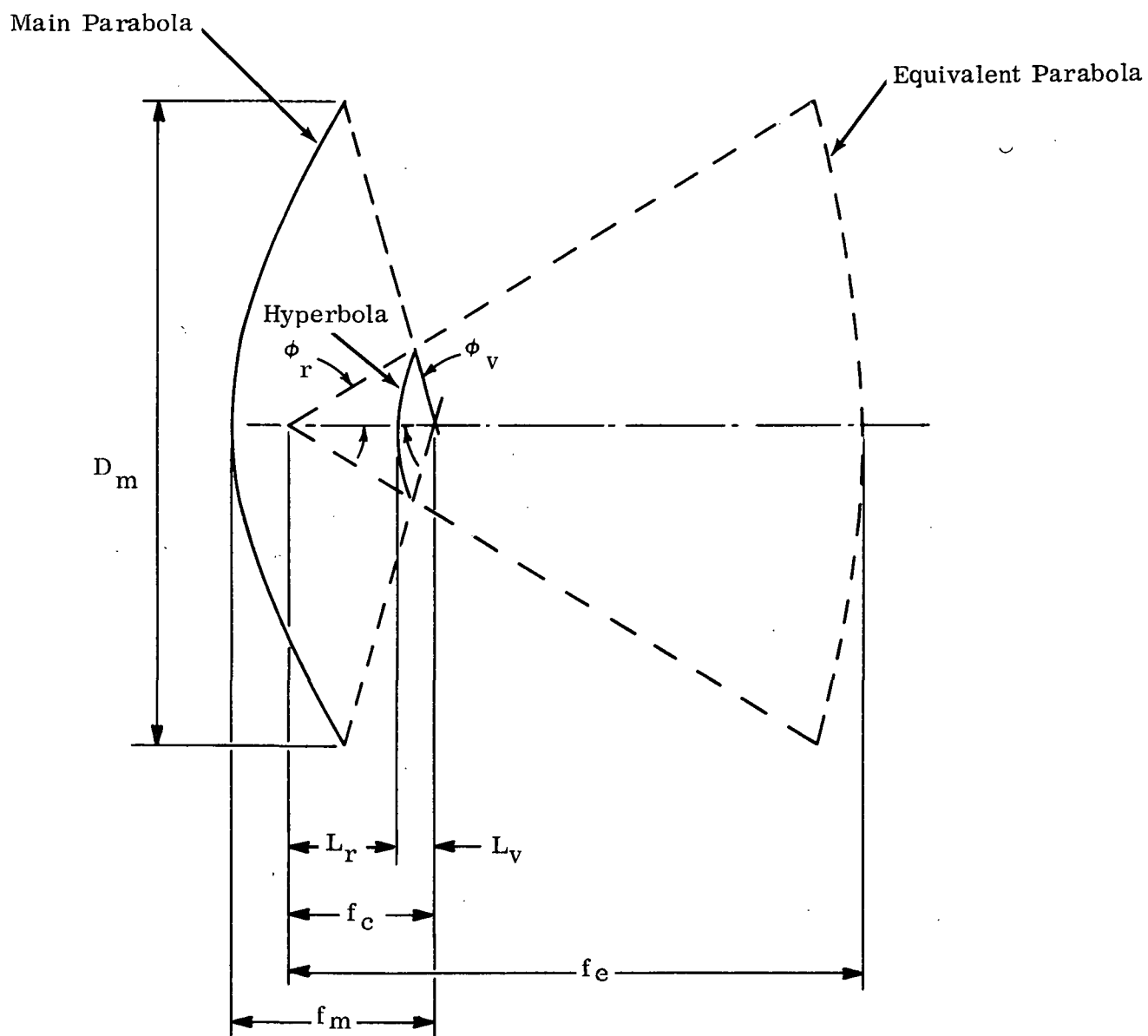


Figure 5.3.7-1. Cassegrain Reflector Geometry

$$2 \frac{L_v}{f_c} = 1 - \frac{\sin 1/2 (\phi_v - \phi_r)}{\sin 1/2 (\phi_v + \phi_r)} \quad (5)$$

The contour of the main reflector is given by

$$X_m = \frac{Y_m^2}{4f_m} \quad (6)$$

The contour of the subreflector is given by

$$X_s = a \left[ \sqrt{1 + \left( \frac{Y_s}{b} \right)^2} - 1 \right] \quad (7)$$

where

$$e = \frac{\sin 1/2 (\phi_v + \phi_r)}{\sin 1/2 (\phi_v - \phi_r)}$$

$$a = \frac{f_c}{2e}, \quad b = a \sqrt{e^2 - 1}$$

The quantities,  $e$ ,  $a$ , and  $b$  are the parameters of the hyperbola:  $e$  is eccentricity,  $a$  is half the transverse axis, and  $b$  is half the conjugate axis. The contour of the equivalent parabola is given by

$$X_e = \frac{Y^2}{4f_e} \quad (8)$$

For simplicity, only the equivalent parabola is shown in Figure 5.3.7-2 along with two feeds, representating the feed cluster for the large reflector. The feed cluster arrangement is shown in Figure 5.3.7-3 as a direct view of the individual radiating apertures. The aperture sizes and spacings in the focal plane (X-Y) are indicated by  $W$  and  $d$  respectively. The orientation of the shaped reflector is indicated by 244 cm and 122 cm dimensions shown along the Y and X axes respectively.

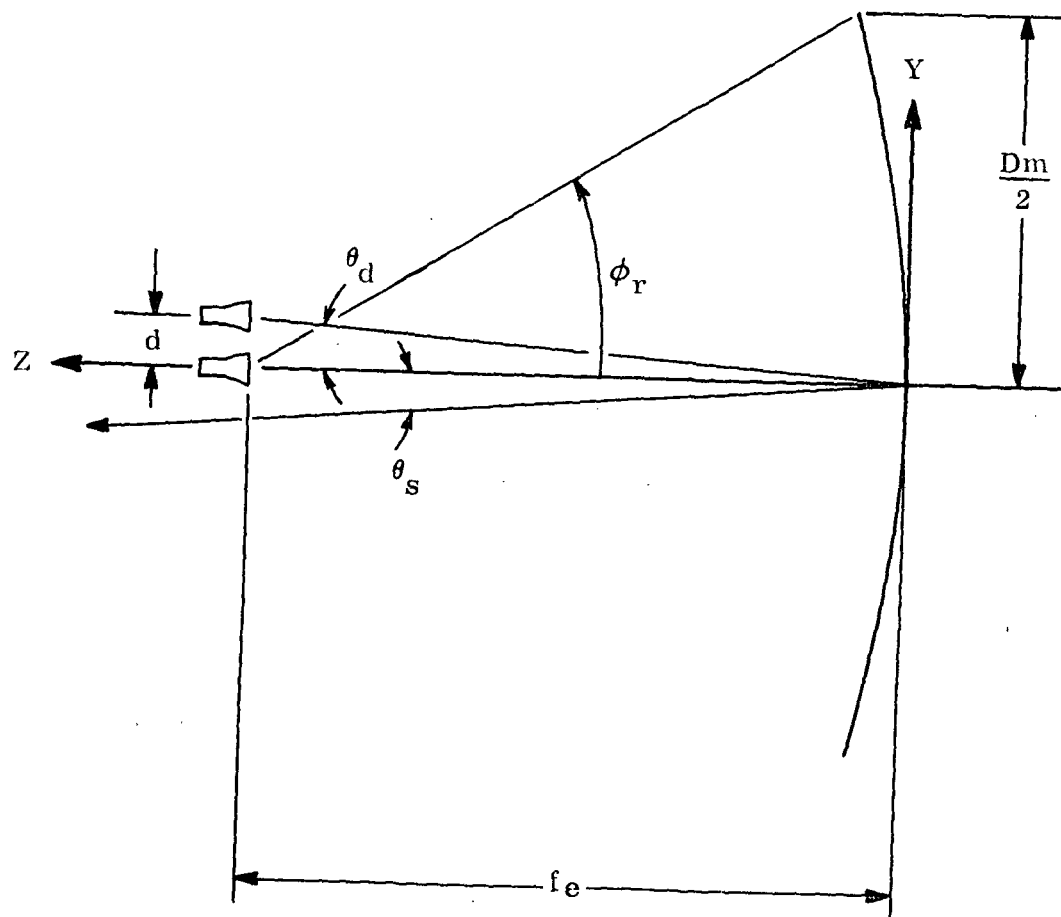


Figure 5.3.7-2. Equivalent Parabola

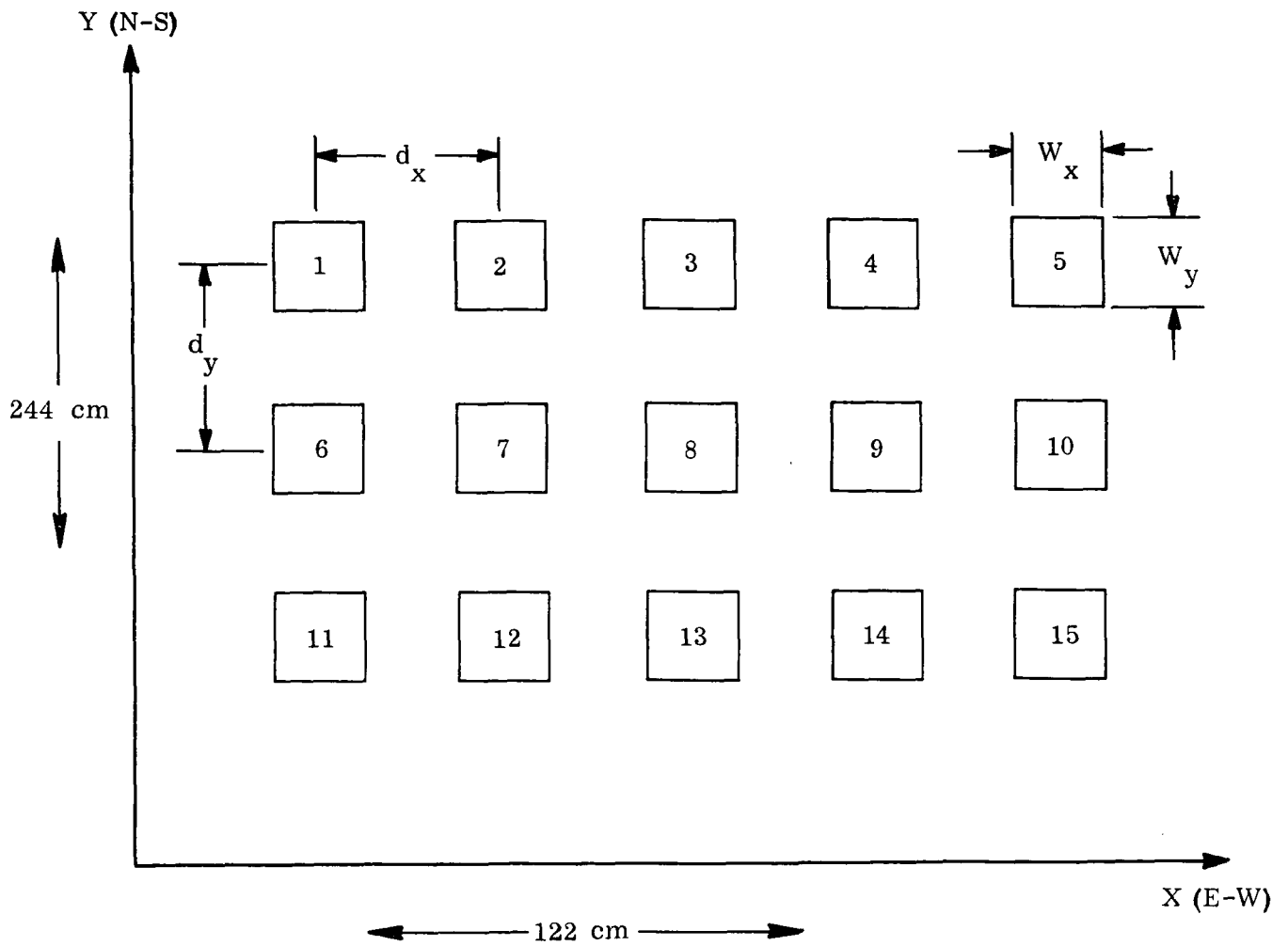


Figure 5.3.7-3. Large Reflector Feed Cluster

Initially an aperture illumination is assumed that produces a beam with half power width of  $0.75^\circ$  in the Y-Z plane and  $1.5^\circ$  in the X-Z plane. This assumption is most applicable for the center feed which is at the focal point and forms a beam on the axis of the parabola. The other feeds form beams which are scanned off axis by an amount proportioned to the feed displacement. A communication link to any spot inside the CONUS is effected by selecting the appropriate beam. Beam formation in the E-W direction is thus assumed to be represented by 5 beams, each of which has a  $1.5^\circ$  beamwidth. The cross over level is -3 dB. Thus the scan angle,  $\theta_s$ , is a multiple of the beamwidth. With the middle beam at the center of the CONUS, complete E-W coverage is obtained by selecting any one of the five beams. The total coverage obtainable from one extreme edge to the other extreme edge is thus  $7.5^\circ$ . Beam formation in the N-S direction is assumed to be represented by 3 beams, each of which have a  $0.75^\circ$  beamwidth and the crossover level is -3 dB. The scan angle in this plane is  $\pm 0.75^\circ$ . Here the total coverage obtainable from edge to edge is  $2.25^\circ$ . Since the included angle subtended by the north and south boundaries of the CONUS is approximately  $3^\circ$ , this edge to edge coverage is lacking from the total desired by  $0.75^\circ$ ; however, this situation can be improved by adding another row of feeds or by increasing the scan angle slightly which places the cross over level further down on the antenna pattern.

The scan angle,  $\theta_s$ , measured from the axis of the reflector, is proportional to the feed displacement angle,  $\theta_d$ . The proportionality factor is called the Beam Deviation Factor and is dependent on the  $f/D$  ratio of the reflector. With reference to geometry of Figure 5.3.7-2.

$$\tan \theta_d = \frac{d}{f_e} ;$$



however, assuming a BDF of unity,

$$\tan \theta_s = \frac{d}{f_e}$$

and the focal length,  $f_e$  is determined by  $\theta_s$  and the feed displacement,  $d$ . From the  $f/D$  ratio, the angle  $\phi_r$  can be obtained which determines the radiation requirements of the feed for a given edge illumination. While large  $f/D$  ratios result in reflectors with good scan characteristics, they also result in reflectors which require highly directive feeds to achieve a low edge illumination and correspondingly low sidelobes.

The smallest required focal length will be obtained when the feed displacement distance is equal to the width of the feed horn aperture, i.e. when the edges of the feed horns are touching each other. Since the small scan angles in the N-S plane will require the longest focal length, they will be used to determine the required geometry. Therefore, the design procedure is as follows :

- Assume a feed aperture dimension
- Calculate the required focal length for a given scan angle and the assumed displacement distance
- Calculate the angle  $\phi$  from the reflector geometry
- Estimate the radiation pattern of the feed for both uniform and tapered aperture excitation
- From the feed radiation pattern and the angle  $\phi$ , estimate the edge illumination of the reflector
- Estimate the reflector radiation pattern with respect to beam-width and side lobe level
- Estimate the crossover level for the beams

In order to obtain moderate directivity at 12 GHz, a feed aperture of 3 cm is assumed. For a scan angle of  $0.75^\circ$  in the N-S plane and assuming a Beam Deviation Factor of unity, a focal length of 230 cm

is required. In this plane, the reflector aperture is 244 cm; therefore, the  $f/D$  ratio is almost unity, which justifies the BDF assumption, and the angle  $\phi$  is  $28^\circ$ . Since the reflector dimension in the orthogonal plane (E-W plane) is only 122 cm, the  $f/D$  ratio is almost 2.0 and the angle  $\phi$  is about  $14^\circ$ . The allowable feed displacement in this plane is about 6 cm for a scan angle of  $1.5^\circ$ . Thus, the feed aperture can be twice as large in this plane, however, this increased aperture is necessary, since the angle subtended by the reflector,  $14^\circ$ , is half as much in this plane.

The feed horn can thus have an aperture that is 3 cm by 6 cm. When the flare angle is small, a simple waveguide fed horn is characterized by uniform amplitude distribution in the E-plane and sinusoidal distribution in the H-plane. Taking into account the space attenuation factor and the radiation at an angle of  $28^\circ$  from the axis of a 3 cm linear aperture, the edge illumination of the parabola in the N-S plane is estimated at -5.8 dB for uniform excitation of the 3 cm aperture and -3.2 dB for cosine excitation. Conversely, the edge illumination of the parabola in the E-W plane for an angle of  $14^\circ$  from the axis of a 6 cm aperture is estimated at -3.8 dB for cosine excitation of the 6 cm aperture and -7 dB for uniform excitation. Choosing uniform excitation for one plane dictates the cosine excitation for the other plane. Since this produces an edge illumination as high as -3 dB, this is not a good design. Consequently other reflector geometries were considered and the results are summarized in Table 5.3.7-1. As the reflector becomes deeper (small  $f_e/D$  ratio), the sidelobe performance improves; however, the scan angle increases and beam crossover occurs at a lower level on the radiation pattern. For example with  $f_e/D$  of 0.6, the radiation at the crossover point is 9 dB down from maximum. A good compromise is obtained when the equivalent focal length is 171 cm (67 in). This value was used as a basis for the design of the Cassegrain system.

Table 5.3.7-1. ATS-AMS I and II Large Reflector Design Summary

Parameter	Value					
	D (cm)	244			122	
$f_e/D$	0.8	0.7	0.6	1.6	1.4	1.2
$f_e$ (cm)	195	171	146	195	171	146
$\phi_r$ (deg)	34.7	39.4	45	17.8	20.2	23.6
$\phi_d$ (deg)	0.895	1.02	1.19	1.5	1.5	1.5
$\phi_s$ (deg)	0.868	0.98	1.12	1.5	1.5	1.5
d (cm)	3.0	3.0	3.0	5.14	4.47	3.86
Edge Taper (in dB for uniform)	-9.4	-12.8	-17.4	-7.1	-7.2	-7.3
Edge Taper (in dB for cosine)	-5.3	-6.8	- 8.2	-3.9	-4.0	-4.1
Sidelobe level (dB)	-21	-22	-23	-22	-22	-22
Beamwidth (deg)	0.64	0.65	0.66	1.3	1.3	1.31
Crossover level (dB)	-5.2	-6.4	-9.0	-3.9	-3.9	-3.9
Edge to Edge Coverage (deg)	2.4	2.6	2.9	7.3	7.3	7.31

The subreflector causes aperture blockage; however, so does the feed horn matrix. A minimum blocking condition is obtained by means of the following relationship:

$$\frac{f_e}{f_m} \approx \frac{D_f}{D_s} \quad (9)$$

where  $D_s$  is the physical or blocking diameter of the subreflector and  $D_f$  is the physical or blocking diameter of the feed aperture. Using this relationship, the previous equations, the equivalent focal length of 171 cm (67 in) and choosing an  $f_m/D_m$  of 0.35 for the main reflector for compact packaging, the Cassegrain reflector system shown in Figure 5.3.7-4 is obtained.

#### 5.3.7.2

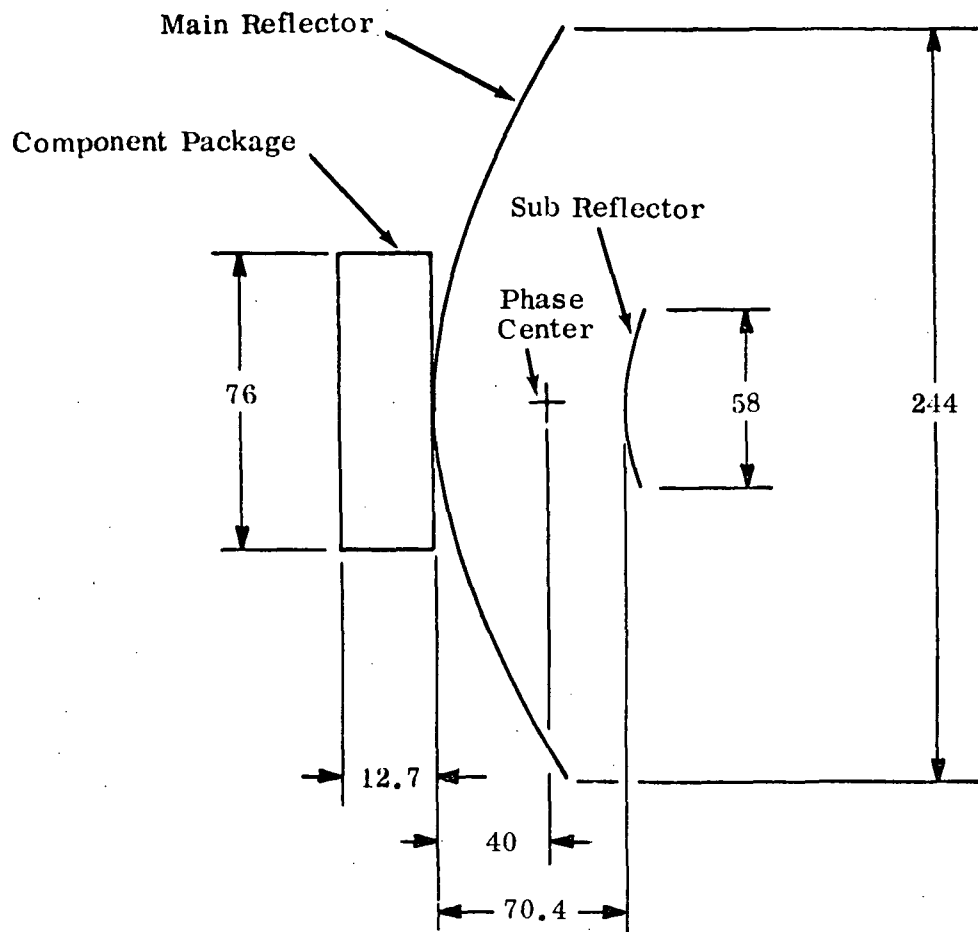
##### Small Reflector

The size of the small reflector does not create an installation problem on the spacecraft. Space is available within the shroud volume for installation of this antenna; however, the feed, the waveguide runs, and the beam forming and selection matrix create an aperture blockage problem. Therefore the decision has been made to obtain a compromise on the aperture blockage by using a Cassegrain reflector system for this antenna also.

A similar design procedure as that described for the large reflector is used, involving the use of the equivalent parabola for analysis.

The feed horn cluster as viewed in the focal plane is shown in Figure 5.3.7-5. The initial assumption is that this cluster will form a beam such that the N-S beamwidth is  $5.0^\circ$  and the E-W beamwidth is  $7.5^\circ$ .

The CONUS beam in the N-S direction is formed by adding pairs of feed horns (such as 1 & 4). It is estimated that two beams which are scanned approximately  $\pm 1.7$  degrees from the axis will produce a single beam of approximately 5 degrees when added together. Again



Dimensions in cm

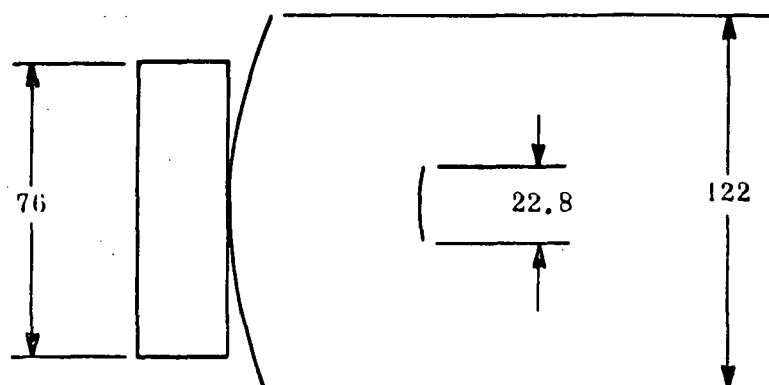


Figure 5.3.7-4. Large Antenna Dimensions

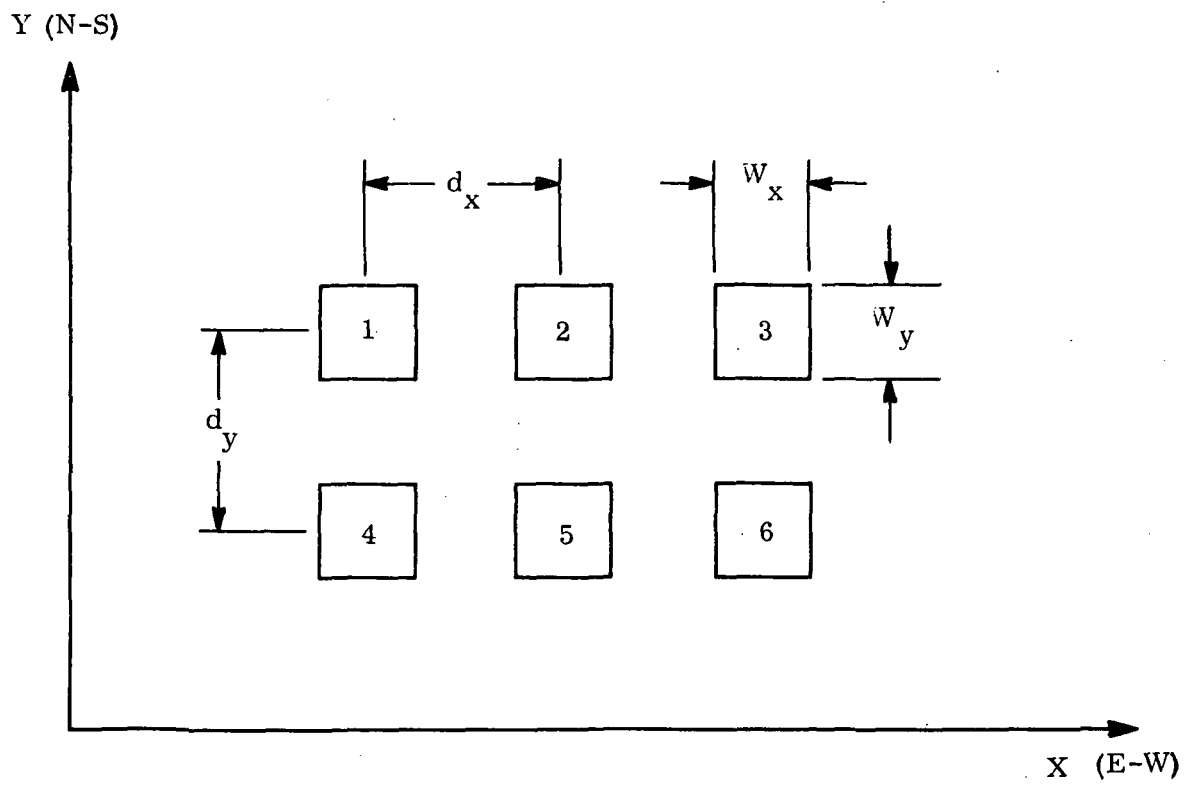


Figure 5.3.7-5. ATS-AMS I & II Small Reflector Feed Cluster

assuming a horn aperture of 3 cm, this scan angle requires a focal length of 50.8 cm, and an  $f_e/D$  ratio of 0.67 for the 76.2 cm (30 in) reflector. Thus the peak to peak angular beam separation will be 3.4 degrees, and the angle  $\phi$  of the equivalent parabola will be 41.1 degrees.

The CONUS beam in the E-W direction is formed by adding the three pairs of feed horns. With a horn aperture of 3 cm in this plane and a focal length of 50.8 cm, (20 in) the peak-to-peak angular separation of the beams will also be 3.4 degrees. It is estimated that three beams scanned at this separation will produce a beam of approximately 7.5 degrees when added together.

The 3 cm x 3 cm horn is used as a basis for design. The assumption is a cosine excitation of the horn aperture in the N-S plane and a uniform excitation in the E-W plane. From the geometry of the equivalent parabola and the radiation patterns of the assumed excitations, it is estimated that the reflector illumination at the edge will be -7.2 dB in the N-S plane and -14.4 dB in the E-W plane. For a single feed, it is estimated that this illumination will produce a beam with half power width of  $2.1^\circ$  in the N-S plane with -22 dB sidelobes and half power width of  $2.25^\circ$  in the E-W plane with -25 dB sidelobes. This beam will be used as the regional beam. By combining two of these beams it is estimated that the resultant beam will have a beamwidth of  $4.2^\circ$  in the N-S plane and  $7.5^\circ$  in the E-W plane. These results are listed in Table 5.3.7-2 for operation at 12 GHz.

Although the beamwidth is somewhat narrower in general than that initially predicted, it is felt the typical performance shown in Table 5.3.7-2 will be satisfactory for the intended application. Using an equivalent focal length of 50.8 cm (20 in) an  $f_m/D_m$  ratio of 0.3 for the main reflector, and equation [1] through [9], the Cassegrain reflector system shown in Figure 5.3.7-6 is obtained.

Table 5.3.7-2. Beam Formation Summary

Beam Location	Beam Size (in deg.)	Feed(s) Excited
Center (CONUS)	7.5 x 4.2	all six
left (western time zone)	2.25 x 4.2	1 & 4
center (center time zone)	2.25 x 4.2	2 & 5
right (eastern time zone)	2.25 x 4.2	3 & 6
upper left	2.25 x 2.1	1
lower left	2.25 x 2.1	4
upper center	2.25 x 2.1	2
lower center	2.25 x 2.1	5
upper right	2.25 x 2.1	3
lower right	2.25 x 2.1	6



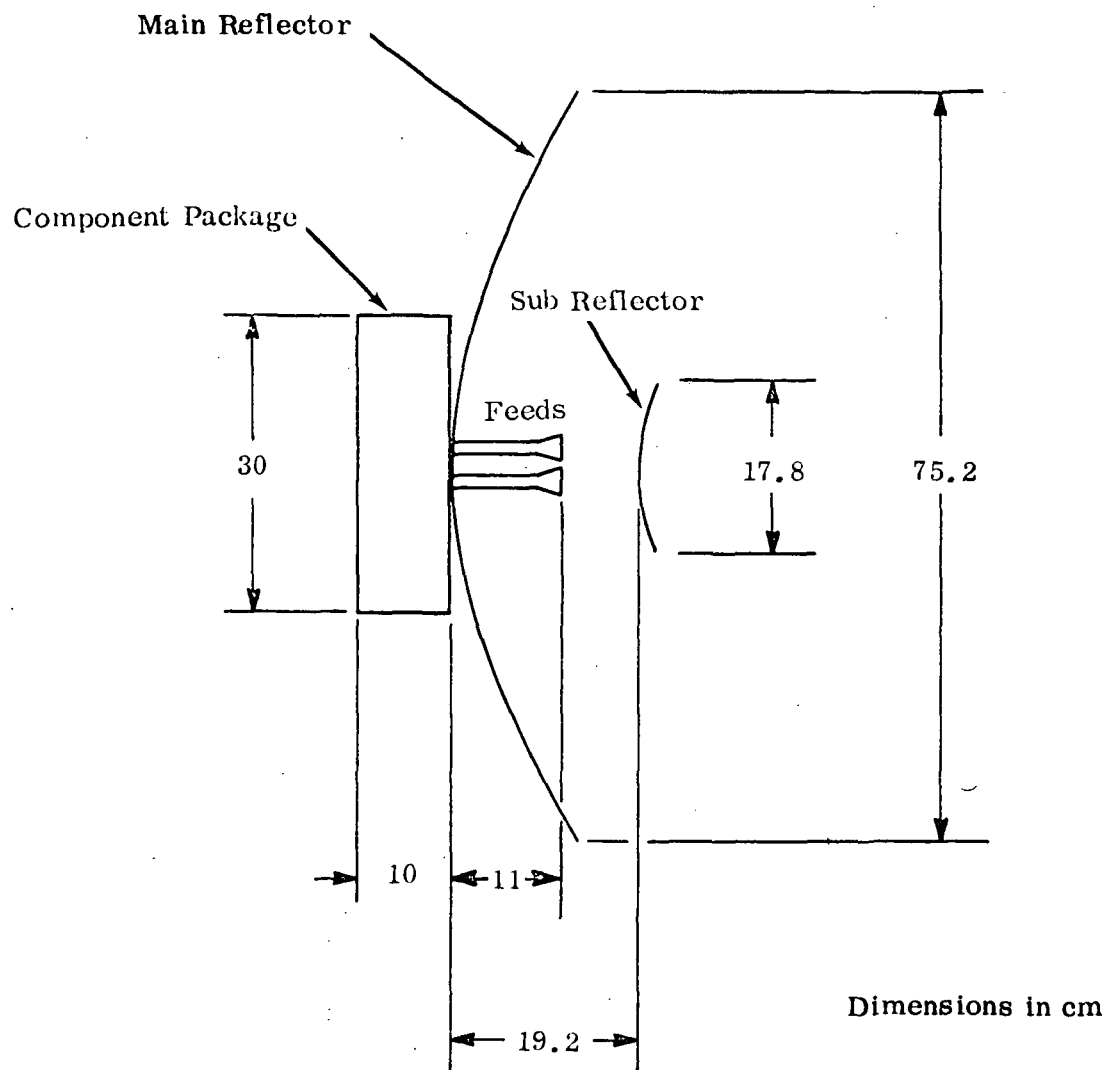


Figure 5.3.7-6. Small Antenna Dimensions

### 5.3.8 AMS I AND II SWITCHING MATRICES

#### 5.3.8.1 Small Reflector

The beam forming and beam selection matrix for the small reflector is shown schematically in Figure 5.3.8-1. With reference to the figure, the first SPDT switch at the input allows selection between the  $7.5^\circ \times 4.2^\circ$  CONUS beam and either a  $2.25^\circ \times 4.2^\circ$  time zone beam or  $2.25^\circ \times 2.1^\circ$  regional beam, depending on the state of the other switches. Beam formation is reviewed briefly in the following paragraphs.

The six feeds shown in Figure 5.3.8-1 may be energized individually, in pairs, or all six at once. Each feed pair utilizes a set of three SPDT switches. The pair of SPDT switches connected directly to a pair of feeds are used to connect the feeds either to the arms of a hybrid junction or to the ports of the third SPDT switch. When connected to the hybrid, the two feeds are fed in parallel (thereby forming a two element array with higher directivity) and the  $2.25^\circ \times 4.2^\circ$  time zone beam is obtained. Three such beams may be formed - left, right, and center. When the two feeds are connected to the third SPDT switch (switch C), this switch is used to select either one of the two  $2.1^\circ \times 2.25^\circ$  regional beams which are generated by each feed.

Left, right, and center beam positions are selected by the SPDT switch at the input, while up or down beam positions (in the case of regional beams) are selected by switch C. Selection of either the  $2.25^\circ \times 4.2^\circ$  time zone beam or  $2.1^\circ \times 2.25^\circ$  regional beam is provided by the transfer switches.

With the switch positions shown in Figure 5.3.8-1 feed pairs are summed to form three  $2.25^\circ \times 4.2^\circ$  beams. The transfer switches are set to sum these three beams through the hybrid junction, 4.8 dB coupler, and phase shifter combination. Thus, a  $7.5^\circ \times 4.2^\circ$  beam is obtained and selected by the input SPDT switch. The estimated insertion loss is 1.45 dB for the formation of the  $7.5^\circ \times 4.2^\circ$  CONUS beam, 1.1 dB for the formation

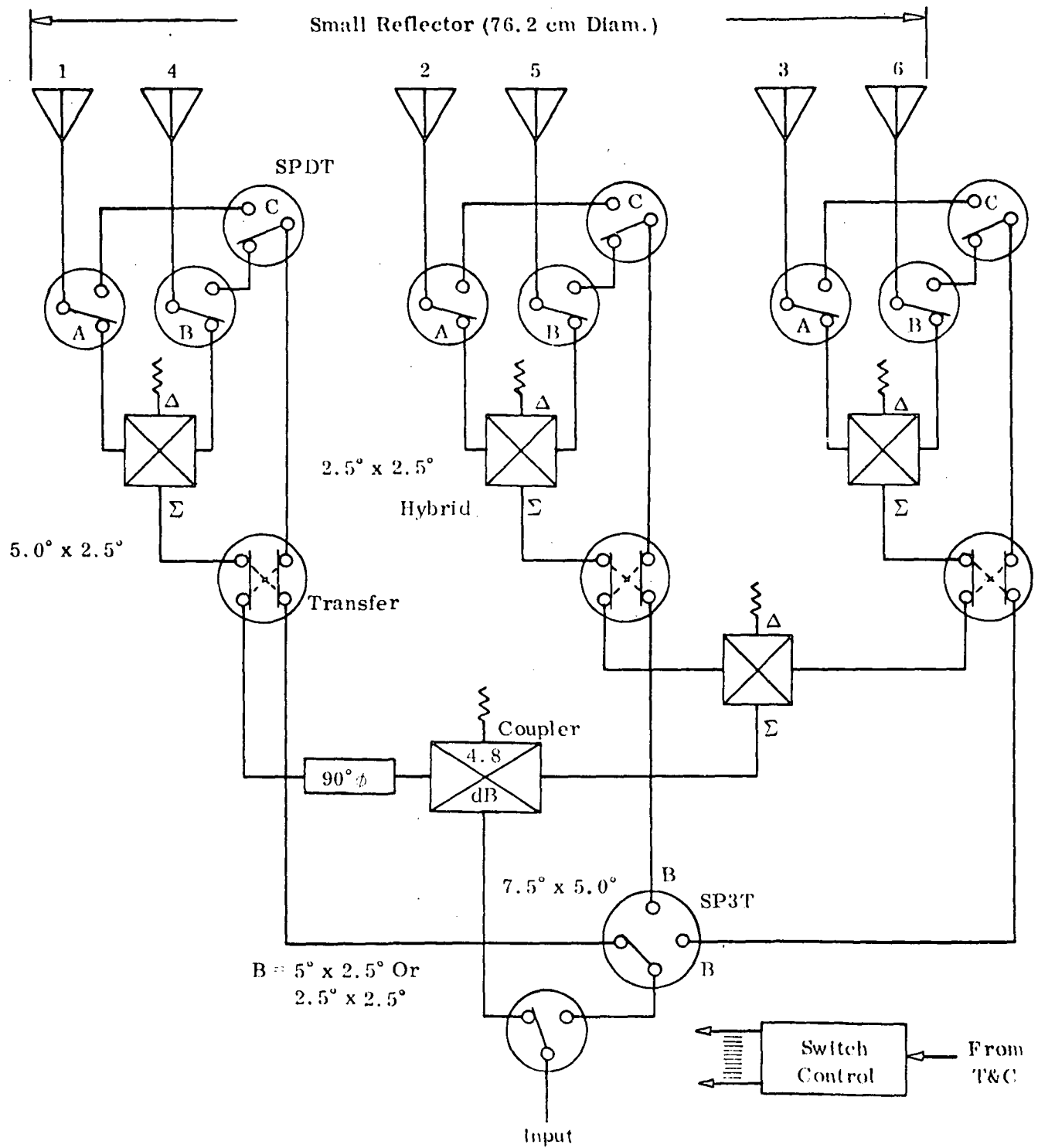


Figure 5.3.8-1. Small Reflector Beam Forming Matrix

of the  $2.25^\circ \times 4.20^\circ$  time zone beam, and 0.9 dB for the formation of the  $2.1^\circ \times 2.25^\circ$  regional beam. The cross over level in the E-W plane is estimated at -4 dB.

#### 5.3.8.2 Large Reflector

The matrix switching problem has been examined in order to isolate the problems of using waveguide switches and to develop alternate configurations. The problem as it presented itself was to develop a matrix able to receive on any four of fifteen beams and transmit on any four of the fifteen beams. All possible combinations and permutations of transmit and receive beams being allowable.

##### 5.3.8.2.1 Waveguide Switches

The first approach considered is the use of high power waveguide switches. A portion of a system using this approach is shown in Figure 5.3.8-2. The total system would be Figure 5.3.8-2 repeated three times for the transmit portion and three more times for the receive portion. Table 5.3.8-1 is a hardware list with a weight estimate for a system offering full flexibility in the transmit mode. Table 5.3.8-2 shows that same estimate for a system offering full flexibility in both transmit and receive modes. Examination of Table 5.3.8-2 shows that a weight problem exists whenever waveguide switches are used to generate the required matrix. The waveguide switches however have the definite advantage of providing a very low insertion loss (approximately 0.9 dB). In order to resolve the weight problem several alternatives have been considered.

##### 5.3.8.2.2 Alternate Configurations

No satisfactory alternate configurations could be found which could provide full flexibility in the transmit mode. The requirements that the transmit switching matrix be able to handle large powers (as high as 2 Kw) imposes the use of high power waveguide switches with their inherent weight characteristics.

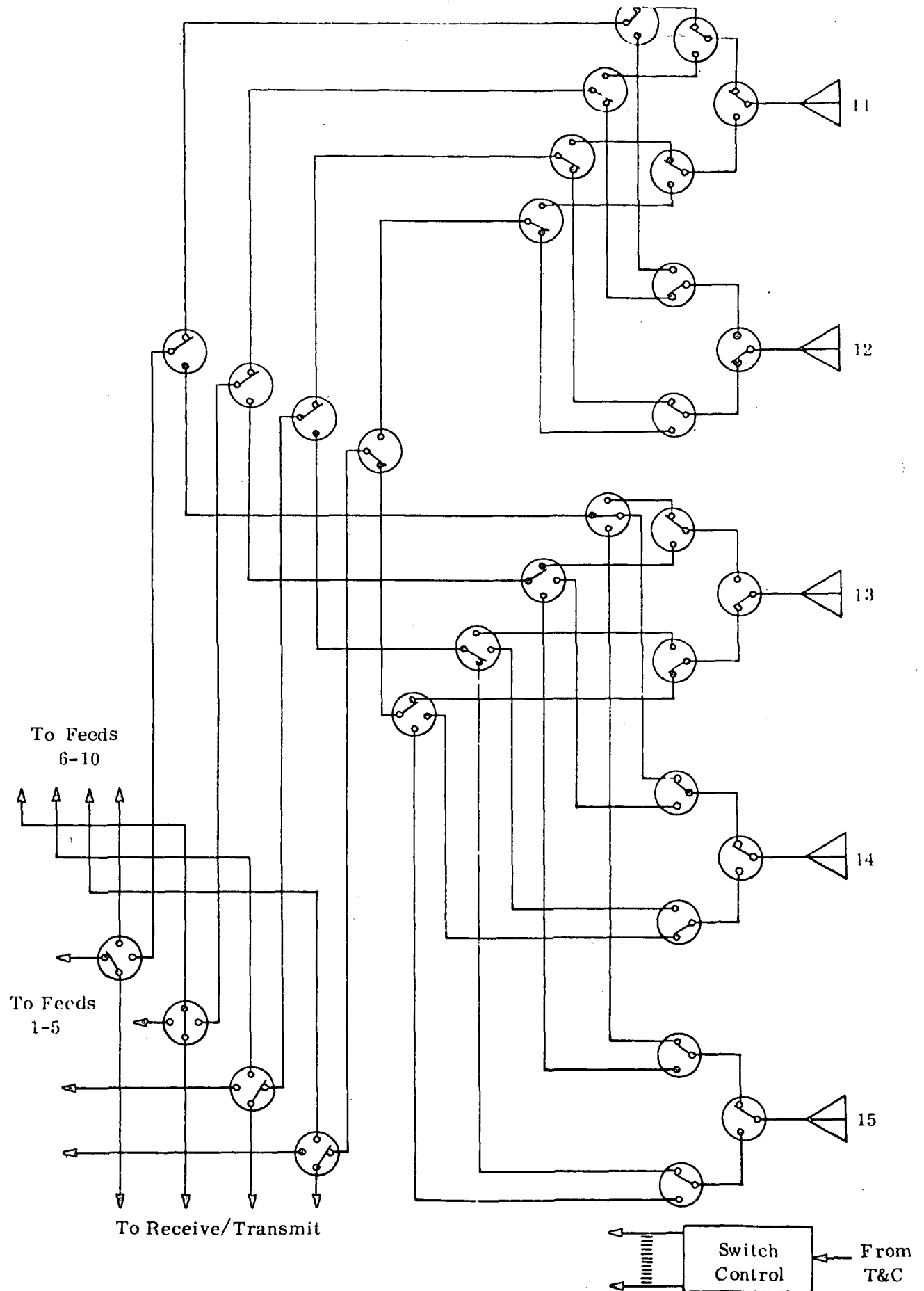


Figure 5.3.8-2. Spot Beam Switching Matrix

Table 5.3.8-1. Transmit Hardware Weight Characteristics

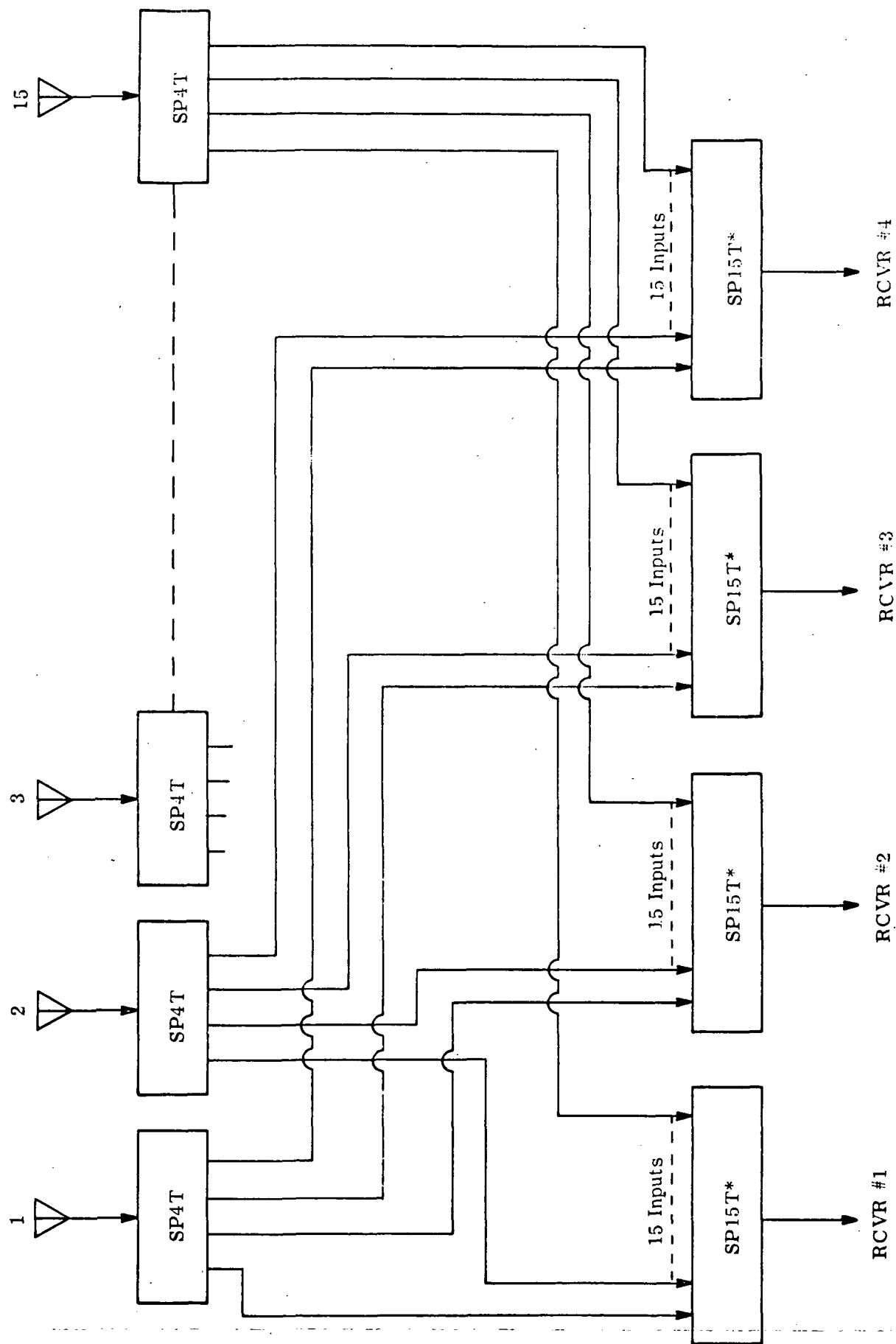
Item	Qty. Req.	Weight Per Unit kg (lb)	Total Weight kg (lb)
Single pole 3 Throw Switch	16	1 (2.2)	16 (35.2)
Single pole 2 Throw Switch	69	.454 (1)	31.4 (69)
Waveguide	39.5 m	.41 kg/m	16.2 (35.6)
Total			63.6 (140)

Table 5.3.8-2. Transmit and Receive Hardware Weight Characteristics

Item	Qty. Req.	Weight Per Unit kg (lb)	Total Weight kg (lb)
Single pole 3 Throw Switch	32	1 (2.2)	32 (70.4)
Single pole 2 Throw Switch	138	.454 (1)	62.8 (138)
Waveguide	79 m	.41 kg/m	32.4 (71.2)
Total			127.2 (280)

The receive switching matrix, not being required to handle large amounts of power, offers several alternatives. These various alternatives outlined below provide the full flexibility of being able to receive from any four of the fifteen beams.

- 5.3.8.2.2.1 Solid State Switches - The use of solid state coaxial switches to reduce the weight of the receive switching matrix has been considered. The configuration of a typical matrix using solid state switches is shown in Figure 5.3.8-3. Various manufacturers have been consulted with the results that the best which could be expected is about 8 db insertion loss with a weight of approximately six kilograms. Compared with the sixty four kilograms which the waveguide switch receive matrix would weigh, this represents a considerable weight reduction. However, the 8 db insertion loss of the solid state switches is too high to be practical.
- 5.3.8.2.2.2 Coaxial Solenoid Switches - The use of coaxial solenoid switches was also considered. These represent a compromise between the heavy waveguide switches with their very low insertion losses and the solid state coaxial switches which are much lighter but which have excessive insertion losses. The basic configuration for a switching matrix utilizing coaxial solenoid switches is the same as that of the solid state switches shown in Figure 5.3.8-3. It was estimated that the switching matrix would weigh approximately 23 kilograms (50 lb) and would have about 3.5 dB insertion loss. The weight is about one third that of the waveguide switches and four times that of the solid state switches. The insertion loss is approximately half way between the waveguide switches and the solid state switches.
- 5.3.8.2.2.3 Separate Front Ends - While the coaxial switching techniques described in the preceding two sections are appealing from the viewpoint of versatility and lightweight, they both suffer from the disadvantage of increasing the noise figure of the receiver. The effects of the insertion loss due to switching can be minimized by using separate front ends for each of the feed horns and performing the switching at IF as shown in Figure 5.3.8-4.



\*NOTE: SP15T switch is made up of 3 SP5T switches cascaded with one SP3T switch.

Figure 5.3.8-3. Solid State Switches Matrix Configuration



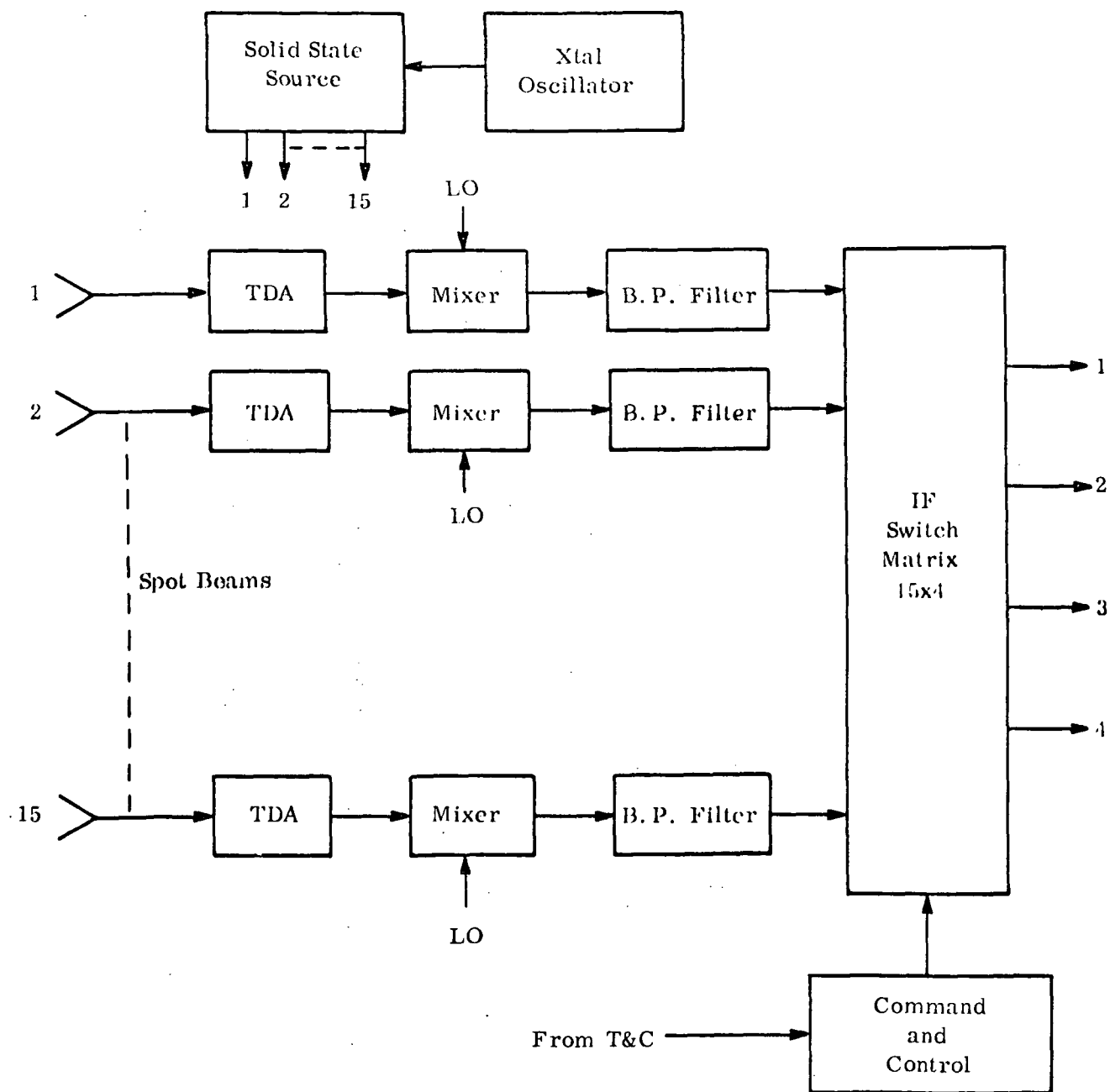


Figure 5.3.8-4. Alternate Transponder Front End

Defining insertion loss here as that measured between a feed and a TDA, the insertion loss using this approach is at most 0.1 db. The estimated weight from the TDA input to the switch matrix output (assuming no redundancy for the TDA's) is 17 Kg. (37.4 lbs).

#### 5.3.8.3

#### Summary and Recommendations

Table 5.3.8-3 shows the weight and insertion loss characteristics of all the configurations considered. In order to compare all the systems on the same basis, the weight of the front ends required were added to the matrix weights. Systems number 1, 2 and 3 require the same front end weighing 3.6 kg. The weight breakdown for these systems is shown in Table 5.3.8-4. On system # 4, the multiple front ends add up to 17.0 Kg. (37.4 lb). The weight breakdown for that system is shown in Table 5.3.8-5. When compared on the basis of weight and insertion loss characteristics, system # 4 with the separate front ends stands out as the best for the AMS I and II requirements.

From the previous analysis, it is readily apparent that a considerable weight penalty has to be paid for having the flexibility of being able to transmit and receive on any four of fifteen beams, transmit and receive channels being totally independent. For the receive portion of the system this penalty has been reduced to an acceptable level by the use of separate front ends and by performing the switching at I. F. For the transmit portion of the system, the high power levels which must be handled do not allow the use of light weight coaxial switching devices. Therefore, some type of waveguide switch must be used. The problem here is that the weight of a waveguide switch matrix is intolerable and some compromise must be reached which still maintains some of the system's flexibility while keeping the overall weight at an acceptable level.

One approach which would satisfy these constraints is shown in Figure 5.3.8-5. In the transmit mode, the feeds are divided into four areas A-B-C-D with the beams being divided on a 4-4-4-3 basis. Each of the four areas is allocated one of the four channels with the limitation that

Table 5.3.8-3. System Comparison Table

NO.	SYSTEM	(1) TRANSMIT MATRIX WEIGHT kg (lb)	(2) RECEIVE MATRIX WEIGHT kg (lb)	(3) RECEIVE MATRIX PLUS FRONT END WEIGHT kg (lb)	TOTAL WEIGHT 1 + 3 kg (lb)	RECEIVE INSERTION LOSS (dB)	TRANSMIT INSERTION LOSS (dB)
1	Waveguide Switches	64 (141)	64 (141)	67.6 (149)	131.6 (290)	0.9	0.9
2	Waveguide Switches (Trans.) Solid State Switches (Rec.)	64 (141)	6 (13.2)	9.6 ( 21)	73.6 (162)	8.0	0.9
3	Waveguide Switches (Trans.) Coax Sole- noid Switches Rec.)	64 (141)	21 (46.2)	24.6 ( 54)	88.6 (195)	3.5	0.9
4	Waveguide Switches (Trans) Separate Front Ends (Rec.)	64 (141)	6 (13.2)	17 ( 37.4)	81 (178)	0.1	0.9
5	Limited Transmit Matrix	7.8 (17)	-	-	-	-	0.3

Table 5.3.8-4. Weight Breakdown for System 1, 2 and 3 Front End

NO	ITEM	QUANTITY	PER UNIT WEIGHT kg (lb)	TOTAL kg (lb)
1	Isolator	4	0.20 (.44)	0.8 (1.76)
2	Combiner	1	0.4 (.88)	0.4 (.88)
3	Filter	1	1.0 (2.2)	1.0 (2.2)
4	TDA	2	0.25 (.55)	0.5 (1.1)
5	Mixer	1	0.25 (.55)	0.25 (.55)
6	Filter	1	0.25 (.55)	0.25 (.55)
7	Multicoupler	1	0.4 (.88)	0.4 (.88)
			TOTAL WEIGHT	3.6 kg (7.9 lb)

Table 5.3.8-5. Weight Breakdown for System 4 Front End

No	ITEM	QUANTITY	PER UNIT WEIGHT kg (lb)	TOTAL kg (lb)
1	TDA	15	0.25 (.55)	3.75 (8.25)
2	Mixer	15	0.25 (.55)	3.75 (8.25)
3	Filter	15	0.25 (.55)	3.75 (8.25)
4	IF Switches	15	5.75 (12.65)	5.75 (12.65)
			TOTAL WEIGHT	17.0 kg (37.4 lb)

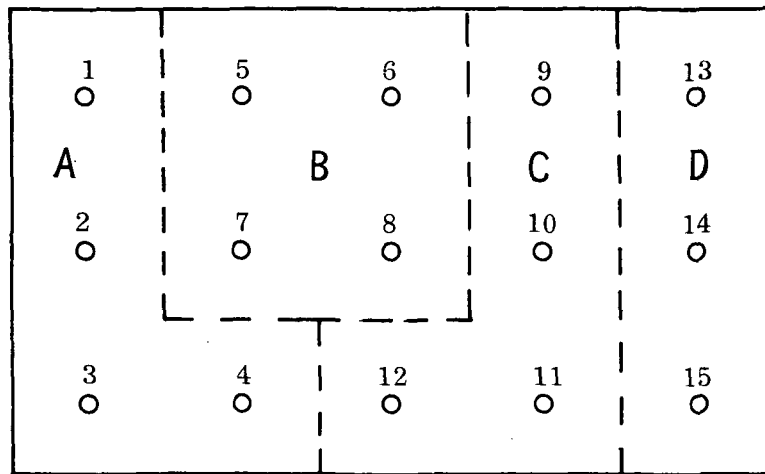


Figure 5.3.8-5. Beam Assignment

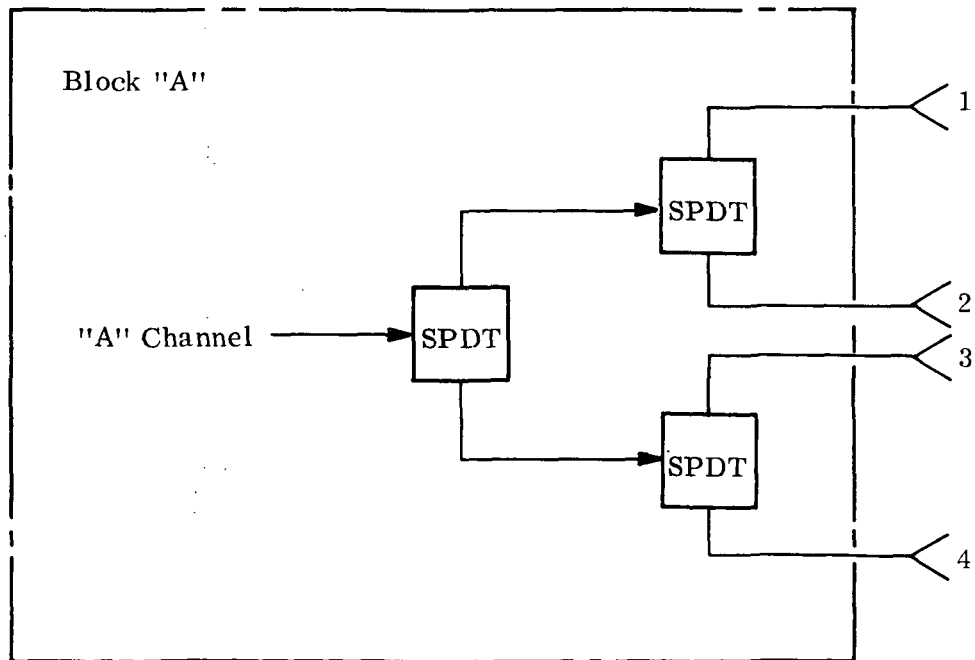


Figure 5.3.8-6. Channel Routing

only one channel be transmitting to a given area at any one time. For such an arrangement, as shown in Figure 5.3.8-6 only 3 SPDT switches are needed to route the A channel to its appropriate feed. For the entire 15 beam switching matrix, a total of only 12 SPDT switches will be required. The characteristics of this switching matrix is shown as system 5 in Table 5.3.8-3.

It is felt that the combination of separate front ends for receive and the limited matrix described above for transmit represents the best configuration for this system and as such is recommended for the AMS I and II satellite.

The spaceborne communications transponder configurations described in Section 4.4 have been designed to demonstrate the capability of high power TWT and Klystron amplifiers in conjunction with a beam forming antenna feed matrix to retransmit acceptable quality video, voice and data to a variety of widely dispersed network and community ground stations under diverse weather environments. To achieve this capability, projections are required of the future performance of components and sub assemblies making up the transponder assembly.

## 5.4.1

## TRANSPONDER CONFIGURATION - ATS-AMS-III

Since the video and voice/data messages to be relayed will not require signal processing in the satellite (such as for modulation conversion or reduction to baseband in a demodulator-modulator repeater) a simple linear repeater is proposed for the transponder configuration. The linear repeater accepts frequency modulated carriers from the ground stations, translates the carrier frequency and retransmits the signal. Translation of frequencies to IF and back to transmit frequencies may be either by single or dual conversion with the decision as to which mode to use depends on many factors including transmit/receive frequencies and separation, signal bandwidths, RF-to-IF frequency separation, filter design feasibility, numbers of channels and acceptable performance criteria. In dual conversion, as proposed in the satellite transponder for ATS-AMS-III (Section 4.4.2), the 14 GHz input signal is translated to a first IF of approximately 1 GHz and then to a 2nd conversion IF of 150 MHz with an up conversion to approximately 1 GHz followed by translation to the 12 GHz transmit frequency. Flexibility of switching up-link to down-link channels is provided with the common 150 MHz IF. Since a coherent transponder is not specified, separate local oscillators are used for up and down conversion, avoiding the weight and design complexity of a synthesizer and permitting flexibility in choice of receive and

and transmit frequencies. A single oscillator source frequency will be used for the RF conversions (from 14 GHz and to 12 GHz) with multiple LO's reserved for lower frequency conversion to/from the 150 MHz IF. Dual conversion permits maintaining the transmit-to-local oscillator separation larger and filtering of harmonics in the LO chain less complex than for single conversion. More detailed analysis is required to establish the best conversion design with optimum selection of LO frequencies and filters. The cutoff strip inserted in front of each TDA isolates frequencies between the undesired 12 GHz frequencies and the receive frequency.

Other design features that are desirable in the transponders are the backup redundancy provided by multiple IF and TWT amplifiers, reliability and size/weight advantages of solid state and microwave components at these frequencies, balanced amplifier/mixers, AGC detector amplifiers and low noise receivers.

#### 5.4.1.1

##### Power Amplifiers

Power amplifiers for the spacecraft communication transponder are required to operate at output powers of from 5 watts in a multicarrier back-off mode up to 2000 Watts in both single and multiple carrier back-off modes. Tests of TWT's operating with a two-tone input signal have shown that third order intermodulation products vary from 20 to 30 dB below the fundamental with a 6 dB output power backoff below saturation. While it is expected that the third order products of the higher power Klystron and TWT will fall at the same general power levels, actual tests will have to be run to determine the effects of intermodulation in the high power spacecraft designs where up to four or more TV channels are transmitted through a single 160 MHz TWT or 100 MHz Klystron.

The projection for multi-channel audio operation in low powered TWT's noted in Section 4.4.2.3 with analysis in Section 5.1, identifies



the need for experimentation and development on a range of low and high power microwave amplifiers to minimize effects of intermodulation distortion and to optimize for multi-carrier operation.

Other features of spaceborne microwave amplifiers which are projected and for which further development and/or experimentation are required include:

Increased efficiency particularly of high power amplifiers through multistage depressed collectors with directional thermal radiation capabilities.

Development of microwave solid state drivers with increased dynamic range for varying the input power of high power TWT's and Klystrons over a linear range compatible with minimizing intermodulation distortion effects of multi-carrier operation.

Development to achieve essentially constant collector power requirements over the range of output power operation.

#### 5.4.2

#### TRANSPONDER CONFIGURATION -ATS-AMS-I/II

The spaceborne communications transponder configuration, described in Section 4.4.3 has been designed to satisfy the constraints imposed by the particular high power TWT and Klystron-amplifiers, while keeping in mind the desire for operation with 15 spot beams and a variable beam-forming matrix.

The TWT amplifier has an instantaneous bandwidth of 160 MHz capable of transmission of up to 4 RF channels. Necessary power division for multi carrier operation, plus an additional "back-off" ratio to reduce intermodulation combine to limit the high power capability of the power amplifier to single channel operation. However, the additional complexity in implementing the transponder for multi-channel operation offers added flexibility in conducting various experiments with geographically separated earth terminals.

The added complexity begins with the four-fold switching hierarchy in the feed matrix. Further, in order to maintain the integrity of each spot beam, at least 20 dB of isolation must be provided between beams. This might possibly be accomplished with ferrite isolators, which represent a simpler expedient than by using independent receivers for each channel.

Redundant, active functional modules (TDA, IF amplifier LO source, solid-state power amplifier) are provided to insure reliable operation. The high power vacuum tube amplifiers, the TWT and Klystron, in a sense provide back-up for each other.

The use of multiple IF amplifiers permits high gain narrow band operation with attendant reduction in noise bandwidth. While the advantages of this method are not significant, it does provide additional redundancy. Also with additional switching the IF signals could be routed to separate output power amplifiers operating at reduced power.

The key experiment for the ATS-AMS transponder involves the use of the full 2 KW RF power delivered by the TWT or the Klystron operating in single and multiple carrier modes. Development of high power TWT's and Klystrons and/or predistortion circuitry to provide efficient multicarrier operation is required.

### 5.4.3

#### Transmitter/Receiver Isolation

To keep the transmitter signal levels at 12 GHz nominal below the 14 GHz receiver noise level of -124 dBW, it is required that filtering be provided for (1) out-of band-noise generated by the power amplifiers and (2) transmitter output power. Figure 5.4.3-1 shows the isolation network to accomplish the desired isolation with a single feed as a typical junction for (1) transmitting voice/data and video/ voice signals in the 11.7 - 12.2 GHz range and (2) receiving video/voice signals at 14.0 - 14.5 GHz.

#### 5.4.3.1

##### Filtering of Power Amplifier Generated Noise

For the video/ voice signals, out-of-band noise from the TWT is estimated to be -30 dBm (-60 dBW) in a 23-24.5 MHz bandwidth. For the isolation shown in the network the signal in the 14 GHz receive band is as follows:

TWT out-of-band noise level	-60 dBW (24.5 MHz)
Filter isolation	-40 dB
Splitting network power reduction	-9 dB
Antenna polarization isolation	<u>-30 dB</u>
TWT noise level at receiver	-139 dBW

This noise level is 15 dB below the -124 dBW in-band noise level at the receiver. The 40 dB filter is made of WS62 waveguide in three sections and approximately 3 1/2 inches long.

The voice/data transmitter out-of-band noise level at the receiver is computed from the following values:

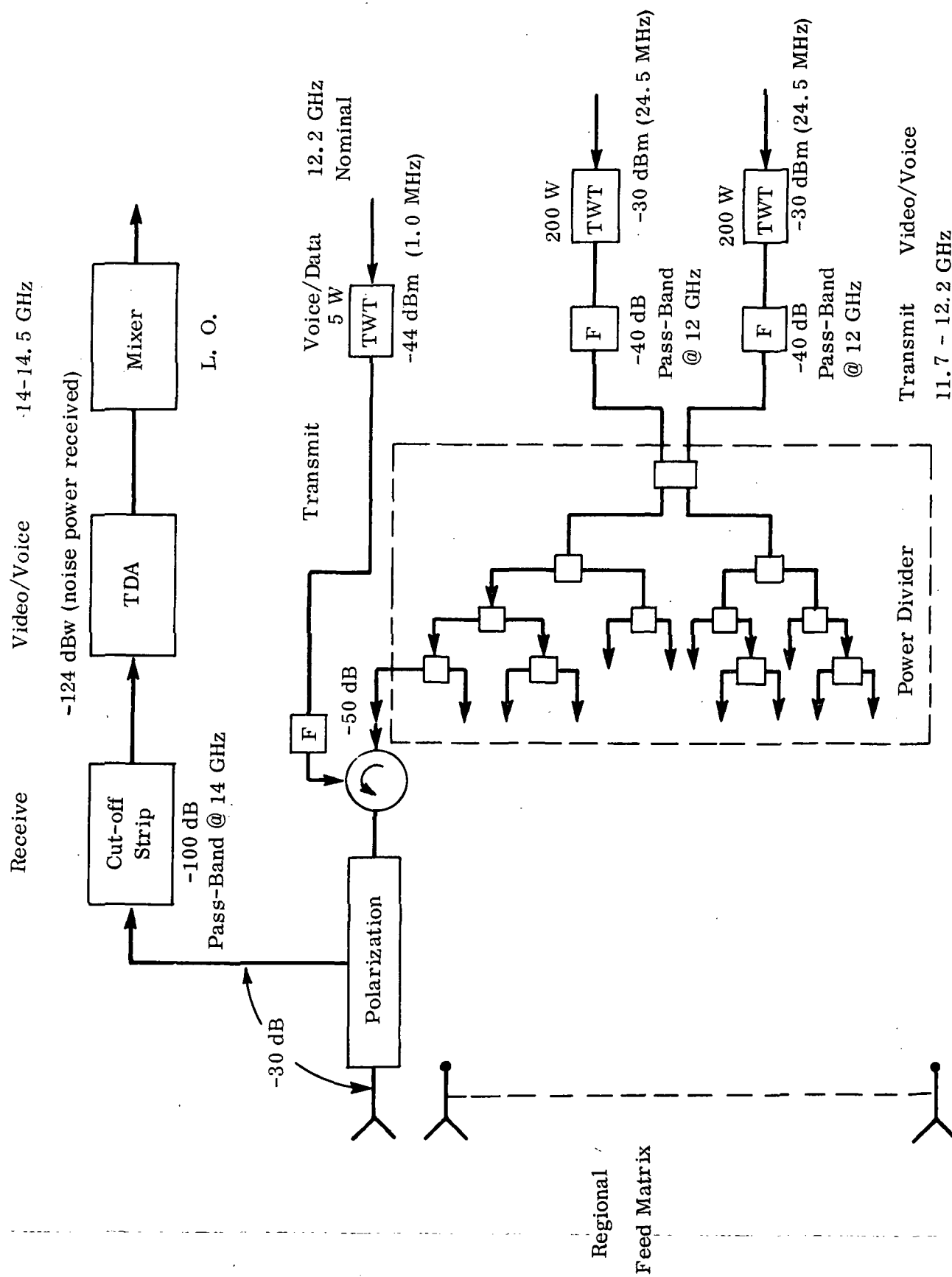


Figure 5.4.3-1. Simplified Transmitter/Receiver Isolation Network

P.A. out-of-band noise level (-44 dBm; 0.6 MHz)	-74 dBW
Filter isolation	-50 dB
Antenna polarization isolation	<u>-30 dB</u>
TWT noise level at receiver	-154 dBW

The noise level is below the -124 dBW in band receiver noise level by 30 dB with a 4 section filter to achieve the desired isolation. Other power amplifiers are not expected to generate out-of-band noise requiring isolation in excess of these levels.

#### 5.4.3.2 Isolation of Transmitter Output Power from Receiver

The 12 GHz satellite output power must be isolated from the satellite receiver for proper operation of the tunnel-diode amplifier (TDA). This can be achieved by inserting in front of the TDA a strip of waveguide with cut-off frequency between the undesired 12 GHz frequencies and the receive frequency (14 GHz).

The allowable transmitter power level at the receiver input is:

Noise level	-124 dBW
Out-of-band rejection (TDA)	<u>15 dB</u>
Tolerable level	-109 dBW

Consequently, out-of-band filtering by the cut-off waveguide strip must be:

Transmitter power (Video/voice)	23 dBW
Splitting network power reduction	-9 dB
Antenna polarization isolation	<u>- 30 dB</u>
Power level before strip	-16 dBW
Tolerable level	-109 dBW
Power level before strip	<u>-(-16 dBW)</u>
Required filtering	-93 dB

For additional margin, filtering of -100 dB is recommended.

Choice of the actual cut-off frequency for the isolating waveguide strip is made as follows: Higher cut-off frequencies give more isolation of undesired signal (12.2 GHz) but also greater insertion loss at the receiver frequencies (14.0 - 14.5 GHz). This is shown in Figure 5.4.3-2. The cut-off frequency which gives the most isolation with least insertion loss is therefore the best choice. As shown in figure 5.4.3-3, the least insertion loss for 100 dB isolation is given by a waveguide strip with cut-off frequency of about 13.0 GHz. This corresponds to 12.27 cm (4.83 inches) of copper waveguide with dimensions 1.154 cm x 0.762 cm (0.4543 inches x 0.30 inches), to give -100 dB filtering at 12.2 GHz with 0.066 dB insertion loss at 14.0 GHz. Since the output power for the voice/data transmitter (5W) is less than for the video transmitter the -100 dB cut-off filter provides adequate isolation.

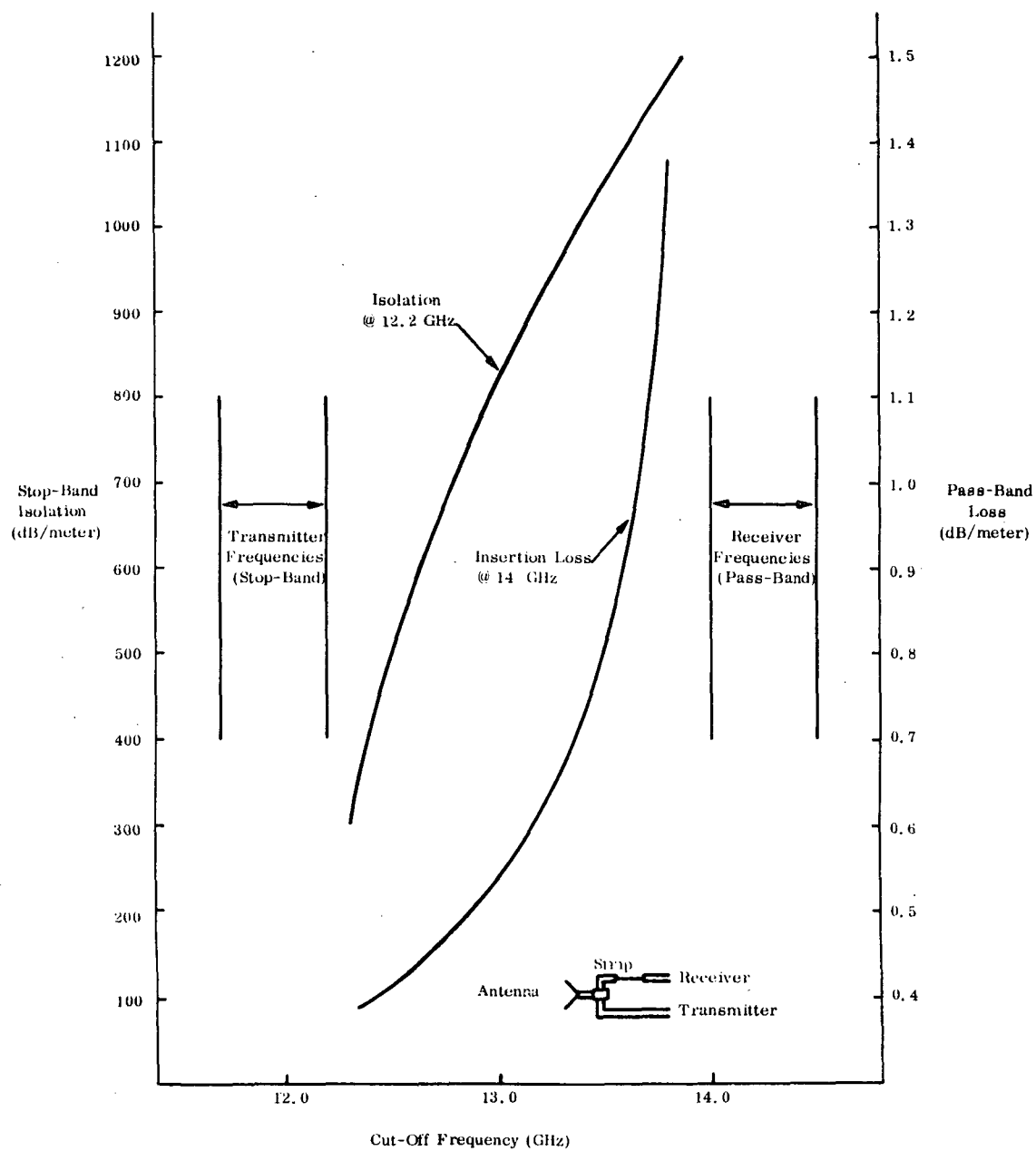


Figure 5.4.3-2. Waveguide Strip Isolation & Loss vs. Cut-Off Frequency

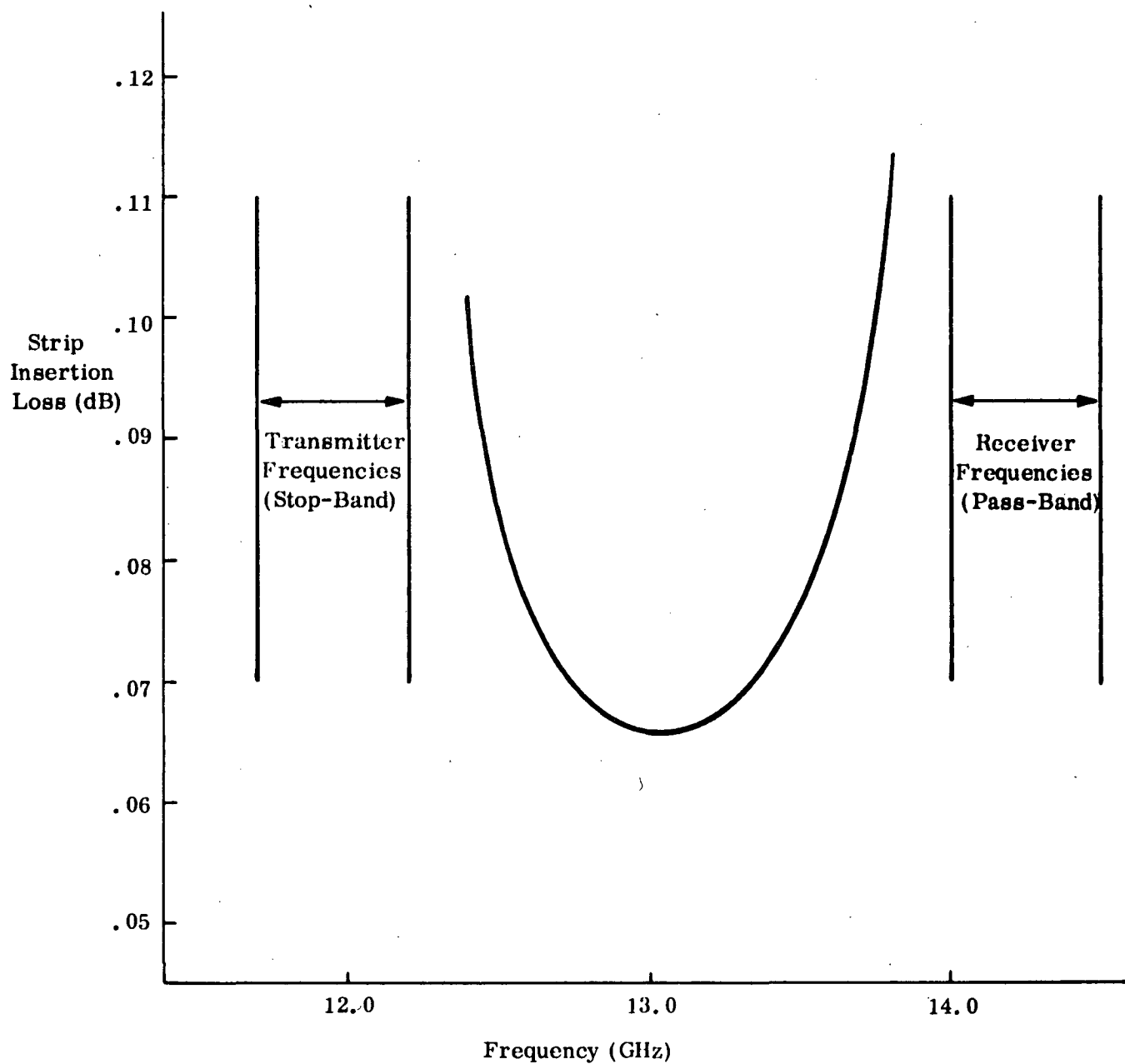


Figure 5.4.3-3. Waveguide Strip Insertion Loss vs. Cut-Off Frequency  
(for 100 dB Isolation)



## 5.5

## POWER SUPPLY SUBSYSTEM

### 5.5.1

### ATS-AMS-III POWER SUBSYSTEM CONFIGURATION

#### 5.5.1.1

#### Load Profile Analysis

Load profiles for ATS-AMS-III may be defined for the long time (2-5 years) and short term (daily). During the long term, solar array power will degrade approximately 18% over the initial two years because of design/manufacturing tolerances and operation in a synchronous radiation environment resulting in decreasing power levels available for performing experiments and required housekeeping and stationkeeping (orbit control) functions. During equinox, the spacecraft is in darkness (occult) for varying time periods to a maximum of 72 minutes (1.2 hours) per day.

The daily load profile during solstice (no darkness) and equinox both include orbit control (0.5 hour/day) with ion engine power (at high voltage) and housekeeping (at 30.5 V) required during that period. During occult (equinox only) battery discharge (30.5 V) is required to supply housekeeping power. For the remainder of the daily cycle (minimum of 22.3 hours) at equinox, solar array power supplies power (through a 67 volt bus) for daytime 30.5 V power (housekeeping plus low voltage for communications), battery recharge, high voltage power for communications and undefined experiments plus margin. A daily power budget distribution during equinox is illustrated in Figure 5.5.1-1.

The load profile shown in Figure 5.5.1-1 illustrates the basis for sizing the ATS-AMS-III power subsystem. The following assumptions were made in constructing this load profile:

- With decreasing solar array power over the first two years of operation the primary mode communications has been estimated for the end of life (end of 2 year period). Additional functions with increased power amplifier applications may be performed at the start of mission.

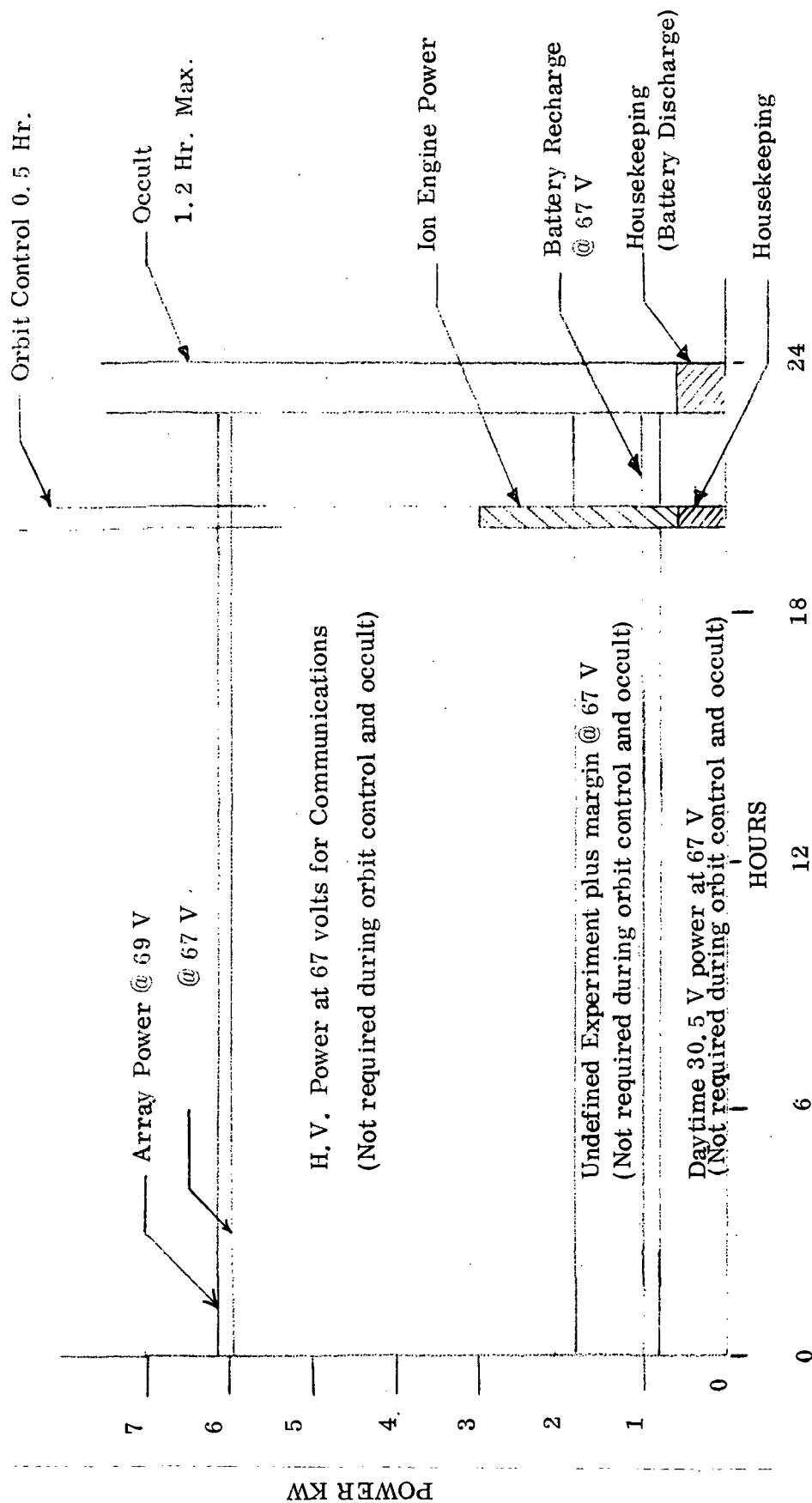


Figure 5.5.1-1. ATS-AMS-III B Daily Power Budget Distribution During Equinox (EOL)

- o The DC to RF conversion efficiency of all high power amplifier tubes is 50 percent, operating at saturation.
- o The cathode heaters of the high power amplifiers are maintained at a 50 percent power level when the tubes are not in use. The 50 percent power requirements for the heaters of the 2 kW TWT, 1 kW klystron and 200 W TWT are estimated as 65 W, 33 W and 6.5 W, respectively at 30.5 Volts.
- o Ten percent of the power for the Communications Subsystem switching matrix and low power amplifiers is ON during occult.

#### 5.5.1.2

#### Power Subsystem Capability Analysis

To estimate the power requirements for ATS-AMS-III reference is made to the power subsystem block diagram, Figure 4.5-1 and the power subsystem description. The following conversion values using a primary bus voltage of 67 V are of interest to this analysis:

Unarticulated array power = articulated power  $\times \cos 23.5$  (0.9171)  
(seasonal sun angle variation =  $\pm 23.5^\circ$ )

Array power at 67 V bus = Array power at 69 V  $\times \frac{67}{69}$  (allowing for 2 V harness and diode drop)

Buck regulator efficiency (for converting 67 V to 30.5 V and for discharging battery) = 89%

Diode voltage drop, 67 V bus to buck regulator input = 1 V

Converter network efficiency (67 V bus power to high voltage power for power amplifiers and ion engines) = 86%

Table 5.5.1.2-1 summarizes the power subsystem budget for the primary communication mode of ATS-AMS-III A, indicating typical communication options that may be exercised during the mission period. Referring to Table 5.5.1.2-1 the raw array power (Column D)

Table 5.5.1.2-1. ATS-AMS-III A Power Budget, Primary Communication Mode

Mission Phase	I Array Power at 69 V	II Power at 67 V Bus (1)	III 67 V Bus Power Less 30.5 V Daytime Power, 725 W (2)	IV (3)	V Power Margin @ 67 V	VI DC Comm. Power @ 67V	VII DC Comm. Power @ HV	Options (Typical)	200 W-TWT (Video)	2000 W-TWT (Rainfall)	2000 W-TWT (2-4 carriers)	1000 W Klystron (Rainfall)	5 W TWTS (Audio)	Maximum Power Required
Start of Mission at Equinox (Unarticulated Array Power)	9.6 kW	9.34 kW	8.52kW	8.51kW	1.33kW	7.15kW	6.16kW	$\frac{1}{2} \frac{3}{4}$	10 8 9 5	1* 1* 1* 1	- 1 - -	- 1 - -	10 10 10 6	4.05 kW 5.25 kW 5.65 kW 6.05 kW
Solstice	8.79kW	8.58 kW	7.76kW	7.75 kW	1.23kW	6.42kW	5.52kW	$\frac{1}{2} \frac{3}{4}$	10 8 8 3	1* 1* 1* 1	- 1 - -	- 1 1 -	10 10 9 4	4.05 kW 5.25 kW 5.24 kW 5.22 kW
End of Mission at Equinox (Unarticulated Array Power)	7.55 kW	7.68 kW	6.86 kW	6.85kW	1.33kW	5.52kW	4.75kW	$\frac{1}{2} \frac{2}{3}$	10 6 6	1* 1* 1*	- 1 -	- - 1	10 10 7	4.05 kW 4.45 kW 4.44 kW
Solstice	7.2 kW	7.0kW	6.15kW	6.17 kW	1.33kW	4.54kW	4.15kW	$\frac{1}{2} \frac{2}{3}$	10 5 5	1* 1* 1*	- 1 -	- - 1	10 9 6	4.05 kW 4.04 kW 4.03 kW

Notes: (1) Array power less isolation diode and harness drop (2V)  
 (2) Less buck regulator efficiency (89%) to convert to 30.5 V bus  
 (3) Less isolation diode drop (1V)  
 \* Indicates interchanging 2000 W TWT or 1000 W Klystron for 200 W TWTS.

at start of mission suffers a power degradation of 18% (design/manufacturing 8% and radiation environment 10%) over a two year period to end of mission. Since the array may not articulate to account for seasonal sun angle variations ( $\pm 23.5$  degrees), the array size required is the solstice array power required/ $\cos 23.5^\circ$  or,  $8.78 \text{ kW}/\cos 23.5^\circ = 9.6 \text{ kW}$ . The power available at the 67 volt bus (Column II) has been decreased by the two-volt drop (array power  $\times 67 \text{ V}/69\text{V}$ ) through the isolation diode and harness. Columns III and IV result from subtracting the 30.5 volt daytime power (referred to the 67 V bus) required for housekeeping and communications (other than for high voltage). For ATS-AMS-III A the normal 30.5 V daytime power is estimated to be:

Communications (Transponder plus P.R. 30.5 V power)	400 W
Antenna Tower drive	10 W
Telemetry and Command	45 W
Attitude Control	170 W
Margin	<u>100 W</u>
Total 30.5 V daytime power	725 W

Allowing for a buck regulator efficiency of 89% and a one volt isolation diode drop the power reduction at 67 V to arrive at the power levels in Column IV of Table 5.5.1.2-1 is:

$$\frac{725 \text{ W}}{0.89} \times \frac{67 \text{ V}}{66 \text{ V}} = 830 \text{ W}$$

The 67 V power shown in Column IV is apportioned between power margin (Column V) and communication power at 67 V (Column VI). The available high voltage DC communication power (Column VII) is obtained by multiplying the Column VI values by the converter network efficiency of 86%. The

power margin (Column V) includes allowance for additional undefined experiments and for recharging batteries (see battery discharge/charge description following).

Depending upon the high voltage D. C. power available (Column VII) various communication experiments may be postulated as indicated by the typical options listed in the table. The quantities are shown for each P. A. with asterisks indicating alternate experiments interchanging 200 W TWTs for either the 2000 W TWT or 1000 W Klystron. In selecting these options, the saturated efficiencies of the 2000 W and 200 W TWT's and 1000 K Klystron have been assumed at 50% and the 5 W TWT. With the 2000 W TWT and the 5 W TWT at 30%, the output (and input) are backed off from saturation with less than saturated power required at the output. Back-off of 10.8 dB (see section 5.1.3.1) on the 5 W TWT reduces the efficiency to about 10%.

Back-off of 6 dB for the 2000 W TWT (500 W output) reduces the efficiency to about 25% (2000 W input). Input DC power estimated for the various modes are as follows:

<u>P. A.</u>	<u>Mode</u>	<u>DC Power Input</u>	<u>Status</u>
200 W TWT	Single carrier	400 W	Saturation
2000 W TWT	Single carrier (Rainfall)	4000 W	Saturation
2000 W TWT	2-4 carrier (500 W output)	2000 W	6 dB backoff
1000 W Klystron	Single carrier (Rainfall)	2000 W	Saturation
5 W TWT	Multi-carrier (500 mW output)	5 W	10.8 dB backoff

The power subsystem budget at the bottom of the Table (underlined) has been identified with the communication mode described in Volume I and represents, along with the options shown, a conservative communication capability as evidenced by the expanded capability for the earlier mission phases and the typical options in the Table. By allowing most of the margin (Column V) for communications additional high voltage transmitter experiments may be performed.

During occult (with power supplied by battery) or orbit control, housekeeping power requirements are estimated to be:

Communications	213 W
Antenna tower drive	10 W
Telemetry and Command	45 W
Attitude Control	170 W
Margin	<u>100 W</u>
Total at 30.5 V	538 W

Converted to the 67 V bus the power becomes

$$\frac{538}{.89} \times \frac{67}{66} = 601 \text{ W (buck regulator efficiency = 89\%)}$$

For orbit control 2000 W (at 1.2 kV) is required for station-keeping which at 67 V becomes  $2000/0.86 = 2330 \text{ W}$  (Converter network efficiency = 86%). The total power during orbit control (at 67 V) is then  $2330 \text{ W} + 601 \text{ W} = 2931 \text{ W}$  considerably less than for primary communications (the primary mode for which the power subsystem was sized).

To determine battery capacity, C, the battery discharge power during occult is first estimated from the expression:

$$P_{LBD} = \frac{P_{LN30} N V_{BD \text{ AVG}}}{e_D (N V_{BDAVG} - 1.0V)}$$

where

$P_{LN30}$  is the 30.5 VDC occult load power (538 W)

$V_{BDAVG}$  is the average cell discharge voltage (1.2 V)

$e_D$  is the buck regulator efficiency (0.89)

N is the number of battery cells

$$P_{LBD} = \frac{(538W) (N) (1.2)}{(0.89) (1.2N - 1.0)} = \frac{725N \text{ W}}{1.2N - 1.0}$$

Discharge occurs over a 1.2 hour maximum occult period

$$\text{for a watt hour discharge of } \frac{725N}{1.2N - 1.0} (1.2) = \frac{725N}{N - 0.84}$$

Battery capacity, C, is then found from  $C = \frac{725N}{N - 0.84} / N V_{BDmin} D$

Where  $V_{BD \text{ min}}$  is the minimum cell discharge (1.0 volts)

and D is the maximum depth of discharge (0.50)

$$C = \frac{725N}{N - 0.84} \bigg/ N (1.0) (0.5) = \frac{1460}{N - 0.84} \text{ ampere-hours}$$

For a 32 cell system

$$C = 1460 / (32 - 0.84) = 47 \text{ ampere hours (A hrs)}$$

Four strings of 12 A hrs. capacity will be connected in parallel to meet the requirement.



Based on a 20 hour charging rate for nickel-cadmium cells and a battery recharge efficiency of 0.53 the time required to restore charge to the battery is:

$$\frac{\text{DC}}{(0.53) (c/20)} = \frac{(0.5) (48 \text{ A hr})}{(.53) (48/20)} = 19 \text{ hours}$$

This is less than the minimum amount of sunlight available to the spacecraft during equinox season in synchronous orbit. The power required at 67 volts for recharging = 161 W assuming a simple charge controlled for the 32 cell battery.

#### 5.5.1.3

### ATS-AMS-III A Power Subsystem Physical Characteristics

#### Solar Array

The array area is found from

$$\text{Area} = \frac{P_{A69}}{(1400 \text{ W/m}^2 E_{28} F D_1)} = \frac{9.6 \text{ kW}}{130(0.018) (0.86) (.85)} = 87 \text{ m}^2 (935 \text{ ft}^2),$$

where

$E_{28}$  is the bare solar cell efficiency (0.108) at  $301^\circ\text{K}$ , AMO (standard) conditions.

$F$  is a temperature-correction factor applied to a bare cell efficiency to account for operation at  $331^\circ\text{K}$ .

$D_1$  is a solar cell packing factor

The array weight is estimated to be 177 kg (390 lb).

#### Battery

Battery weight is 94 kg (207 lb) estimated from .045 kg (0.1 lb/A hr./ cell) and multiplying by 1.35 for frame, heat sink and auxiliary hardware.

### Shunt Dissipator

The shunt dissipator proposed is a partial shunt dissipator, with a tap point 67 percent of the series length from array ground.

Based on measured specific weights of comparable spacecraft units approximately 54 W/lb. the shunt dissipator is estimated to weigh

$$\frac{9600 \text{ W (0.67)}}{54 \text{ W/lb}} \times 0.454 \text{ kg/lb} = 54 \text{ kg (119 lb)}$$

### Power Converter Network (PCN)

Based on a weight/power relationship of 7 kg/1kW \* for the power conversion network and a maximum high voltage output load power of 6.16 kW (7.18 kW x 0.86) the power conversion network weighs 7 x 6.16 = 43 kg (95 lb)

### Power Regulation Unit

The Power Regulation Unit consisting of charge controllers and the discharge buck regulator is estimated to weigh 7 kg (15.4lb) based upon the same weight/power factor of 7 kg/1 kW as for the Power Conversion Network. The maximum power through the PRU will be just under 1 kW (D.C. daytime power of 830 W and maximum battery charge of 161 W, both at 67 V).

---

\* From a paper by Moore, Wilson and McIntire, "Lightweight Power Conditioning System for Ion Engines Using Energy-Storage Transformers for Conversion, Non-dissipative Regulation and Protection", IEEE Transaction on Aerospace and Electronic Systems, Vol AES-2, No. 4, July 1966, work performance on a Lewis (NAS 3-6264) contract we obtain the following estimates

56 V input 8 lb/kW

28 V input 10.3 lb/kW

Applying judgement we elected to use 11.5 lb/kW multiplied by a factor of 1.33 to account for source-load mismatch effects. Therefore

$$(11.5 \text{ lb/kW}) + (1.33) + (0.454 \text{ Kg/lb}) = 7 \text{ kg/kW}$$

### ATS-AMS-III B Power Budget

Table 5.5.1.4-1 summarizes the power subsystem budget for the primary communication mode of ATS-AMS-III B with the various power levels and typical options established by the same process as for ATS-AMS-III A, (Table 5.5.1.2-1). For ATS-AMS-III B the normal 30.5 V daytime power is estimated to be:

Communications(Transponder plus P. A. 30.5 V power)	275 W
Antenna tower drive	10 W
Telemetry and Command	45 W
Attitude Control	170 W
Margin	<u>75 W</u>
Total 30.5 V daytime power	575 W

With a buck regulator efficiency of 89% and a one volt isolation diode drop the required power at 67 V is  $\frac{575}{0.89} \times \frac{67V}{66 V} = 660 \text{ W}$ , which is subtracted from entries in Column II to arrive at those in Column IV.

The power subsystem budget (underlined) at the bottom of the Table represents that identified with the communication mode described in Volume I. By transferring the bulk of the power margin in Column V to communications (Column VII) (with the 86% efficiency conversion) additional communications capability experimentation may be achieved.

During occult and orbit control housekeeping power requirements are estimated to be:

Table 5.5.1.4-1. ATS-AMS-III B Power Budger, Primary Communication Mode

Mission Phase	I Array Power at 69V	II Power at 67 V Bus (1)	III 67 V Bus Power Less 30.5 V Daytime Power, 575 W (2)	IV Power Margin @ 67 V (3)	V Power Margin @ 67 V	VI DC Comm Power @ 67V	VII DC Comm Power @ HV	Options (Typical)	200 W TWT (Video)	2000 W TWT (Rainfall)	2000 W-TWT (2-4 Carriers)	1000 W Klystron (Rainfall)	5 W TWT's (Audio)	Maximum Power Required
Start of Mission at Equinox Unarticulated Array Power	7.5 kW	7.3 kW	6.79	6.64 kW	840 W	5.50 kW	4.93 kW	$\frac{1}{2}$ $\frac{2}{3}$	5 4 2	1* 1* 1	- - -	- 1 -	5 5 -	4.00 kW 4.00 kW 4.80 kW
Solstice	6.9 kW	6.7 kW	6.19 kW	6.04 kW	840 W	5.20 kW	4.41 kW	$\frac{1}{2}$ $\frac{2}{3}$	5 4 1	1* 1* 1	- - -	- 1 -	5 5 -	4.00 kW 4.00 kW 4.40 kW
End of Mission Array Power at Equinox	6.15 kW	5.98 kW	5.47 kW	5.32 kW	840 W	4.45 kW	3.55 kW	$\frac{1}{2}$ $\frac{2}{3}$	3 4	- -	1 1*	1* 1	5 5	3.22 kW 3.62 kW
Solstice	5.64 kW	5.47 kW	4.97 kW	4.81 kW	840 W 160 W	3.97 kW 4.65 kW	3.4 kW 4.00 kW	$\frac{1}{2}$ $\frac{2}{3}$	5 4	- 1*	- -	1* 1	5 -	2.02 kW 4.00 kW

Notes: (1) Array power less isolation diode and harness drop (2 V)  
(2) Less buck regulator efficiency (89%) to convert to 30.5 V bus  
(3) Less isolation diode drop (1V)

\* Indicates interchanging 2000 W TWT or 1000 Klystron for 200 W TWT's

Communications	158 W
Antenna tower drive	10 W
Telemetry and command	45 W
Attitude Control	<u>170 W</u>
Total at 30.5 V	383 W

At 67 V this power is  $\frac{383}{.89} \times \frac{67}{66} = 437 \text{ W}$

For orbit control the same requirement exists as for ATS-AMS-III A namely 2000 W at high voltage or 2330 W at 67 V. The total 67 V requirement for orbit control is then 2767 Watts.

To accommodate a 383 W discharge during occult battery capacity is estimated at 33.4 ampere hours for 132 nickel-cadmium cells. At a 20 hour charging rate the recharge power to be supplied by the solar array is 121 W. Four 9 A hr. strings, storing a total of 36 A hr. capacity will be used to meet the requirement.

#### 5.5.1.5

#### ATS-AMS-III B Power Subsystem Physical Characteristics

The power subsystem for ATS-AMS-III B has been sized similarly to that for ATS-AMS-III. The solar array is estimated to be 68 m<sup>2</sup> in area and to weigh 134 kg.(295 lb). The shunt dissipator, power regulation unit (PRU) and power converter network (PCN) are estimated at 42 kg (92.5 lb) and 35 kg (77 lb) respectively. Battery weight is 71 kg(156 lb). The same conversion factors are used as for estimating the physical characteristics of the ATS-AMS-III A power subsystem.

### 5.5.2

#### ATS-AMS II POWER SUBSYSTEM CONFIGURATION

The functional block diagram of the Shunt Regulator power subsystem selected for this mission is shown in Figure 4.5-2. From the primary communications mode, the end-of-mission equinox array bus (30.5 V) load capability, is 3900 W. Array power is then

$$\frac{(32.5V)(3900 W)}{(30.5V) \cos 24.5^\circ} = 4600 W, \text{ and the array area is}$$

51 m<sup>2</sup> (550 ft<sup>2</sup>). Array power at start of mission is 5500 W.

Battery capacity requirements are estimated to be 42 A hr. requiring three batteries of 15 A hr. cells weighing 48 kg (105 lbs). The power regulation unit weight is estimated as 5 kg (11 lb) the shunt dissipator 33 kg (73 lb). The power control unit 3 kg (7 lb), power converter network 28 kg (62 lb) and harness 14 kg (31 lb).

### 5.5.3

#### ATS-AMS I POWER SUBSYSTEM CONFIGURATION

The functional block diagram of the power subsystem for the ATS-AMS I is shown in Figure 4.5-3.

The primary communications mode end-of-mission array bus (30.5V) load capability is 4400 watts. Array power is estimated at 5.5 KW and the array area at 144 m<sup>2</sup>. Array power for the start of mission is 13 KW.

To provide for the battery discharge requirements during occult 6 15 A hr. batteries weighing about 100 kg (220 lb) are estimated to supply a housekeeping plus P.A. heater power requirements during occult. Other power subsystem weights are estimated to be:

Solar Array	306 kg (673 lb)
PRU	7 kg (15 lb)
Shunt Dissipator	8 kg (18 lb)
PCU	3 kg (6 lb)
PCN	10 kg (23 lb)
Harness	14 kg (31 lb)

## 5.6 ATTITUDE CONTROL

### 5.6.1 EQUIPMENT TRADEOFFS FOR ATS-AMS III & II

The selection of equipment (sensors, signal processors, torquers) for the Attitude Control System is dictated primarily by the pointing accuracy requirements for a geostationary orbit ( $\pm .03^\circ$  for all axes). Since the system can not be any more accurate than the sensors, the accuracies of the sensors selected is a critical parameter.

A wide range of sensors, signal processors and torquers was investigated. An excellent reference source for this information is in Appendix C of the "Small Applications Technology Satellite Program and Spacecraft Study Report", X-730-70-350, Sept. 1970, Goddard Space Flight Center. Rather than include the large quantity of fold out sheets (approximately 70) cataloging these data, reference will be made to the approximate page of this study report. Where additional information is available, it will be included in this report.

It is good engineering practice to have sensor errors an order of magnitude smaller than the allowable system errors. For the  $\pm .03^\circ$  requirements that would mean a maximum sensor error of  $\pm .003^\circ$ . Digital solar sensors can approach this accuracy (The Adcole Aspect Sensor Model #15380 has a resolution of  $1/256^\circ$  or  $.0039^\circ$ ) but the best available earth sensor (Quantic Model 15380) has a null accuracy of  $.05^\circ$  for a non-moving part radiation balance sensor with a limited altitude range around synchronous altitude. A much heavier radiation balance edge Tracker with thermostatic non-periodic mirrors (also Quantic) has a null accuracy on the order of  $.015^\circ$  and a very wide altitude range (143.6 km to 46,300 km). Complexity and weight make the use of this unit on the Advanced Mission spacecraft questionable. The earth sensor will be used in a back-up mode only.

The following lists may be used as a cross reference (note, only items concerning the ACS will be listed):

Excerpts from "Small Application Technology Satellite Program and Spacecraft Study Report, " X-730-70-350, September 1970, GSFC, Appendix C.

<u>Topic</u>	<u>Report Page Number</u>
Altitude Control Systems	C-43
Earth Sensors	C-45
Earth Sensors	C-47
Sun Sensors	C-49
Sun Sensors	C-51
Star Trackers	C-53
Momentum Wheels	C-57
Control Moment Gyros	C-59
Auxiliary Propulsion Systems	C-65
Auxiliary Propulsion Systems	C-67
Propulsion Thrusters	C-69
Propulsion Valves	C-71
Propulsion Valves	C-73

Specific Details on chosen equipment will be found in the sections on Component Description.

For the coarse sun sensors,  $4\pi$  steradian coverage is required to locate the sun at any time the spacecraft is in sun light regardless of spacecraft orientation and six Sun Sensors with greater than  $120^\circ$  coverage in two orthogonal planes will provide the necessary coverage. Tight accuracy is not required and the standard  $1/2^\circ$  resolution (the angle subtended by the sun at earths orbital distance) will suffice.

An interferometer is suggested for use as the primary mode attitude sensor. This will provide 3 axis information. The interferometer being used on ATS/F has a three sigma accuracy of  $\pm .02$  degrees. At present this appears to be the most accurate sensor available. Derived rate information can also be obtained electronically from the interferometer angular position information. This will permit shutting off the gyros after the geosynchronous station has been attained.



For truly equatorial or near-equatorial orbits, the use of Polaris as a stellar reference is indicated by Figure 5.6.1-1 which shows a Polaris sensor stabilized in roll, pitch, and yaw in a rotating earth-centered coordinate system. Yaw motions appear as true translation in the sensor field of view, which looks out parallel to the orbit normal. Roll motions merely displace the yaw motion in a direction orthogonal to itself, and provided that there is sufficient field of view coverage in the roll-sensitive direction, yaw motions are still sensed as translations away from the yaw null axis. This method is insensitive to motions about the spacecraft pitch axis, which is parallel to the orbit normal and to the line-of-sight to Polaris.

A spacecraft having a truly equatorial or geostationary orbit of zero inclination angle, zero roll and yaw angles, and Polaris as a yaw reference would oscillate in yaw once per orbit due only to the diurnal motion of Polaris (about  $\pm 55$  arc-minutes). A Polaris sensor with 2-axis sensitivity in roll and yaw would oscillate likewise in roll as well as yaw by that amount. There is no South Celestial Pole star corresponding to Polaris at the North Celestial Pole, so Polaris is the logical choice for a yaw-sensing guide star.

Momentum wheels (one for each psuedo inertial axis) appear best suited to store the effects of cyclic disturbance torques. The momentum storage capability of the wheels should be selected to provide in excess of an integrated half cycle of cyclic disturbance. A biased momentum system in which a large momentum wheel (203 N-m-s nominal momentum) is mounted within the spacecraft with its momentum vector parallel to the  $Y_I$  axis was investigated; but, since the momentum vector would precess approximately  $.06^\circ$  in 28.7 min. due to the secular disturbance torque, it was not considered as a candidate.

For back-up operation, an earth sensor could be used in conjunction with a Polaris sensor. 3 sigma accuracy on the order  $.024^\circ$  will permit operation within the backup mode limits of  $\pm 0.1^\circ$ . The Polaris sensor provides roll and yaw information as described previously.

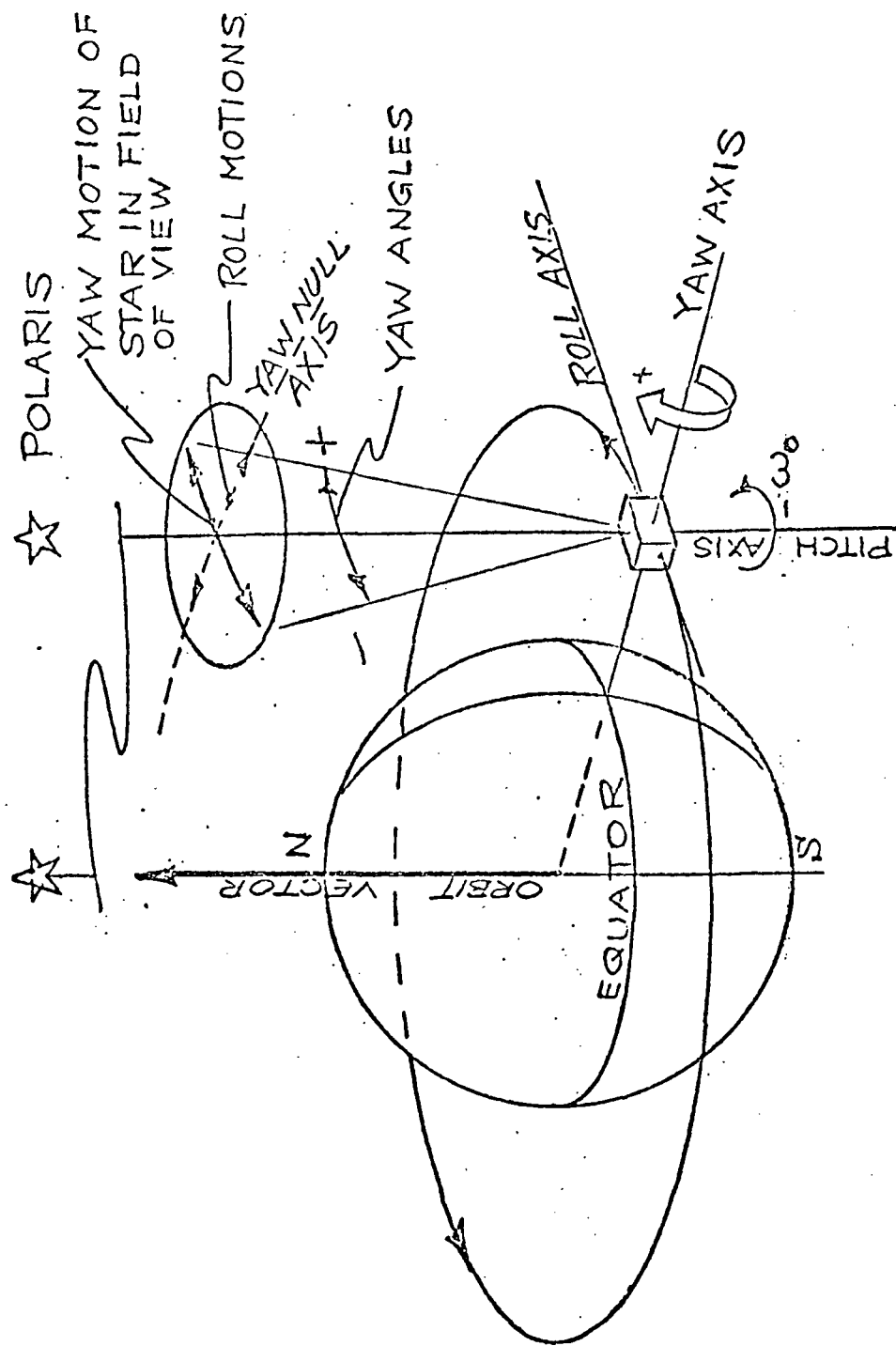


Figure 5.6.1-1. Polaris Yaw Sensing in Equatorial Orbit

## 5.6.2 ATTITUDE CONTROL DISTURBANCE TORQUE ANALYSIS FOR ATS-AMS III

### 5.6.2.1 Solar Torques and Momentum Storage Requirements

This section describes the method used to compute the solar torque (for the equinox condition) acting on the spacecraft and the resulting momentum requirements for the momentum wheels.

The solar torques were determined by computing the torque contributions of each element (i.e. the module, reflector, and solar panels) which are then summed to arrive at the total solar torque acting in each axis.

The torque computations were carried out at specific points in an orbit where (1) zero degrees point in orbit is the point in orbit closest to the sun and (2) 180° point in orbit is the point in orbit further from the sun. The reflectivity coefficients used for each element were:

Module	.8
Reflector	.8
Panels	.2

The center of gravity (CG) was considered to be at  $X_I = 0$ ,  $Y_I = -463$  cm and  $Z_I = 10.1$  cm. The center of pressure (CP) was assumed to vary with the rotation of the reflector.

The spacecraft configuration with the pertinent C G location, C P location and other dimensions required for solar torque computations at specific points in an orbit is shown in Figures 5.6.2.1-1 through 5.6.2.1-3.

Curves showing the solar torque and the resulting momentum requirements for the  $Y_I$  and  $Z_I$  axes are shown in Figures 5.6.2.1-4 and 5.6.2.1-5.

The solar torques for the  $X_I$  axis are approximately zero.

The buildup in momentum is 10.7 N-m-s per orbit for the  $Z_I$  axis and 3.52 N-m-s per orbit for the  $Y_I$  axis. This amount must be incorporated in the jet fuel requirements for attitude hold.

The actual wheel storage is a function of cyclic torque, average torque, and amount of momentum to be unloaded.

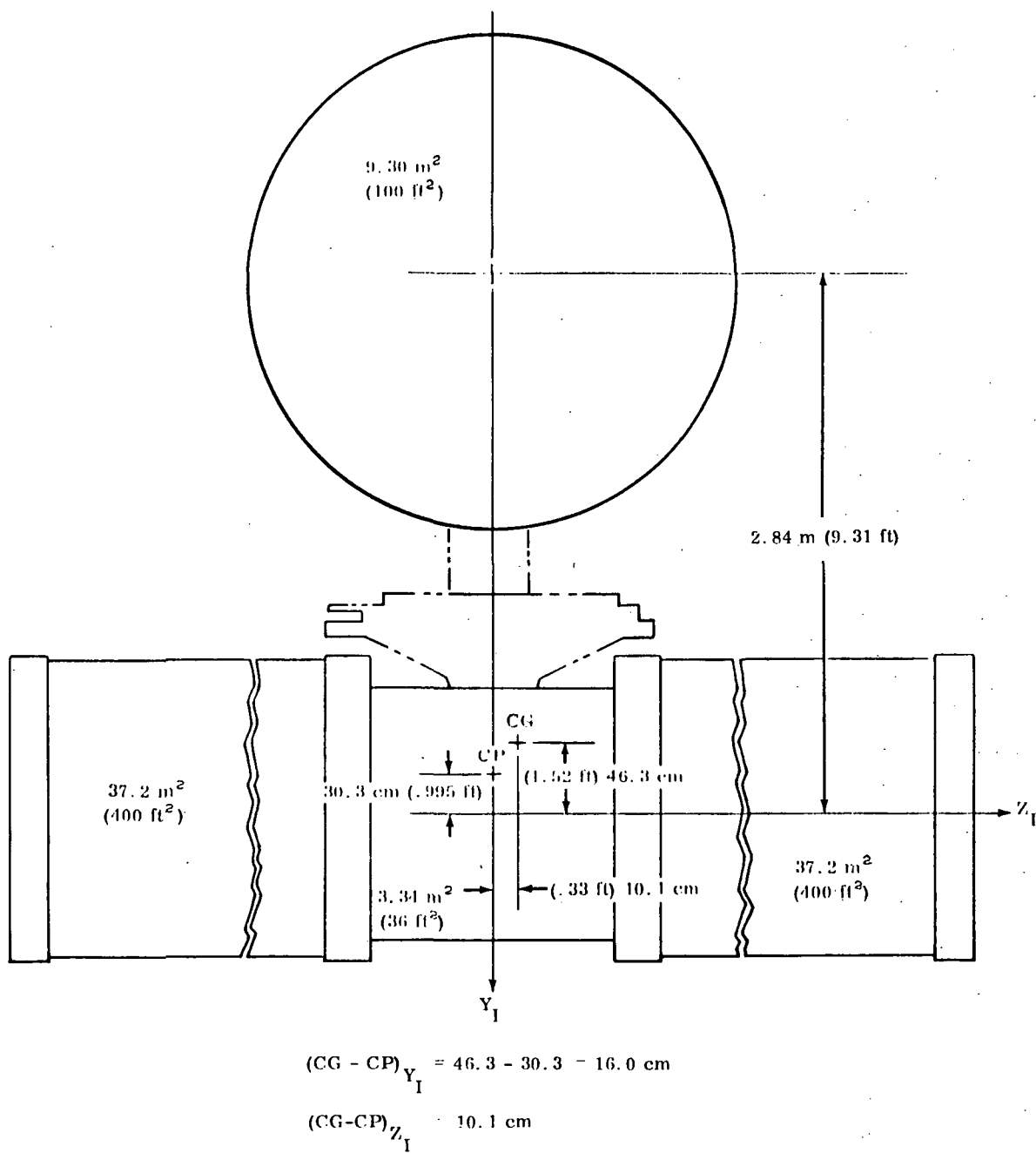


Figure 5.6.2.1-1. Spacecraft Configuration at 0° and 180°

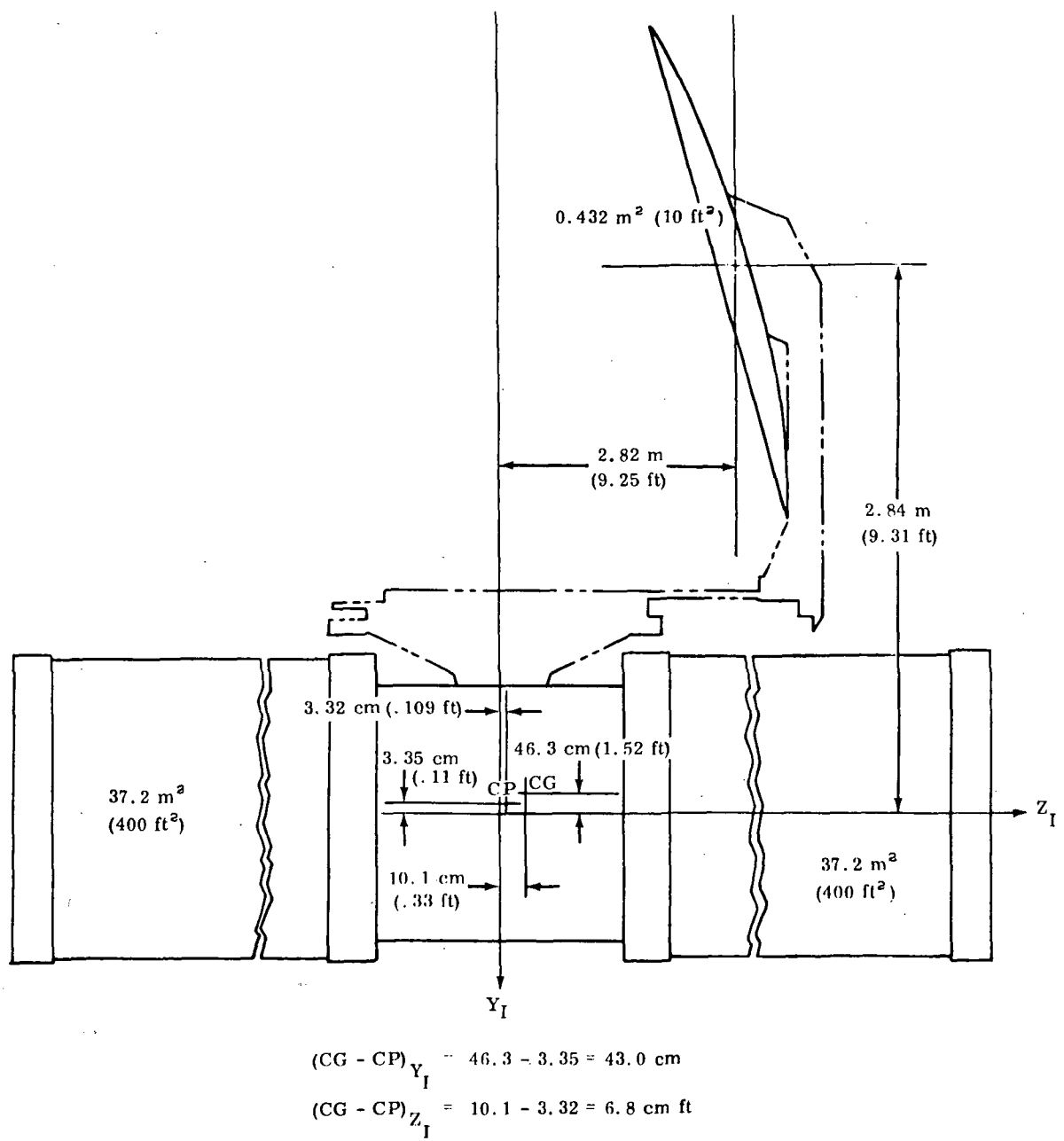


Figure 5.6.2.1-2. Spacecraft Configuration at 90° Point in Orbit

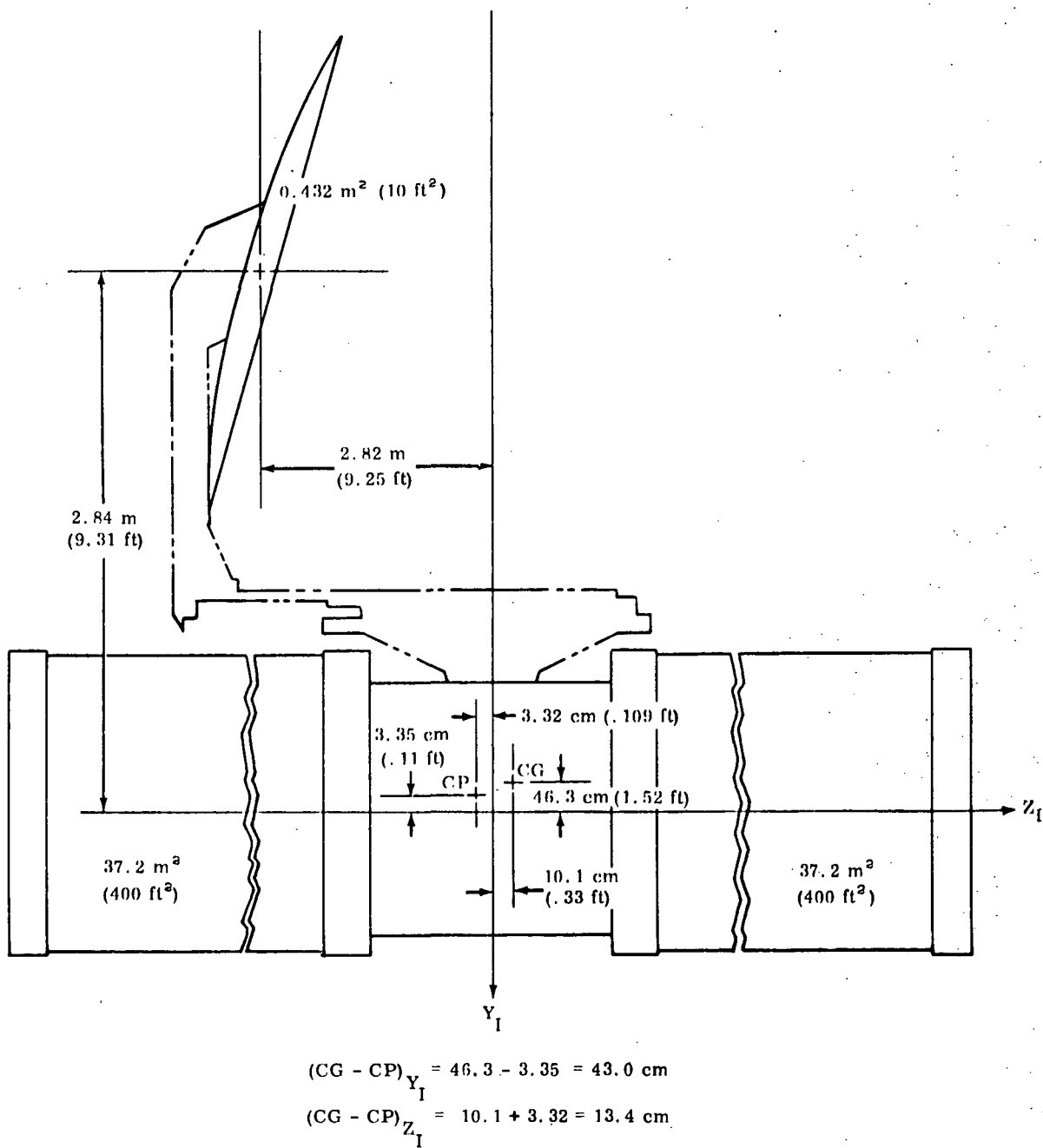


Figure 5.6.2.1-3. Spacecraft Configuration at 270° Point in Orbit

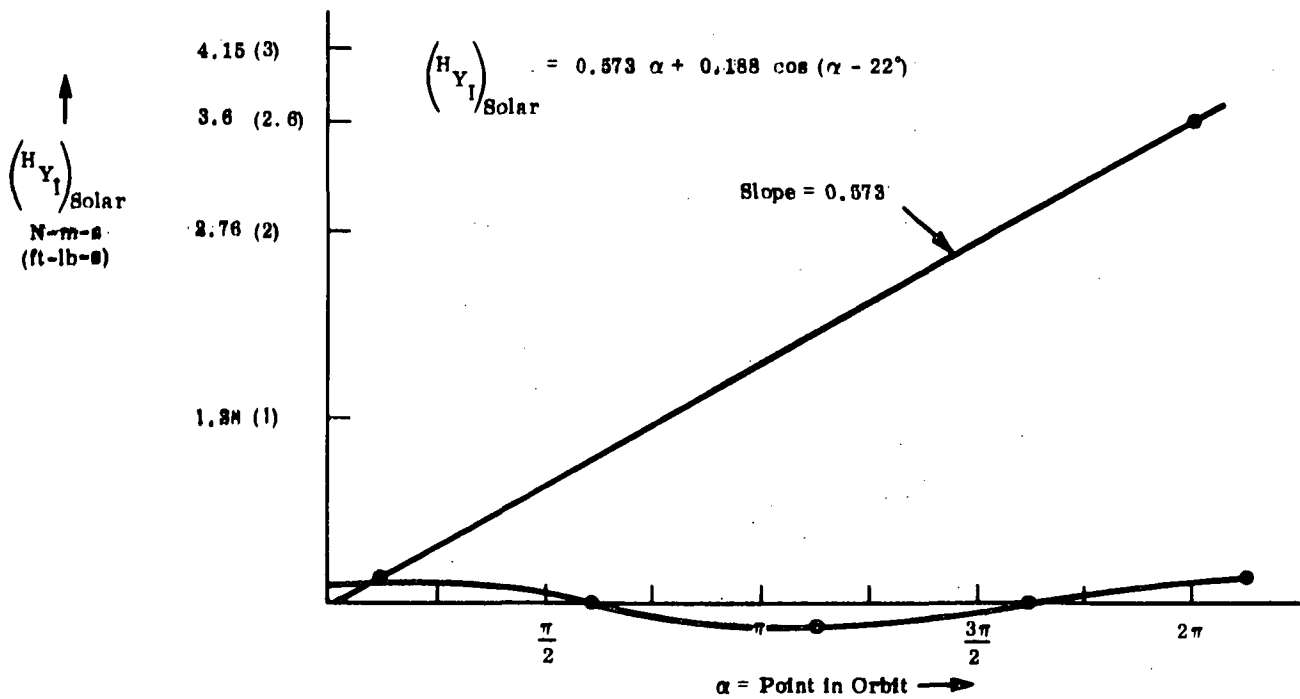
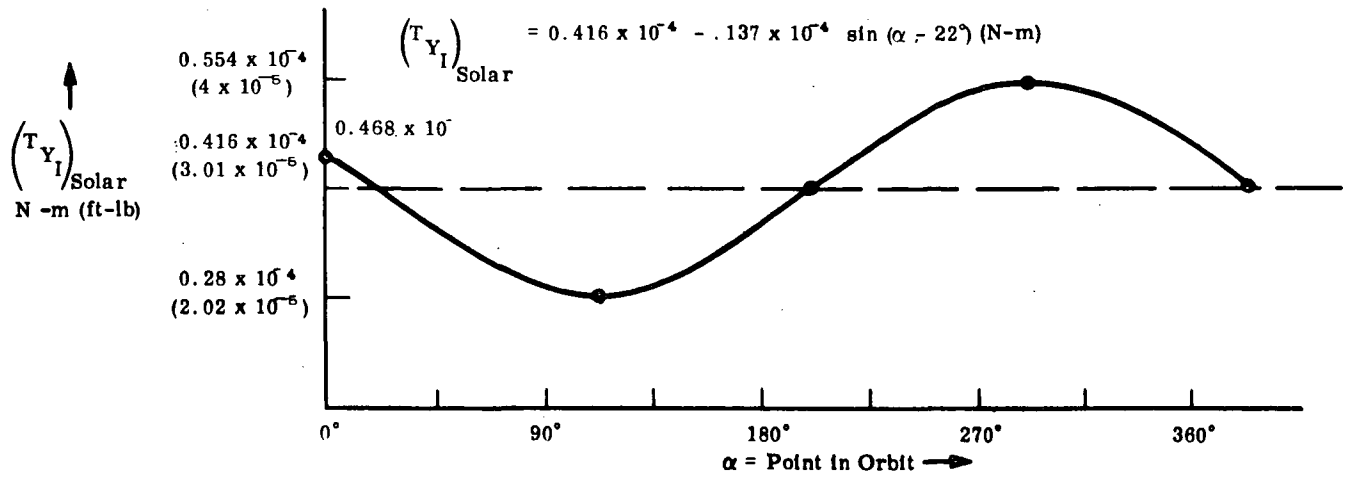


Figure 5.6.2.1-4. Solar Torques and Resulting Momentum Requirements

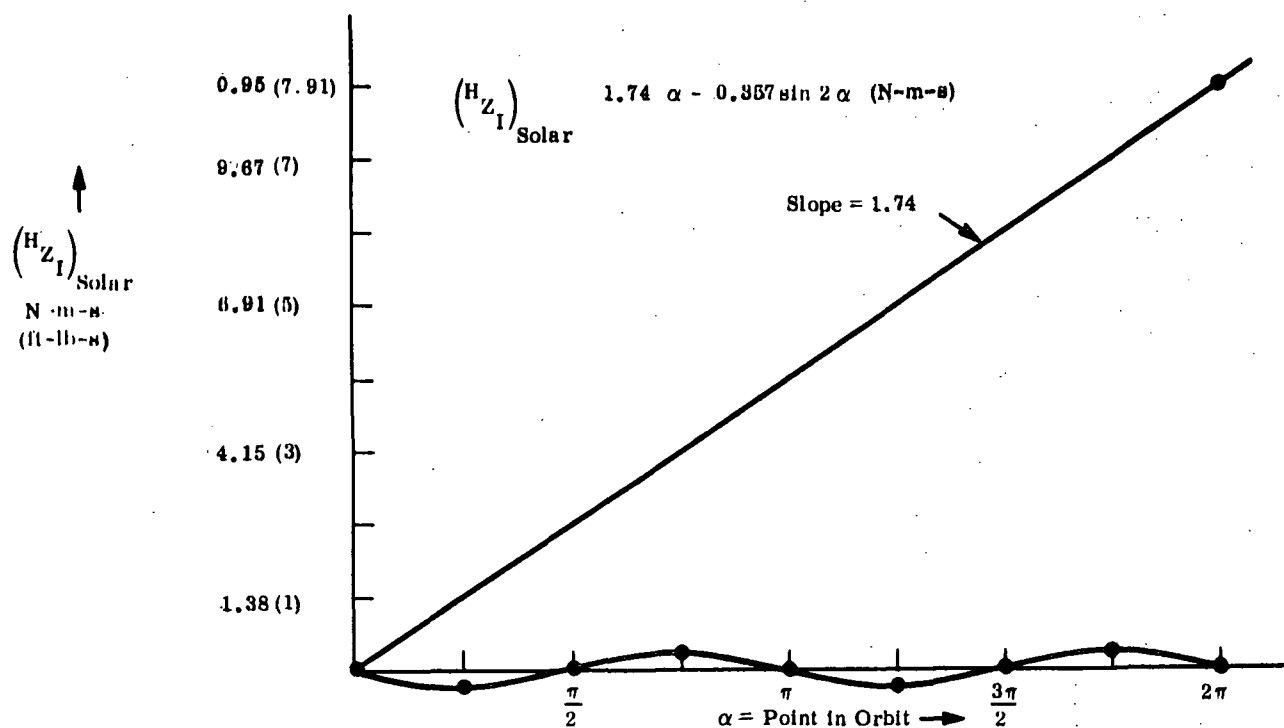
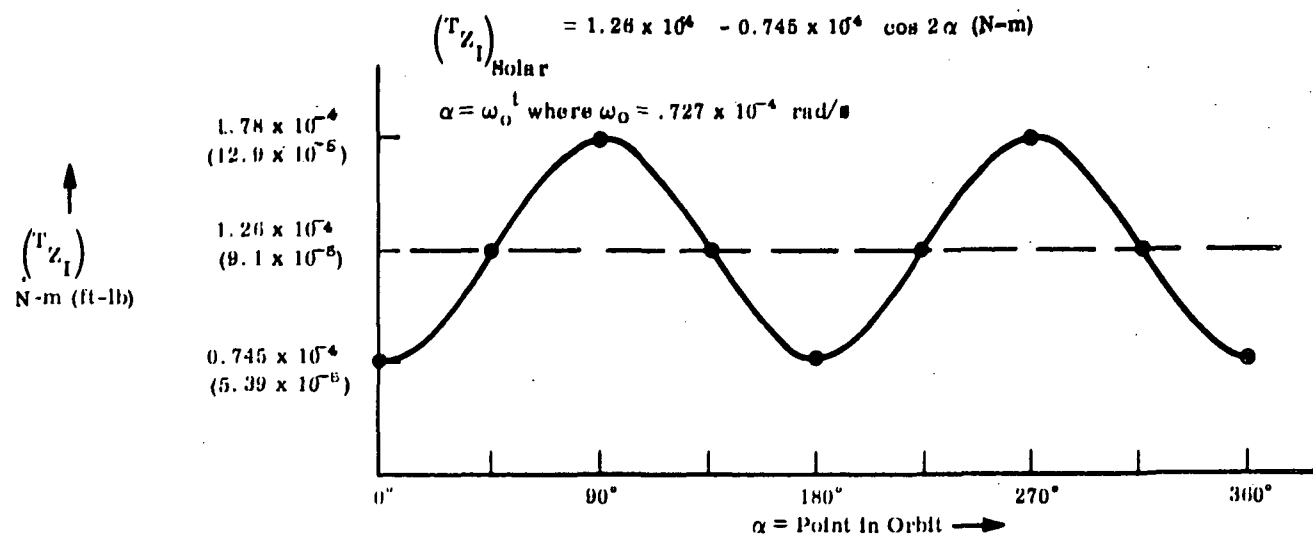


Figure 5.6.2.1-5. Solar Torques and Resulting Momentum Requirements



The purpose of this section is to develop an expression for the gravity gradient torque and to compute the gravity gradient torque acting on the spacecraft and the resulting momentum requirements for the momentum wheels.

Curves showing the gravity gradient torque and the resulting momentum requirements for the  $Y_I$  axis (with  $\phi = 0$ ) are shown in Figure 5.6.2.2-1. The maximum gravity gradient torque about the  $X_I$  and  $Z_I$  axes for a roll offset angle of  $.03^\circ = 5.23 \times 10^{-4}$  rad. is given below:

$$\begin{aligned} \left( T_{GG_{XI}} \right)_{\text{Max}} &= \left| 3 W_o^2 \left( I_{ZI} - I_{YI} \right) \phi \right| = 3 (.727 \times 10^{-4})^2 (16 \times 10^3) (5.23 \times 10^{-4}) \\ &= (13.3 \times 10^{-8} \text{ ft-lb}) = 18.0 \times 10^{-8} \text{ N-m} \\ \left( T_{GG_{ZI}} \right)_{\text{Max}} &= \left| \frac{3}{2} W_o^2 \left( I_{XI} - I_{YI} \right) \phi \right| = (1.5) (.727 \times 10^{-4})^2 (.9 \times 10^3) (5.23 \times 10^{-4}) \\ &= (3.74 \times 10^{-9} \text{ ft-lb}) = 5.05 \times 10^{-9} \text{ N-m} \end{aligned}$$

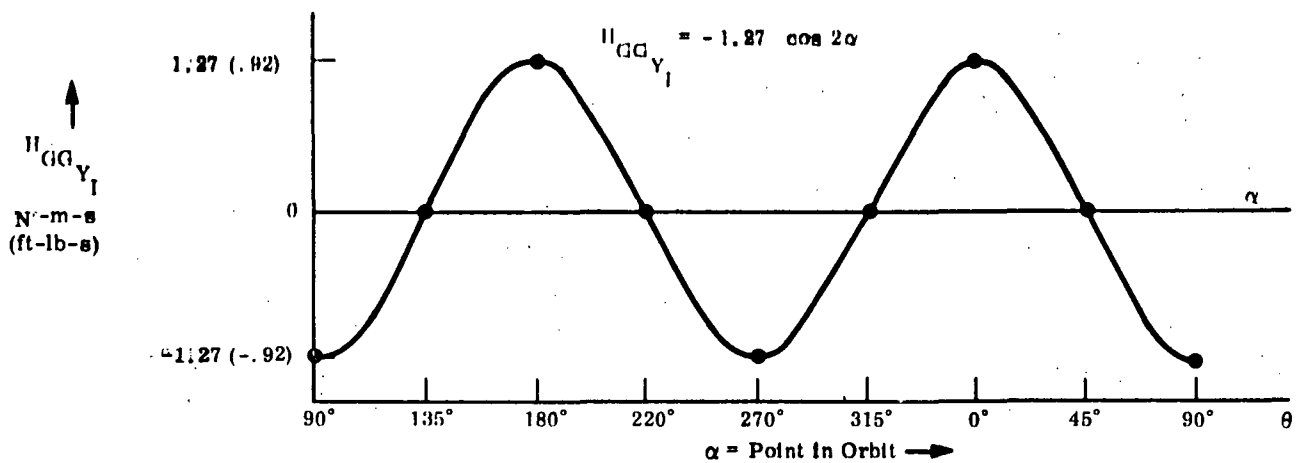
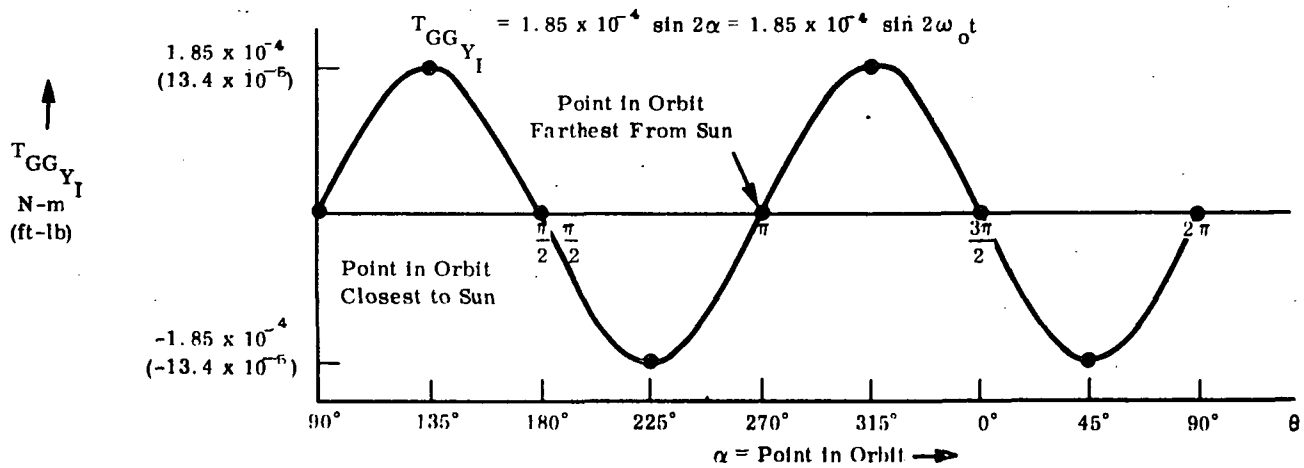
The differential force of gravity on the elemental mass  $dm$  (Figure 5.6.2.2-2) is

$$d\vec{F} = - \frac{GM}{R^2} \hat{R} \, dm$$

The torque about the vehicle c. m. due to  $dF$  follows as:

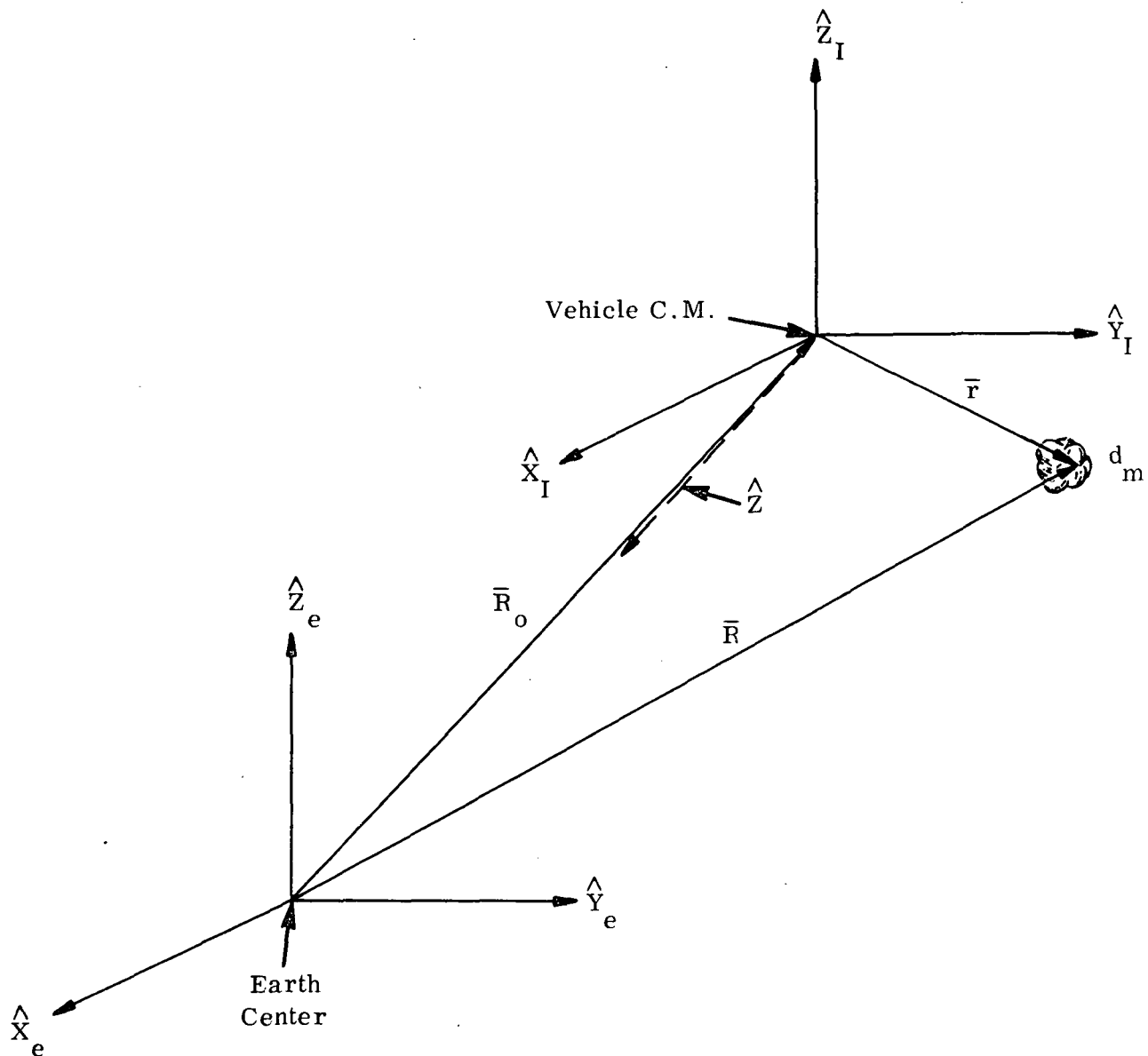
$$(1) \quad d\vec{T}_{GG} = \vec{r} \times d\vec{F} = - \frac{GM}{R^3} (\vec{r} \times \vec{R}) \, dm$$

$$\text{where } R^3 = R_o^3 \left[ 1 + \frac{r^2}{R_o^2} + \frac{2 \vec{R}_o \cdot \vec{r}}{R_o^2} \right]^{3/2}$$



$$\begin{aligned}
 T_{GG_{Y_I}} &\approx \frac{3}{2} \omega_0^2 \sin 2\theta \cos \phi (I_{Z_I} - I_{X_I}) \\
 &\approx \frac{3}{2} \omega_0^2 \sin 2\theta (I_{Z_I} - I_{X_I}) \text{ for } \phi = 0 \\
 &= (1.5)(.727 \times 10^{-4})^2 (1.7 - 18.6)10^3 \sin 2\theta \\
 &= (-13.4 \times 10^{-6} \sin 2\theta \text{ ft-lb}) = -1.85 \times 10^{-4} \sin 2\theta \text{ (N-m)}
 \end{aligned}$$

Figure 5.6.2.2-1. Gravity Gradient Torque and Resulting Momentum Requirements



$\hat{X}_I, \hat{Y}_I, \hat{Z}_I$  is the vehicle body axes unit triad.

$\hat{X}, \hat{Y}, \hat{Z}$  is the local vertical unit triad where the  $\hat{Z}$  axis is pointed toward the earth and the  $\hat{X}$  axis is in the direction of flight.

Figure 5.6.2.2-2. Geometry for Gravity Gradient Torques

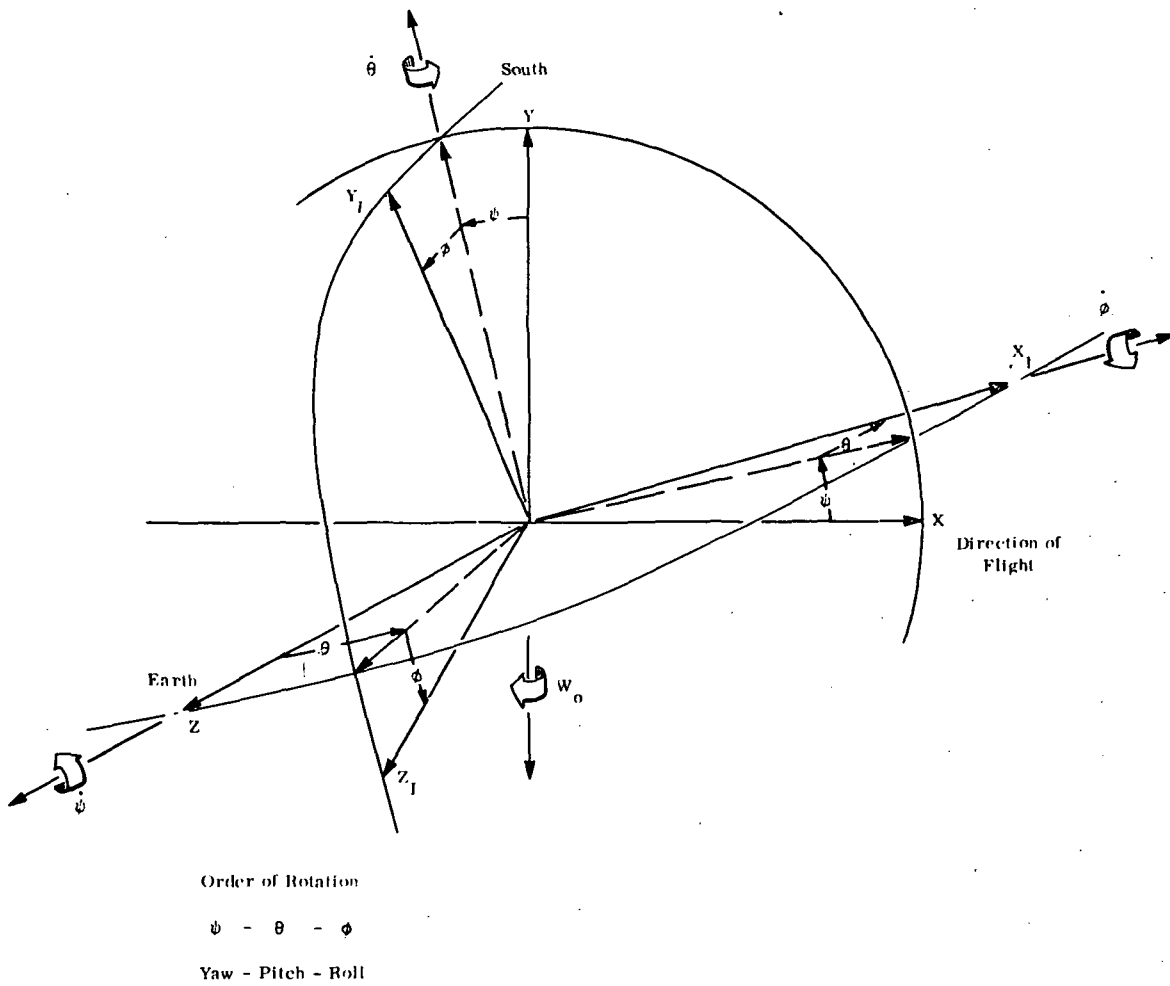


Figure 5.6.2.2-3. Euler Angles

For  $\left(\frac{r^2}{R_o^2}\right) \ll 1$ , the expression  $\frac{1}{R^3}$  becomes

$$\frac{1}{R^3} = \frac{1}{R_o^3} \left[ 1 + \frac{2 \bar{R}_o \cdot \bar{r}}{R_o^2} \right]^{-3/2} \quad \text{which reduces to:}$$

$$\frac{1}{R^3} = \frac{1}{R_o^3} \left[ 1 + \frac{3 \bar{R}_o \cdot \bar{r}}{R_o^2} \right] \quad \text{since}$$

$$(1 + X)^{-3/2} = 1 - \frac{3}{2} X + \frac{3(5)}{(2)(4)} X^2 - \frac{3(5)(7)}{(2)(4)(6)} X^3 \approx 1 - \frac{3}{2} X \quad \text{for } X \ll 1.$$

Substituting into Equation 1 yields

$$\begin{aligned} d\bar{T}_{GG} &= -\frac{GM}{R_o^3} (\bar{r} \times \bar{R}) \left[ 1 - \frac{3 \bar{R}_o \cdot \bar{r}}{R_o^2} \right] d_m \\ &= -\frac{GM}{R_o^3} \left[ R_o \left( \bar{r} \times \frac{\bar{R}}{R_o} \right) - \left( \frac{3 \bar{R}_o \cdot \bar{r}}{R_o} \right) \left( \bar{r} \times \frac{\bar{R}}{R_o} \right) \right] d_m \\ &\approx -\frac{GM}{R_o^3} \left[ R_o \left( \bar{r} \times \frac{\bar{R}_o}{R_o} \right) - \left( \frac{3 \bar{R}_o \cdot \bar{r}}{R_o} \right) \left( \bar{r} \times \frac{\bar{R}_o}{R_o} \right) \right] d_m \end{aligned}$$

where  $\bar{R} = \bar{R}_o + \bar{r} \approx \bar{R}_o$  for  $\bar{r} \ll \bar{R}_o$ .

Defining  $\hat{\bar{Z}} = -\bar{R}_o/R_o$ , the gravity gradient torque acting on the vehicle may be obtained from

$$(2) \quad \bar{T}_{GG} = -\frac{GM}{R_o^3} \left[ R_o \int_{\text{Vol.}} (\bar{r} \times \hat{\bar{Z}}) d_m - 3 \int_{\text{Vol.}} (\hat{\bar{Z}} \cdot \bar{r}) (\bar{r} \times \hat{\bar{Z}}) d_m \right]$$

Because the origin of the vehicle body axes is taken with respect to the vehicle configuration center of mass, Equation 2 reduces to

$$\bar{T}_{GG} = 3 W_o^2 \int_{Vol} (\bar{r} \cdot \hat{Z}) (\bar{r} \times \hat{Z}) d_m \text{ where}$$

$$W_o^2 = \frac{GM}{R_o^3}$$

The gravity gradient torque acting on the vehicle expressed in the vehicle body axes reference frame is

$$\begin{aligned} T_{GG} = & 3 W_o^2 \int_{Vol.} \left\{ Y_I (\hat{Z} \cdot \hat{Z}_I) \left[ X_I (\hat{Z} \cdot \hat{X}_I) + Y_I (\hat{Z} \cdot \hat{Y}_I) + Z_I (\hat{Z} \cdot \hat{Z}_I) \right] \right. \\ & - Z_I (\hat{Z} \cdot \hat{Y}_I) \left[ X_I (\hat{Z} \cdot \hat{X}_I) + Y_I (\hat{Z} \cdot \hat{Y}_I) + Z_I (\hat{Z} \cdot \hat{Z}_I) \right] \left. \right\} \hat{X}_I d_m \\ & + 3 W_o^2 \int_{Vol.} \left\{ Z_I (\hat{Z} \cdot \hat{X}_I) \left[ X_I (\hat{Z} \cdot \hat{X}_I) + Y_I (\hat{Z} \cdot \hat{Y}_I) + Z_I (\hat{Z} \cdot \hat{Z}_I) \right] \right. \\ & - X_I (\hat{Z} \cdot \hat{Z}_I) \left[ X_I (\hat{Z} \cdot \hat{X}_I) + Y_I (\hat{Z} \cdot \hat{Y}_I) + Z_I (\hat{Z} \cdot \hat{Z}_I) \right] \left. \right\} \hat{Y}_I d_m \\ & + 3 W_o^2 \int_{Vol.} \left\{ X_I (\hat{Z} \cdot \hat{Y}_I) \left[ X_I (\hat{Z} \cdot \hat{X}_I) + Y_I (\hat{Z} \cdot \hat{Y}_I) + Z_I (\hat{Z} \cdot \hat{Z}_I) \right] \right. \\ & - Y_I (\hat{Z} \cdot \hat{X}_I) \left[ X_I (\hat{Z} \cdot \hat{X}_I) + Y_I (\hat{Z} \cdot \hat{Y}_I) + Z_I (\hat{Z} \cdot \hat{Z}_I) \right] \left. \right\} \hat{Z}_I d_m \\ (3) \quad T_{GG} = & 3 W_o^2 \left\{ \left[ (\hat{Z} \cdot \hat{Y}_I) (\hat{Z} \cdot \hat{Z}_I) \int_{Vol.} (Y_I^2 - Z_I^2) d_m \right] \hat{X}_I \right. \\ & + \left[ (\hat{Z} \cdot \hat{X}_I) (\hat{Z} \cdot \hat{Z}_I) \int_{Vol.} (Z_I^2 - X_I^2) d_m \right] \hat{Y}_I \\ & \left. + \left[ (\hat{Z} \cdot \hat{Y}_I) (\hat{Z} \cdot \hat{X}_I) \int_{Vol.} (X_I^2 - Y_I^2) d_m \right] \hat{Z}_I \right\} \end{aligned}$$

$$\text{where: } \bar{\mathbf{r}} = X_I \hat{\mathbf{X}}_I + Y_I \hat{\mathbf{Y}}_I + Z_I \hat{\mathbf{Z}}_I$$

$$\hat{\mathbf{Z}} = (\hat{\mathbf{Z}} \cdot \hat{\mathbf{X}}_I) \hat{\mathbf{X}}_I + (\hat{\mathbf{Z}} \cdot \hat{\mathbf{Y}}_I) \hat{\mathbf{Y}}_I + (\hat{\mathbf{Z}} \cdot \hat{\mathbf{Z}}_I) \hat{\mathbf{Z}}_I,$$

$$\bar{\mathbf{r}} \cdot \hat{\mathbf{Z}} = X_I (\hat{\mathbf{Z}} \cdot \hat{\mathbf{X}}_I) + Y_I (\hat{\mathbf{Z}} \cdot \hat{\mathbf{Y}}_I) + Z_I (\hat{\mathbf{Z}} \cdot \hat{\mathbf{Z}}_I),$$

$$\begin{aligned} \bar{\mathbf{r}} \times \hat{\mathbf{Z}} &= \hat{\mathbf{X}}_I \left[ Y_I (\hat{\mathbf{Z}} \cdot \hat{\mathbf{Z}}_I) - Z_I (\hat{\mathbf{Z}} \cdot \hat{\mathbf{Y}}_I) \right] \\ &+ \hat{\mathbf{Y}}_I \left[ Z_I (\hat{\mathbf{Z}} \cdot \hat{\mathbf{X}}_I) - X_I (\hat{\mathbf{Z}} \cdot \hat{\mathbf{Z}}_I) \right] \\ &+ \hat{\mathbf{Z}}_I \left[ X_I (\hat{\mathbf{Z}} \cdot \hat{\mathbf{Y}}_I) - Y_I (\hat{\mathbf{Z}} \cdot \hat{\mathbf{X}}_I) \right], \text{ and} \end{aligned}$$

the products of inertia are assumed to be zero, i. e.

$$(\hat{\mathbf{Z}} \cdot \hat{\mathbf{i}}_I) (\hat{\mathbf{Z}} \cdot \hat{\mathbf{j}}_I) I_{jk_I} = (\hat{\mathbf{Z}} \cdot \hat{\mathbf{i}}_I) (\hat{\mathbf{Z}} \cdot \hat{\mathbf{j}}_I) \int_{\text{Vol.}} j_I k_I d_m = 0$$

$$i = X, Y, Z$$

$$j = X, Y, Z$$

$$k = X, Y, Z$$

$$j \neq k.$$

The moments of inertia about the vehicle body axes are defined as

$$\begin{aligned} I_{XI} &= \int (Y_I^2 + Z_I^2) d_m \\ I_{YI} &= \int (X_I^2 + Z_I^2) d_m \\ I_{ZI} &= \int (X_I^2 + Y_I^2) d_m \end{aligned}$$

From the above definitions,

$$I_{ZI} - I_{YI} = \int (X_I^2 + Y_I^2) d_m - \int (X_I^2 + Z_I^2) d_m = \int (Y_I^2 - Z_I^2) d_m$$

$$I_{XI} - I_{ZI} = \int (Y_I^2 + Z_I^2) d_m - \int (X_I^2 + Y_I^2) d_m = (Z_I^2 + X_I^2) d_m$$

$$I_{YI} - I_{XI} = \int (X_I^2 + Z_I^2) d_m - \int (Y_I^2 + Z_I^2) d_m = (X_I^2 - Y_I^2) d_m$$

Substituting into Eq. (3) gives

$$(4) \quad \bar{T}_{GG} = 3 W_o^2 \left\{ \left[ (\hat{Z} \cdot \hat{Y}_I) (\hat{Z} \cdot \hat{Z}_I) (I_{ZI} - I_{YI}) \right] \hat{X}_I \right. \\ \left. + \left[ (\hat{Z} \cdot \hat{X}_I) (\hat{Z} \cdot \hat{Z}_I) (I_{XI} - I_{ZI}) \right] \hat{Y}_I \right. \\ \left. + \left[ (\hat{Z} \cdot \hat{Y}_I) (\hat{Z} \cdot \hat{X}_I) (I_{YI} - I_{XI}) \right] \hat{Z}_I \right\}$$

The following are defined in Figure 5.6.2.2-3:

$$\hat{Z} \cdot \hat{X}_I = \cos(90 + \theta) = -\sin \theta$$

$$\hat{Z} \cdot \hat{Y}_I = \cos \theta \sin \phi$$

$$\hat{Z} \cdot \hat{Z}_I = \cos \theta \cos \phi$$

Substituting into Eq 4 gives

$$\bar{T}_{GG} = 3 W_o^2 \left\{ \left[ \cos^2 \theta \sin \phi \cos \phi (I_{ZI} - I_{YI}) \right] \hat{X}_I \right. \\ \left. + \left[ -\sin \theta \cos \theta \cos \phi (I_{XI} - I_{ZI}) \right] \hat{Y}_I \right. \\ \left. + \left[ -\sin \theta \cos \theta \sin \phi (I_{YI} - I_{XI}) \right] \hat{Z}_I \right\}$$

$$(5) \quad \bar{T}_{GG} = \frac{3}{2} W_o^2 \left\{ \left[ \cos^2 \theta \sin 2 \phi (I_{ZI} - I_{YI}) \right] \hat{X}_I \right. \\ \left. + \left[ \sin 2 \theta \cos \phi (I_{ZI} - I_{XI}) \right] \hat{Y}_I \right. \\ \left. + \left[ \sin 2 \theta \sin \phi (I_{XI} - I_{YI}) \right] \hat{Z}_I \right\}$$



Assuming small angle approximations yields

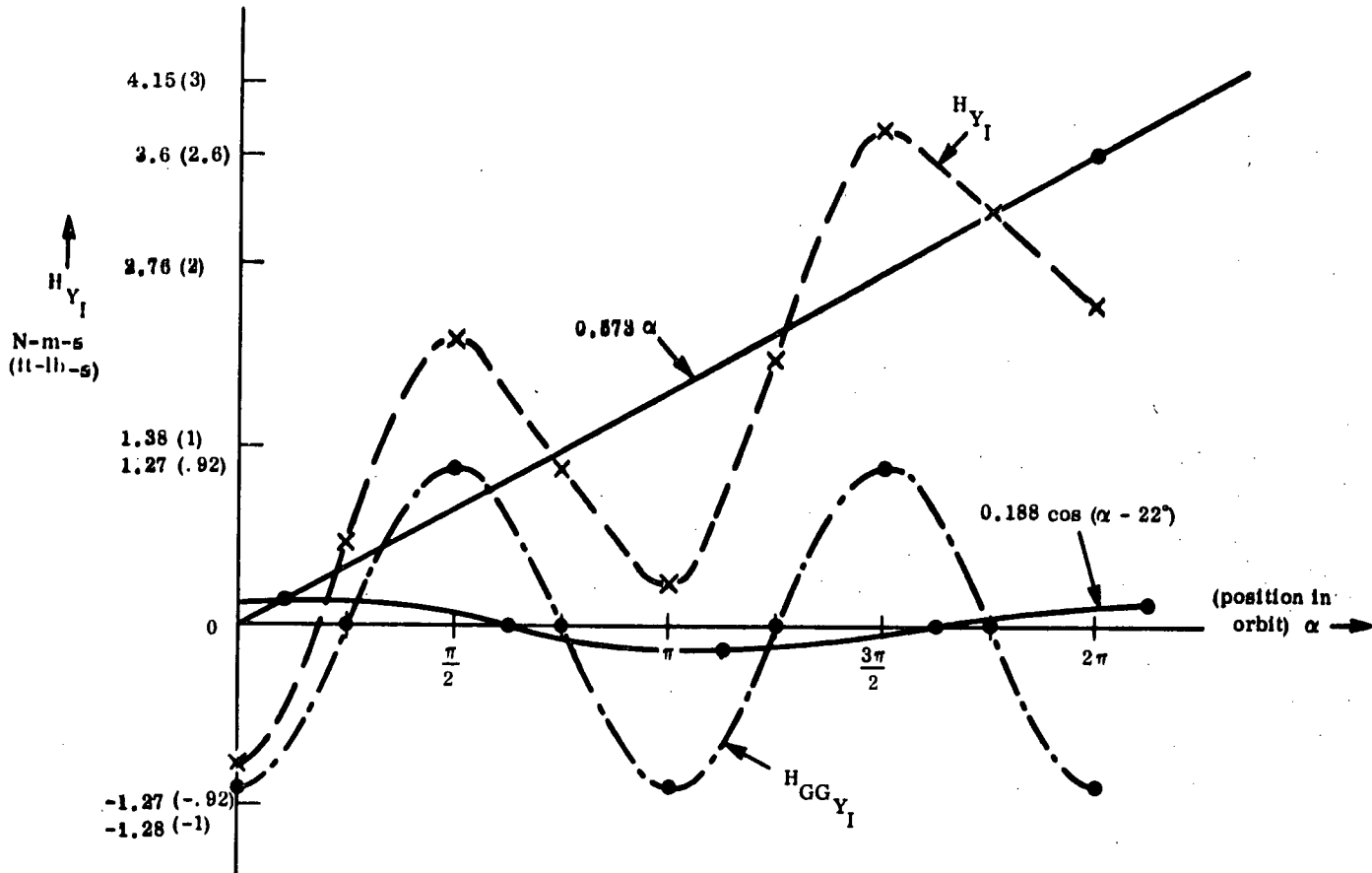
$$(6) \quad \bar{T}_{GG} = 3 W_o^2 \left\{ \Phi(I_{ZI} - I_{YI}) \hat{X}_I + \Theta(I_{ZI} - I_{XI}) \hat{Y}_I + \Theta\Phi(I_{XI} - I_{YI}) \hat{Z}_I \right\}.$$

Neglecting products of small angles gives

$$(7) \quad \bar{T}_{GG} = 3 W_o^2 \left\{ \Phi(I_{ZI} - I_{YI}) \hat{X}_I + \Theta(I_{ZI} - I_{XI}) \hat{Y}_I \right\}.$$

### 5.6.2.3 Summary of Momentum Storage Requirements

The momentum storage requirements due to solar and gravity gradient disturbance torques are shown in Figures 5.6.2.3-1 and 5.6.2.3-2.

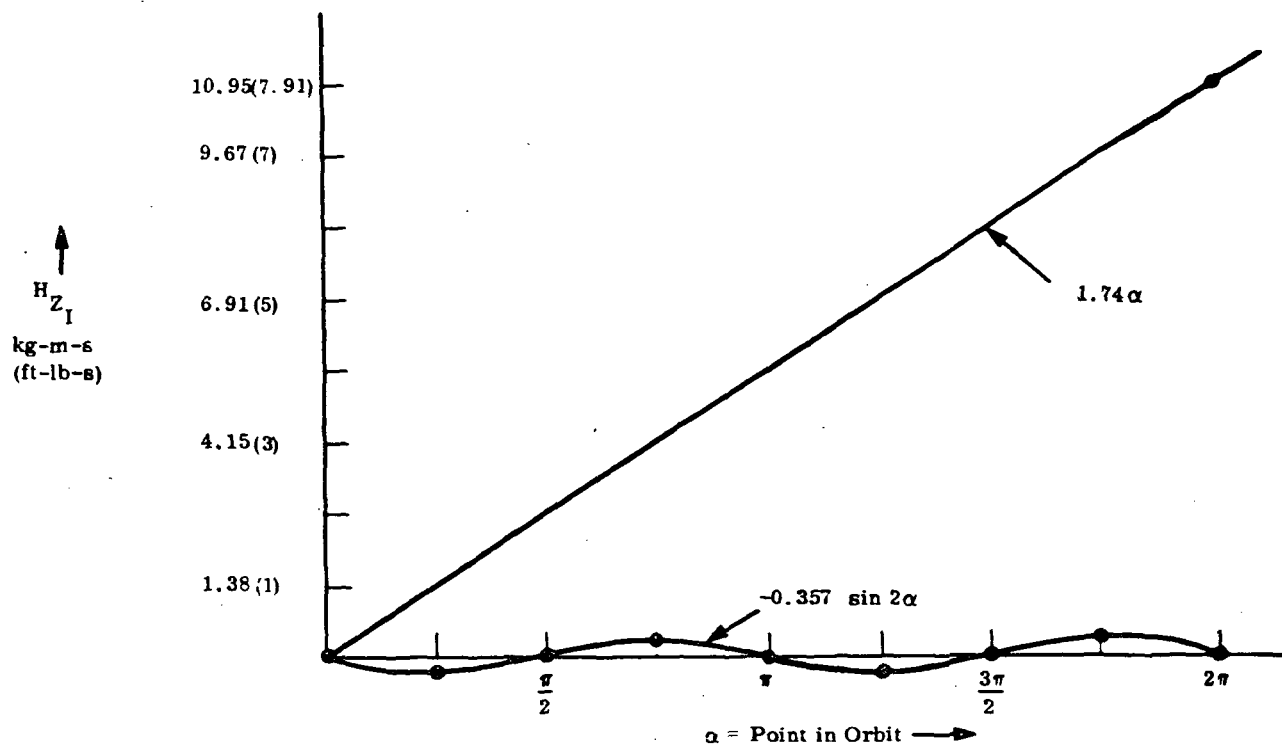


$$\left( H_{Y_I} \right)_{\text{Solar}} = 0.573 \alpha + 0.188 \cos (\alpha - 22^\circ) \quad (\text{N-m-s})$$

$$H_{GG_{Y_I}} = -1.27 \cos 2\alpha \quad (\text{N-m-s})$$

$$H_{Y_I} = \left( H_{Y_I} \right)_{\text{Solar}} + H_{GG_{Y_I}} \quad (\text{N-m-s})$$

Figure 5.6.2.3-1. Momentum Storage Requirements



$$H_{Z_I} = (H_{Z_I})_{\text{Solar}} + \int T_{GG_{Z_I}} dt$$

$$\approx (H_{Z_I})_{\text{Solar}} = 1.74 - 0.357 \sin 2\alpha$$

$$\text{where: } (T_{GG_{Z_I}})_{\text{max}} = 5.17 \times 10^8 \text{ N-m}$$

$$H_{X_I} = (H_{X_I})_{\text{Solar}}^0 + \int T_{GG_{X_I}} dt$$

$$\text{where: } (T_{GG_{X_I}})_{\text{max}} = 1.84 \times 10^7 \text{ N-m}$$

Figure 5.6.2.3-2. Momentum Storage Requirements

### 5.6.3 EQUIPMENT TRADEOFFS FOR ATS-AMS I

The equipment tradeoffs for ATS-AMS I are essentially identical to those for ATS-AMS II & III (Section 5.6.1) with the exception of the parts dealing with the momentum wheels and the IRU.

For geostationary use, a momentum wheel appears best suited to store the effects of the sinusoidal solar torque about the pitch axis caused by the relatively large c.p. - c.g. offset. Over half an orbit, the pitch torque will vary from essentially zero at one terminator to maximum at high noon and back to zero at the other terminator. A momentum wheel of sufficient capacity can store up the angular momentum acquired by the spacecraft and dump it back during the next half-orbit. This does not require the expenditure of attitude control propellant.

For the spiral out mode and initial stabilization, an Inertial Reference Unit (IRU) is the best choice to provide for the variety and complexity of maneuvers needed. If the spacecraft could always have one axis (yaw) pointed toward the earth, then by using a variable field of view earth sensor, 2 axes of information could always be obtained (roll and pitch). Rotational information about yaw could be obtained by a sun sensor once or twice each orbit, but drift in between these check points would be a problem. In addition, commanded yaw maneuvers could not be performed at all points in the orbit. Thus, an inertial reference appears to be necessary.

Linear acceleration and velocity information could be obtained from accelerometers to monitor ascent engine performance.

The IRU could be used in geostationary orbit, but the best gyro system drift rates currently attainable are on the order of .01 degree/hr. Updating by sun sensor for pitch could be done only twice an orbit (once every 12 hrs.) and the resulting 0.12 degree drift exceeds the pointing accuracy requirement of  $\pm .03^\circ$ .

## 5.7

### ORBIT CONTROL

#### 5.7.1

##### EQUIPMENT TRADEOFFS FOR ATS-AMS III & II

Use of the 30 cm mercury bombardment ion engine was an initial study constraint and the only possible tradeoffs concern the proper number to be used. Initially a cluster of three engines was considered. Subsequent analysis reveals that one engine is sufficient.

The orbit plane will precess in the North/South direction approximately  $.8525^\circ/\text{year}$  due primarily to earth's oblateness and ellipticity of the equatorial section. This will require a corrective change in velocity in the North/South direction of  $46 \text{ m/yr}$  ( $152 \text{ ft/yr}$ ) or  $.125 \text{ m/day}$  ( $.41 \text{ ft/day}$ ). One 30 cm ion engine thrusting for 25 minutes/day will give the required change in velocity. The fuel required over a five-year period would be approximately  $13.4 \text{ kg}$  ( $29.5 \text{ lb}$ ).

#### 5.7.2

##### EAST-WEST DRIFT ANALYSIS

The spacecraft will have a tendency to drift in the East/West direction due primarily to the perturbing effects of the sun and the moon. This will require a corrective change in velocity in the East/West direction of  $2.3 \text{ m/yr}$  ( $7.6 \text{ ft/yr}$ ) or  $.0063 \text{ m/day}$  ( $0.2 \text{ ft/day}$ ). Two  $.023 \text{ kg}$  ( $.05 \text{ lb}$ ) hydrazine jets thrusting for 24.2 sec/day will give the required change in velocity. The fuel required over a five year period would be approximately  $9.1 \text{ kg}$  ( $20 \text{ lb}$ ). As a back-up mode, the spacecraft can be oriented to allow the 30 cm ion engine to provide East/West station keeping. Reorientation and return to the original altitude will be via the inertia wheels.

#### 5.7.3

##### EQUIPMENT TRADEOFFS FOR ATS-AMS I

Again, use of the 30 cm mercury bombardment ion engine was an initial study constraint, and the tradeoffs concern the proper number to be

used. Initially a matrix of five engines was considered since such a pattern permitted a high initial thrust and incremental shutdown of the engines as the solar array degraded during passage through the Van Allen belt. Subsequent analysis of the power requirements of the ion engine and its power efficiency, fuel utilization efficiency and specific impulse parameters indicated that a matrix of three engines resulted in a more optimum utilization of the spacecraft's payload and power capabilities.

## 5.8 THERMAL CONTROL ANALYSIS

### 5.8.1 ATS-AMS IIIA

#### 5.8.1.1 Power Dissipation

The preliminary thermal design is based on the assumption that the solar array produces 9200 Watts of raw DC power for the spacecraft at the beginning of the mission. Of this 9200 Watts, a minimum of 7540 Watts is required to maintain the spacecraft in full time operation. For this reason 1660 Watts must be dissipated in the shunts at the beginning of life and practically nothing at the end of life (186 W). This power range is sufficient to maintain the shunt radiator between  $373^{\circ}\text{K}$  and  $208^{\circ}\text{K}$  throughout mission life so that the shunt transistor junction temperature will always fall between  $208^{\circ}\text{K}$  and  $413^{\circ}\text{K}$ .

The remaining power is distributed to the spacecraft module and antenna platform as shown in Table 5.8.1.1-1.

#### 5.8.1.2 Antenna Platform Temperature Control

The mounting platform for the RF Power Amplifier and the DC to DC power converter represents the single most difficult problem in thermal control. While the amplifiers contain their own radiators and are allowed to radiate at a high temperature the converter must dissipate 1000 Watts from a relatively small volume at a maximum of  $308^{\circ}\text{K}$ . A thermal balance on the platform shows that the entire platform area  $4.5\text{ m}^2$  ( $48\text{ ft}^2$ ) must be used as a radiator to maintain the converter and transponder at a reasonable temperature. Should the power amplifiers be turned off during the 1 hour period the ion engines are on, then the platform could drop below the minimum allowable temperature because the heat radiated by the amplifiers is not sufficient to keep the platform warm. In this situation, use of high capacity constant temperature (variable conduction) heat pipes would be an excellent way to resolve the problem. This type of heat pipe would automatically reduce the converter/transponder effective radiator area as the heat load changes. A detailed design study of the

Table 5.8.1.1-1. Power/Heat Distribution Watts

Equipment Platform	MODE I		MODE II	
	Power	Heat	Power	Heat
2 KW TWT	4100	2100	50*	50*
1 KW Kly	50*	50*	50*	50*
10-200 W TWT	200*	200*	4400	2400
Switches	400	400	400	400
Subtotal	4750	2750	4900	2900
DC/DC Converter	1000	1000	1000	1000
Transponders	400	400	400	400
Totals	6150	4150	6300	4300

Spacecraft Module Heat Load	Min.	Max.
Battery	72	106
T T & C	45	45
AC	170	170
Converter	340	900
Antenna Drive	10	10
Experiments	100	225
Totals	737	1356

\* Heater power on 100%



platform heat load and mission requirement is needed to adequately define its thermal design requirement.

#### 5.8.1.3 S/C Module Temperature

The spacecraft module temperature is controlled by louvers which regulate the module emittance as required by the heat load. The louver control characteristics are shown in Figure 5.8.1.3-1.

Subtracting the area blocked by the solar array storage volume from both solar array sides and the anti-solar side of the spacecraft, there is  $8.39 \text{ m}^2$  ( $90.4 \text{ ft}^2$ ) available for thermal radiators. If 100% of this area were covered by louvers the spacecraft module could dissipate between 400 and 2250 Watts with a temperature range of from  $273^\circ\text{K}$  to  $293^\circ\text{K}$ . This is in excess of 737 to 1356 watts required, therefore only 59% of the area ( $4.51 \text{ m}^2$ ) needs to be covered with louvers. The remainder of the surface is insulated.

#### 5.8.1.4 High Voltage Array Experiment

The High Voltage Experimental Array is located on the sub-solar side of the spacecraft. The solar cells, having a high solar absorptance to emittance ratio, can get very hot on this surface. A high temperature is undesirable for both the spacecraft interior and the solar array voltage characteristics, therefore a highly reflective coating is interspaced with the solar cells so that the temperature is reduced. A long life coating suitable for this purpose is the Optical Solar Reflector (OSR) having an  $\alpha/\epsilon$  ratio of 0.1/.8. Figure 5.8.1.4-1 shows the variation in temperature as the % OSR covering is increased. At least 80% OSRs could be used to control the temperature of the surface between  $273^\circ\text{K}$  to  $293^\circ\text{K}$ . This is in excess feasible to mount equipment to the interior of the subsolar side.

#### 5.8.2 ATS-AMS II

The ATS-AMS II is a smaller spacecraft which is launched directly into a sun oriented synchronous orbit. Lack of space on the space viewing sides of the spacecraft necessitates an internal equipment shelf which must be cooled by heat pipes.

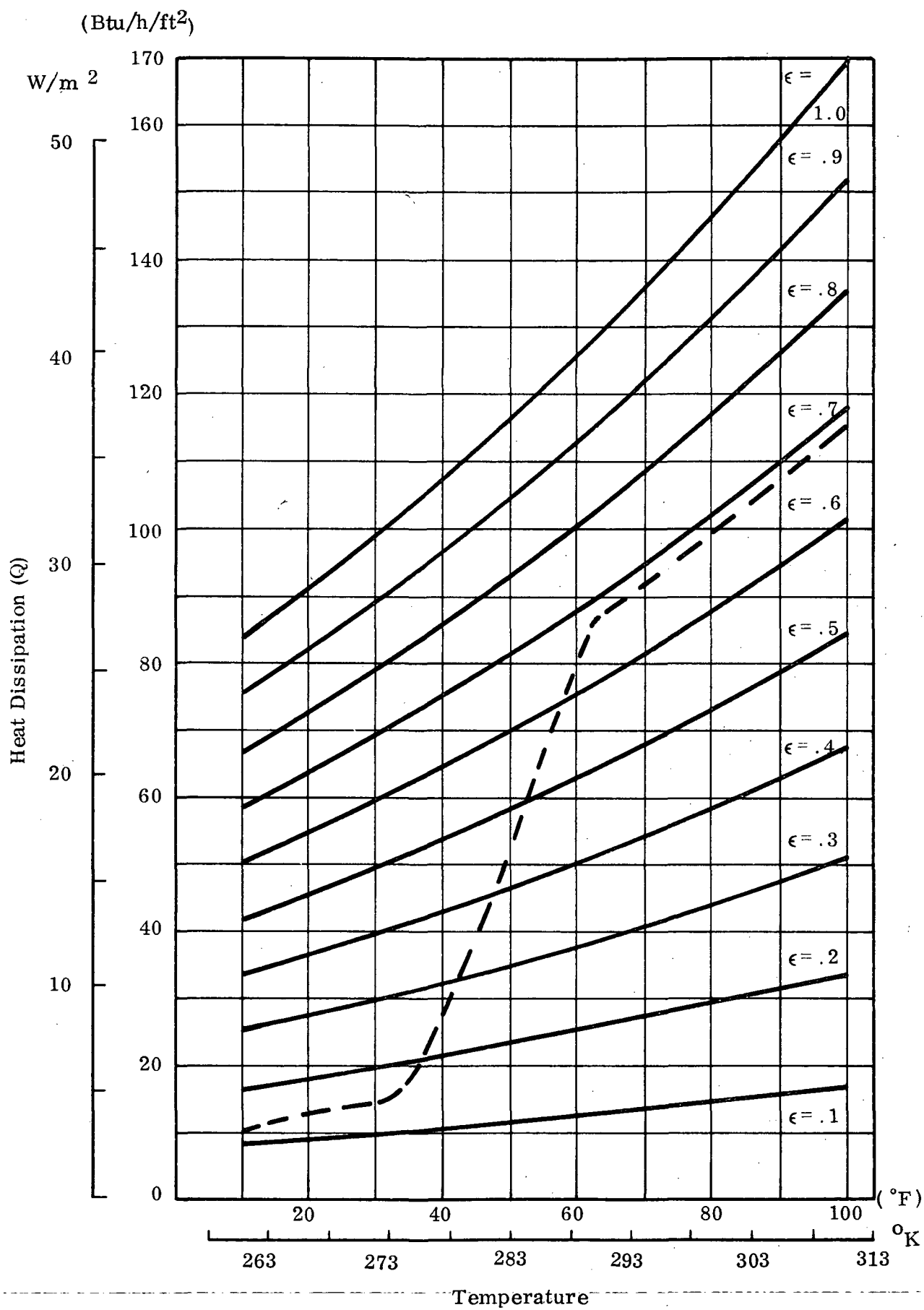


Figure 5.8.1.3-1. Louver Control Characteristics

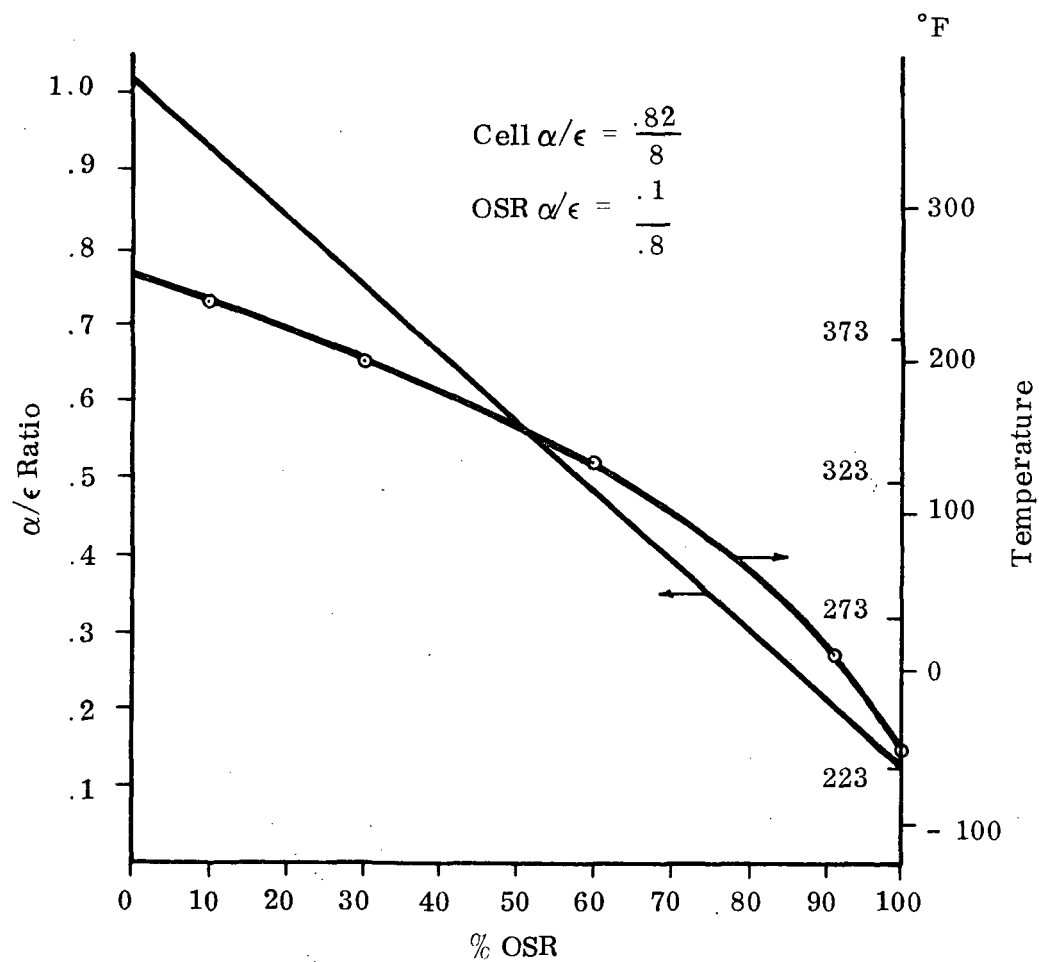


Figure 5.8.1.4-1. Temperature of High Voltage Solar Array Experiment as a Function of Percent Ratio of Optical Solar Reflection

The spacecraft thermal control design is dictated primarily by the electronic and optical components' functional reliability for a five year mission life. Due to power fluctuation and changing orbital environmental conditions, the spacecraft heat rejection requirements vary from 300 to 1000 watts. The thermal design proposed provides the flexibility to accommodate the variations in heat rejection rates while maintaining the temperatures within the required limits. The flexible heat rejection in narrow radiator temperature band is achieved by louver assemblies which vary the effective emittance of the spacecraft radiator surfaces. A typical louver assembly is capable of an effective emittance variation from 0.14 to 0.7. Hence the heat rejection turndown ratio of 5, would require 100% louvered radiator. Lower turndown ratios are achieved by proportioning a louvered radiator and passive radiator such that the heat rejection variations are achieved within the operating temperature ranges.

The ATS-AMS II has low temperature radiators on 2 sides only. The north side of the spacecraft is  $1.0 \text{ m}^2$  ( $10.8 \text{ ft}^2$ ) louvered area. The side facing away from the sun has  $2.0 \text{ m}^2$  ( $21.6 \text{ ft}^2$ ) of passive radiator area. The two radiators and internal equipment shelf are conductively coupled by "U" shaped heat pipes.

#### 5.8.3

##### ATS-AMS I

The preliminary thermal design of the ATS-AMS I earth oriented spacecraft uses a  $4.5 \text{ m}^2$  ( $48.5 \text{ ft}^2$ ) low temperature radiator. The two sides of the spacecraft where solar arrays are mounted will be louvered to give  $2.25 \text{ m}^2$  ( $24 \text{ ft}^2$ ).

louvered radiator. The side facing away from the earth will have 2.25 m<sup>2</sup> (24 ft<sup>2</sup>) passive radiator. The louvered radiator sides will be conductively coupled with heat pipes to achieve the required load distribution to maintain 278-308°K radiator temperature. The passive radiator surface may require heaters to maintain the equipment temperature above 278°K during quiescent mode. The heat pipes shall be 1.27 cm (.5 in) outside diameter grooved/ammonia configuration similar to those used on ATS/F&G spacecraft. The heat pipes spacing of 8.9 cm (3 1/2 inches) is based on Fairchild in-house evaluations. The remaining three sides will be superinsulated with 30 layers of 1/8 mil perforated double aluminized mylar separated by 15 denier nylon netting. The perforations shall be random and shall not exceed .5% area. The effective emittance of this insulation will be better than 0.01.

#### 5.8.4

##### ION ENGINE TEMPERATURE CONTROL

The ion engine cluster external surfaces are painted black and thermal control is achieved by passive radiation. Heaters are provided for quiescent thermal control of the propulsion equipment. The inboard side of the engine cluster is insulated by superinsulation consisting of 10 layers of Nickel foil/Inconel Mesh, 20 layers of 1/2 mil aluminized Kapton, and 20 layers of 1/8 mil perforated double aluminized mylar separated by 15 denier nylon netting. The effective emittance of such composite, based on tests, is expected to be 0.005. The inboard maximum heat leak of 12 watts is anticipated.

The baseline spacecraft design shows a cluster of three ion engines mounted on -X surface of the spacecraft. Figure 5.8.4-1 shows the 16 node diagram of a thermal model which was used to predict engine operating temperatures. Table 5.8.4-1 shows the steady state temperatures of the 16 nodes when one, two or three thrusters are operating.

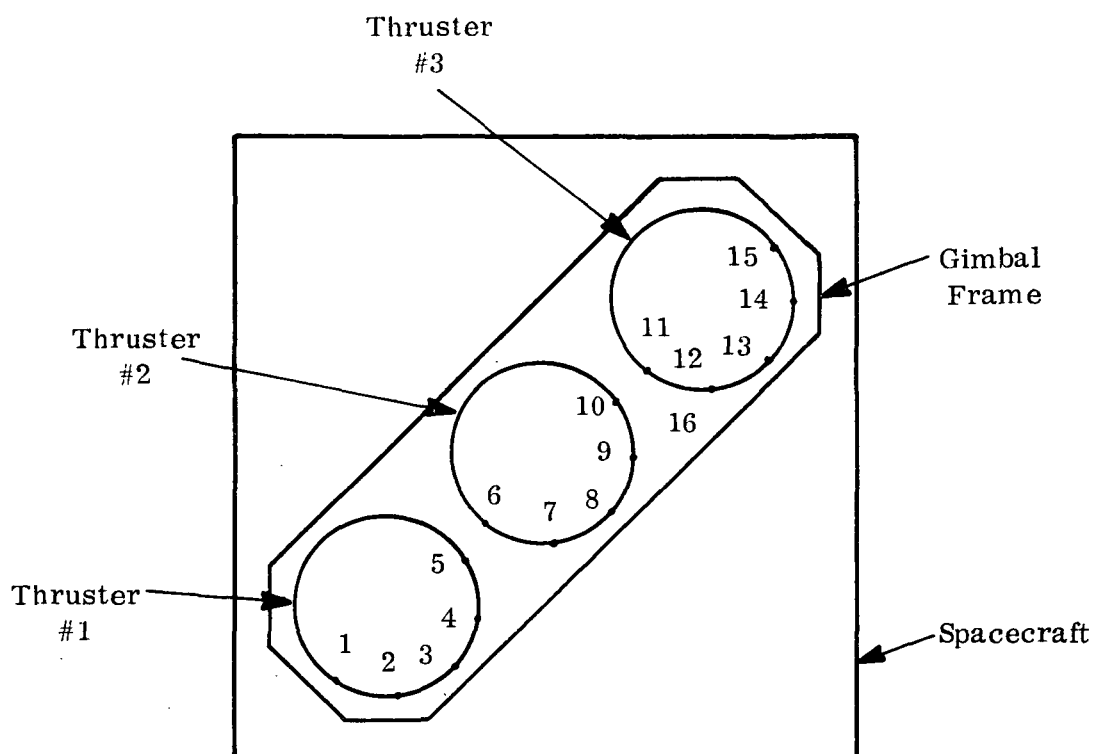


Figure 5.8.4-1 Ion Engine Cluster Node

Table 5.8.4-1. Ion Engine Cluster Thermal Analyses Steady  
State Node Temperatures - °K

Node #	Thrusters 1, 2, & 3 On	Thrusters 1 & 3 On	Thruster 2 On
1	455	455	197
2	458	456	209
3	464	458	257
4	520	468	386
5	600	507	463
6	600	414	505
7	520	392	467
8	471	290	459
9	521	317	467
10	600	320	505
11	600	339	463
12	520	388	386
13	464	450	257
14	458	465	209
15	455	529	197
16	512	425	1

## SOLAR ARRAY TEMPERATURES

Maximum solar array temperatures occur in the ATS AMS I version which starts out in a low orbit. The earth albedo tends to increase the the array temperature at low altitudes. The AMS II and III versions are not affected by albedo due to their high altitudes. Figure 5.8.5-1 shows how the array temperature will vary with altitude.

The minimum low temperature of the array occurs at the end of occult period in synchronous orbit. The minimum temperature is calculated to be  $144^{\circ}\text{K}$  ( $-200^{\circ}\text{F}$ ) for this condition. At exit from occult the low temperature causes a voltage surge from the array. The transient analysis of the array emerging from earth's shadow is shown in Figure 5.8.5-2. The curves are plotted for maximum ( $1532 \text{ Joules}/\text{m}^2 \text{ }^{\circ}\text{K}$ ) and minimum ( $613 \text{ Joules}/\text{m}^2 \text{ }^{\circ}\text{K}$ ) of array thermal mass (mass per unit area x specific heat of the array composite). This information can be used to determine the solar array power surge and to design power management system. The array initial temperature of  $144^{\circ}\text{K}$  ( $-200^{\circ}\text{F}$ ) has been used in developing the transient response curves.



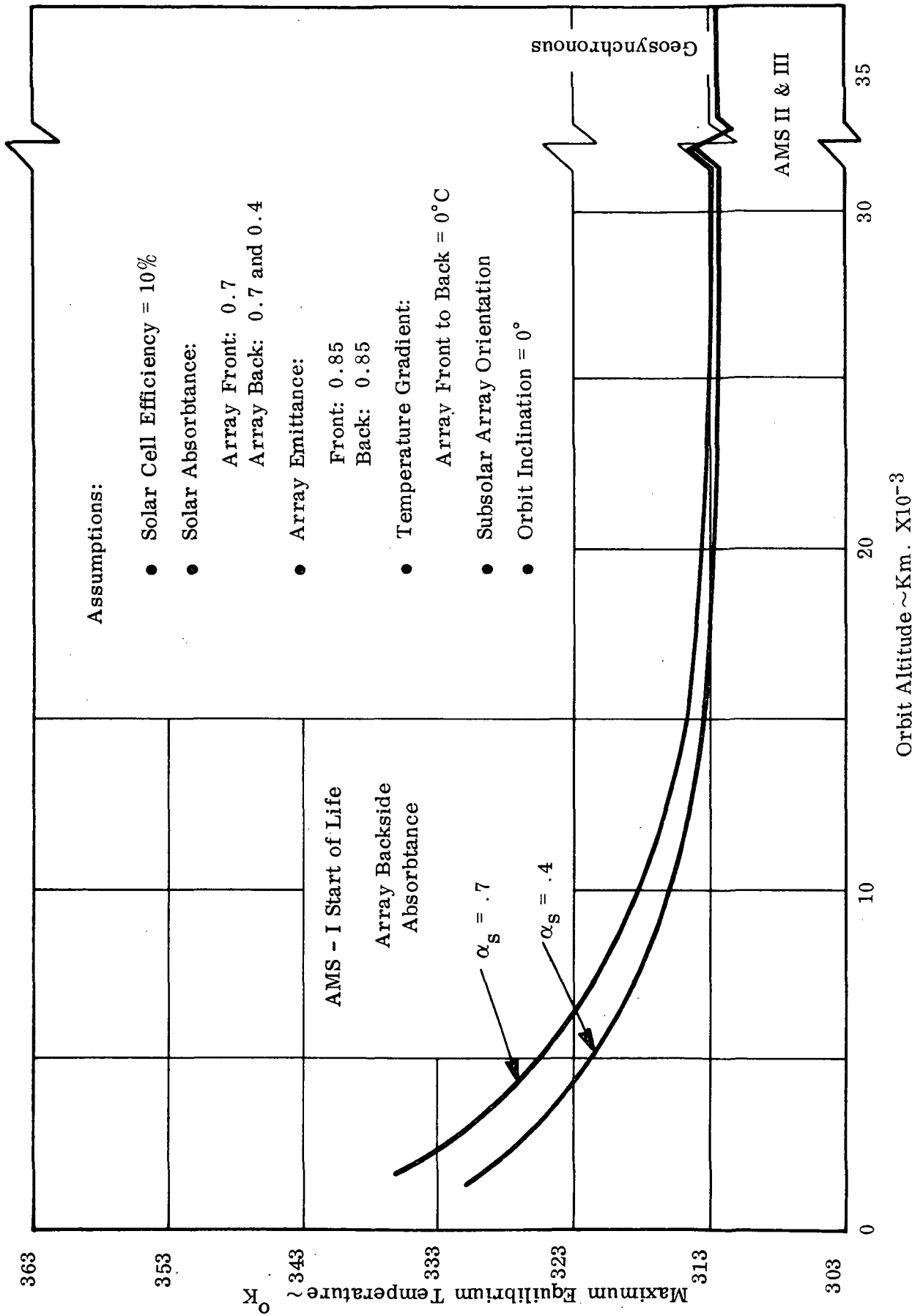


Figure 5.8.5-1 Maximum Temperatures of Flexible Solar Arrays

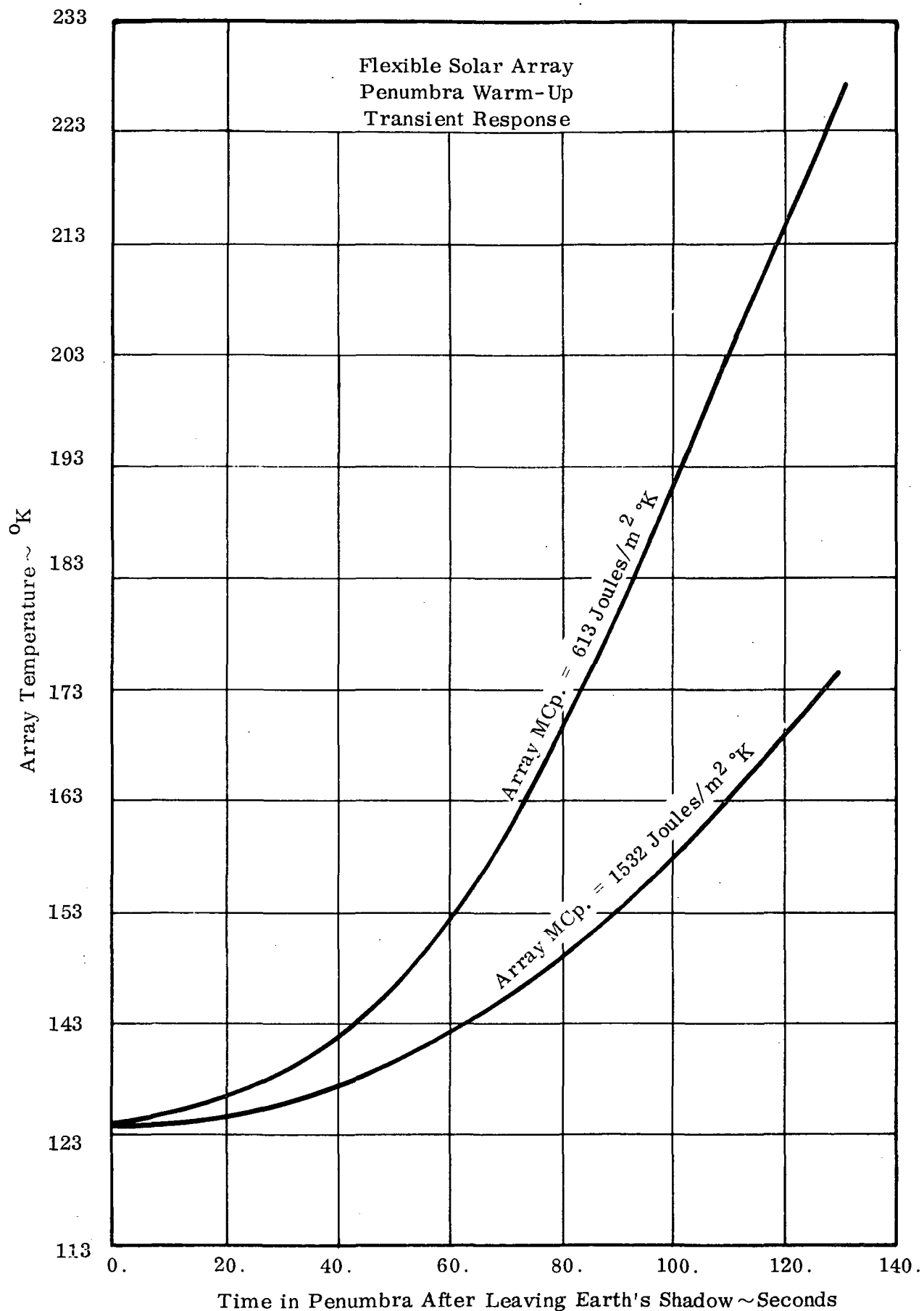


Figure 5.8.5-2 Array Transient Warm-Up

## SPACECRAFT INSULATION

Multilayer insulation performance depends upon the reflecting properties and the separation characteristics of the insulation composites. The insulation system effectiveness depends upon thermal leakage characteristics of the penetrations and the insulation support system. The penetration heat leak can be minimized by good design practice using low conductivity penetrations and covering all optical holes in the insulation. The number of insulation layers in the composite depends upon the trade-off between the weight penalty of the insulation system and with the heat leakage associated with the system. The ideal insulation system would have no conduction between the layers and minimum radiation coupling between the layers. ATS spacecraft insulation system consists of  $.32 \times 10^{-3}$  cm ( $.12 \times 10^{-3}$  in) double aluminized mylar having aluminum side emittance between .025 and .03, corresponding to approximately two ohms per square.

The spacing material will be 15 denier nylon netting. The performance of the insulation blanket is best presented as variation of effective emittance with number of layers of aluminized mylar. It is evident that the maximum number of layers for aluminized mylar multi-layer insulation should not exceed 30 layers.

#### 5.8.7

##### HEAT PIPES

The heat pipes are used to achieve structure isothermalization and thermal load distribution with minimum temperature gradient. Of all the heat pipes tested, the grooved ammonia heat pipes are the most successful. The latest test data of these heat pipes, obtained from reference (1), is used for the design of ATS AMS spacecraft thermal control system. Figure 5.8.7-1 shows the variation of the heat pipe temperature gradient with the heat transfer rate for grooved ammonia (1.27 cm inside diameter, 89 cm long) heat pipe. The data is used to determine the number of heat pipes required for a given load transfer rate to isothermalize the structure.

#### 5.8.8

##### SHUNT RADIATOR

The passive radiator operating temperature  $233^{\circ}\text{K}$  to  $373^{\circ}\text{K}$  differs significantly from the louvered radiator  $278^{\circ}\text{K}$  to  $308^{\circ}\text{K}$ . When the spacecraft shunt dissipators are turned off, the passive radiator panels must be maintained above  $233^{\circ}\text{K}$ . Heaters are provided to achieve the required temperature. The variation of passive radiator heater power with the passive radiator area is shown in Figure 5.8.8-1.

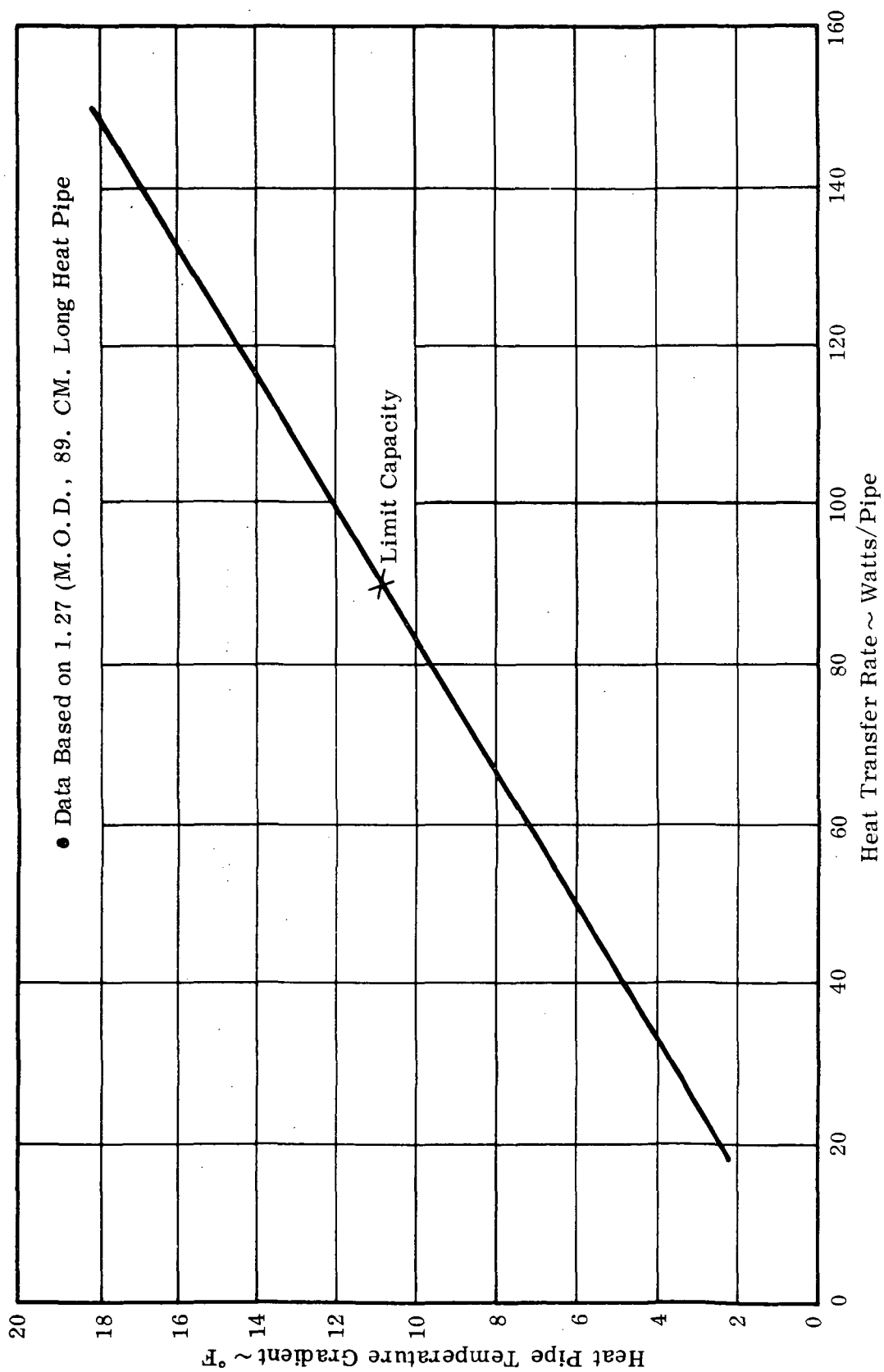


Figure 5.8.7-1. Performance of Grooved Ammonia Heat Pipes

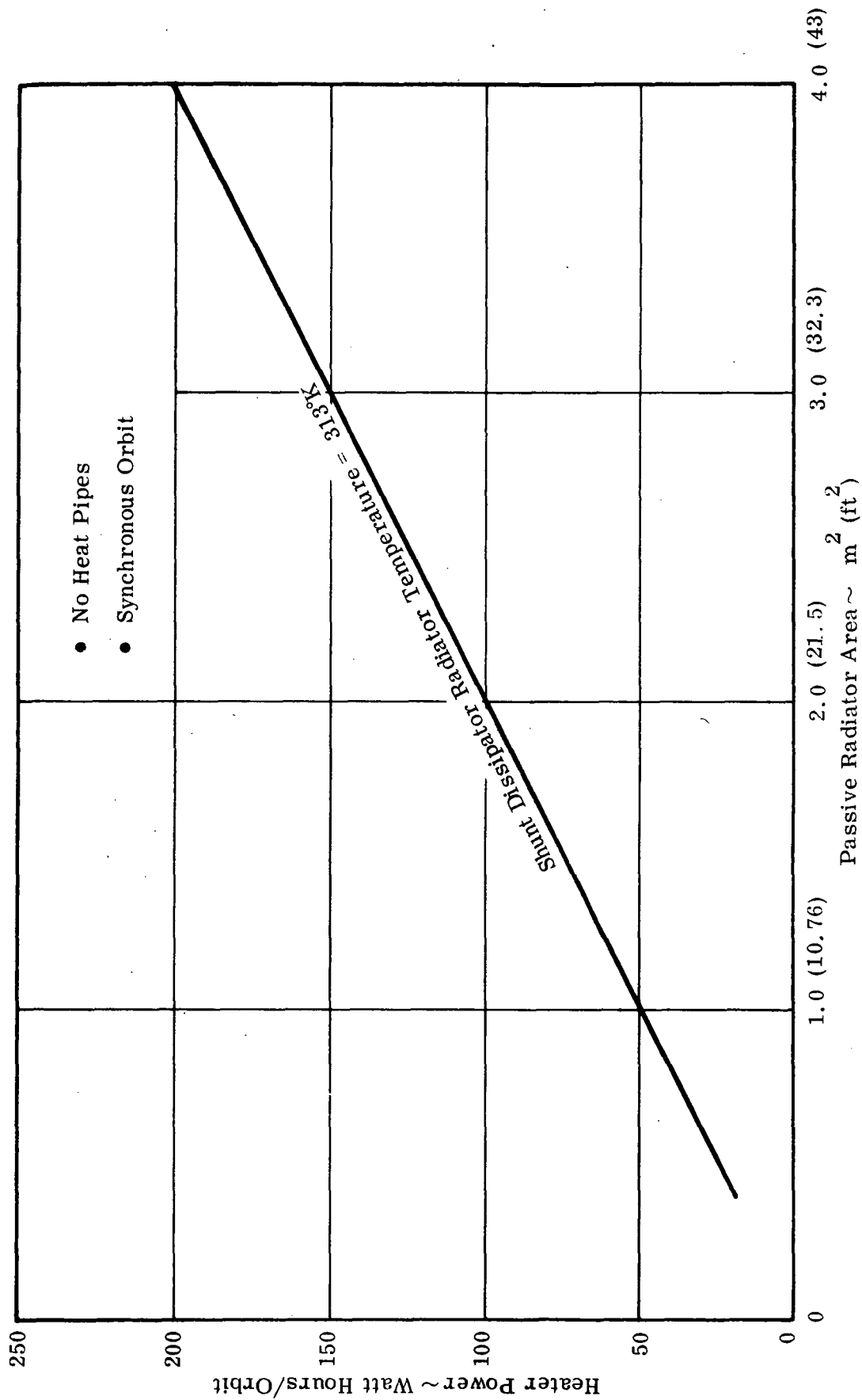


Figure 5.8.8-1. Heater Power Required for Passive Radiator

Since the Telemetry and Command subsystem is to be of conventional design, compatible for operation within the STADAN network and satisfying the requirements of the Aerospace Data Systems Specification, the design of that system was straightforward with no real tradeoff analysis required. The Telemetry and Command subsystem was thus developed as an adaptation of the ATS-F/G T & C to allow it to satisfy the specialized requirements of the ATS-Advanced Mission Spacecraft.

Analysis of the command and telemetry communication links indicates that sufficient margin exists for both the  $\pm 17^\circ$  cone with antenna gain of -3 dB and for the 90% spherical with -10 dB gain to insure satisfactory performance; i.e.  $10^{-5}$  bit error rate. For the VHF telemetry link, spacecraft transmitter power is 3 dBW with the ground antenna gain 21 dB and ground receiver noise figure 3 dB. For the command link, ground transmitter power is 34 dBW,  $G_T$  is 17 dB and the spacecraft receiver noise figure is 8 dB (TA - 1000°K).

STRUCTURAL ANALYSIS

The analysis of the ATS-AMS III was pursued to the conclusion that the concept was structurally feasible and could meet the structural and vibration requirements. The analysis was performed in three principal investigations: weight estimation, mass properties and design criteria.

## 5.10.1

## WEIGHT ANALYSIS

The structure weight was determined and summarized in Table 5.10.1-1. These weights are based on a detailed weight analysis of each subsystem and a breakdown of these subsystem weights may be found in Tables 5.10.1-2 thru 5.10.1-7. The weights are based on empirical data derived from the ATS-F spacecraft where ever possible, and from preliminary structural sizing where similarity did not exist.

All of the subsystem weights include a nominal contingency ranging from 2% to 10% depending upon the weight maturity to account for the difference between the analytically determined weight and the most probable weight the subsystem will have when built.

Table 5.10.1-1. Structural System Weight Summary

Subsystem	Weight	
	kg	(lbs)
Adapter Assembly	32.8	72.2
Equipment Module	149.9	330.8
Rotating Platform	68.6	151.1
Reflector Deployment	33.3	73.4
Solar Array	248.2	407.0
Parabolic Reflector	45.0	99.0
TOTAL 577.8		(1,133.5)



Table 5.10.1-2. Equipment Module Weight Summary

Item		Weight	
		kg	(lbs)
Frame Structure Assembly		47.7	105.1
Corner Fittings	11.5 (26.4)		
Frame Assembly	23.0 (50.7)		
Corner Angles	1.4 ( 3.1)		
Separation Guides	4.5 (10.0)		
Fittings, Hwd, Angles	6.8 (14.9)		
Non-Rotating Tunnel		12.3	27.2
Ring Frames	7.8 (17.2)		
Webs	3.4 ( 7.4)		
Stiffeners	0.6 ( 1.4)		
Att. Hwd.	0.5 ( 1.2)		
Exterior Panels		77.1	170.2
External Walls	61.6 (136.0)		
Fwd. Shelf	6.8 ( 14.9)		
Aft. Shelf	5.1 ( 11.3)		
Att. Hwd.	3.6 ( 8.0)		
Ion Engine Support Assy.		5.7	12.6
Contingency		7.1	15.7
		—	—
TOTAL		149.9	(330.8)

Table 5.10.1-3. Rotating Platform Weight Summary

Item			Weight	
			kg	(lbs)
Tunnel Structure			18.2	39.9
Ring Frames	8.1	(17.8)		
Webs	7.2	(15.9)		
Stiffeners	2.4	( 5.2)		
Att. Hwd.	0.5	( 1.0)		
Platform Assembly			36.0	79.5
Sandwich Panel	20.2	(44.5)		
Outer Ring	8.4	(18.5)		
Gussets	5.7	(12.7)		
Att. Hwd.	1.7	( 3.8)		
Bearing Installation			8.2	18.0
Contingency			6.2	13.7
TOTAL			68.6	(151.1)

Table 5.10.1-4. Reflector Deployment System Weight Summary

Item			Weight	
			kg	(lbs)
Reflector Deployment System			15.3	33.7
Glides	4.8	(10.6)		
Truss Members	2.5	( 5.5)		
Guides	7.2	(15.9)		
Fittings	0.8	( 1.7)		
Feed Deployment System			7.5	16.5
Glides	1.9	( 4.2)		
Truss Members	1.0	( 2.2)		
Guides	2.9	( 6.4)		
Fittings	0.3	( 0.7)		
Feed Supt.	1.4	( 3.0)		
Deployment Mechanisms			7.5	16.5
Contingency			3.0	6.7
TOTAL			33.3	(73.4)

Table 5.10.1-5. Solar Array Weight Summary

Item		Weight	
		kg	(lbs)
Solar Array Blanket		90.0	200.0
Boom Assembly		28.0	62.0
Arms	12.7 (28.0)		
Fittings	3.6 ( 8.0)		
Depl. Mechanisms	9.0 (20.0)		
Att. Hwd.	2.7 ( 6.0)		
Storage System		18.0	40.0
Drum	13.5 (30.0)		
Fittings	1.8 ( 4.0)		
Bearings	0.9 ( 2.0)		
Misc.	1.8 ( 4.0)		
Array Support System		7.2	16.0
Spreader Bar	4.5 (10.0)		
Fittings	2.7 ( 6.0)		
Hoist Mechanism		9.0	20.0
Cable Drum	1.8 ( 4.0)		
Cable, Pulleys	2.7 ( 6.0)		
Motor, Gear	4.5 ( 10.0)		
Launch Restraints		14.4	32.0
Contingency		16.8	37.0
TOTAL		248.2	(407.0)

Table 5.10.1-6. Parabolic Reflector Weight Summary.

Item		Weight	
		kg	(lbs)
Reflector Assembly		29.6	65.0
Parabolic Reflector	28.2 (62.0)		
Supt. Ring, Misc.	1.4 ( 3.0)		
Tower Assembly		11.3	25.0
Tower Structure	9.5 (21.0)		
Adapter, Misc.	1.8 ( 4.0)		
Contingency		4.1	9.0
TOTAL		45.0	(99.0)

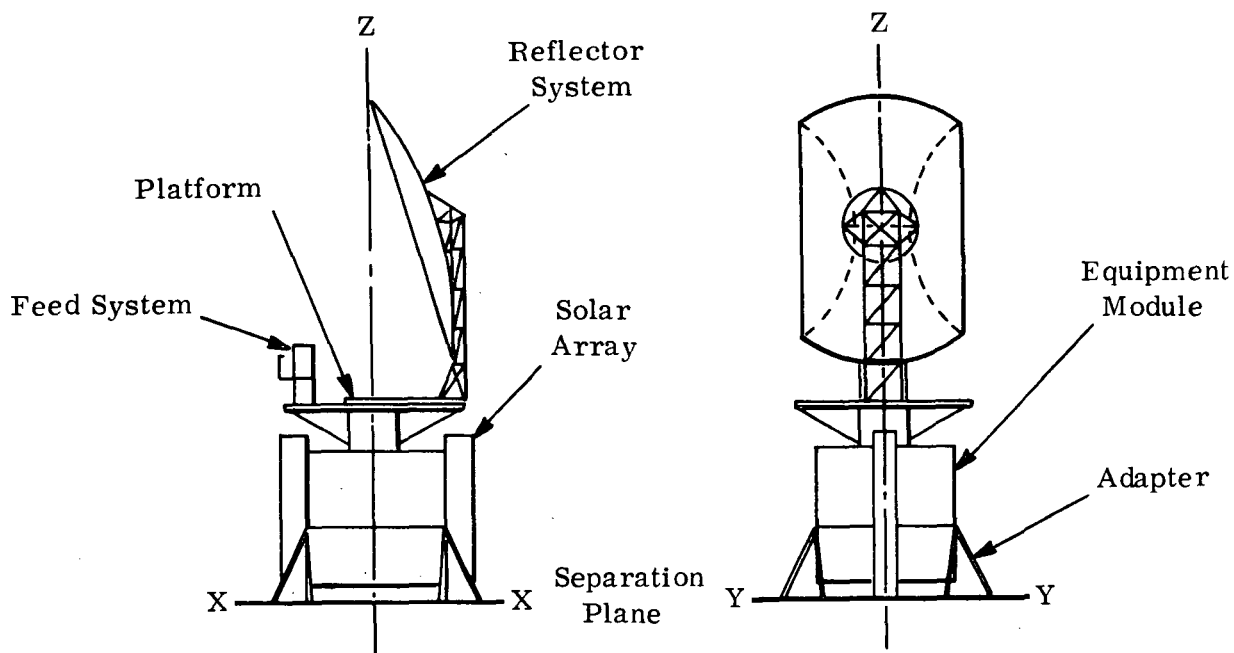
Table 5.10.1-7. Adapter Assembly Weight Summary

Item		Weight	
		kg	(lbs)
Struts		17.3	38.0
Lower Fittings		2.0	4.4
Upper Fittings		4.9	10.8
Separation Mechanisms		8.0	17.6
Contingency		0.6	1.4
TOTAL		32.8	(72.2)

#### 5.10.2

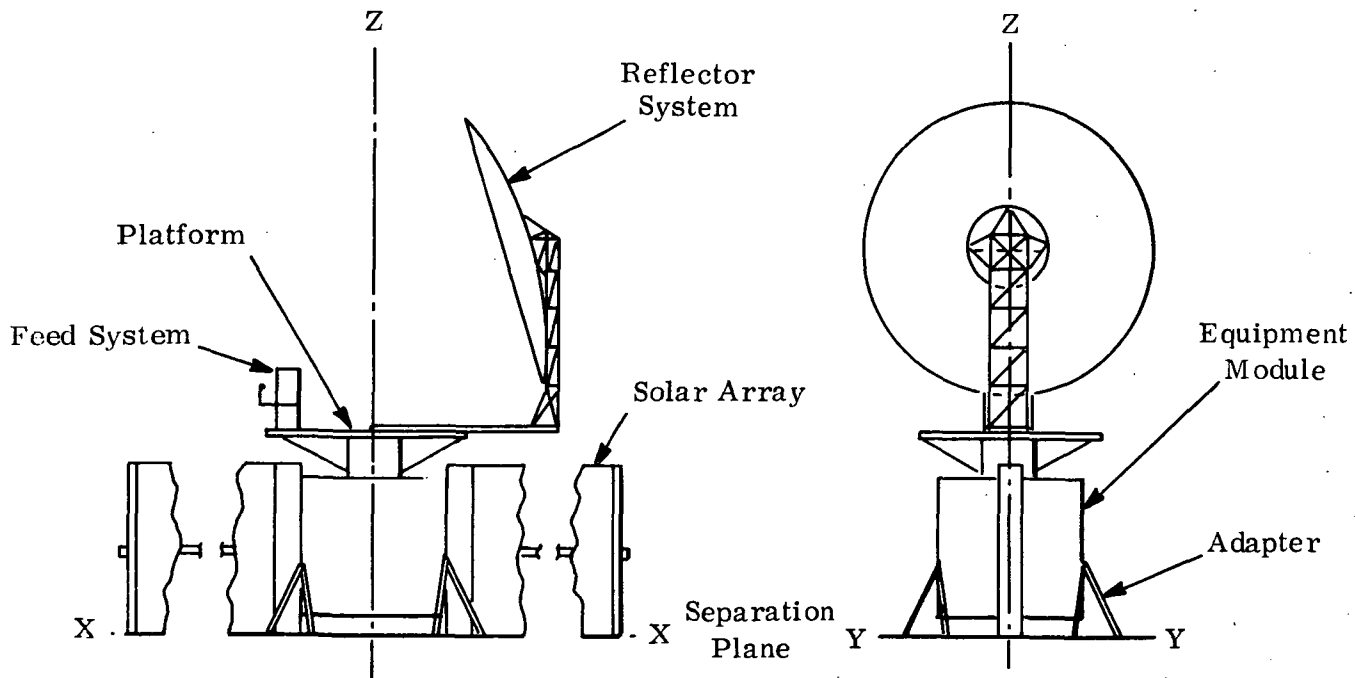
#### MASS PROPERTIES

A summary of the total ATS-AMS III mass properties is shown in Tables 5.10.2-1 and Table 5.10.2-2. Included is the resultant spacecraft center of gravity for the deployed configuration as well as the launch configuration. The weight moment of inertias about the roll, pitch and yaw axes for the orbiting spacecraft is also included.



COMPONENT	WEIGHT kg      (lbs.)	CENTER OF GRAVITY - m (in)		
		X	Y	Z
EQUIPMENT MODULE	997    (2,152)	0        (0)	0    (0)	1.14    (45)
PLATFORM ASSEMBLY	395    (870)	0        (0)	0    (0)	2.67    (105)
ADAPTER	33     (72)	0        (0)	0    (0)	.66    (26)
ARRAYS	185    (407)	0        (0)	0    (0)	1.22    (48)
REFLECTOR SYSTEM	45     (99)	.74      (29)	0    (0)	4.60    (181)
FEED SYSTEM	91     (200)	-1.02    -(40)	0    (0)	3.12    (123)
TOTAL SPACECRAFT	1,726    (3,800)	-.033    -(1.3)	0    (0)	1.68    (66.3)

Figure 5.10.2-1. ATS-AMS III Mass Properties Launch Configuration



COMPONENT	WEIGHT	CENTER OF GRAVITY m (in.)			WEIGHT OF MOMENT OF INERTIA kg - m <sup>2</sup> (10 <sup>6</sup> lbs. - in. <sup>2</sup> )		
	kg (lbs.)	X	Y	Z	I <sub>X</sub>	I <sub>Y</sub>	I <sub>Z</sub>
EQUIPMENT MODULE	977 (2,152)	0 (0)	0 (0)	1.14 (45)	510 (1.76)	510 (1.76)	510 (1.76)
PLATFORM ASSEMBLY	395 (870)	-0.08 (-3)	0 (0)	2.67 (105)	150 (.50)	150 (.50)	290 (1.00)
ADAPTER	33 (72)	0 (0)	0 (0)	.66 (26)	35 (.12)	35 (.12)	67 (.23)
ARRAYS	185 (407)	0 (0)	0 (0)	1.22 (48)	60 (.20)	22,470 (76.80)	22,410 (76.60)
REFLECTOR SYSTEM	45 (99)	2.82 (111)	0 (0)	4.60 (181)	220 (.76)	130 (.44)	130 (.43)
FEED SYSTEM	91 (200)	-1.09 (-43)	0 (0)	3.12 (123)	3 (.01)	3 (.01)	0 (.00)
TOTAL SPACECRAFT	1,726 (3,800)	0 (0)	0 (0)	1.66 (66.3)	2,300 (7.83)	25,100 (85.71)	23,900 (81.62)

Figure 5.10.2-2. ATS-AMS III Mass Properties Deployed Configuration



## DESIGN CRITERIA

This section presents the preliminary simplified criteria to which the spacecraft have been designed.

The design load factors and frequencies used are based on "ATS-F & G Environmental Test Specification for Spacecraft System Tests," S-320-ATS-1B, for launch loads and upon past experience for the orbital load factors. A summary of the criteria used is shown in Table 5.10.3-1.

The structure which is similar to ATS-F & G, the center body and launch vehicle adapter, is sized by ratioing ATS-F & G structure weights by the AMS weights. Modifications are made to account for differences in designs, for example, the region influenced by the rotating platform.

The platform and rigid antenna is sized for the launch load factor criteria, while the tower is sized so that the subsystem has a frequency 40% above the minimum allowable spacecraft frequency.

The array system analysis follows guidelines set forth in the "Applications Technology Satellite Advanced Mission Study" monthly progress report (Volume IV, Appendix F) for May 1971 (Contract No. NAS3-14360). An array blanket tension of 3.6 kg (8 lb) is used which yields a system frequency of 0.10 Hz.

Table 5.10.3-1. Design Criteria Summary

	Configuration	
	Launch	Orbit
Design Ultimate Longitudinal Load Factor	11.3 g	.13 g
Design Ultimate Lateral Load Factor	4.9 g	.13 g
Minimum Longitudinal Frequency	24 Hz	1.0 Hz (except as noted)
Minimum Lateral Frequency	6 Hz	1.0 Hz (except as noted)

## SECTION 6

### CRITICAL RESEARCH AND DEVELOPMENT

The projected spacecraft configurations and capabilities that have resulted from this Advanced Mission Study require only reasonable extrapolations from the present state of the various technologies. Even with this conservative approach, it has become apparent that reducing the results of this study to optimum hardware will require development in certain critical areas of spacecraft, earth terminal and communication system technology. The need for these critical developments are in addition to studies required to define subsystems to a level of detail beyond the scope of this contract and to further explore user requirements.

#### 6.1 SPACECRAFT TECHNOLOGY CRITICAL R & D

##### 6.1.1 THERMAL

The ATS-AMS is the highest power spacecraft now being planned. The kilowatts of RF and DC power create unique thermal problems. Specific techniques for the more critical areas are outlined here and should be pursued further.

- The high power tube collector structure geometry as presently envisaged is consistent with the thermal radiation requirements. This configuration does not, however, attempt to control the thermal radiation pattern. Selective application of thermal coatings and configuration can be used to direct radiation.

A program to apply this technology to the depressed collector is suggested. The suggested program would encompass thermal modelling of the tube, thermal vacuum testing of the model, measurement of the thermal radiation field from the model, and assessment of the effect of selective coating application on these fields; all of this in addition to, and supported by, computer modelling.

- Typical presently available heat pipes can transfer one watt over a temperature differential of one °C for a one cm diameter pipe two meters long. The high power and resultant heat loads in the AMS spacecraft would benefit from an order of magnitude increase in the capacity (power transferred times length divided by cross sectional area) and efficiency (power transferred divided by temperature differential) of heat pipes.

A program including analysis and experimentation to force this improvement in the state of the heat pipe art is suggested.

- The ATS-AMS III is sun oriented with a transponder tower that rotates to keep the antennas pointing at the earth with the result that the satellite body has most of the shaded area suitable for heat rejection while the transponder tower has many of the heat sources (even taking into account that the tube collectors are direct radiators). One very attractive way to solve this problem would be to have a heat pipe with a rotary joint. Heat pipes are very susceptible to contamination, therefore, a sealed rotary joint presents too high a risk; an alternate is to have the heat pipe split into two sealed sections free to rotate with respect to each other and thermally "connected" by being immersed in conducting fluid (e. g. , mercury) in a

suitable container with a stuffing tube or other rotary seal. A program to develop and evaluate such a heat pipe rotary joint including environmental, life and performance testing is suggested.

This joint would permit the heat from the High Voltage converter to be transferred to the south face of the spacecraft where the ion engines and shunts are located. This heat would then keep these elements above minimum temperatures.

#### 6.1.2

#### HIGH POWER ELECTRICAL TECHNOLOGY

The requirement for the AMS spacecraft to generate up to ten kilowatts of electrical power and to supply the microwave amplifiers with voltages as high as fourteen kilovolts will require improvements in existing technology in three areas.

- If the AMS spacecraft is earth oriented; and/or if the solar array is to follow the seasonal solar angle; and/or if the solar array is to vary its sunlight acceptance angle for pre-regulation; it will obviously be necessary to be able to rotate the solar array about its long axis. This rotation requirement coupled with the large area (ten square meters) of the array present new problems for the deployment devices utilized. The requirement here is for a study to uncover the two or three most promising light weight deployment mechanisms and structure followed by a detailed design. The design developed must then be stress and vibration analyzed. It is to be expected that this program will enjoy the same success as similar NASA studies of other electromechanical devices such as deployable antennas.

- Another electromechanical device that required further development to meet the peculiar requirements of the AMS mission is the rotary joint. All of the spacecraft configurations require a rotary joint that completes one revolution in a day and transmits kilowatts of power. Several approaches to the joint and its drives appear viable and should be explored further. Stiction, for example, may be overcome by rotating the joint faster than the net relative rotation of the two ends. Liquid metal slip rings, as mentioned in the Statement of Work for this study, also reduce stiction. A contactless system with "chopping" on the array and reducing the slip ring to a rotating transformer also has some good features. For the drive both stepping and continuous rotators have advantages and disadvantages. Recommended is a study to select the most promising combination of options for drive, bearings and slip rings in terms of reliability, electrical losses, electrical noise, and thermal considerations. Then to breadboard and test the selected configuration for electrical and mechanical performance.
- The unique electrical configuration of the depressed collector microwave power amplifiers to be utilized for the ATS-AMS II coupled with the high power, impose new demands upon the power processing system in terms of efficiency, number and size of voltages, and power.

It will be necessary to select and qualify semiconductor devices as well as circuits. The Communication Technology Satellite program transmitter experiment package faces many of the same problems. A high power parallel study will result in significant benefit to both programs.

### 6.1.3

#### ION ENGINE

The NASA decision to halt development of the cesium contact ion engine created a need for an alternate attitude control electric engine. The LeRC-developed 5cm mercury bombardment ion engine fulfills this requirement as regards available thrust; but it has one drawback, as presently configured; the thrust is not electrically vectorable. A program to add electric steering of the thrust vector to this engine is strongly recommended. A goal of this program should be to provide  $\pm 45^\circ$  minimum steering of the thrust vector.

### 6.2

#### EARTH TERMINAL TECHNOLOGY CRITICAL R&D

NASA has a history of continuing support of critical spacecraft user technology. In addition, other agencies of the U. S. Government have been supporting the development of user terminals. The most common questions raised by potential satellite users concern the cost of terminals. Suggested here is a program to compile the work already done to develop the various user terminal configurations of receive-only, transmit-only, duplex, mobile, fixed, video, voice, data, fax, etc., realistic parameters attached to each configuration as a function of non-recurring costs, quantity, and signal quality. The study will identify the most expensive components so that development to lower these costs may be commenced. Such a review will provide a valuable user-planning aid and tend to reduce duplication of development effort.

### 6.3

#### COMMUNICATION SYSTEM TECHNOLOGY REQUIRED R & D

The ATS-AMS spacecraft is unique in that as a result of the high power and short wavelength utilized, this will be the first NASA satellite that has the potential to provide experimental information networking to low cost terminals, wide area direct-to-the-schoolhouse TV, and computer-aided instruction, all of the highest technical

quality to extremely low cost terminals. To realize this potential, developments in certain areas of satellite communication systems are required. These needs have come about because up until this time, most work in spacecraft communications has been for point-to-point links with low power spaceborn transponders and elaborate earth terminals.

#### 6.3.1 NARROW BAND TRANSPONDERS (See Sections 4.4 and 5.4)

For the service where a voice or data back link is used in conjunction with educational TV, a multiple access transponder is required in the 14/12 GHz band. Many channels - each with a three KHz base band bandwidth are required. As the down link is to the origination terminal which is relatively elaborate (G/T on the order of 13 dB Hz.) the power per channel may be very low (on the order of 200 milliwatts) solid state and linear integrated circuits seem very promising. In order to maintain separation, minimize cross talk and prevent intermodulation, it will be necessary for the transponder to be ultralinear and each channel will have to be heavily filtered. A direct frequency translator would require many heavy microwave filters, therefore, a system which converts down to I. F. is a logical choice. The suggested program is one to develop both the multiple access transponder and the miniature IF/RF amplifier and mixer incorporating the required active filters.

#### 6.3.2 BROADBAND TRANSPONDER (See Sections 4.4 and 5.4)

The high power and multiple service capability of the ATS-AMS spacecraft requires the development of a transponder that is new and different in more than the novel radio frequencies employed. Questions of multiple carrier versus composite baseband operation and "back-off" effect on intermodulation must be answered. The proposed program is to build a highly instrumented breadboard



transponder and measure the effects of varying the operating parameters and modulation techniques on efficiency, and output signal quality. It is to be expected that during the course of this measurement program improvements in the transponder design will become apparent. These advances will be incorporated into the breadboard and tested. The result of the effort will be both an optimized transponder design and firm data on its performance.

#### 6.3.3

#### MICROWAVE POWER AMPLIFIERS

Recommended here is continuation of the program to develop the power output tubes now being carried on under the aegis of LeRC. The only clarification of direction suggested by this study is concentration on output power levels variable from 150 to 2,000 watts and control of the thermal radiation patterns. The possibility of varying the output power by ground command or in an adaptive mode provides a new degree of freedom in communication experiment design.

#### 6.3.4

#### MILTIBEAM ANTENNA (See Sections 4.3 and 5.3)

To efficiently utilize the ATS-AMS spacecraft high power it is necessary to direct this power to the user. Previous spacecraft have provided relatively large area coverages from small antennas with essentially circular or elliptical patterns. The flux densities were so low that the slopover into non-user areas could safely be ignored. Alternately, point-to-point satcoms have provided small spot beams from large antennas as there was no requirement for dispersed users. The high power of the AMS spacecraft and the recent decisions of the WARC prohibit the carelessness of the former and the mission requirements preclude the latter. In recognition of this delimma, LeRC has instructed this contractor to study the problem. NASA LeRC is also attacking the contoured beam problem with two AAFE programs. Both of these programs

emphasize the radiating elements and give short shrift to the development of the switchable microwave matrix that drives these elements. What is suggested here is further extension of the AAFE program with special emphasis on the tapered offset feeds, together with the commencement of parallel programs to develop the switchable microwave matrix. Additional trade-off analysis to determine optimum  $f/D$  ratios, beam-to-beam cross-over levels and side-lobe minimization are also required. This analysis will be supported by extensions of the computer modelling now being performed on the AAFE program.

#### 6.3.5

#### MODULATION TECHNIQUES

In order for the spacecraft transponder to operate at maximum efficiency the output tube must be operated saturated. Unfortunately, as mentioned elsewhere in this section, this class of amplification creates a severe intermodulation distortion problem. The technique for minimizing this distortion by utilizing a composite baseband is not applicable to the cases where the transponder must accept signals from dispersed ground stations. An alternate to the frequency division multiplex approach is time division multiplexing of either digital or sampled analog signals. TDM has been used for digital data transfer between fixed points and, of course, in spacecraft telemetry a simple form of TDM is employed. The program proposed is to synthesize a TDM multiple access system bread-board the crucial components and test its performance against standards based upon the work of J. Miller at GSFC and E. Miller at LeRC. Special attention must be paid to the synchronization problem as complicated by the diurnal motion of the spacecraft and to the method of final RF modulation (e.g., PCM/PSK and sampled analog proportional FM). The outcome of this research will be a modulation technique for multiple access from dispersed originators that will still permit the power amplifier to be operated at saturated efficiencies while preserving signal quality.

RECOMMENDED FUTURE STUDIES

This Advanced Mission Study, in the manner of all studies, has uncovered areas that merit further attention. The topics presented here differ from those given in sections 6.1, 6.2, and 6.3 in that no hardware activity is suggested.

## 6.4.1

## MULTIPOINT ACCESS CUEING AND CONTROL

There is a vast body of prior art in methods and techniques for multiple access cueing and control. Unfortunately, essentially all of this work has been based upon ground systems in which all parts of the network are equally accessible and equally amenable to increased complexity. In a satellite system one of the major topological nodes of the system is inaccessible and increasing its complexity is extremely expensive. This point in the satcom network is, of course, the satellite transponder. A study is suggested to model the problem of many dispersed ground stations (more than the number of available channels) wishing access to the transponder to communicate with either a central or each other. The problems of cueing and annunciating may be analyzed with the help of this model. Various systems will be synthesized and tried against the problem model. By iterating system synthesis and trial, an optimum system and or realizable constraints on the system requirements will be developed.

## 6.4.2

## USER AND EXPERIMENTER SUPPORT

The ATS-AMS spacecraft will present opportunities for both on-board experiments and communications user experiments as discussed in section 7 of this report. In order for potential experimenters to be prepared to present their experiments in an

intelligent manner, they will need to be supported. Suggested here is a program to support these users with the necessary communications and spacecraft technologies in addition to preparing experimenter handbooks for distribution as directed by NASA. Such an effort coordinated with and supported by NASA and Contractor guidance meetings with this community will result in NASA being presented with a plethora of experiments in a uniform and complete manner so that an optimum complement can be selected.

#### 6.4.3 DEPLOYABLE MICROWAVE LENS

Most of the multibeam antenna efforts have been toward improvement of parabolic reflectors and their feed arrays. Microwave lenses have generally been considered a poor choice for satellite use because of weight and deployment problems. Suggested here is a two pronged study to evaluate the potential benefits of a lens and to investigate means of stowing and deploying dielectric, waveguide and metal plate lenses.

#### 6.4.4 NUCLEAR PRIME POWER (See Section 1.4 and Appendix A)

This study has concentrated upon solar arrays as the source of prime power. A possible alternate is a reactor-thermoelectric device. The weight of these devices preclude their use in a direct ascent mission. A non-solar power source does have some advantages, therefore dismissing it just because of weight may be unwise. These advantages which include deletion of the requirement to have at least part of the spacecraft sun oriented and immunity of the power source to Van Allen belt damage suggest a mission worthy of further study. This proposed nuclear Advanced Mission Study is for a satellite with at least the capability of AMS III to be placed in a subsynchronous orbit by a Titan or shuttle and then to be orbit

raised by ion engines. Once at synchronous altitude the initial prime power would still be available and the spacecraft would be earth oriented with no rotating joints. Performing the nuclear study now that this AMS is complete will save duplication of antenna and communications effort.

#### 6.4.5

#### USE OF UPLINK FOR ATTITUDE SENSING

The AMS antenna will contain many feeds and will be continually receiving 14 GHz transmission from various earth stations. Considering this, a study should be instituted to examine the possibility of utilizing this received radiation in a monopulse or interferometer mode for attitude sensing in lieu of the 6GHz interferometer.

## SECTION 7

### ADDITIONAL EXPERIMENTS

#### 7.1 OPERATIONAL EXPERIMENTS

##### 7.1.1 POSSIBLE APPLICATIONS

A literature search was performed to define possible applications which might benefit most from high power communication satellites such as the ATS-AMS. The investigation included the review of documents such as references 3 and 12 (Table 7.1.1-2). Applications which benefit the general public and applications with commercial benefits were both considered.

The applications which were isolated as a result of the search have been tabulated into an application matrix shown as Table 7.1.1-1.

Each horizontal row of the matrix represents a specific application. Since a number of these applications fall into the same general category, they have been grouped by type of service.

Each vertical column represents a different characteristic or requirement of the application. These characteristics are:

- a) Beamwidth and Geographical Deployment - defines the area to be covered and the approximate (non-contoured) beamwidth which would be required to illuminate the area from a geostationary satellite.
- b) Network configuration - describes the network topology in terms of combinations of points

Table 7.1.1-1. Application Matrix (Sheet 1 of 3)

	Type of Service	Particular Application	Beamwidth & Geographic Deployment	Network Configuration	Direction of Traffic Simplex/Duplex	Channel Assignment	Period of Usage	Info. Type of Bandwidth	Usage	Digital Bits/Year	Type of Mod.	Type of Receive Terminal	Type of Transmit Terminal	Message Quality	
a	Regional Information Networks	Alaska Communication	2.6°x0.5° Alaska	Multipoint to Multipoint	Two-Way 1/2 Duplex	Demand Assigned (1, vol 9, p45) (11, p1)	24 hrs. Daytime Hrs. Mostly	Voice	250 x 10 <sup>3</sup> Chan-Hrs/yr		TDM-FM (2, p12)	Small	Small	20 Db	1975 Total Pop Est = 300,000 - 50,000 require service - 50 calls per person per year - 6 min/call - Maintenance support for remote areas, Medical emergencies, general communication.
b		Appalachian Communication	0.5x1.6° Appalachia	Multipoint to Multipoint	Two-Way 1/2 Duplex	Demand Assigned (1, vol 9, p45) (11, p1)	24 hrs. Daytime Hrs. Mostly	Voice	250x10 <sup>3</sup> Chan-Hrs/yr		TDM-FM (2, p12)	Small	Small	20 Db	
c		Rocky Mts. Communication	1.4x2.8° Rocky Mountains	Multipoint to Multipoint	Two-Way 1/2 Duplex	(Demand Assigned (1, vol 9, p45) (11, p1)	24 hrs. Daytime Hrs. Mostly	Voice	250x10 <sup>3</sup> Chan-Hrs/yr		TDM-FM (2, p12)	Small	Small	20 Db	
d		Pacific Trust Territory	4° x 8° Pacific Trust	Multipoint to Multipoint	Two-Way 1/2 Duplex	Demand Assigned (1, vol 9, p45)	24 hrs. Daytime Hrs. Mostly	Voice	250x10 <sup>3</sup> Chan-Hrs/yr		TDM-FM (2, p12)	Small	Small	20 Db	
e	Government Agency Information Network	Biomedical Communication	7° x 3.5° CONUS	Multipoint to Multipoint	Two-Way Duplex	Dedicated and Demand	8 am to 5 pm	Video Voice Data	20 x 10 <sup>3</sup> Chan-Hr/yr (3, p90) 180x10 <sup>6</sup> items/yr(10, p5)	6 x 10 <sup>14</sup> bits/year (12, p54, 51)	PCM, PSK (10, p7)	Medium	Medium	42 Db 10 <sup>-6</sup> (3, p10)	Remote Medical diagnosis remote medical browsing electro cardiogram analysis, 50 char/trans; 8 bits/char.
f		Law Enforcement	7 x 3.5° CONUS	Multipoint to Multipoint	Two-Way Duplex	Demand Assigned & Dedicated	24 Hrs. Daytime Mostly	Video Voice Data Fax	282 x 10 <sup>6</sup> Items/yr (10, p8)	1 x 10 <sup>14</sup> bits/year (12, p51, p53)	PCM, PSK	Medium	Medium	10 <sup>-6</sup> (13, p3-29)	Stolen vehicle information transfer stolen property information transfer facsimile: mug shot, finger print, court records, nat'l crime information center, nat'l information center
g		Post Office Corporation	7° x 3.5° CONUS	Multipoint to Multipoint	Two-Way 1/2 Duplex	Dedicated and Demand Assigned	24 Hrs. Night Mostly	Data Fax	50 x 10 <sup>9</sup> Items/yr. (12, p51)	1.5 x 10 <sup>16</sup> (12, p55)	PCM-PSK	Medium	Medium	10 <sup>-6</sup> (13, p3-29)	3 x 10 <sup>5</sup> bits/letter 50 x 10 <sup>9</sup> letter/year (12, p55)

Table 7.1.1-1. Application Matrix (Sheet 2 of 3)

	Type of Service	Particular Application	Beamwidth & Geographic Deployment	Network Configuration	Direction of Traffic Simplex/Duplex	Channel Assignment	Period of Usage	Info. Type of Band-Width	Usage	Digital Bits/Year	Type of Mod.	Type of Receive Terminal	Type of Transmit Terminal	Message Quality	
h	Regional Broadcast ETV/ITV	Alaska	2.6 x 0.5 Alaska	Point to Multipoint	One Way Simplex	Dedicated Channels	8 am to 5 pm	Video Voice	1540 Chan Hrs./yr		FM	Small	Large (U. of Alaska)	37 Db (3, p90)	
i		Appalachia	0.5 x 1.6 Appalachia	Point to Multipoint	One Way Simplex	Dedicated Channels	8 am to 5 pm	Video Voice	1540 Chan/Hrs./yr (3, p90)		FM	Small	Large	37 Db (3, p90)	
j		Rocky Mountains	1.4 x 2.8 Rocky Mts.	Point to Multipoint	One Way Simplex	Dedicated Channels	8 am to 5 pm	Video Voice	1540 Chan/Hrs/yr (3, p90)		FM	Small	Large	37 Db (3, p90)	
k		Migrant Workers	0.5 x 0.5 Regional Fla, Cal, Conn, South	Point to Multipoint	One-Way Simplex	Dedicated Channels	8 am to 5 pm	Video Voice	1540 Chan/Hrs/Yr (3, p90)		FM	Small	Large	37 Db (3, p90)	
l		U.S. Indian	0.5 x 0.5	Point to Multipoint	One Way Simplex	Dedicated Channels	8 am to 5 pm	Video Voice	1540 Chan/Hrs/Yr (3, p90)		FM	Small	Large	37 Db (3, p90)	
m	Special Purpose Broadcast System	Disaster Warnings	7° x 3.5° CONUS	Point to Multipoint	One Way Simplex	Dedicated Channels	24 hrs.	Voice	121 Chan Hrs/Yr (3, p90)	180 x 10 <sup>3</sup> (3, p90)	FM	Small	Large	31 Db (3, p90)	230 x 10 <sup>6</sup> People (3, p90)
n		Talking Books for the Blind	7° x 3.5° CONUS	Point to Multipoint	One Way Simplex	Dedicated Channels	8 am to 5 pm	Voice			FM	Small	Large	25 Db	
o	General Needs Information Network	Records, Business & Computer Data Network	7° x 3.5° CONUS	Multipoint to Multipoint	Two-Way Duplex	Demand Assigned	8 am to 5 pm Night-time to	Data		196 x 10 <sup>16</sup> (3, p90)	PCM-PSK	Medium	Medium	10 <sup>-6</sup> (3, p90)	350 x 10 <sup>3</sup> customers (3, p90) Insurance, claims and records sales and orders, in inventory
p		Tele Conferencing	7° x 3.5° CONUS	Multipoint to Multipoint	Two-Way Duplex	Demand Assigned	8 am to 8 pm mostly	Voice and Video	44 x 10 <sup>5</sup> Chan/Hrs/yr (3, p90)	2.3 x 10 <sup>15</sup> (10, p7, p8)	PCM-PSK	Medium	Medium	37 Db (3, p90)	Video telephone 6 min/call 6.3 x 10 <sup>6</sup> bits/sec. 1 x 10 <sup>6</sup> calls/year
q		Public Information (Libraries)	7° x 3.5° CONUS	Multipoint to Multipoint	Two-Way Duplex	Dedicated & Demand Assigned	8 am to 8 pm mostly	Data or Video	53 x 10 <sup>6</sup> Items/yr (10, p8)	7 x 10 <sup>14</sup> (12, p51, p 53)	PCM-PSK	Medium	Medium	10 <sup>-6</sup> 37 Db	Remote library browsing remote title and abstract searches intercalibrary loans



Table 7.1.1-1. Application Matrix (Sheet 3 of 3)

	Type of Service	Particular Application	Beamwidth & Geographic Deployment	Network Configuration	Direction of Traffic Simplex/Duplex	Channel Assignment	Period of Usage	Info. Type of Band-Width	Usage	Digital Bits/Year	Type of Mod.	Type of Receive Terminal	Type of Transmit Terminal	Message Quality	
r		Remote Printing of Books	7° x 3.5° CONUS Possibly Spot Beams	Point to Multipoint	One Way Simplex	Dedicated Channel	Night Mostly	Data or Fax	60 x 10 <sup>3</sup> Newtitles/Yr (10, p8)	540 x 109 (10, p8, 9)	DCM-PSK	Medium	Medium	10 <sup>-6</sup>	300 pages/book-30,000 bits/page
s		Remote Printing of Newspaper	7° x 3.5° CONUS Possibly Spot Beams	Point to Multipoint	One Way Simplex	Dedicated Channel	Twice Daily	Data or Fax	10 Newspaper using service (10, p8)	3 x 10 <sup>3</sup> (12, p55, p 51)	PCM-PSK	Medium	Medium	10 <sup>-6</sup>	
t		Reservation Services	7° x 3.5° CONUS	Multipoint to point point to Multipoint	Two Way Duplex	Demand Assigned or Dedicated	24 hrs. mostly 8 am to 5 pm	Data	710 x 10 <sup>6</sup> Items/yr (10, p8)	2.5 x 10 <sup>12</sup> (12, p51, 54)	PCM-PSK	Small/Medium Large	Large Small/Medium	115 <sup>-6</sup>	Airline reservation auto rental, hotel/motel entertainment, 50 char/trans; 8 bits/char
u		Financial Services	7° x 3.5° CONUS	Multipoint to Point Point to Multipoint	Two Way Duplex	Demand Assigned or Dedicated	Daily Mostly 8 am to 8 pm	Data	140 x 10 <sup>9</sup> Items/yr (10, p8)	7 x 10 <sup>3</sup> (12, p51, 54)	PCM-PSK	Small/Medium Large	Large Small/Medium	10 <sup>-6</sup>	Checks credit cards transactions and verifications. Stock Exchange quotations stock transfers - 50 char/trans; 8 bits/char.
v		Weather Map Dissemination	7° x 3.5° CONUS	Point to Multipoint	One Way Simplex	Dedicated	24 Hrs.	Fax	50 Maps/Day	6 x 10 <sup>8</sup> bits/yr.	PCM-PSK	Small/Medium	Large	10 <sup>-6</sup>	Retransmission of weather maps to forecasting stations and local broadcasting stations - 50 maps/day x 3 x 10 <sup>6</sup> bits/page
w	Direct Commercial TV Transmission	Alaska	2.6° x 0.5°	Point to Multipoint	One Way Simplex	Dedicated	Normal Broadcasting Schedule	Video	3 channels 120 MHz		FM-FM	Small	Large	Tasco Grade II	TV Transmission to isolated areas in Alaska 3 Channels
x		Remote Areas Appalachia Rocky Mts.	1.4 x 2.8	Point to Multipoint	One Way Simplex	Dedicated	Normal Broadcasting Schedule	Video	3 channels 120 MHz		FM-FM	Small	Large	Tasco Grade II	TV Transmission to remote areas within the continental U. S. 3 channels

Table 7.1.1-2. Key Index for References Used in the Preparation of the Application Matrix for the Study.

Key Number	Source and Title of Reference
1	National Academy of Sciences, National Research Council Useful Applications of Earth Oriented Satellites
2	National Aeronautics and Space Administration A Survey of Space Applications for the Benefit of Mankind
3	Lockheed Missile and Space Company for NASA Final Report: Information Transfer Systems Requirements Study
4	Fairchild Hiller Corporation for NASA Proposal for: TV Relay Using Small Terminals for ATS-G
5	General Electric Company for NASA Television Broadcast Satellite Study
6	General Electric Company and the Indian National Committee for Space Research. Study of Community Broadcast Systems for India
7	Communication Satellite for Alaska and the Mountain States. J.A. Fager and C. W. Kinkade. Convair Division of General Dynamics, San Diego, California
8	Special Report on Communications for Alaska from U. S. Senator Mike Gravel, June 1970
9	An Instructional Communication Satellite System for the United States - E. M. Sheppard, University of Maine, Orond Maine. AIAA Paper No. 70-450, AIAA 3rd Communication Satellite Systems Conference Los Angeles, California, April 6-8, 1970.
10	Roger W. Hough, "Information Transfer in 1990" AIAA Paper No. 70-4443, 3rd Communications Satellite Systems Conf., Los Angeles, California, April 6-8, 1970.
11	J.G. Puente. "A PCM-FDMA Demand Assigned Satellite Multiple Access Experiment", AIAA Paper No. 68-451, 2nd Communication Satellite System Conference, San Francisco, California, April 8-10, 1968.
12	Hough, R. W. et.al., "A Study of Trends in the Demand for Information Transfer", Stanford Research Institute, Menlo Park, California February 1970 (NASA CR-73426)
13	Fairchild Hiller Corporation. "Proposal for Applications Technology Satellite Advanced Mission Study" prepared for NASA Lewis Research Center (August 1970).

- c) Direction of traffic - identifies the direction of information flow as well as its characteristics in terms of "simplex" (which signifies information flows in two directions but only in one direction at any instant of time) and "duplex" (which signifies that information can flow in both directions at the same time).
- d) Channel assignment - defines the channel assignment method which would provide the most efficient usage of available channels.
- e) Period of usage - shows the period of day when the service should be available as well as the hours of peak service when such periods could be identified.
- f) Information type - describes the type of information involved in each application in terms of voice, fax, video or data or combinations of the four.
- g) Usage - shows the number of channel hours per year that would be required to satisfy the application.
- h) Digital bits/year - identifies wherever applicable the number of digital bits per year expected to be generated by the application.
- i) Type of modulation - lists the type of modulation which is best to the application.
- j) Type of receive terminal - classifies the receive terminals as small (antenna diameter of 1 meter or less), medium (antenna size between 1 and 3 meters), and large (antenna greater than three meters).
- k) Type of transmit station - classifies the transmit terminals similarly as small, medium, or large. In the one-way links or in the balanced links, only one entry is made in the receive and transmit column. In the two-way unbalanced links, two entries were made in each column, one for each direction.

1. Message quality - shows, as applicable, the maximum allowable error rate or S/N ratio of the signal as received by the end user.

Throughout the matrix, whenever numbers or information were extracted directly from a reference, the reference and the page where the information is to be found is identified in the block along with the information. The references are coded with a number and the corresponding title can be found from the table of references shown in tabular form by Table 7.1.1-2. This table is not intended to represent a total list of the documents consulted in the search, but is a key to the source of the numerical values shown in the matrix.

From the application matrix (Table 7.1.1-1) the requirement matrix shown in Table 7.1.1-3 was developed. This table groups together applications which place similar requirements upon the satellite and was utilized in generating a compatible set of mission objectives and equipment requirements.

The six groups which were identified are:

1. Regional Networks - In this application the satellite would provide a communication link within remote areas such as Appalachia, Alaska, the Rocky Mountains and the Pacific Trust Territory. The need for such communication links is well demonstrated in the special report on communications for Alaska by U.S. Senator Michael Gravel. Personal contact with Mr. Bernard Poirier, Technical Assistant to Senator Gravel, has confirmed that the requirement to provide reliable voice communications to remote areas is both very real and very pressing.
2. Regional TV Networks - People in regions such as Alaska, Appalachia, and the Rocky Mountains and minority groups such as migrant workers and US Indians all have a common characteristic in that the benefits of television are not available to them either due

to their geographical location or nomadic nature. A satellite-distributed television network would be beneficial to these people in two ways.

First it would provide an economical way to bring educational and instructional television to these people. Second it would also provide at reasonable cost a means for these people to end their isolation and provide them with the ability to share in the day to day activities around the world.

3. Remote Printing of Books & Newspapers and Dissemination of Weather Maps - These applications all involve the distribution of information from a central point to multiple users, a task which a high power satellite is ideally suited to perform.

In the case of newspaper remote printing, two different applications are envisioned. The first application arises in the case of newspapers with national distribution, which must be distributed overnight. In cases such as these, it becomes necessary to have printing facilities situated in widely separated locations. The composition and editing is done at one central location and the finished pages would be transmitted, via satellite, by facsimile to the remote printing sites.

The second application of newspaper printing is in remote areas which have limited or no access to newspapers. In this case, news information would be transmitted, via satellite, from a central distribution point to the isolated locations. There, a community antenna (part of an ETV/ITV reception facility) would receive the news information, duplicate it and distribute it, possibly through the children attending the school facilities. Such a scheme would allow people in isolated areas to be kept up to date on the most recent news developments.

The dissemination of annotated weather maps via satellite would make available to all forecasting stations the latest weather information. The improved forecasting reliability resulting from a service of this type would be very beneficial to farmers and other groups which are very vulnerable to the weather conditions.

4. Financial Services and Reservation Services - These services, such as credit card verification and travel reservations, which involve communications to a central computer complex are now handled through land lines. The same services routed through a satellite should provide better services at a lower cost.
5. Data Exchange - In these applications, such as teleconferencing, biomedical communications, law enforcement data exchange, computer data exchange, and first class letter transmission, a geostationary high power satellite would make available to a small user large banks of data in real time which until now have been available only to large users.
6. Books for the Blind - This application would alleviate the loneliness of the blind person by providing to him either directly in his home or through a library a wide selection of books in recorded form.

The applications listed above are described in detail in the literature. The list is by no means exhaustive and there are countless other applications where satellites could be used to facilitate communications. As a means of ensuring that all useful satellite applications would be considered, the NASA Scientific and Technical Information Facility was requested to run a literature search and this is now available as Literature Search Number 14653 dated 24 March 1971.

The summarized and regrouped applications shown by Figure 7.1.1-3 has been further regrouped to define requirements for the spacecraft

Table 7.1.1-3. Requirements Matrix

No.	Coverage	Network Configuration	Direction of Traffic	Channel Assign.	Baseband Bandwidth	Rf Band-Width & Mod. Type	Transmit Terminal	Receive Terminal	Number of Applications Demonstrated	Line No. on Main Matrix	List of Applications Demonstrated
1	0.75 x 1.5 APACA 0.75 x 2.6 (225 x 1.5) 1.4 x 2.8 (1.5x2.25) 4 x 8 (4.5 x 2.25)	Multipoint to Multipoint	Two-Way 1/2 Duplex	Demand Assigned	Voice 4 KHz	80 KHz	Small	Small	4	(a, b, c, d)	Regional information networks for Appalachia, Alaska, Rocky Mountains, Pacific Trust
2	0.75 x 1.5 0.75 x 2.6 (2.5x1.5) 1.4 x 2.8 (2.25x1.5)	Point to Multipoint	One Way Simplex	Dedicated	Voice and Video 4 MHz	34 MHz	Large	Small	7	(h, i, j, k, l, w, x)	Regional ETV/STV Broadcasts for Alaska, Appalachia, Rocky Mountains, Migrant workers, U.S Indians, remote area entertainment T.V.
3	7° x 3.5° (7.5 x 5.0)	Point to Multipoint	One Way Simplex	Dedicated	Fax 32 KHz Data 6.3 M bits	12 MHz or 500 KHz	Medium	Medium	3	(z, s, v)	Newspaper remote printing books remote printing. Weather map dissemination.
4	7° x 3.5° (7.5 x 5.0)	Point to Multipoint Multipoint to Point	Two Way 1/2 Duplex	Demand Assigned	Data 32 KHz	500 KHz	Large Small/Med	Small/Med Large	2	(t, u)	Financial services (credit card verification stock exchange listing and transactions) reservation services (car, hotel, airplane entertainment)
5	7° x 3.5° (7.5 x 5.0)	Multipoint to Multipoint	Two Way Duplex	Demand Assigned	Voice and Video, Fax, Data	34 MHz or 500 KHz	Medium	Medium	6	(e, f, g, o, p, q)	Data Exchanges, public information, libraries teleconferencing. Biomedical communications, Law enforcement. Post Office communications. Computer Data.
6	7° x 3.5° (7.5 x 5.0)  Note numbers in Parentheses are closest available beamwidths	Point to Multipoint	One Way Simplex	Dedicated	Voice 4 KHz	80 KHz	Medium	Small	2	(m, n)	Special Purpose - Talking bodies for blind, disaster warning

communications equipment (transponder, feed switching and antenna (s)). The requirements are shown by Table 7.1.1-4 and are based on the assumption that 2 KW of RF power will be available for allocation at all times and that good engineering practice will be observed in defining the quality of service to be provided.

#### 7.1.2

#### PROPOSED OPERATIONAL EXPERIMENTS

The matrix of applications, with services categorized by similar communication requirements (Table 7.1.1-4), served as a basis for establishing communication subsystem parameters that would permit a number of experiments to be performed in demonstrating one or more applications in each service category. Link calculations were performed to define more specifically the communication equipment requirements for the satellite and earth stations, giving due consideration to equipment cost and complexity factors. A summary tabulation derived from link calculations for the various services, is shown as Table 7.1.2-1. It may be seen that viable communications experiments are possible with earth stations having antenna diameters of 1.0 meter or less, receiver noise figure as poor as 13 dB, and transmitter power as low as 0.25 W. (assuming spacecraft transmitter power up to 33 dBW, receiver noise figure of 6 dB, and antenna configuration to provide the coverage area required).

Table 7.1.2-2 summarizes the experiments which might be performed with the ATS-AMS. These proposed experiments are grouped according to their antenna requirements for area or spot beam coverage. Notation has been made of those experiments which require or could most advantageously use high satellite power in performing their communications mission.

The following paragraphs briefly describes each of the candidate experiments.

- A1 ITV This experiment would demonstrate instructional TV direct to remote schools via the satellite and small receiver satellite at the school site.



Table 7.1.1-4. ATS - AMS Simplified Service Matrix

	Service	Beamwidth	Power/Bandwidth Ratio	Reference to Application Matrix	Remarks
1	Emergency Warning One-Way Voice	Conus Region Locality	Maximum	m, n	See Section 4.9 for definition of beamwidths
2	Voice	Region	Dependent on Ground Station Complexity	a, b, c, d	
3	Data Distribution	Conus Region	Depends on Ground Rcvr. Data Rate + Quality of service	r, s, v, q	See Section 11 for tradeoff curves
4	Data Exchange	Multi- beam	Varies From Teletype to High Speed Link, High Quality of Service	e, f, g, o, t, u	
5	Video Distribution	Conus Region Locality	Minimal Quality into Budget Receiver	h, i, j, k, p, q, w, x	
6	Video Exchange	Multi- beam	High quality with Medium Station	e, f, p	See Appendix E. for link calculations

Table 7.1.2-1A. ATS-AMS Communication System Requirements

	ETV	Voice Exchange	Video Exchange	High-Speed Data Exchange	Voice Distribution (Mobile)	Video Distribution (Ships)
<u>Down-Link (11.7 - 12.2 GHz)</u>						
Coverage Area	Time Zone	Spot	Spot	Spot	Spot	Region
Spacecraft Trans. Power*	2 kW	4 W	100 W	200 W	2 kW	400 W
Spacecraft Ant. Gain	33.4 dB	43.8 dB	43.8 dB	43.8 dB	43.8 dB	36.4 dB
Max. Mod. Freq./Data Rate *	4 MHz	3.5 kHz	4 MHz	6.3 Mbps	3.5 kHz	4 MHz
RF Bandwidth *	34 MHz	35 kHz	34 MHz	13 MHz	35 kHz	34 MHz
Earth Station Ant. Size	2 m	0.5 m	2 m	1 m	omni H, 40° V	1.5 m
Earth Station Rec. Quality (NF)	11 dB	13 dB	11 dB	11 dB	13 dB	6 dB
Output Sig.-to-Noise Ratio	49.4 dB	39.4 dB	49 dB	10.9 dB	39.4 dB	49 dB
<u>Up-Link (12.75-13.25 GHz)</u>						
Earth Station Trans. Power *	300 W	4 W	200 W	400 W	4 W	200 W
Earth Station Ant. Size	5 m	0.5 m	2 m	1 m	0.5 m	2 m
Max. Mod. Freq./Data Rate *	4 MHz	3.5 kHz	4 MHz	6.3 Mbps	3.5 kHz	4 MHz
RF Bandwidth *	34 MHz	35 kHz	34 MHz	13 MHz	35 kHz	34 MHz
Spacecraft Ant. Gain **	43.8 dB	43.8 dB	43.8 dB	43.8 dB	43.8 dB	43.8 dB
Spacecraft Rec. Quality (NF)	6 dB	6 dB	6 dB	6 dB	6 dB	6 dB
Carrier-to-Noise Ratio	28 dB	21 dB	21 dB	20.4 dB	21 dB	21 dB
* Per Channel (Trans. Power required is directly proportional to no. of channels.)						
** Beamwidth 0.75° x 1.5°						

Table 7.1.2-1B. ATS-H Advanced Mission Study Communication System Requirements

	Voice Distribution	Video Distribution	Voice Exchange	Low-Speed Data Exchange	Video Exchange	High-Speed Data Exchange
<u>Down-Link (11.7-12.2 GHz)</u>						
Coverage Area	CONUS	CONUS	Region	Region	Region	Region
Spacecraft Trans. Power *	35 W	2 kW	10 W	1 W	400 W	300 W
Spacecraft Ant. Gain	28.6 dB	28.6 dB	36.4 dB	36.4 dB	36.4 dB	36.4 dB
Max. Mod. Freq. / Data Rate *	3.5 kHz	4 MHz	3.5 kHz	2400 bps	4 MHz	6.3 Mbps
RF Bandwidth *	35 kHz	34 MHz	70 kHz	5 kHz	34 MHz	13 MHz
Earth Station Ant. Size	1 m	3 m	1 m	1 m	3 m	2 m
Earth Station Rec. Quality (NF)	13 dB	11 dB	13 dB	13 dB	11 dB	11 dB
Output Sig. -to-Noise Ratio	39.8 dB	49.4 dB	52.4 dB	10.9 dB	49 dB	10.9 dB
<u>Up-Link (12.75-13.25 GHz)</u>						
Earth Station Trans. Power *	0.5 W	300 W	4 W	0.25 W	200 W	150 W
Earth Station Ant. Size	5 m	5 m	1 m	1 m	3 m	2 m
Max. Mod. Freq./Data Rate *	3.5 kHz	4 MHz	3.5 kHz	2400 bps	4 MHz	6.3 Mbps
RF Bandwidth *	35 kHz	34 MHz	70 kHz	5 kHz	34 MHz	13 MHz
Spacecraft Ant. Gain **	43.8 dB	43.8 dB	43.8 dB	43.8 dB	43.8 dB	43.8 dB
Spacecraft Rec. Quality (NF)	6 dB	6 dB	6 dB	6 dB	6 dB	6 dB
Carrier-to-Noise Ratio	28 dB	28 dB	21 dB	20.4 dB	21 dB	20.4 dB
* Per Channel (Trans. Power required is directly proportional to no. of channels.)						
** Beamwidth $0.75^{\circ} \times 1.5^{\circ}$						

Table 7.1.2-2. Communications Experiments

Experiments requiring CONUS, Time Zone of half time zone beams and a small (3/4 meter) satellite antenna.	
<u>Ref. Number</u>	<u>Experiment Title</u>
A-1*	ITV Alaska and other areas
A-4*	CCS Citizen's Communication Service
A-5*	MCS Mobile Communication Service
A-6*	TV to Ships
B-8	ARIS Antenna range in space
Experiments requiring spot beams and a large (2 1/2 x 1 1/4 meter) satellite antenna	
A-9	MVS Mail via Satellite
A-12*	IATV Interactive television
C-4	TRIM Vernier trim of off-axis feeds
_____	Ability to reuse frequency spectrum by two spot beams using the same frequency.
Experiments that could be performed with either a small or large satellite antenna	
A-7	DFRA Duplex Facsimile to remote areas
A-13	SLS Satellite Library Service
Note: Experiments which require or could most advantageously use high satellite power are indicated by an asterisk.	

- A4 Citizens Communication Service - This experiment would demonstrate the technology for providing useful communications services for individual citizens. This may include emergency warning, civil defense, time, weather. Narrow band receivers would be used.
- A5 Mobile Communication Service - This experiment would demonstrate the technology for providing data to mobile users such as truckers, railroads, boats, giving traffic data or home office communications. Further work in the development of receiver terminals may be required. The use of 12 GHz for mobile communication services, in fact for any type of services in which a very low gain (or omnidirectional) antenna is employed by the user is questionable. In general, lower frequencies (unless other considerations such as frequency allocation, terrestrial interference, or man-made noise dictate otherwise) are preferred. This arises from the fact that in the "constant aperture to constant gain link", much less coverage is obtained at higher frequencies, the complexity is significantly greater, and the required transmitter power in the satellite is equal or greater than at lower frequencies. A simple example will show the validity of this conclusion.

For a typical link calculation for mobile communications assume  $.75^\circ \times 1.5^\circ$  beam and an omni-directional receiving antenna. With the same spacecraft antenna aperture size and the same transmitted power, full CONUS coverage of approximately  $3.75^\circ \times 7.5^\circ$  could be obtained with a transmission frequency of 2.4 GHz. At this frequency, atmospheric losses would be less, the receiver would be more easily produced, and in fact, since lower NF front ends would be available (than at 12 GHz), a better C/N would be obtainable. Trade-offs would then be possible to allow the same quality of reception with less transmitter power.

A sample calculation will show this in terms of two factors:

## COVERAGE VS. FREQUENCY

### RECEIVED CARRIER POWER FREQUENCY

#### Coverage:

$$S = \frac{72}{DF}$$

where: D = transmitting antenna  
diameter in feet  
(symmetrical parabola)

F = freq. in GHz

S = angular coverage area  
(3 dB Beamwidth)

For a fixed transmitting antenna aperture, or dish diameter, S is proportional to  $\frac{1}{F}$ . Therefore a wider coverage area can be obtained for the same aperture size as frequency is decreased.

#### Received Carrier Power:

$$1) P_R = G_T + P_T + L_S + G_R \quad \text{where } P_R = \text{received carrier power in dBW}$$

$$\text{But } G_T = 20 \log F + 20 \log D + 7.4$$

$P_T$  = transmitter power  
in dBW

$$\text{and } L_S = (92.45 + 20 \log F + 20 \log R) \quad G_T = \text{transmitting antenna in dB}$$

$G_R$  = receive antenna gain  
in dB

$L_S$  = space loss in dB

F = Carrier Freq. in GHz

D = transmitting antenna  
diameter in ft.

R = Range in km

$$\begin{aligned}
P_R &= 20 \log F + 20 \log D + 7.4 + P_T + G_R \\
&- 20 \log F - 20 \log R - 92.45 \\
&= 20 \log D - 20 \log R - 85.05 + P_T + G_R
\end{aligned}$$

Since all quantities  $D$ ,  $R$ ,  $P_T$ ,  $G_R$  have been constrained as the same, it is seen that the received power  $P_R$  is independent of frequency.

We therefore conclude that because a constant gain antenna had to be utilized as the receiving element, the usual advantage of increasing frequency (providing increased receiving gain) no longer exists. This coupled with the poorer coverage area dictates that lower, rather than higher, frequencies be used in the mobile communication case.

A6 TV to Ships - This experiment would demonstrate the practicality of TV entertainment and instruction to U.S. Navy ships at sea. This may require the development of a simple tracking system for the shipboard receiving antenna.

A7 Facsimile to and from Remote Areas - This experiment would demonstrate the practicality of duplex facsimile to provide, for example, newspaper services to remote areas such as the Rocky Mountains, Trust Territory and Alaska.

A9 Mail via Satellite - This experiment would demonstrate techniques of rapid mail transit via satellite. This experiment would require development of sending and receiving terminals.

A12 Interactive TV - This experiment would demonstrate the use of 2-way TV for medical diagnostic aid. This would provide real time communication between consulting physicians.

- A13 Library Service - This experiment would demonstrate access to library services such as Talking Books and the recording of tapes from this library service. Receiving terminal hardware including rapid-recording tape machines would have to be developed.
- B8 Antenna Range in Space - This experiment would use the high power transmitter as a signal source to determine antenna patterns of ground antennas.
- C4 Version Off-Axis Feed Trim - This experiment would be to demonstrate adaptive feeds in conjunction with the high power transmitter and a multiple feed arrangement. The feed mechanism has to be developed for this experiment.

## 7.2

### TECHNOLOGY EXPERIMENTS

This section describes additional technology experiments proposed for the ATS-AMS.

### 7.2.1

#### LIST OF PROPOSED EXPERIMENTS

Reference Number	Experiment Name	Abbrev.
A11	Earth to Satellite to Satellite to Earth Link	ESSE
A14	Centralized Computer Communication	CCS
B1	Laser Communication Experiment	LCE
C2	Thermal Control Flight Experiment	TCFE
C10	Mechanical Battery	MBAT
C11	Satellite Station Measurement	SSM
C13	Thermal Coating Degradation Experiment	TCDE

Each of the above experiments are described in the following paragraphs.

- A11 Earth to Satellite to Satellite to Earth Link - The earth-satellite-satellite-earth link experiment, using laser communications between satellites, would verify the acquisition techniques as



well as the communication link. This experiment would provide data transmission between earth locations not feasible via a single satellite.

A14 Centralized Computer Controlled Communications System -

This experiment would demonstrate the effectiveness of a centralized computer to authorize, via satellite, communications channel assignments, on demand, for uses of the voice communication system.

B1 Laser Communication Link - A demonstration of the use of a high bit rate FM laser communication to provide an auxiliary link between earth and satellite.

C2 Thermal Control Flight Experiment - This experiment would demonstrate the use of variable conductance and self priming heat pipes to transfer large amounts of heat power in a space environment. The experiment would be implemented by using absorber and radiator panels located outside the satellite envelope.

C10 Mechanical Battery - To demonstrate the practicality of a mechanical battery for space application, to be used during occult.

C11 Satellite Station Measurement - To demonstrate the use of a scanning celestial attitude determination system in conjunction with monopulse to provide station sensing.

C13 Thermal Coating Degradation Experiment - To investigate the degradation of terminal coatings and solar cells during extended exposure to the Van Allen Belt radiation. This mission provides the unusual opportunity to test various coatings and cells as the exposure in the belt may be several months. This experiment would be particularly applicable in a spiral-out configuration such as AMS I.

## SECTION 8

### MANUFACTURING, TESTING AND SUPPORT

#### 8.1

#### MANUFACTURING AND ASSEMBLY

The ATS AMS spacecraft is a logical follow-on to the manufacturing and assembly technique being utilized for the ATS F and G. An appraisal of the major assemblies follows:

- o Spacecraft - Truss Adapter. This is a tubular aluminum-fittings weldment of a debugged design used for ATS F and G.
- o Equipment Module. The frame construction of this module is of aircraft type design similar to that used on ATS F and G. Precision assembly tooling is required to accurately control the location of the equipment. The external surfaces are honeycomb panels also requiring the use of precision tooling during the bonding and insert installation to properly position all internal equipment.
- o Rotary Joint. Radar antenna manufacturing techniques are employed in fabricating this item, including the use of aluminum for the turret stem.
- o Deployable Platforms. The antenna feed and reflectors slide on rails which are an integral part of the rotating platform. The moving portions are driven along the rails by a rotating lead screw which accurately sets the focal length. The feed to reflector alignment is maintained by the tightly toleranced and located rails.
- o Antenna Tower. The antenna support tower is a weldment of thin wall aluminum tubing, similar to the boom construction used for

ATS F and G. Precision, certified welding, heat treating and welding techniques provide the dimensional accuracies.

- Antenna. The antenna is a sectionalized assembly of honeycomb segments. Stretch forming provides the exact shape required. The curing ovens must have more than adequate capacity for the length of the 6.9 m (23 ft) segments with room for the required tooling.
- Solar Arrays. The two deployable solar arrays employ storage rollers for the solar cell blankets and are supported outboard from the equipment module by a folding mechanism that results in a rigid boom on each side. The precision required to make such a mechanism function correctly has been proven on the Nimbus and ATS F and G. Precision tooling is used to ensure the correct linkage centers. Previous experience with solid lubricants, viscous dampers and negator type spring drives ensure smooth, positive, precision deployment. The solar cells are applied to the flexible array structure with specialized laying up and back wiring techniques currently being used on ATS F and G.
- Alignment. Precision alignment techniques as used on the ATS F and G are used to ensure the step-by-step progression of accuracy from one major subsystem to the next so that the final assembly of the spacecraft will have sighting and tracking capabilities well within specification.

## 8.2

### TESTING AND SUPPORT

Aerospace ground equipment is defined as the electrical and mechanical equipment required to support the assembly, test, integration, and launch of the spacecraft. Within this framework, AGE is required for all the major elements of the spacecraft in order to perform pre-system level and system level tests during acceptance and qualification testing. In addition, AGE is required at the launch site. The categories

of AGE may be classified as follows:

- o Component/Subassembly Test Equipment (Bench Test Equipment)
- o Subsystem Test Equipment
- o System Test Complex

Component/subassembly test equipment is equipment which is used to conduct tests on major components, assemblies, or subassemblies of a major subsystem (e. g. , solar array of the power subsystem).

Subsystem test equipment is equipment used to conduct tests on the major subsystems of the spacecraft for acceptance and qualification test purposes (e. g. , power subsystem, communications subsystem, etc.).

A system test complex is used for in-plant system integration and environmental tests and pre-launch/launch activities. It is anticipated that all three classes of AGE will be required.

#### 8.2.1

#### AGE GUIDELINES

The basic guidelines for the AGE may be summarized as follows:

- o Provide the minimum amount of equipment in terms of cost and complexity consistent with adequately supporting pre-system level tests, integration and performance tests, and launch activities.
- o Utilize "building block" concepts to the greatest extent possible, whereby a component/subassembly test set is essentially identical to a module/panel in the subsystem test set, and a subsystem panel/console is essentially identical to a rack in the spacecraft system test complex.
- o Maximum utilization of commercial equipment and test harnesses.

#### 8.2.2

#### COMPONENT/SUBASSEMBLY TEST

Component/subassembly test equipment is required on a selective basis to support the engineering, acceptance test and qualification programs.

The subsystems which require subassembly test sets are:

- Power Subsystem
- Attitude Control Subsystem
- Communications Subsystem
- Telemetry and Command (T&C) Subsystem

There is no requirement for an antenna subassembly test set as the antenna will be checked out at the subsystem level.

### 8.2.3 SUBSYSTEM TEST

Subsystem test equipment is equipment that is required for pre-system level testing. As previously stated, the "building block" concept is utilized whereby subassembly test equipment is integrated into the subsystem test set designs, providing greater utilization of test equipment. For pre-system level testing, the following subsystem tests are required:

- Power Subsystem Test
- ACS Subsystem Test
- Antenna Subsystem Test
- Communication Subsystem Test
- T&C Subsystem Test
- Ion Engine Subsystem Test
- Cable Harness Subsystem Test
- Experiments Subsystem Test

### 8.2.2 SYSTEM TEST

#### 8.2.2.1 Electrical AGE

System level electrical AGE is required to monitor and control the spacecraft systems during integrated testing. This equipment is assembled and integrated in order to establish a system test complex

(STC) which serves as the focal point and single control source for the conduct of all spacecraft level tests both in the factory and at the launch site.

Mechanical design of the STC is based upon a modular concept, where each module is an independently transportable unit mechanically interconnected to the other modules of the STC. Each module also contains a patch panel which will provide access to any of the recording and/or readout equipment contained in the STC. With this approach, redundant equipment is minimized.

Electrical design of the STC is based on an end-to-end spacecraft system test concept. Spacecraft test input and control will be through the command system, communications system, and stimulation of the various on-board sensors. Functional verification of the spacecraft operation is accomplished through telemetry readout and downlink RF transmission. Telemetry readout is accomplished through selected word display, analog recording, printout of selected subcoms and the entire bit stream.

The power subsystem portion of the STC consists of the subsystem test set and a power control panel for ON-OFF Control and Monitoring. This console will have the capability of remote operation when physically removed from the rest of the STC. This feature eliminates the requirement for long power cable runs during environmental testing and launch operations. Spacecraft power will be provided through the umbilical connector.

Anechoic chamber facilities are necessary for electrical testing (far field) with the antennas mounted on the spacecraft during system level acceptance and qualification test programs. With this arrangement, all tests of the communications and T&C subsystems will be RF closed loop tests with the up-link signal originating at the STC, transmitted to the spacecraft through an antenna coupler and processed by the

communications subsystem. Verification of performance will be via telemetry readout and/or analysis of down-link data transmission from the spacecraft via the antenna coupler to the STC.

#### 8.2.2.2 Mechanical AGE

The mechanical AGE includes all items of mechanical equipment required throughout the program for handling, testing and transporting the spacecraft and its components, subsystems, and systems. Those items identified are:

- Handling Fixtures. Fixtures and slings used in the fabrication and assembly of the spacecraft and subassemblies are used to support the integration and test program. Of particular interest in the area of mechanical AGE are the fixtures to accommodate the equipment module, solar panels and booms and the complete spacecraft.
- Spacecraft Holding Fixture. The spacecraft holding fixture which is used to support and transport the spacecraft within the test area consists of a wheeled dolly used for the assembly and integration of the spacecraft. It holds the spacecraft in the Z-axis vertical and must meet the requirements for assembly operations and for support during various tests, such as the thermal vacuum tests.
- Spacecraft Hoisting Slings. Hoisting slings, designed for the assembly process are used for lifting and positioning of the spacecraft. Lifting of the spacecraft are restricted to the Z-axis vertical condition.
- Spacecraft Vibration Fixture. A test fixture having no significant inherent resonances which can amplify or attenuate the required input excitations is required.
- Spacecraft Mass Properties Fixture. This fixture consists of an interface plate which allows the spacecraft (with adapter ring) to be mounted on the mass properties platform.

- o Spacecraft Separation Test Fixture. This fixture provides for suspension cables to support the spacecraft and simulated transtage masses at the respective center of gravity.
- o Spacecraft Alignment Fixture. The alignment fixture is a precision rotary table consisting of a platform capable of handling the spacecraft.
- o Spacecraft Transport Container. The container consists of an inner shock-and-vibration-isolated supporting frame, an outer fixed frame and cover. Seals are used to permit internal use of dry nitrogen under pressure to protect the spacecraft from the corrosive effects of uncontrolled ambient atmosphere.
- o Solar Array Transport Dolly. The solar array transport dolly consists of a metal frame configuration designed to support and transport the solar array.
- o Equipment Module Dolly. This dolly accomodates the equipment module and allows for assembly and transportation within the integration and test areas.
- o Solar Boom Deployment Fixture. The solar boom deployment fixture allows for mounting the deployment mechanism and supports the solar panels in the deploying mode of operation. A zero-g condition is simulated to the extent practicable with the use of low friction devices offering minimum restraint as the solar panels are deployed.
- o Antenna Dolly. The antenna dolly allows for support and transport as required for integration and test.
- o Protection Covers. Protection covers are required for all critical components which require protection during handling and transportation. Among these are covers for all sun and earth sensors, solar panels and thermal control louvers.



- Optical Equipment. A theodolite, vertical tool bar, optical cubes, mirrors and other optical measuring equipment are used in conjunction with special test fixtures for alignment purposes.

## SECTION 9

### GROUND SUPPORT SYSTEM

#### 9.1

#### EARTH TERMINALS

The baseline information networking experiments demonstrating the feasibility of a multiservice system serving the needs of the Public Broadcasting Service (PBS) and the Office of Education (OE) and interactive TV (ITV) will require the types of Earth terminals as listed in Table 9.1-1. The link analysis covered previously has shown that wide area distribution of CCIR relay quality television signals using medium size (3.3m) antenna terminals and of TASO Grade 1 signals using small low cost terminals before reception (downlink) is possible if high power amplifiers are used in the satellite. The transmission (uplink) of these signals is accomplished with moderately high transmitter power using medium size (3.3m) antenna terminals for ITV service. However, due to the requirement placed upon the PBS storage stations, these stations must have a larger antenna (7.6m) to provide a high receive G/T. The following sections will describe in detail the characteristics and configuration of these stations.

#### 9.1.1

#### MAJOR STATIONS

At least one originating station for PBS and ITV will be located in its associated time zone or cultural region. These stations will function as the major center for origination of the appropriate television program material, for monitoring of the signals transmitted to their respective zones, for recording and relay transmission in the case of PBS, and for reception and processing of the interactive audio/data signals. The wideband signals transmitted to and from the satellite

Table 9.1-1. Types of Earth Stations

Type	Function	Antenna Size	
		PBS	OE
Originating/Storage Station	Origination and Monitoring	7.6 m (25 ft.)	3.3 m (11 ft.)
Broadcast Station	Receive Only	3.3 m (11 ft.)	--
Community Terminal	Receive, Talkboards	1.0 m (3.3 ft.)	1.0 m (3.3 ft.)
Transportable Station	Origination	3.3 m (11 ft.)	3.3 m (11 ft.)
* Storage Capability Provided			
** Interactive Audio/Data Transmitter Provided			

will always contain both video and high quality program audio together with the necessary cue/control and order wire channels on an FM sub-carrier. In the case of ITV, the return interactive audio/data will also be handled on an FM subcarrier. A block diagram of the originating station for PBS and ITV is shown in Figure 9.1-1. Note that automatic tracking is provided for the PBS originating station because of the narrow antenna beamwidth. The LNA in both stations is an inexpensive tunnel diode amplifier of approximately 6 dB noise figure. Identical receiving equipment is used for both stations, however, the transmitter power for the ITV station must be higher because of the smaller antenna. The high power amplifier (HPA) for the PBS station is a 100 watt TWT and for the ITV station is a klystron amplifier, both air cooled. Table 9.1-2 summarizes the characteristics of these stations.



Table 9.1-2. Major Station Characteristics

Service	PBS	OE/Transportable
TV Channels		
Transmit	1 or 2	1 or 2
Receive	1 or 2	1 or 2
Antenna Diameter	7.6 m (25 ft)	3.3 m (11 ft)
Antenna Polarization		
Transmit	H or V	H or V
Receive	H and V	V or H
Antenna Gain @50%		
Transmit (14 GHz)	57.9 dB	50.8 dB
Receive (12 GHz)	56.6 dB	49.6 dB
EIRP/TV Channel	72.6 dBW	73.6 dBW
System Noise Temperature	1000°K	1000°K
G/T (12 GHz)	26.6 dB/°K	19.6 dB/°K

The PBS station uses one polarization for the uplink. Both polarizations are necessary for the downlink because reception is required from adjacent coverage zones. The ITV station requires only orthogonal linear polarization for transmit and receive. In order to minimize combining costs, non-contiguous frequencies are used for transmitting.

#### 9.1.2 RECEIVE ONLY STATIONS

Receive only stations, are provided in each zone in quantities depending upon the type of service. For a fully implemented system for network distribution, PBS will require a receive only station for

each PBS affiliate now numbering 212. Community service would require a receive only station for each educational unit requiring service estimated by PBS to approach 10,000 stations. The PBS network station will receive television and association program audio for rebroadcast via terrestrial transmitters while the community service will terminate in a conventional TV receiver at the users facility. The community service stations for ITV will have transmit capability for interactive audio origination which is routed back to the originating station in the same zone via the satellite. A block of the receive only stations for both PBS and ITV is shown in Figure 9.1-2. The two stations are identical on receive with the exception that normally the PBS network station has the capability of simultaneously receiving multiple video channels for retransmission while the community station would normally have the capability of one TV channel switchable to any channel available in the area. A tabulation of electrical characteristics of the receive only station is given in Table 9.1-3.

#### 9.1.3

#### TRANSPORTABLE STATION

Transportable transmit stations are required for the purpose of originating sports and special events for storage or live re-broadcast by the PBS originating station, and for originating special programs for live direct broadcast to the small community receiving stations. The station transmitting equipment will be housed in a mobile air conditioned van suitable for road or air transport. The antenna will be manually positioned and also capable of dissassembly and transport. The HPA will be equipped with an air cooled klystron to facilitate transportability. A block diagram of the transportable station is shown in Figure 9.1-3. A tabulation of the electrical characteristics is given in Table 9.1-2.

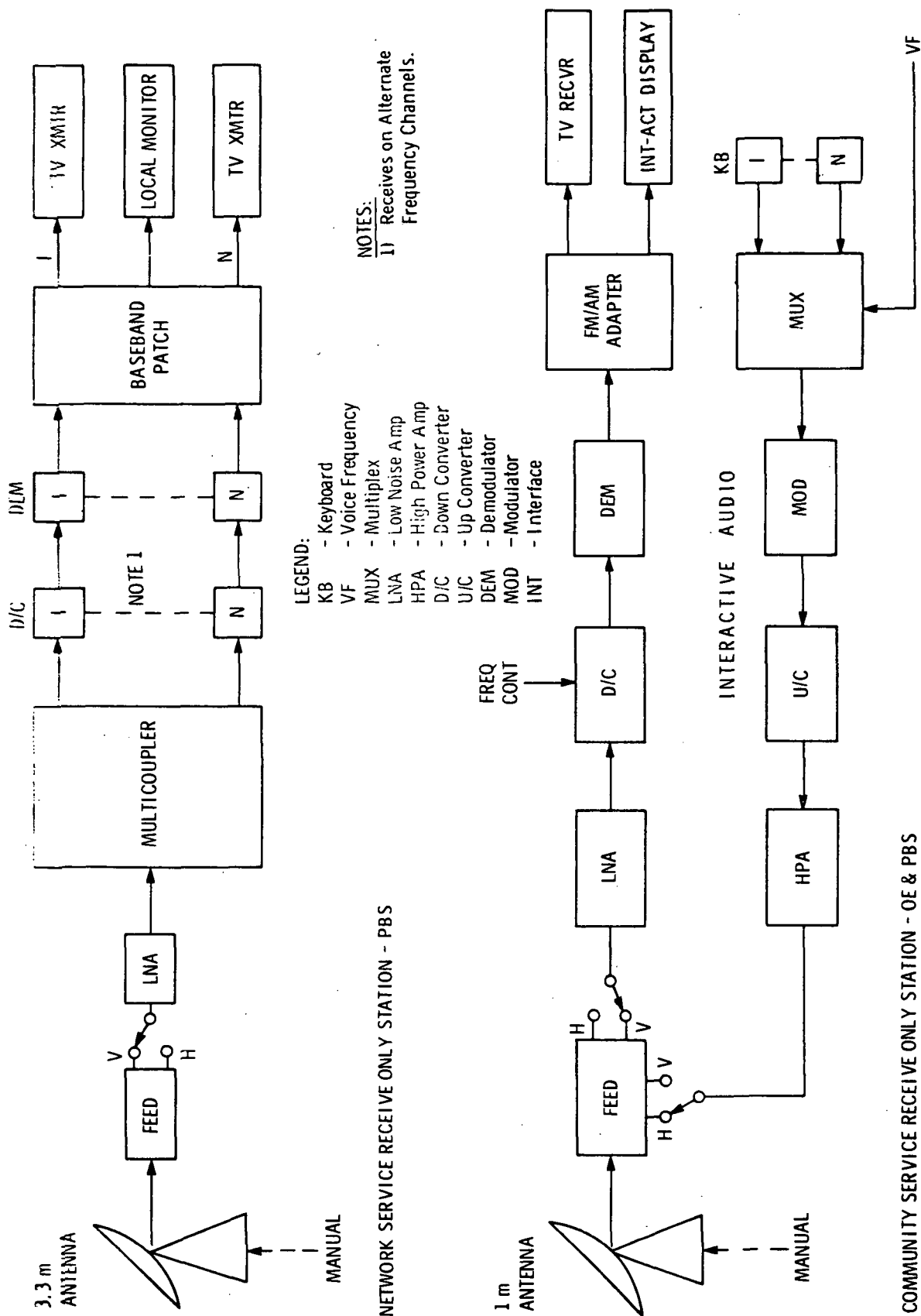


Figure 9.1-2. Block Diagram of Receive Only Stations

Table 9.1-3. Receive Only Station Characteristics

Service	Network	Community
TV Channels (Receive)	1 or 2	1 (switchable)
Antenna Diameter	(3.3 m) 11 ft	(1 m ) 3 ft
Antenna Polarization		
Receive	H or V	H or V
Transmit		V or H
Antenna Gain @50%		
Transmit	50.8 dB	39.5 dB
Receive	49.6 dB	33.2 dB
EIRP/ Audio Channel	54.5 dbW	54.5 dbW
System Noise Temperature	1000°K	1000°K
G/T (12 GHz)	19.6 dB/°K	3.2 dB/°K



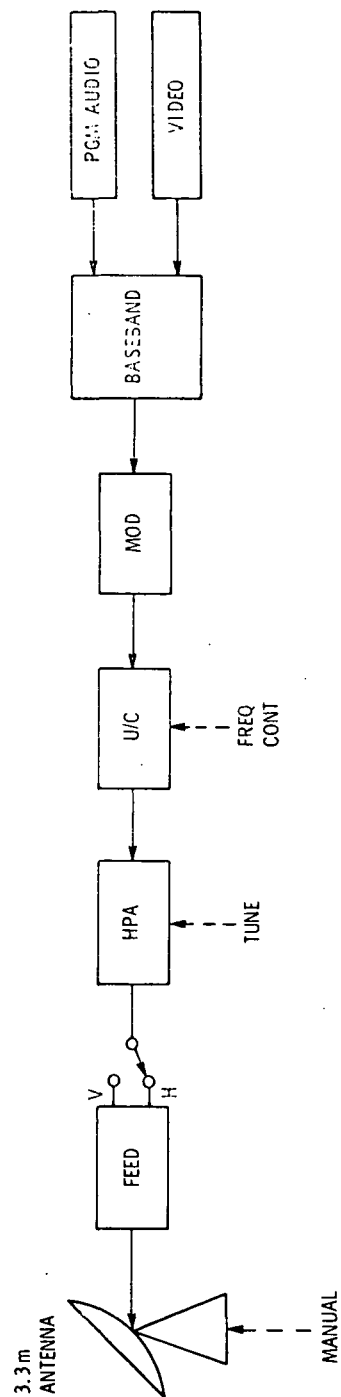


Figure 9.1-3. Transportable Station

SPACECRAFT PERFORMANCE EVALUATION

Evaluation of spacecraft performance is a task which starts with first system level tests and continues to completion of the ATS-AMS mission. A major objective is to quantify spacecraft performance throughout all phases of ground testing, launch readiness, launch and deployment, and in-orbit operations. The approach will provide a normalized basis, in meaningful engineering terms, to assess performance trends and identify incipient failure modes. The specific evaluation categories are:

- (1) Test Data Base Generation
- (2) Test Performance Signature Determination
- (3) Launch Readiness Determination
- (4) Flight Data Base Generation
- (5) Flight Performance Signature Determination
- (6) Degradation Determination & Incipient Failure Predictions
- (7) Final Performance Determination

## 9.2.1

## TEST DATA BASE GENERATION

Gathering of test data is accomplished while the spacecraft is subjected to various environmental and operational orbit simulations. Safety limit checking is performed on critical parameters during all tests, and failures defined, catalogued, and reported by edited computer printout.

## 9.2.2

## TEST PERFORMANCE SIGNATURE DETERMINATION

The dynamic behavior of critical spacecraft parameters under various defined operating conditions establish the test performance signatures which are required for later evaluation of spacecraft performance trends and incipient failure modes. This function is performed in an off-line manner by analyzing the test data base.

9.2.3 LAUNCH READINESS DETERMINATION

This consists of a series of GO-NO-GO tests to ensure that the spacecraft meets the established pre-launch performance requirements.

9.2.4 FLIGHT DATA BASE GENERATION

Gathering of flight data is performed in a similar manner as for the test data base. This data is subjected to various safety limits and operational real time evaluation programs. In addition, spacecraft attitude and pointing accuracies is determined and entered into the flight data base.

9.2.5 FLIGHT PERFORMANCE SIGNATURE DETERMINATION

This is accomplished in a similar manner as for the test operations. The same critical parameters are analyzed utilizing the same hardware and software systems that were previously employed to generate the test signature.

9.2.6 DEGRADATION DETERMINATION & INCIPIENT FAILURE PREDICTIONS

On a regular periodic basis during the flight operations, performance signatures are determined and compared to: (a) the baseline signatures; and (b) signatures determined in previous measurement cycles. An evaluation of the compared signatures result in both degradation determination and conceivably incipient failure prediction.

9.2.7 FINAL PERFORMANCE DETERMINATION

Selected data, taken from the total test base and flight data base is correlated and organized in a suitable final report format that can serve as a summarization of the ATS-AMS spacecraft mission.

## SECTION 10

### LAUNCH THROUGH ORBIT INJECTION

#### 10.1 GROUND SUPPORT EQUIPMENT

Operational Ground Equipment (OGE) is defined as the electrical, mechanical and physical equipment required to launch and inject the spacecraft into orbit. In this context, OGE is differentiated from the AGE required to assembly, test, and integrate the spacecraft prior to launch. However, many of the pre-launch tests are identical to previous system level tests performed during integration and qualification testing of the spacecraft. Therefore, where feasible and appropriate, available AGE is utilized as OGE to the maximum extent possible.

#### 10.2 LAUNCH SITE SUPPORT

The primary facilities to be utilized are a Spacecraft Operations Building and the Titan III C Launch Complex (ATS-AMS III).

##### 10.2.1 Spacecraft Operations Building

Although the flight spacecraft may be shipped directly to the launch pad, a Spacecraft Operations Building will be required for the following reasons:

- o Provide space and working area for the STC
- o Provide storage space for flight spares, tools, and auxiliary equipment
- o Provide space and working area for the spacecraft in the event that the spacecraft must be removed from the pad (due to weather conditions, booster malfunction, experiment malfunction, etc.)
- o Provide office space for the launch team

Preliminary spacecraft operations area requirements are presented in Table 10.2-1. There are probably several existing facilities at Kennedy Space Center which meet these requirements. A building having several antennas located on the roof which will provide a line-of-sight RF link with the launch pad is necessary. An additional feed or diplex arrangement may be required to complement the existing feed and coax lines which will connect to the STC, but this is considered a minor addition.

#### 10.2.2

##### Titan III C Launch Complex

The facilities support requirements for the spacecraft at the Titan III Launch Complex are summarized in Table 10.2-2. As noted in the table, all items are presently available or can be readily provided by incorporation of "standard" modifications.

The launch pads should have an RF window in the gantry to permit direct radiation to and from the pad when the gantry is in place. In addition, RF-transparent segments in the shroud are required.

Table 10.2-1. Preliminary Spacecraft Operations Building Requirements

No.	Item	Requirement	Justification/Need
1	SPACECRAFT LABORATORY		Set-up STC Conduct S/C Tests if required
	a) Floor Space	558 m <sup>2</sup> (6000 ft <sup>2</sup> )	S/C Deployment STC Set-up Misc. Equipment
	b) Overhead Crane	4545 kg (5 ton) 10.3 m (34') hook height	Lift S/C
	c) Environmental Control	Class 300,000 298°K ± 3° < 55% RH	Environmental Test Specification
	d) Access Door	7.6 m (25') high 4.54 m (15') wide	To accommodate S/C shipping container on low-bod truck
	e) Lighting	861 - 1076 lumens/m <sup>2</sup> (80-100 ft. - candles)	Standard working conditions
	f) Power	115 VAC, 60 Hz, 200 A	To provide power for STC, S/C, and misc. equipment
	g) Compressed Air	6328 kg/m <sup>2</sup> gauge (90 psig)	General purpose
	h) Storage	Storage room or cabinets 14 m <sup>2</sup> (150 ft <sup>2</sup> )	To store misc. equipment, supplies and spares
2	OFFICE AREA/EQUIPMENT		
	a) Desks, Chairs, & space (1 small office, 1 large)	14 desks/chairs 2 tables	For contractor personnel
	b) Conference Room, Table, Chairs	23 m <sup>2</sup> (250 sq. ft.)	For status meetings
	c) Communication Equipment	Telephones, Intercom, TWX	For general communications
	d) Standard Office Equipment	Typewriter, Copier, File Cabinets, Bookcases	To process and file documentation
3	MISCELLANEOUS ITEMS		
	a) Bonded Storage Area	Lockable Room or Cabinets	To store GFE items and MRR items
	b) Antenna/Feed/Coax	All RF Links	To permit RF Communica- tion between STC in hanger and S/C on pad
	c) Countdown Clocks	3 locations at STC	For launch pad operations
	d) OIS/MOPS/MITOC	8 headsets and stations (2 S/C Channels)	For test conduct

Table 10.2-2. Spacecraft Launch Complex Support Requirements

No.	Item	Requirements	Justification/Need
1	Environmental Control (within UES and Shroud)	Class 300,000 298° K $\pm$ 3° 55% RH (leak-proof)	Environmental Test Specifications
2	Work Stands and Platforms	Work Stand (Station 77)  Platform 10  Platform 11  Work Stand (Station 148)  Platform 12	Access to Titan Interface  Access  Access  Access Deployment  Access
3	Power MST Deck Levels  AGE Building	115 VAC, 60 Hz, 30A  115 VAC, 60 Hz, 30A	Test Equipment Cooling Cart  STC Power Supply Console
4	Land Lines (between Launch Site and Instrument Room)	3 dedicated	Power on-off control (1) Voltage and Current Monitors (2)
5	MITOC	(2 S/C Channels) 4 headset stations at each deck level; 2 in AGE building	For S/C Operations
6	Standard (Available) Facilities	Overhead Crane Hoist Elevator Lighting RF Window in MST Provisions to Mount Parasitic Antennas Emergency First Aid Kits	For S/C Operations
7	Instrumentation Room	Space to mount remote Power Control Panel Land Line Hook-up (Ref. Item 4) MITOC (2 head-set outlets)	For remote control of S/C external power

## SECTION 11

### IMPLEMENTATION SCHEDULE AND REQUIREMENTS

#### 11.1 WORK BREAKDOWN STRUCTURE (WBS)

11.1.1 The WBS is a "family-tree" type, graphic presentation of the work to be performed for the ATS-AMS program. Once a WBS is adopted, it establishes the baseline for the program schedule and cost control effort. The WBS given in Figure 11.1-1 is an extraction in concept of the ATS F&G WBS; the AMS WBS Level 2 presents the subsystem level from which lower level WBS items are integrated and summarized.

#### 11.2 GROSS RESOURCES REQUIRED

Cost definition and control will be established in accordance with the baseline WBS. A gross matrix, as shown in Table 11.2-1, is predicated on the WBS and the cost data presented is the product of analysis and extrapolation of ATS F&G level 2 historical cost data, coordination and review of cost data from launch vehicle contractors and source data from NASA and DOD agencies. The manpower projection is given in Figure 11.2-1.

#### 11.3 IMPLEMENTATION SCHEDULE

11.3.1 The AMS Program Plan, given in Figure 11.3-1 is predicated on the 1976 launch date given in the Statement of Work. The schedule represents a relatively low risk compression and assumes that the normal NASA program phases C and D will be combined and will start in April 1974. It also assumes that a competitive Phase B will take place during 1973 with final spacecraft contractor selected for Phase C/D, April, 1974. Launch of ATS H - December 1976, and launch of ATS - I, one year later, December 1977.



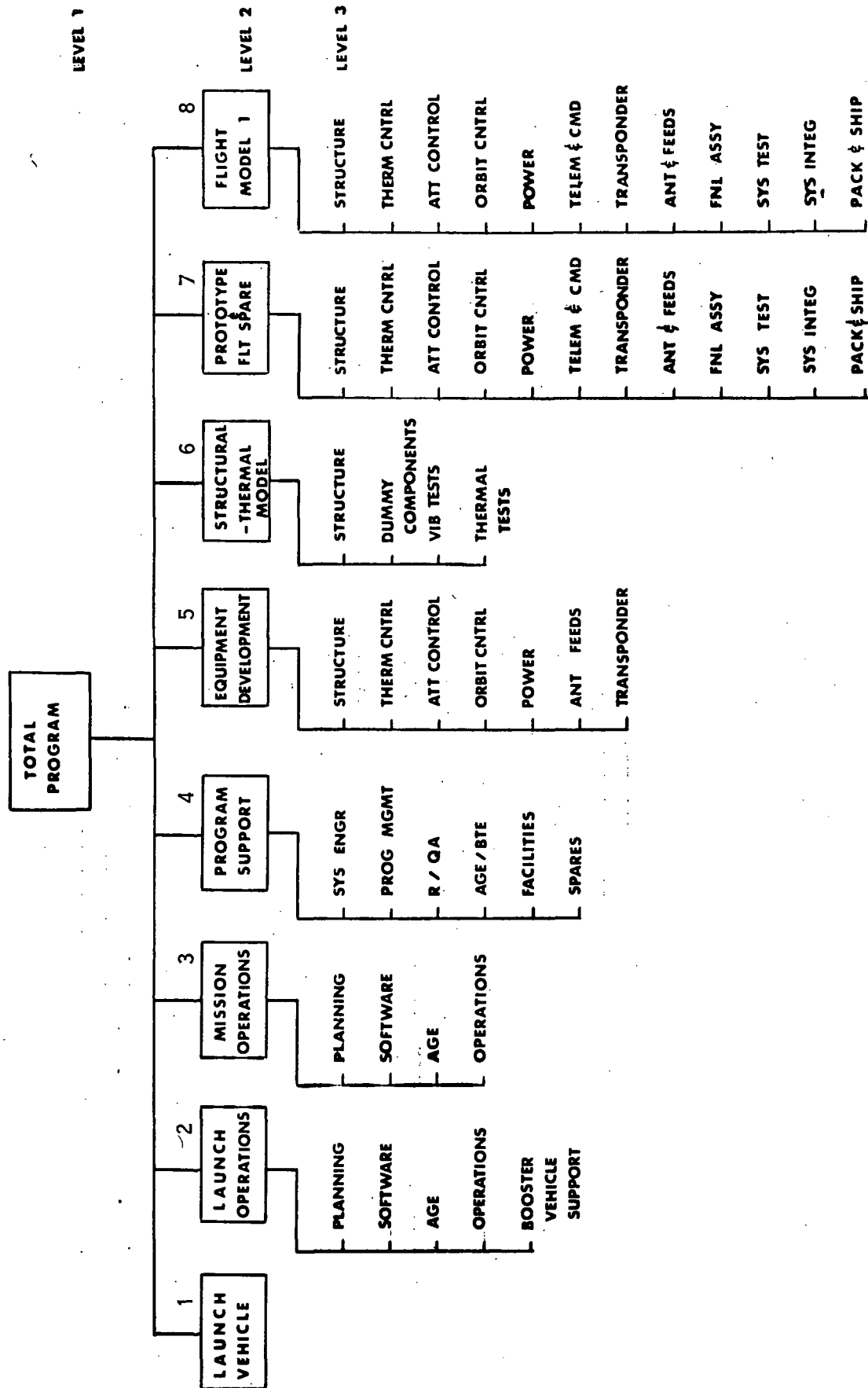


Table 11.2-1. Gross Cost Matrix

WBS DESCRIPTION	COST (MILLIONS)		
	ATS-AMS III	ATS-AMS II	ATS-AMS I
Program Support	18.0	18.0	18.0
Equipment Development	10.7	10.7	10.7
TSM	.7	.4	.6
Prototype	9.0	5.1	7.5
Flight Model H	6.4	3.6	5.3
Flight Model I	5.0	2.8	4.1
M & L Operations	<u>2.4</u>	<u>1.3</u>	<u>1.9</u>
Subtotal	52.2	41.9	48.1
Launch Vehicles	TITAN IIIC	SLV3D-CENTAUR-BII	DELTA 2910
Hdw, Launch Services, Etc.	23.8	11.6	5.7
Range Support (ETR)	<u>3.0</u>	<u>2.7</u>	<u>1.6</u>
Subtotal	<u>26.8</u>	<u>14.3</u>	<u>7.3</u>
TOTALS	79.0	56.2	55.4

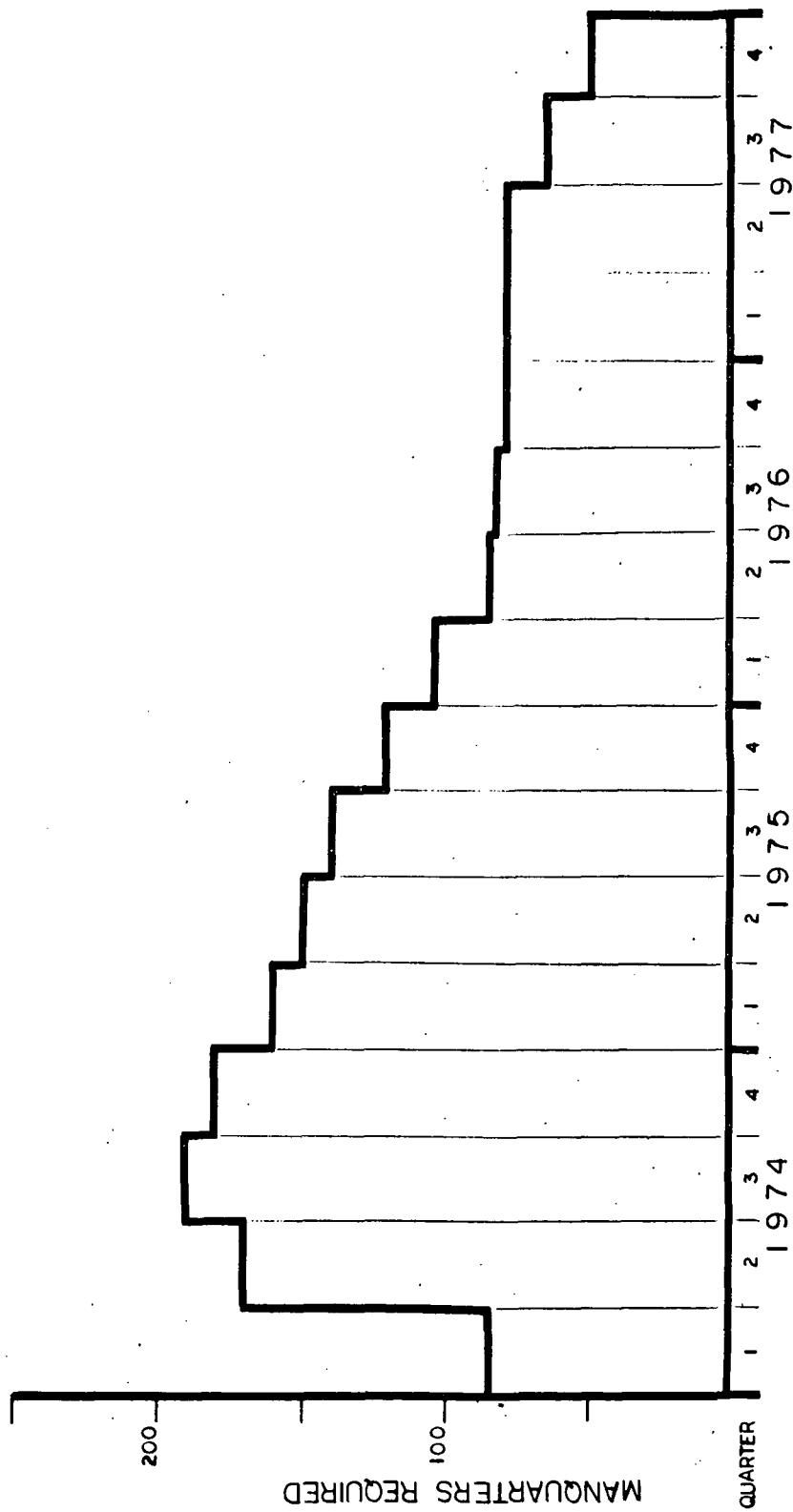


Figure 11.2-1. Manpower Projection

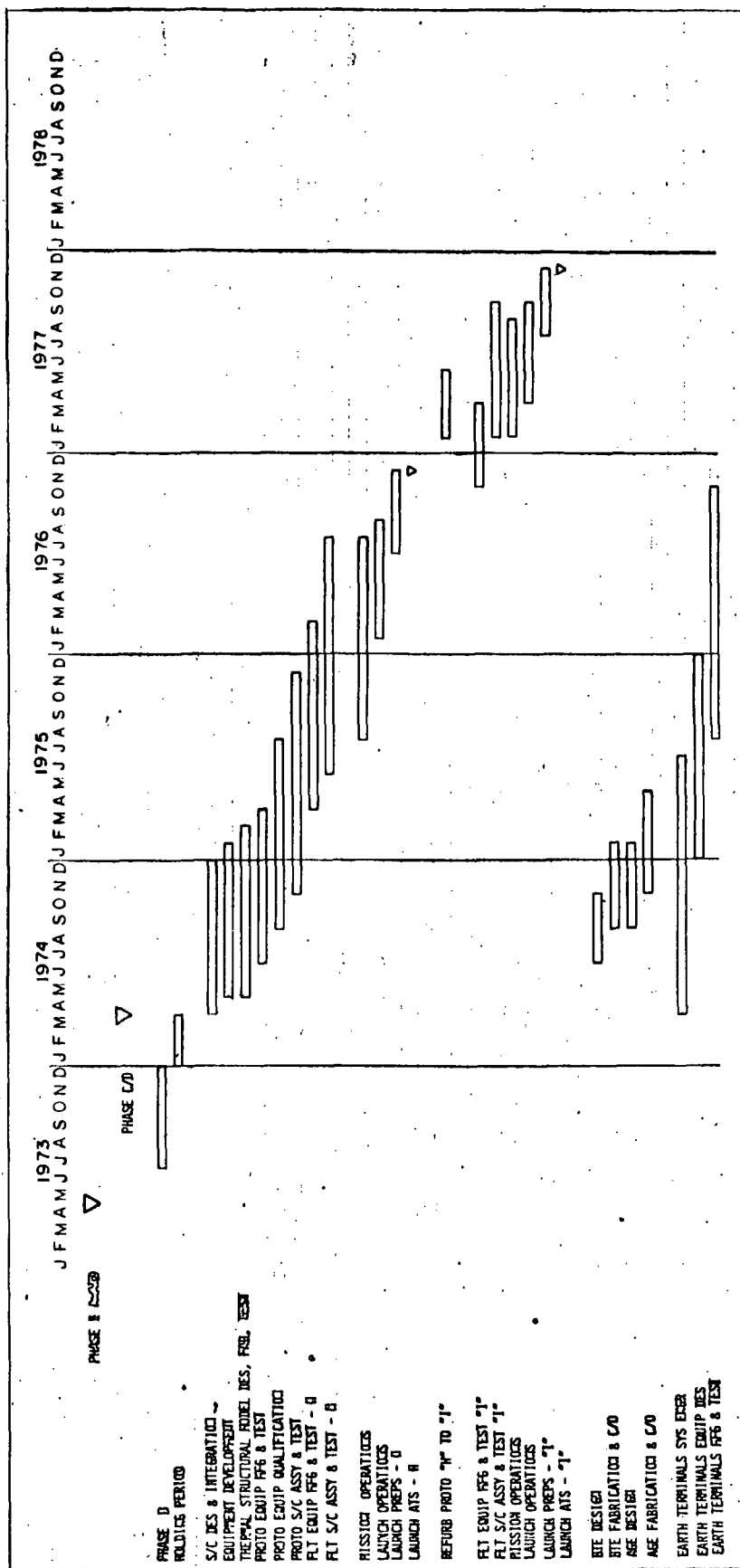


Figure 11.3-1. ATS-AMS Program Plan

## SECTION 12

### CONCLUSIONS AND RECOMMENDATIONS

The preceeding sections document the findings of the ATS-Advanced Mission Study. To highlight the key points developed during the study, specific recommendations and conclusions have been summarized in this Section.

#### 12.1

#### SMALL TERMINAL INFORMATION NETWORKING SYSTEMS

- o There is a real need by potential users for wide-band information networking systems employing geostationary orbit, high power satellites and small user earth terminals.
- o The potential users require experimental data and actual demonstration experience in order to specify their system and to commit resources to ancilliary wares.
- o An ATS-AMS designed to demonstrate the application of maturing spacecraft and communication technologies to the small user information networking system is the ideal response to the user need.
- o The application of 12 GHz to mobile services is not advantageous.
- o For wide area signal distribution, high power RF amplifiers in the satcom is the only way to provide a satisfactory signal to small earth terminals.
- o Discrimination between satellites by earth terminal antennas is less costly at 12 GHz than at lower frequencies.

DEMONSTRATION OF HIGH POWER SATCOM TECHNOLOGY

- The development of efficient high power 12 GHz transmitting amplifiers for satcom applications makes multipoint-to-multipoint information networking systems practical.
- Multibeam antennas producing contoured patterns for controlling the RF illumination of desired geographical areas reduces interference in adjacent areas.
- Although there is a power loss in the satcom by deriving a contoured pattern from multibeam, it is more than offset by the power saved from not illuminating undesired areas.
- The required satcom prime electrical power can be supplied by photovoltaic arrays.
- Precise control of spacecraft attitude and station-keeping makes possible the use of non-tracking earth terminal antennas of up to 3 meters.
- TASO Grade 1 video signals can be received by earth terminals with antennas as small as one meter and with inexpensive (7 dB) receivers.
- Sufficient isolation can be achieved through beam directivity and antenna cross polarization to make frequency reuse practical.

ASSESSMENT OF TECHNICAL FEASIBILITY

- An ATS-AMS is technically feasible for a 1976 launch.
- Contoured multibeam antenna patterns can be best achieved with a parabolic reflector having offset feeds.
- Weight and conversion savings offered by high voltage arrays do not appear to offset advantages of proven low voltage array techniques.

- Multistage depressed collector microwave power amplifiers having 50% RF/DC power efficiency or greater make it feasible to generate over 2 KW of RF power at 12 GHz in a spacecraft.
- Thermal control of a high power ATS-AMS is difficult within the state-of-the-art.
- Station-keeping to within  $0.2^\circ$  for N-S and E-W for 5 years is technically feasible.
- Attitude control permitting antenna beam pointing accuracy of  $\pm 0.2^\circ$  for latitude and longitude at the sub-satellite point and  $\pm 0.2^\circ$  in rotation about the boresight for 5 years is technically feasible.
- Solar arrays for large area-to-mass-ratio spacecraft have specific weights greater than 20.4 kilograms (45 pounds) per kilowatt (including deployment mechanisms) and are practical to beyond 15 kilowatts.

12.4

#### SELECTION OF SPACECRAFT APPROACH

- Direct ascent to synchronous equatorial orbit by the SLV3D/CENTAUR D-1A/Burner II or the Titan IIC, and spiral ascent with ion engines from a lower parking orbit achieved with the Delta 2910 are all feasible launch techniques for the ATS-AMS.
- Either an earth-oriented, rotating solar array spacecraft or a sun-oriented, rotating transponder tower spacecraft is feasible.
- The ATS-AMS I offers the lowest cost approach and the greatest technical risk.
- The ATS-AMS II offers less technical risk than ATS-AMS I at approximately the same cost.
- The ATS-AMS III offers approximately the same technical risk as ATS-AMS II at the highest cost. It has far greater capacity for

additional experiments, design growth and redundancy. The ATS-AMS III is the Fairchild Industries recommended spacecraft approach. The lighter weight ATS-AMS III B would be an excellent candidate for ATS-H, followed by the increased capacity ATS-AMS III A for ATS-I.

12.5

#### RECOMMENDED ADDITIONAL EXPERIMENTS

- Earth to Satellite to Satellite to Earth Link
- Centralized Computer Communication
- Laser Communication Experiment
- Thermal Control Flight Experiment
- Mechanical Battery
- Satellite Station Measurement
- Thermal Coating Degradation Experiment

12.6

#### RECOMMENDED RESEARCH AND DEVELOPMENT

There are no new technology requirements necessary for the ATS-AMS in the sense of invention. There are, however, several items that should undergo further development and evaluation prior to being committed to the spacecraft design. Some of these items are currently in development within the NASA and elsewhere.

- Multibeam parabolic reflector antenna, with a switchable matrix of sharply tapered offset feeds for obtaining minimum sidelobes and additional positioning flexibility to produce shaped patterns with contour coverage required by baseline Information Networking Experiments.
- Efficient, remotely - variable, high power microwave amplifiers having multistage depressed collectors with directional thermal radiation capabilities.



- Broadband microwave transponder/power amplifiers for single and multiple carrier operation in linear and saturated modes.
- Multiple access solid-state linear voice/data talkback transponder.
- Electrically vectorable 5 cm ion engines.
- High current rotating electrical joints.
- High voltage power processors.
- High capacity, high efficiency heat pipes.
- Large articulated photovoltaic array deployment mechanisms.

12.7

#### RECOMMENDED FUTURE STUDIES

- Methods and techniques for multipoint access cueing and control.
- User and experiment planning and coordination.
- Extend tradeoff analysis for offset feed parabolic reflector multibeam antenna to determine optimum f/D ratios, crossover level of multiple beams, feed taper and reflector sidelobes.
- Deployable multibeam microwave lens antenna as alternate to offset-feed parabolic reflector.
- Reactor-thermoelectric device as alternate to photovoltaic array for prime power source.
- Use of 14 GHz uplink signals as reference for attitude sensing as alternate to 6 GHz interferometer.

REACTOR-THERMOELECTRIC POWER SYSTEMS  
FOR THE  
APPLICATIONS TECHNOLOGY SATELLITE -  
ADVANCED MISSION STUDY

## I. SUMMARY

SNAP reactor components and systems have been under development since the 1950's, producing a technology ready to be applied to a variety of space and terrestrial missions. The purpose of this document is to relate this technology to the specific requirements of the Applications Technology Satellite (ATS) - Advanced Mission Study.

Table 1 summarizes the mission requirements. The nuclear system was designed to meet the 5-yr goal rather than the 3-yr requirement. As described in Section II, the power system utilizes a zirconium

TABLE 1  
MISSION REQUIREMENTS

Power Level (EOM)*	5.5 kwe at 30.5 vdc
Life	3-yr required, 5-yr goal
Orbit	geosynchronous
Launch Date	1976-1979
Launch Site	ETR
Power System Weight	minimum

---

\*EOM = end-of-mission.

hydride reactor and lead telluride (PbTe) thermoelectric converters. The power system characteristics are summarized in Table 2. There are a total of 20 thermoelectric modules in the system arranged in four parallel circuits. Each circuit contains 5 modules connected in series electrically to produce 30.5 vdc. Figure 1 is a layout of the power system. It has an overall length of 25.75 ft and a diameter of 4 ft. The system has a total weight of 1850 lb using the U-235 fueled reactor and 1575 lb using the U-233 reactor. The latter system is lighter because the U-233 reactor is lighter and smaller. The smaller reactor also results in a smaller, lighter radiation shield.

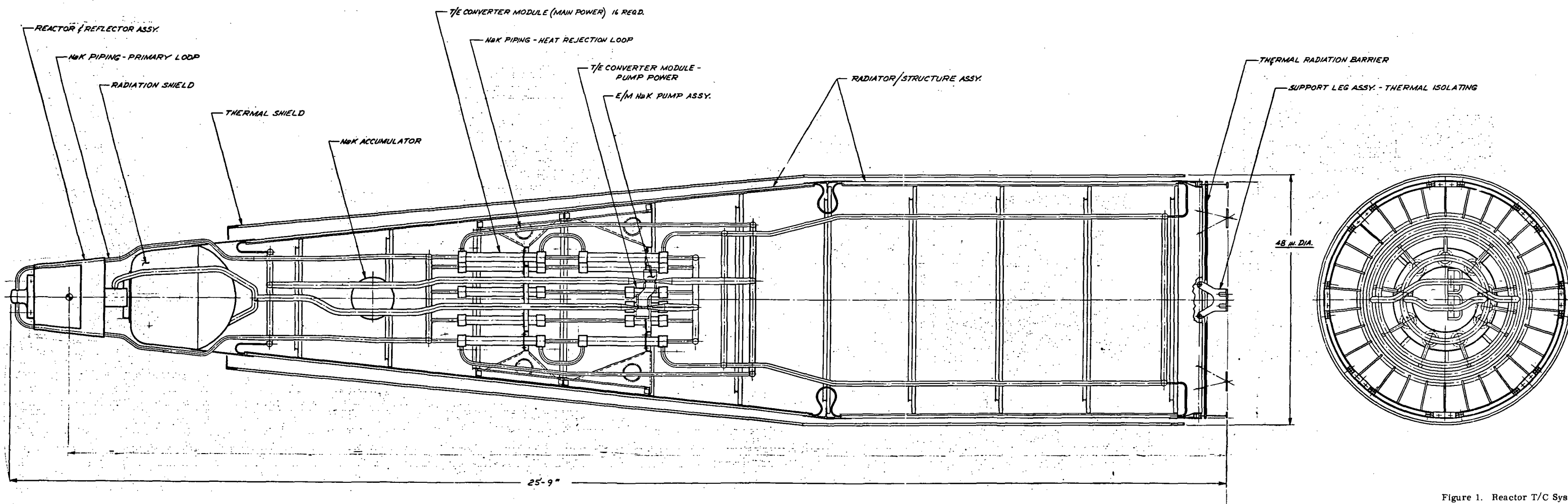


Figure 1. Reactor T/C System

TABLE 2  
POWER SYSTEM CHARACTERISTICS\*

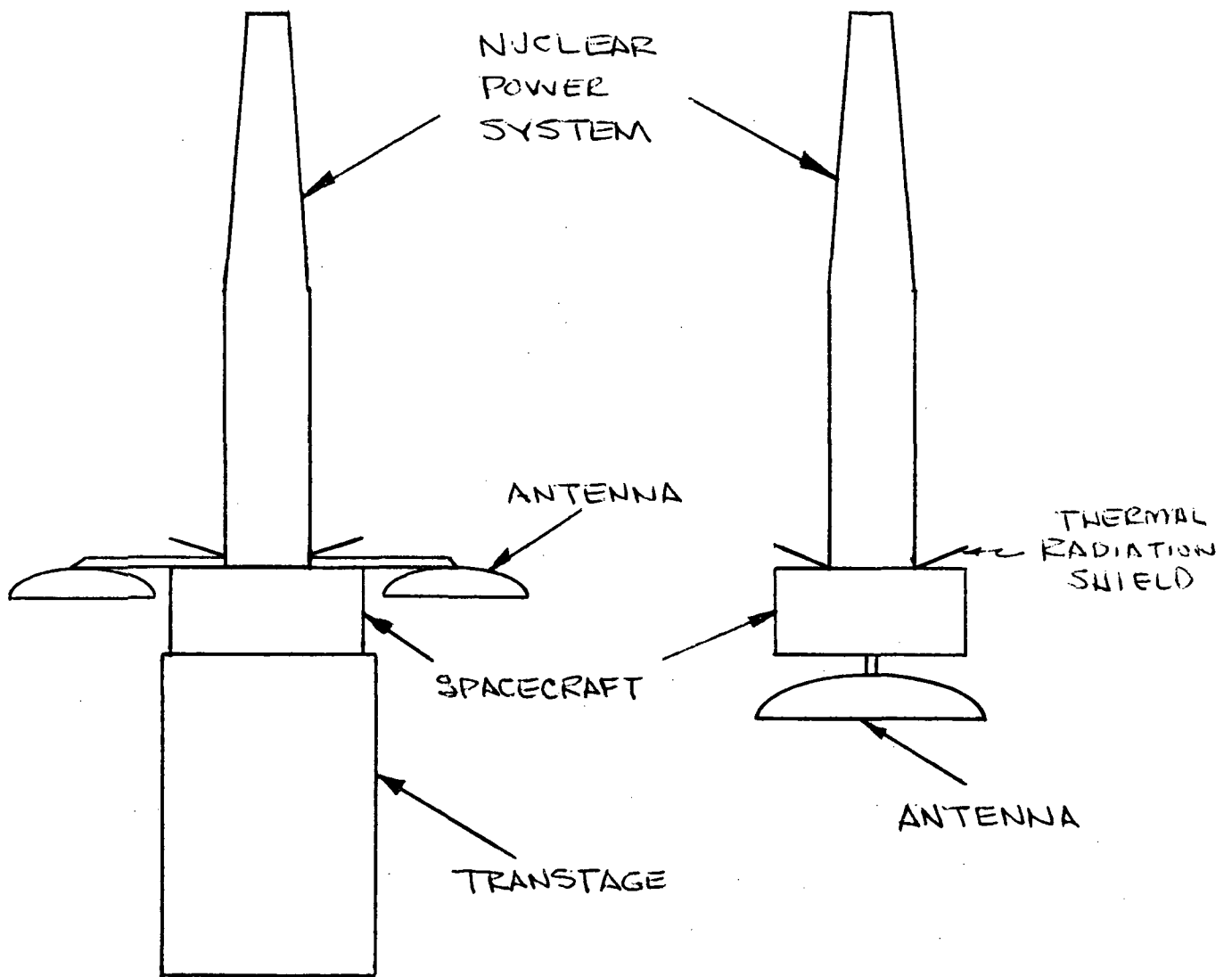
Electrical Power	5.5 Kwe at 30.5 vdc
Reactor Thermal Power	85 Kwt
Reactor Outlet Temperature	1200°F
Thermoelectric Converter Temperature	
Average Hot Clad	1135°F
Average Cold Clad	520°F
Number of TE Modules	4 Strings of 5
Radiator Area	230 Ft <sup>2</sup>
Total System Weight	
With U-235 Reactor	1850 Lb
With U-233 Reactor	1575 Lb

---

\* Performance is given at end-of-mission

Figure 2 shows two versions of the system in its on-orbit configuration. A thermal radiation shield is used to shade any heat sensitive components from the heat rejection radiator. In one case, the spacecraft is still attached to the Transtage and the communications antennas have been deployed. The other configuration shows the propulsion stage separated from the spacecraft. In this latter case, the antenna could be fixed rather than deployed. It was beyond the scope of this present effort to thoroughly investigate the spacecraft/power system integration. Consequently, there may be other configurations which are superior to those shown.

The Titan IIC was the reference launch vehicle for this phase of the study. It has a maximum payload capability of 3800 lbs in geosynchronous



## ON-ORBIT CONFIGURATIONS

FIGURE 2

orbit. Since the primary experiment and spacecraft weigh 1800 lbs, this leaves 2000 lbs for power system and margin. In the case of the U-235 reactor system, the power system weight is 1850 lbs leaving a margin of only 150 lbs or 4 percent. The 1575 lb U-235 system permits a more reasonable margin of nearly 20 percent.

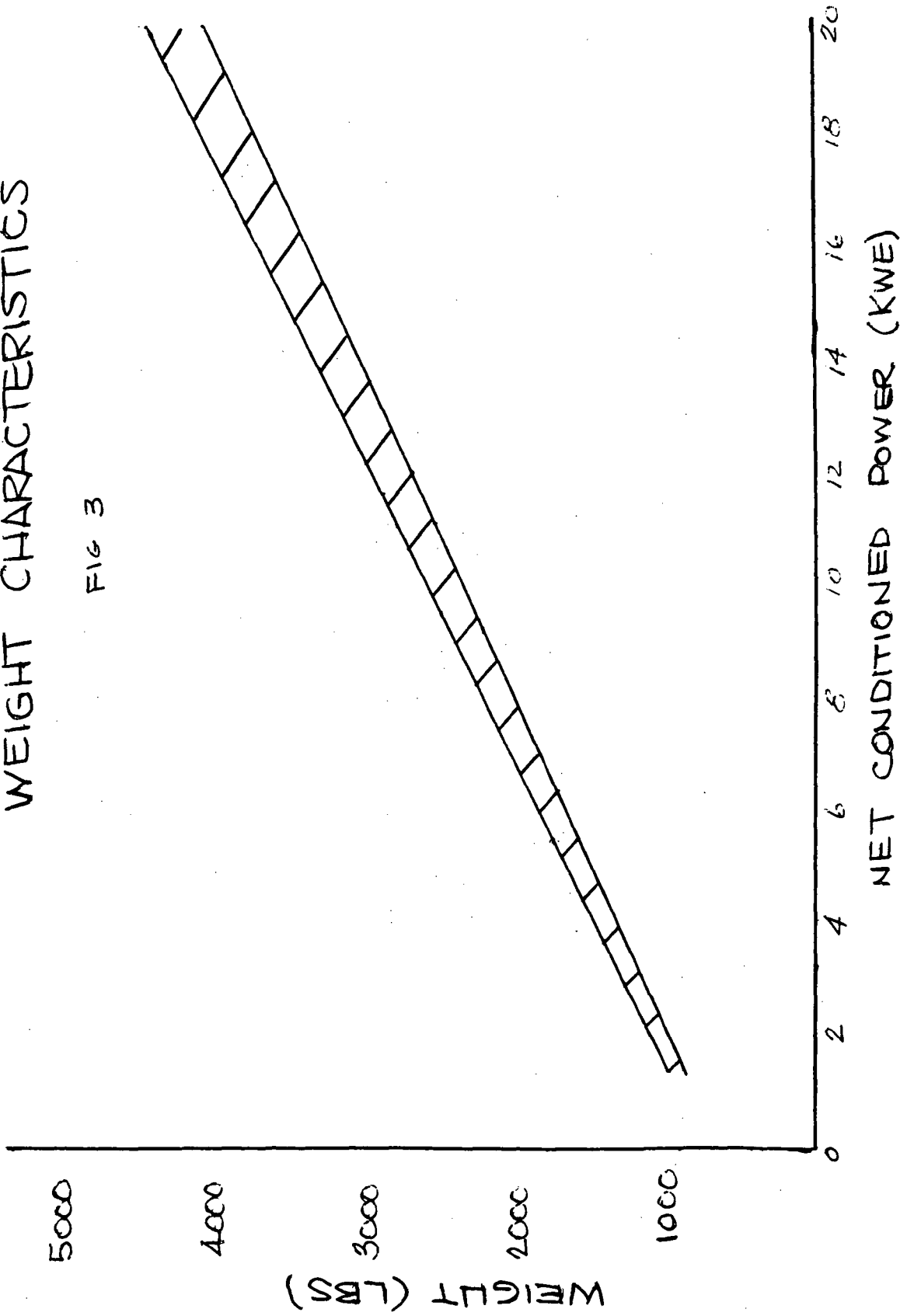
Figures 3, 4 and 5 show system weight, radiator area and cost as a function of power level. These figures show that if the power requirements were doubled from 5.5 kwe to 11.0 kwe, the weight would go from approximately 1575-1850 lbs to 2500-2800 lbs, and the cost would increase from \$1.8 to \$2.7 million. Additionally, the radiator area increase would be small enough for the system to still be used with the existing Titan shroud. These figures illustrate that nuclear power systems offer the advantage of substantial power growth with only modest increases in weight, size and cost.

Although the limited payload capability Titan IIIC launch vehicle does not permit utilization of this potential, there are other launch vehicle options which do. For example, the Titan IIID/Centaur can place approximately 6500 lbs directly into geosynchronous orbit with a launch vehicle differential cost of \$4-6 million. This would mean that an additional 1700 lbs of experiments (nearly double the current payload) requiring up to 11 kwe could be flown with only a 20 percent increase in booster cost.

Another approach would be to use the Titan IIIC to place the spacecraft in a low altitude parking orbit and use the NASA ion engine to spiral out to synchronous orbit. The nuclear power system would provide the electrical power for propulsion. Utilization of the ion engine would in itself be a valuable technology demonstration. Because the nuclear power system is unaffected by Van Allen belt radiation, the only effect on the power system would be to increase the system design life to include the spiral-out time. This would probably be of the order of six months and is not too significant. The Titan IIIC can boost approximately 20,000 lbs into a 1,000 nm orbit or 9,000 lbs in a 5,000 nm orbit. There are obviously trade-offs to be made of weight, altitude and spiral-out time. There are probably additional launch vehicle options which could be investigated.

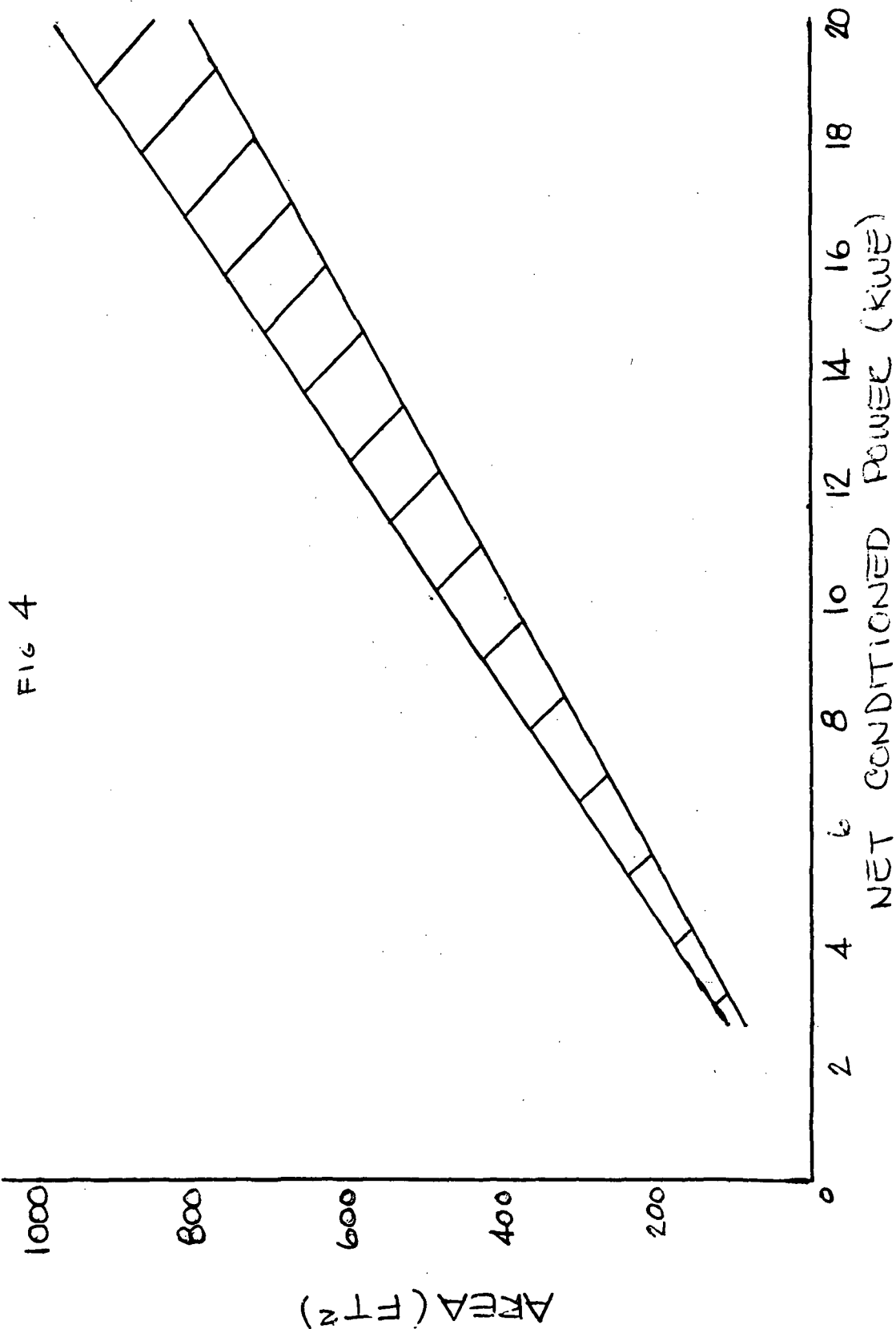
# REACTOR THERMOELECTRIC SYSTEMS WEIGHT CHARACTERISTICS

FIG 3





# REACTOR THERMOELECTRIC SYSTEM RADIATOR AREA



# REACTOR THERMOELECTRIC SYSTEMS RECURRING UNIT COSTS

FIG 5

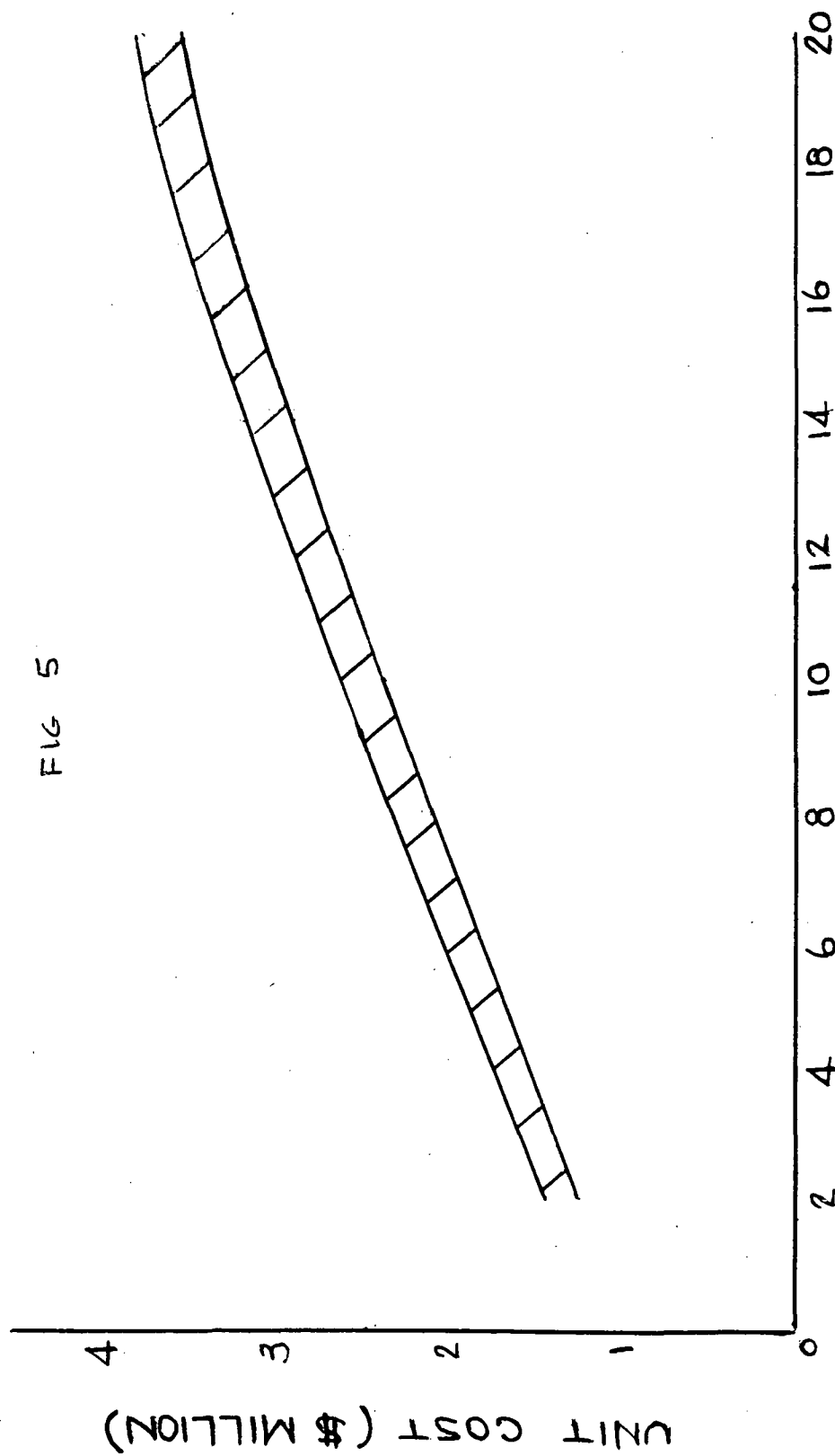


Table 3 summarizes the technology status of each major component in the system. Each component has a technology base of at least 19,000 hours of total test time with the thermoelectric modules having the most with 720,000 hours of testing. Each component has demonstrated a minimum of 10,000 hours in a single continuous test. All components have also been tested to higher temperatures than anticipated in the current design. Not only have reactors operated at 1300°F, they have also operated at powers to 1,000 kw.

TABLE 3  
REACTOR-THERMOELECTRIC SYSTEM  
COMPONENT EXPERIENCE

Component	Number Units Tested	Total Test Hours	Max. Temp (°F)	Max. Duration Single Test (Hrs.)
Reactor	6	41,250	1300	10,000
Thermoelectric Converter Modules	220	720,000	1350	52,000
NaK Pumps	58	212,000	1200	20,000
NaK Accumulators	50	>100,000	750	10,000
Reflector Control Drum Actuators	67	239,000	1125	24,400
Reflector Control Drum Bearings	90	235,000	1500	15,500
Nuclear Radiation Shields	13	19,000	900	10,000

The 1965 flight test of the SNAP 10A system demonstrated reactor system compatibility with all phases of the space mission. That program also provided excellent experience in system design, analysis, and testing. The system test phases included prototype, acceptance and qualification tests as well as spacecraft/power system electrical/mechanical compatibility tests.

The SNAP 10A program also verified the safety of reactor systems during all phases of ground handling, pre-launch operations, and launch. In addition, a recent study confirmed that for earth orbits of altitudes greater than 400 nm no post-operations safety impediments exist.

The heat rejection radiators normally operate at approximately 500-600°F which is high enough not to be effected by solar or earth heat loads. System performance is therefore independent of orbit altitude and inclination and spacecraft orientation. The typical long, slender spacecraft/power system configuration also provides excellent gravity gradient stability, thereby minimizing attitude control system weights. Recent studies for other missions have shown that spacecraft with rather severe pointing accuracy requirements require no attitude control after the desired attitude is initially obtained.

To summarize, nuclear power systems can meet the mission requirements established for this study within the direct ascent payload capability of the Titan IIIC with a weight margin of up to 20 percent. In addition, other launch vehicle candidates have been identified which offer significant potential reductions in launch vehicle cost per pound of experiment in orbit. The critical point is that an effort should be made to determine the most cost effective way of using the resources available for space experiments. It is therefore recommended that an ATS-nuclear power study be initiated to further investigate these and other possible options, and to identify the potential advantages of nuclear power to the ATS program.

## II. POWER SYSTEM DESCRIPTION

This section describes the design and performance of the 5.5 kwe reactor-thermoelectric (TE) power system. Section III presents detail component information.

Figure 6 is a system schematic, Figure 1 shows the system configuration and Table 4 presents a summary of system performance. There are two NaK loops, i. e., one primary and one heat rejection loop. Both loops use liquid metal NaK, a eutectic mixture of sodium (Na) and potassium (K), as the heat transfer fluid. Both loops also have NaK accumulators and electromagnetic (EM) pumps. The accumulators accommodate thermal expansion of the NaK as it heats up during system startup and also maintain system pressure to prevent cavitation.

The EM pumps operate based on Fleming's right-hand rule which states that when a current is passed through a conductor in the presence of a magnetic field, a force is exerted on the conductor. In this case the conductor is the NaK in the pump throat. Permanent magnets provide the magnetic field and the current passes through electrodes brazed to the sides of the pump throats. The net result is a pump which has no moving parts or seals. The pumps are powered by low-voltage/high current thermoelectric modules.

The NaK is heated in the reactor to 1200°F and is pumped to the hot cladding of the thermoelectric converters, where the heat is removed by convection. The primary loop NaK returns to the reactor for reheating. The reactor produces 84.8 kwt. The heat delivered to the hot cladding of the converters is conducted through the thermoelectric couples. A portion of the heat is converted to electricity and the remainder is transferred by convection to the heat rejection loop NaK. This 77.8 kwt is then rejected to space by the radiator which has an average temperature of 510°F.

# TYPICAL REACTOR - THERMOELECTRIC SYSTEM SCHEMATIC

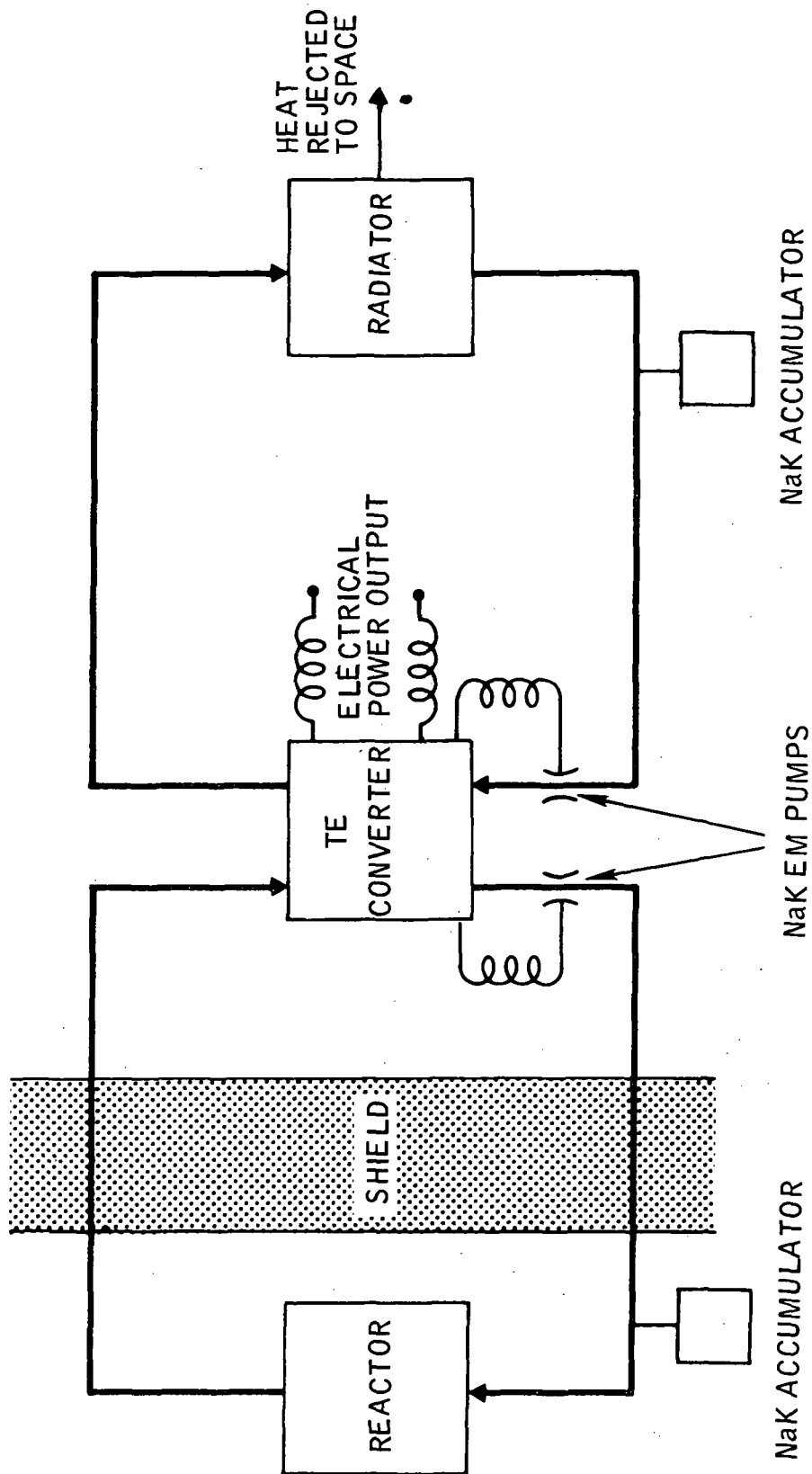


Figure 6

TABLE 4  
 REACTOR TE PERFORMANCE DATA  
 (End-of-Mission)

Electrical Power, kwe	5.5
Reactor Thermal Power, kwt	84.8
TE Module Power, kwt	76.3
Pumo Module Power, kwt	7.3
Thermal Losses, kwt	1.2
Heat Rejection Power, kwt	77.8
Reactor Outlet Temperature, °F	1200
Reactor Inlet Temperature, °F	1100
Average Hot Clad Temperature, °F	1135
Average Cold Clad Temperature, °F	520
Average Radiator Temperature, °F	510
Number of TE Modules	20
Number of TE Modules per String	5
Number of Strings	4
Overall System Efficiency, %	6.50
Radiator Effectiveness	0.85
Radiator Area, Ft <sup>2</sup>	230
System Voltage, Volts	30.5
Nuclear Radiation Dose at Power System/Spacecraft Interface	
Neutrons, nvt/5 years	10 <sup>12</sup>
Gamma Rays, rods/5 years	10 <sup>6</sup>

Figure 1 shows the arrangement of the components in the system. A radiation shield is located next to the reactor and attenuates the reactor neutrons and gamma rays. The standard spacecraft radiation levels of  $10^{12}$  nvt/5 years for neutrons and  $10^6$  rods/5 years for gamma rays are designed for at the power system/spacecraft interface. The other components are located within the shadow of the shield to reduce the radiation dose contribution from scattered neutrons and gamma rays.

The 230 ft<sup>2</sup> system radiator accounts for most of the system size. It is made up of 5/16-inch OD stainless steel NaK tubes with aluminum fins joined together with frames and stringers. The pumps, accumulators, and thermoelectric modules are housed within the radiator structure.

A thermal insulation blanket is located at the base of the system to reduce heat loads to the spacecraft. The heat loads are typically a few watts. A thermal shroud, which is ejected upon reactor startup, covers the radiator to prevent NaK freezing in space during pre-startup orbiting.

There are a total of 20 thermoelectric modules arranged electrically in four strings of five modules each. Each string produces 1.34 kwe at 30.5 volts. Each module is 15-inches long and 1.5-inches in diameter.

At the beginning of the mission, the reactor outlet temperature is 1175°F. Because the TE module performance degrades somewhat with time, the reactor outlet temperature will increase to maintain constant electrical power reaching 1200°F at the end of the five-year mission.

Table 5 presents the component weights for both the U-233 and U-235 fueled reactors. The weights for the two systems are identical except the U-233 reactor and shield are lighter. The radiator structure would also be somewhat lighter, however, this was not taken into account. The total weights for the two systems are 1575 and 1850 for U-233 and U-235 reactor-systems respectively.



TABLE 5  
REACTOR TE WEIGHT BREAKDOWN

	<u>U-233</u>	<u>U-235</u>
Reactor	250	415
Thermoelectric Modules	240	240
EM Pump	37	37
Pump TE Modules	32	32
Primary Piping	100	100
Heat Rejection Piping	82	82
NaK Radiator	367	367
Wiring and Controls	97	97
Accumulators	50	50
Thermal Shroud	63	63
Miscellaneous	49	47
Radiation Shield	<u>208</u>	<u>320</u>
Total	1575	1850

### III. TECHNOLOGY STATUS

This section provides more detail component information, reports the technology status of the components and briefly reviews SNAP 10A system experience.

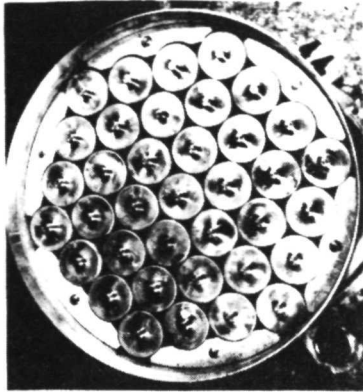
#### A. SNAP 10A SYSTEM

The SNAP 10A system, shown in Figure 7, was a 500-watt reactor-thermoelectric system which was launched into space in 1965. Although it represents a technology which has been surpassed, it is important because it was a demonstration of: (1) reactor system development from conceptual design through flight test, (2) the compatibility of spacecraft and nuclear power systems and (3) contractor and inter-agency cooperation.

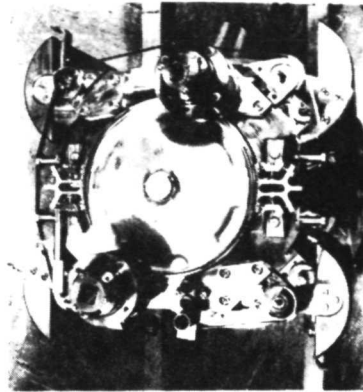
The SNAP 10A test program included: (1) developmental systems hydraulic, thermal and structural tests; (2) nuclear and non-nuclear qualification tests; and (3) the flight test. The non-nuclear qualification test was of a complete system, except the reactor was replaced by electrical heaters. The nuclear test was of a complete system which ran uninterrupted for 10,000 hours. At the end of that time, all test objectives had been met and the system was shut down. The flight test met all of its objectives except for endurance testing. Because of a voltage regulator failure aboard the Agena spacecraft, the system was shut down automatically after only 43 days of operation.

#### B. REACTOR

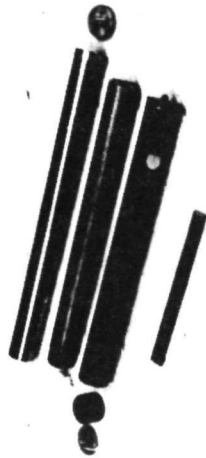
Figure 8 shows a typical zirconium hydride (ZrH) reactor. The fuel element is 90% zirconium and 10% uranium. The element is hydrided so that at operating temperature, its hydrogen density is roughly equal to that of room temperature water. The element is contained within a Hastelloy or Incolloy cladding. The ID of the cladding is coated with a ceramic barrier



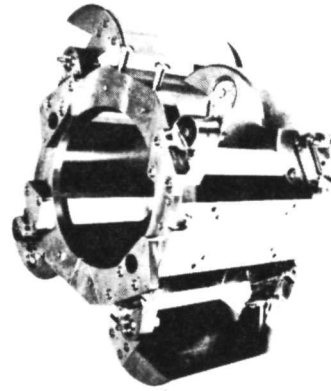
**CORE**



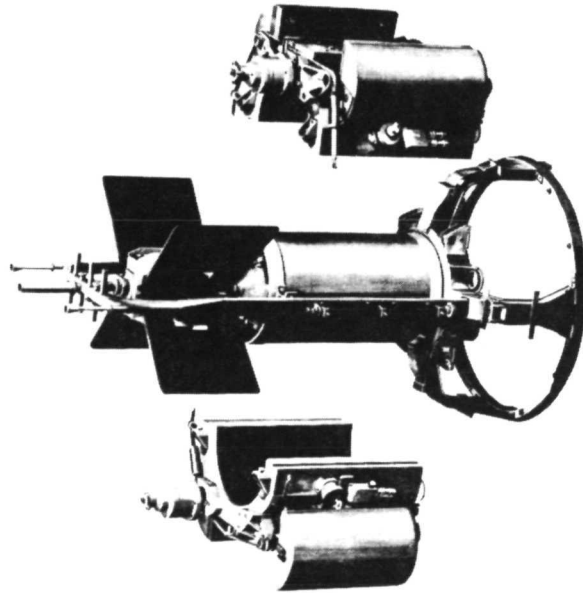
**REACTOR (Top View)**



**FUEL ELEMENT**



**REFLECTOR**



7561-02657A

Figure 8. Zirconium Hydride Reactor Concept

to minimize hydrogen leakage. The elements generally range in diameter from 0.5 - 1.25 in. and in length from 12 - 16 in. The elements are arranged in a hexagonal pattern. The spaces between elements are primary loop NaK flow passages. The reactor vessel is a thin-walled cylinder.

Control of the reactor is achieved through the use of an external beryllium reflector. As shown in the figure, four cylindrical drums rotate within cutouts in the fixed reflector. The position of the drums controls neutron leakage and therefore controls power level. The same effect can be achieved by sliding segments rather than rotating drums.

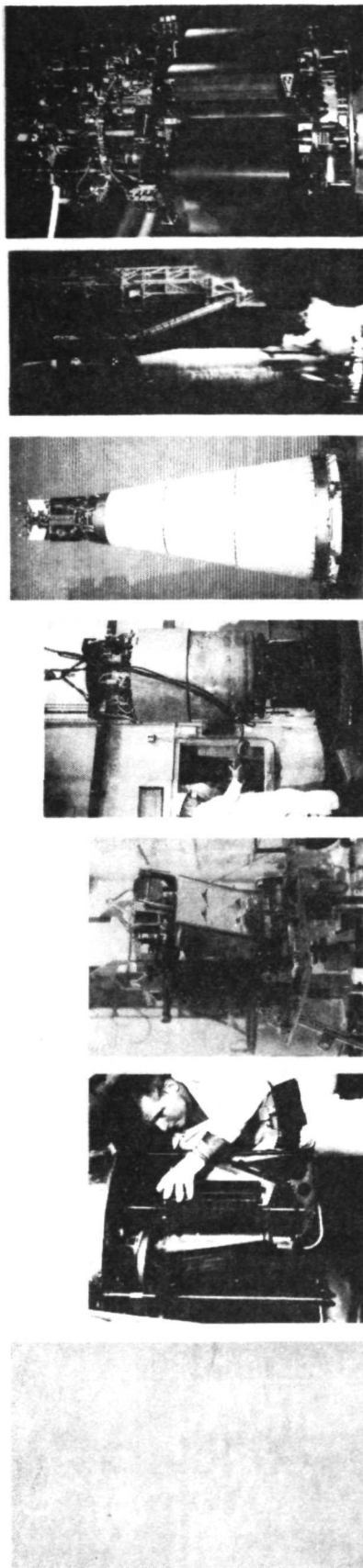
Figure 9 summarizes reactor test experience. A total energy release in excess of  $10^7$  kw-hr has been accumulated for these types of reactors. The longest continuous test was 10,000 hours on the SNAP 10A reactor. The maximum power level on the SNAP 8 DR was 1000 kwt, and the maximum temperature was  $1300^{\circ}\text{F}$  with the power reduced to 600 kwt.

#### C. SHIELD

Figure 10 summarizes nuclear radiation shield experience. It will be noted that considerable fabrication and test experience has been accumulated.

#### D. THERMOELECTRIC CONVERTER

Figure 11 shows a cutaway drawing of the thermoelectric module. The module is constructed using 95% PbTe, 5% GeTe (N) and 95% PbTe, 5% PbSe (P) washers arranged alternately along a central tube. Separating the N and P washers is a mica washer which provides electrical insulation. Conductor rings span adjacent washers on both their I.D. and O.D. to provide a serpentine electrical path through the module. The inner conductor ring is split to allow mechanical insertion of the mica and prevent the diffusion of tellurium around the mica/hot conductor ring interface. Electrical insulation of the inner and outer conductor rings is



	SNAP EXPERIMENTAL REACTOR (SER)	SNAP DEVELOPMENTAL REACTOR (SDR)	SNAP 8 EXPERIMENTAL REACTOR (S8R)	SNAP 10A FLIGHT SYSTEM (FS-3)	SNAP 8 DEVELOPMENTAL REACTOR (S8DR)
CRITICAL	SEPTEMBER 1959	APRIL 1961	MAY 1963	JANUARY 1965	JUNE 1968
SHUTDOWN	DECEMBER 1960	DECEMBER 1962	APRIL 1965	MAY 1965	DECEMBER 1969
THERMAL POWER	50 kw	65 kw	600 kw	38 kw	43 kw
THERMAL ENERGY	225,000 kw-hr	273,000 kw-hr	5.1 x 10 <sup>6</sup> kw-hr	382,944 kw-hr	41,000 kw-hr
ELECTRIC POWER	-	-	-	402 watts	560 watts
ELECTRIC ENERGY	-	-	-	4028 kw-hr	574 kw-hr
TIME AT POWER AND TEMPERATURE	1800 hr AT 1200°F 3500 hr ABOVE 900°F	2800 hr AT 1200°F 7700 hr ABOVE 900°F	1 yr AT 1300°F 400 TO 600 kw	10,005 hr (417 days)	7023 hr 1100-1300°F

9/7041-0006-6C

Figure 9. SNAP Reactor Test Experience

- NEUTRON SHIELDS
  - SELECTED MATERIAL FOR SPACE APPLICATIONS:
    - LITHIUM HYDRIDE (LiH)
  - NUMBER BUILT AND TESTED:
    - 13 (SHOCK, VIBRATION, THERMAL CYCLING, ENDURANCE)
  - ATTENUATION MEASUREMENTS:
    - UP TO 30 in.
- GAMMA SHIELDS
  - CANDIDATE MATERIALS:
    - W, U, AND Pb
  - ATTENUATION MEASUREMENTS:
    - UP TO 2, 5-1/2 AND 7 in., RESPECTIVELY
  - FABRICATION EXPERIENCE:
    - SLABS AND CAPSULES

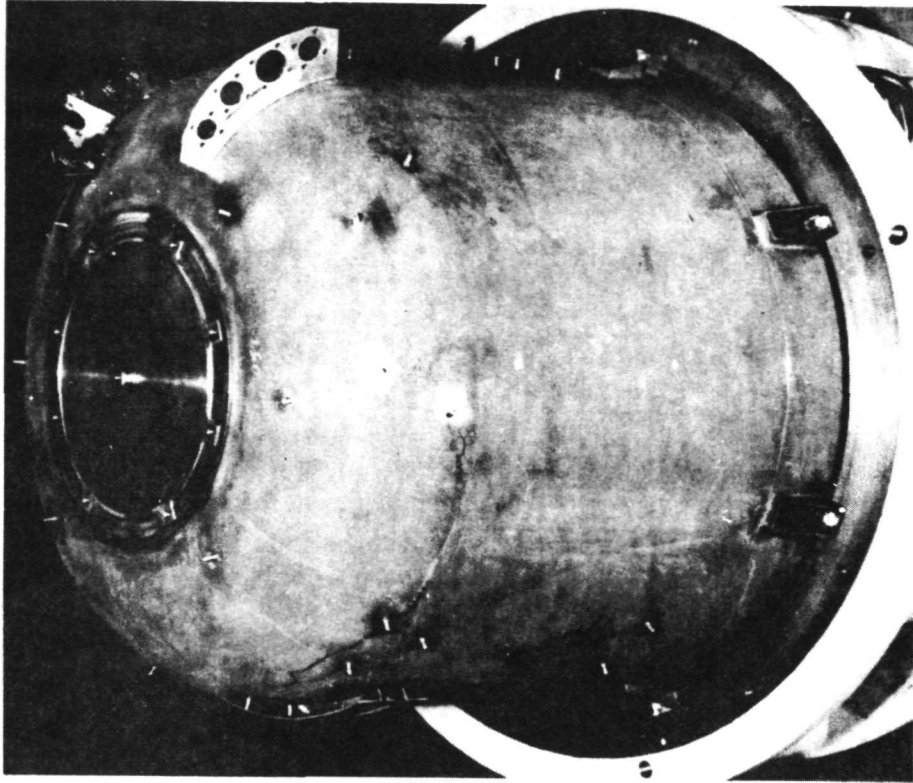
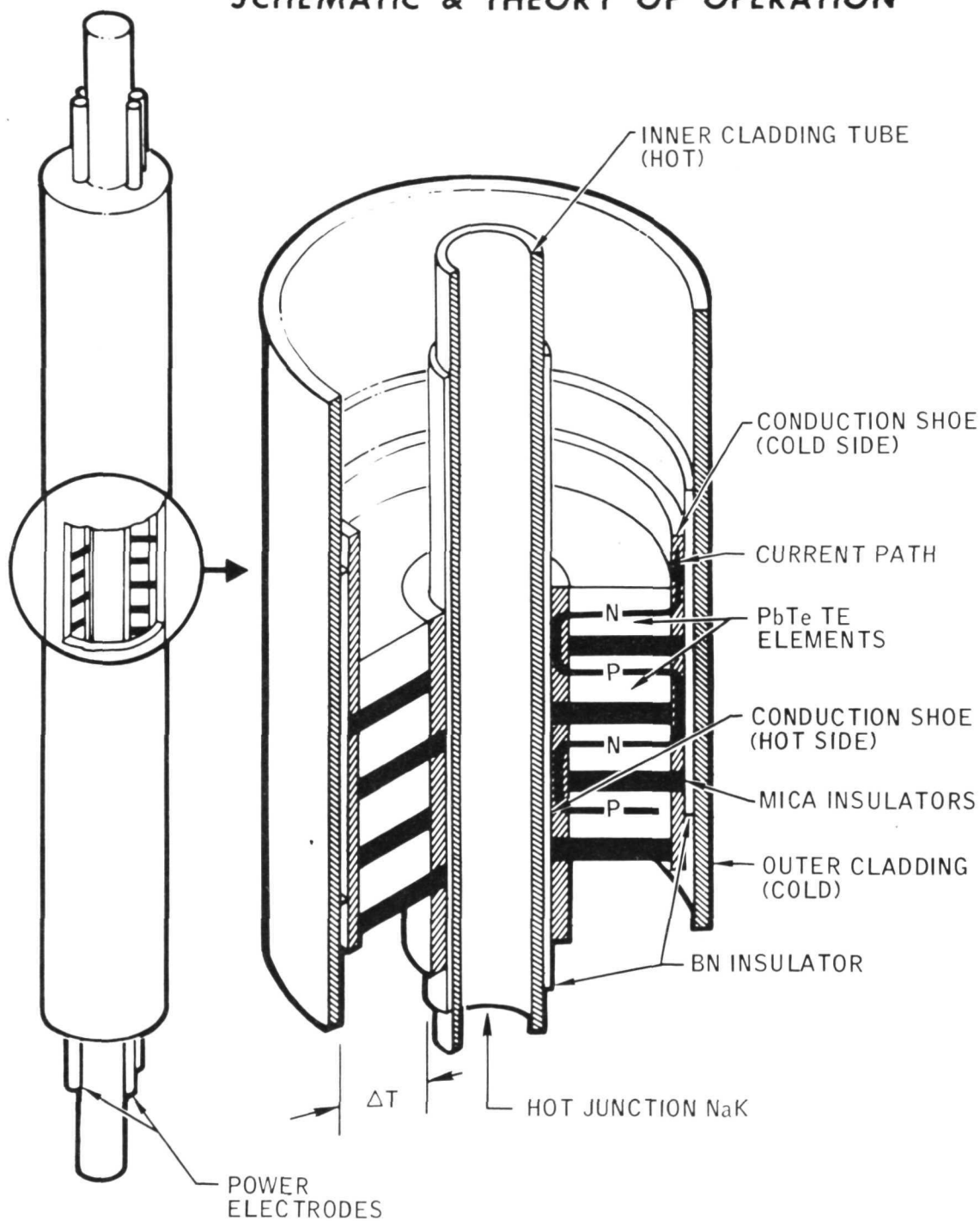


Figure 10. Shield Hardware Experience

7-(95)-273-10B

# COMPACT THERMOELECTRIC TUBULAR MODULE

## SCHEMATIC & THEORY OF OPERATION



70-M18-028-2

Figure 11

provided by thin sleeves of boron nitride which also help to insure a good thermal contact between the cladding and rings. The inner clad is an inconel tube and the outer clad is stainless steel.

The completed assembly, with appropriate end closures containing electrical feedthroughs, is compacted using an autoclaving process into a rugged essentially void-free sealed unit.

In order to provide a passage for the cooling NaK over the outer cladding, a larger diameter tube encloses the module. The annular passage between the module outer clad and enclosure has a wire wrap to improve the heat transfer coefficient. To produce the same effect of increased heat transfer on the hot side of the module, a plug with a helical ridge machined into its O.D. is inserted into the inner clad tube.

The individual tubular modules are manifolded hydraulically in parallel to form a converter assembly. Differential thermal expansion between the hot and cold loops is accommodated by flexibility in the tubes between the tubular modules and the headers while structural support for the individual converters is provided by a rigid bracketry connected to the converters cold NaK outer jacket and the radiator structure.

Typical electrical characteristics of the thermoelectric converter at a given set of operating temperature conditions is presented in Figure 12. This figure gives the current, power, and efficiency of the converter as a function of voltage. Both the matched load and peak efficiency conditions are shown by the vertical lines. It can be noted that higher converter voltages can be obtained by operating at off matched load conditions. Efficiency actually improves due to the Peltier heating effects, and then begins to fall off.



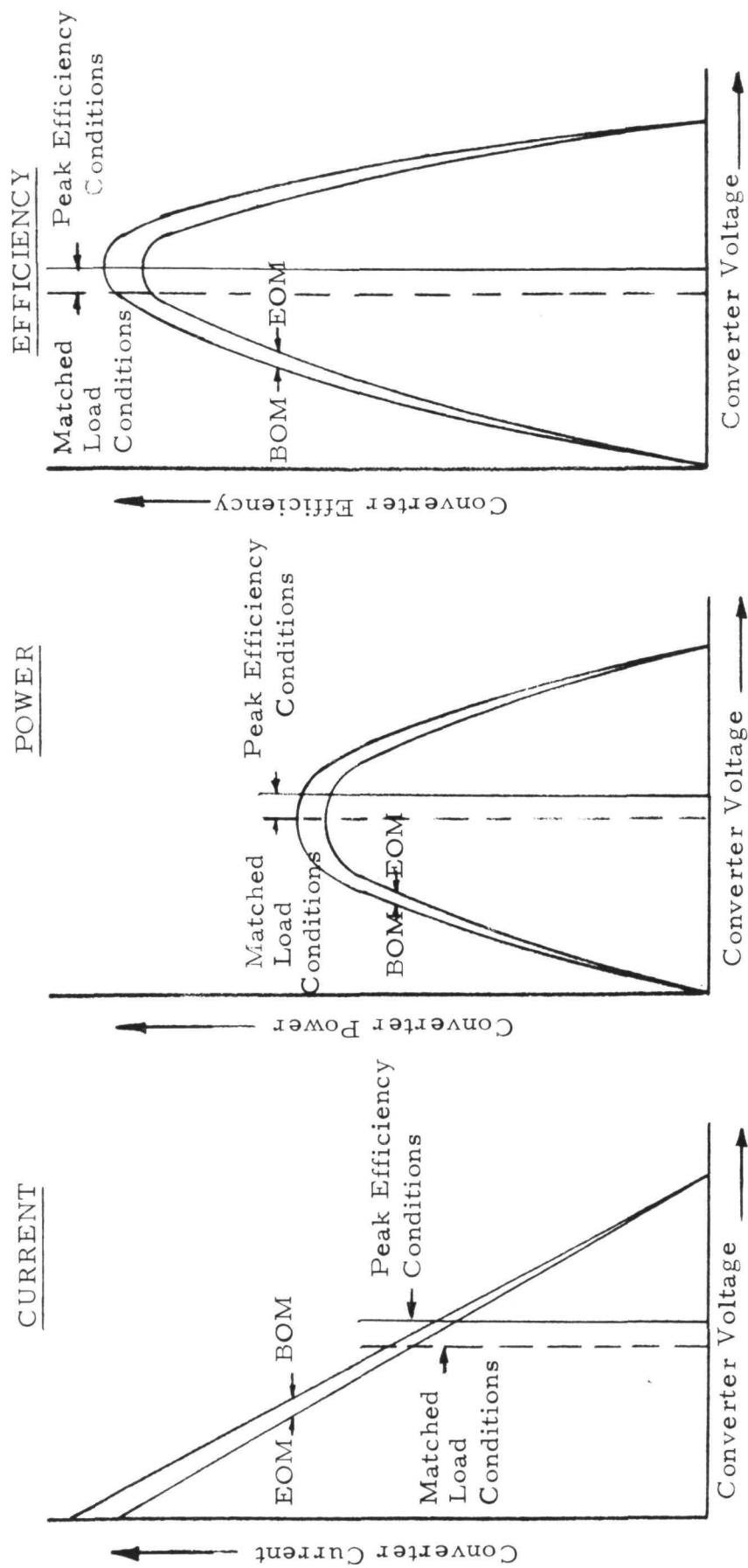


Figure 12. Thermoelectric Converter Operating Characteristics

An illustration of a pump assembly is shown in Figure 13 and a photograph of pump throat and magnet assembly hardware is shown on Figure 14. The assembly contains two throats: one for pumping the primary loop and one for the heat rejection loop. The two identical throats are connected electrically in series. Each throat is a stainless steel tube of rectangular cross section. The copper bus connecting the throats with the thermoelectric modules carries the current. The bus is constructed of flat strips for flexibility to accommodate thermal expansion. An Alnico permanent magnet provides a magnetic field across the throats at right angles to the current and NaK flow.

Thermoelectric pump modules supply power to the bus. The pump thermoelectric modules are the same as the main power modules, except they are shorter and have fewer, but thicker, thermoelectric couples.

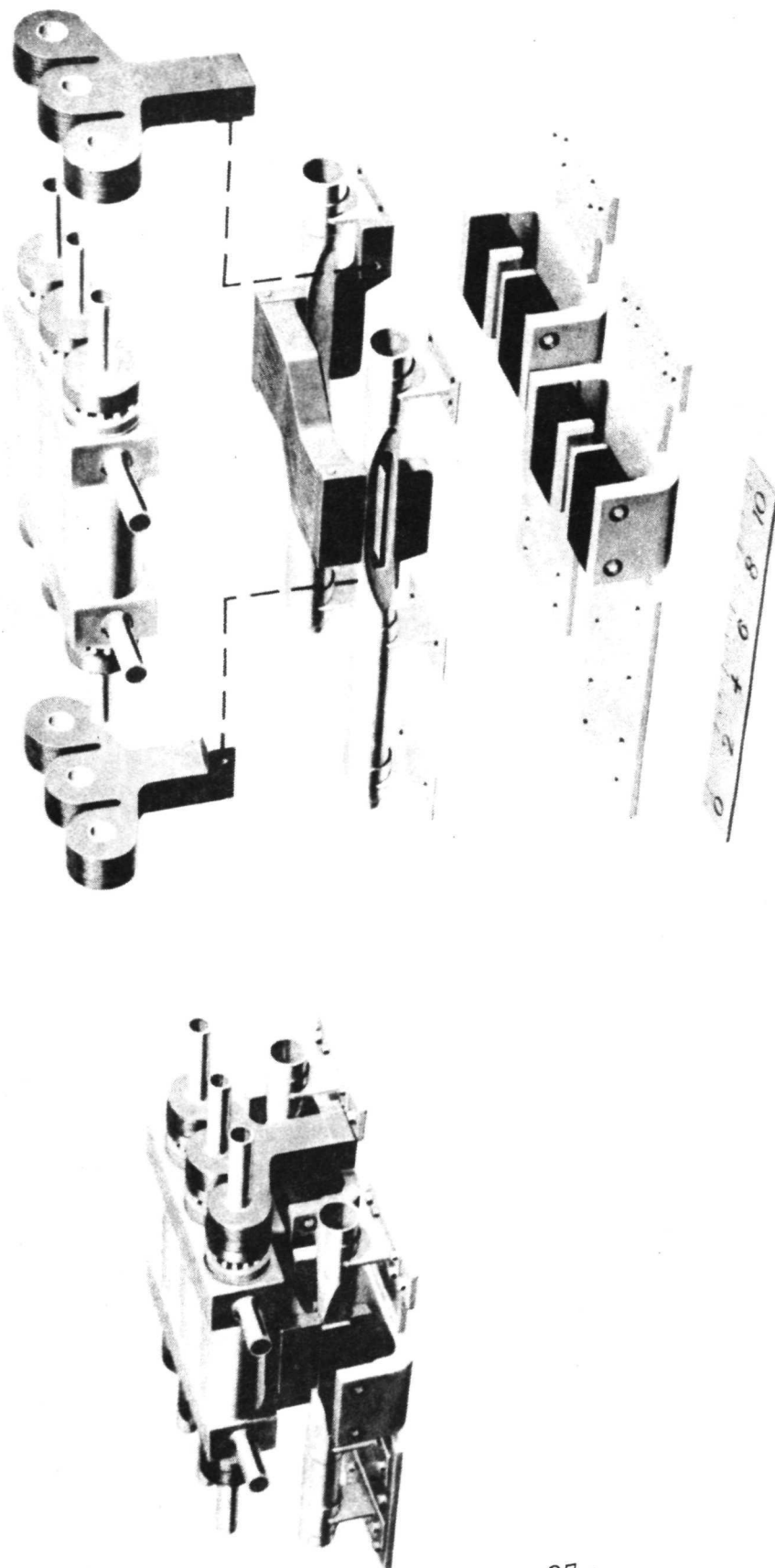
The thermoelectric pump modules are connected electrically and hydraulically in parallel. The two pump modules are also hydraulically in parallel with the main power thermoelectric modules so that they all operate at the same temperature.

Prior to startup in orbit, about 5% of the design NaK flow rate is provided for by a small battery source to preclude the possibility of NaK freezing during the orbital prestart period.

Considerable pump fabrication and test experience on electromagnetic type NaK pumps has been accumulated. This experience is summarized in Figure 15. It can be noted that the total test time is in excess of 400,000 hrs, with more than 100 pumps fabricated and tested.

#### F. NaK ACCUMULATOR

The primary and heat rejection NaK loops are designed to be void free under all system conditions. NaK accumulators are installed in each loop to accommodate the thermal expansion of the NaK



70-F18-003-42

Figure 13. EM Pump Assembly

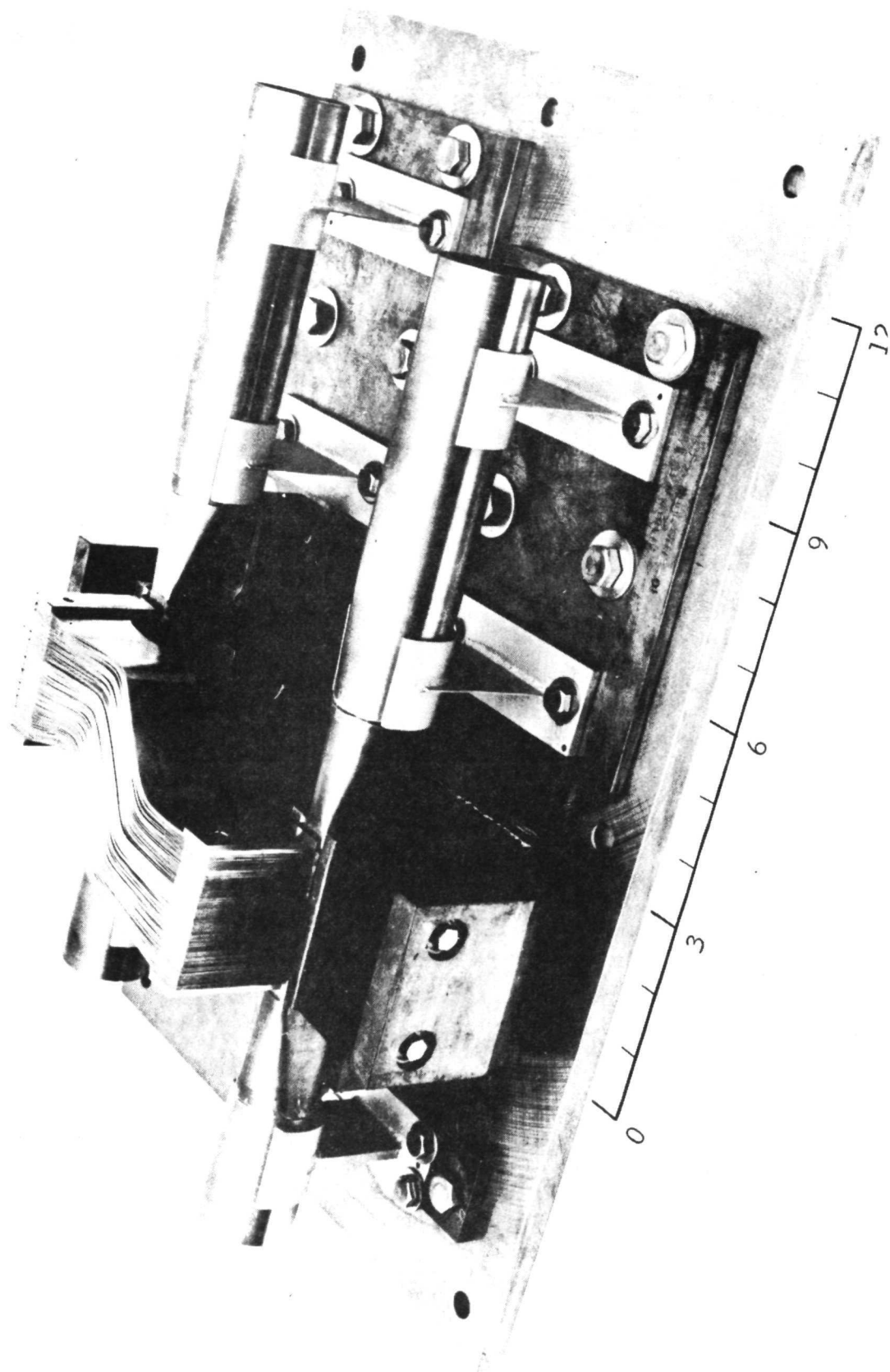
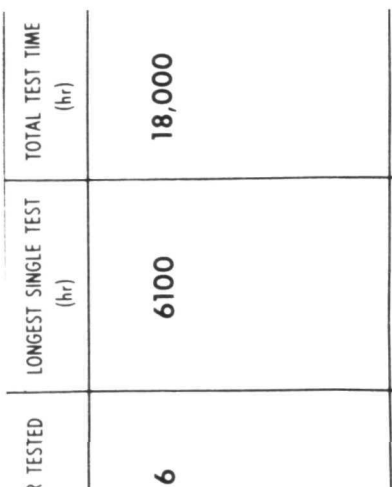
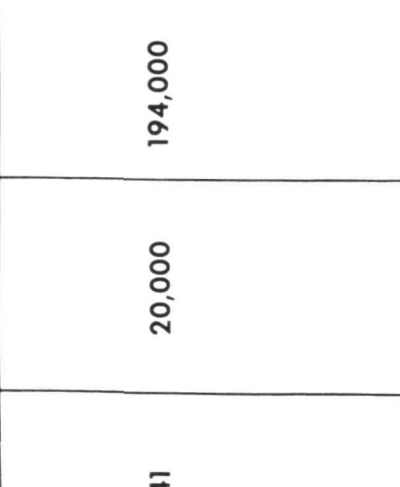
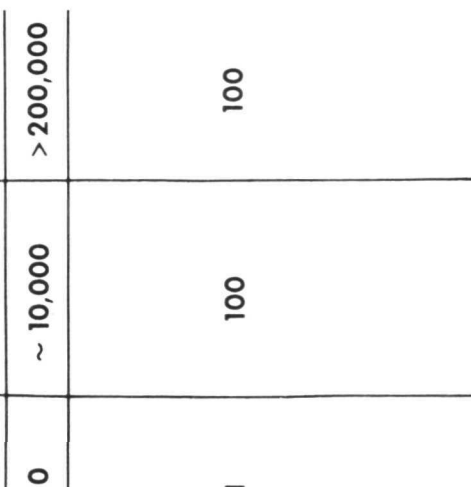


Figure 14. Prototype EM Pump

 <p><b>MERCURY RANKINE PROGRAM INTEGRAL SOURCE PUMP</b></p>	1200 (°F)	16	LONGEST SINGLE TEST (hr)	18,000	TOTAL TEST TIME (hr)
 <p><b>SNAP 10A THERMOELECTRIC PUMP</b></p>	1050	41	20,000	194,000	
 <p><b>TRIPLE PASS PUMP</b></p>	1000-1400	>50	~ 10,000	> 200,000	
	1000	1	100	100	

8-7779-119-4

Figure 15. EM Pump Experience

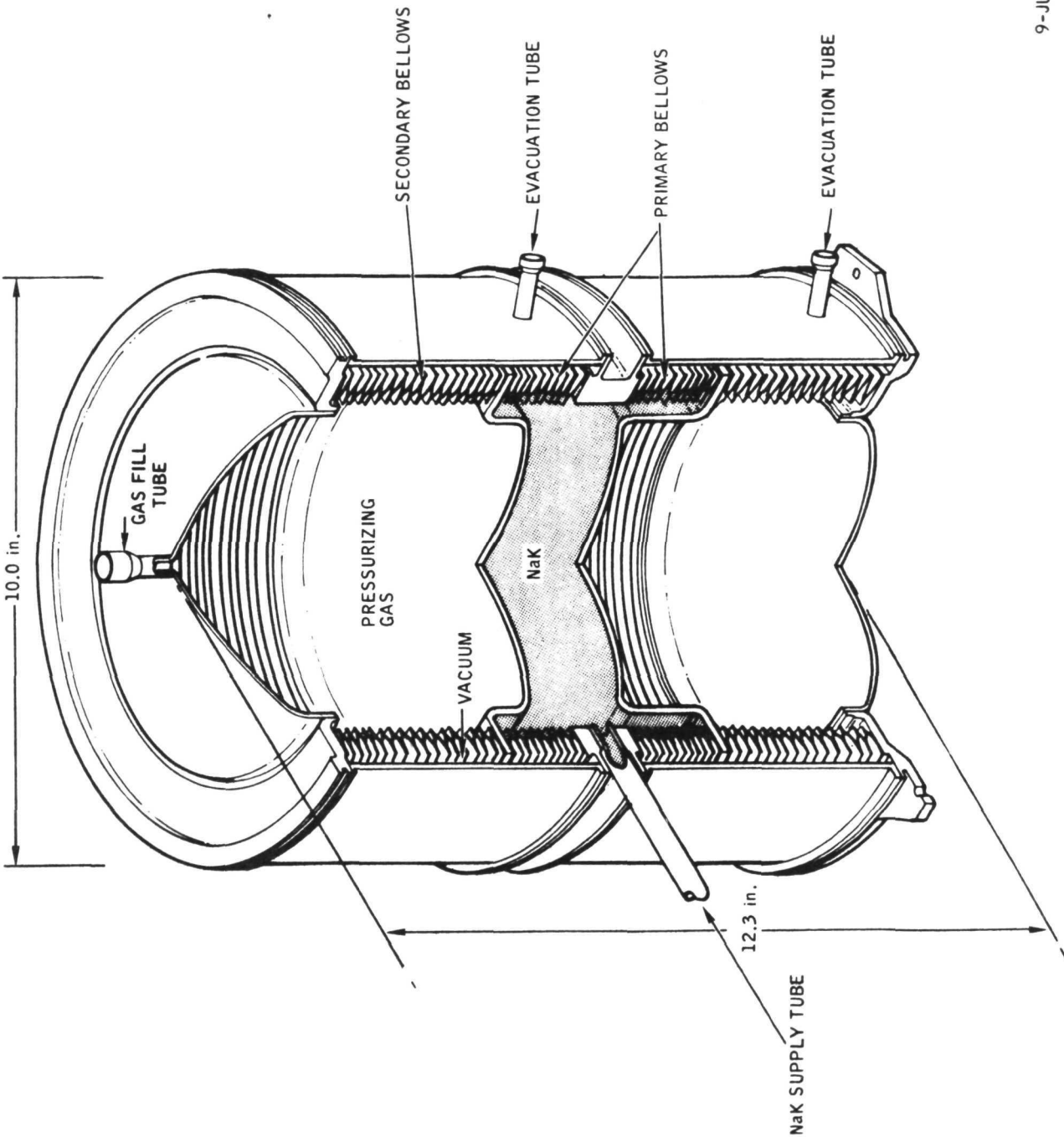
from the cold launch condition to the hot design operation conditions, and to maintain the system at the nominal operating pressure. One NaK accumulator is required in each loop.

The accumulator design is based upon the SNAP 10A flight qualified design. The principle of operation is illustrated in Figure 16. The primary bellows expands as the NaK volume increases, and the secondary bellows is simultaneously compressed. The NaK is contained within the interior surface of the primary bellows and between plates welded between the primary and secondary bellows. The region between the outer surfaces of the primary and secondary bellows and the secondary containment cylinder is evacuated. In the event of a primary bellows failure, the NaK leaks into the secondary containment region, causing the primary bellows to contract slightly but the system is maintained void free. System pressure is maintained by the spring constant of the bellows and by pressurizing gas. Over 50 accumulators were fabricated as part of the SNAP 10A program with over 100,000 hours of testing. The longest, continuous endurance test was 10,000 hours.

#### G. RADIATOR STRUCTURE

The radiator structure design for the nuclear power system is shown in the system layout in Section I. The basic heat rejection surface consists of the integrated radiator structure. An integrated radiator structure was selected since it provides a significant weight savings over separate radiator and structural components.

The radiator structure is constructed from individual extruded aluminum radiator fins. Adjacent radiator fins are riveted to a corrugated aluminum structure along their edges to form a continuous section as shown in Figure 17.



9-JUL13-059

Figure 16. NaK Accumulator

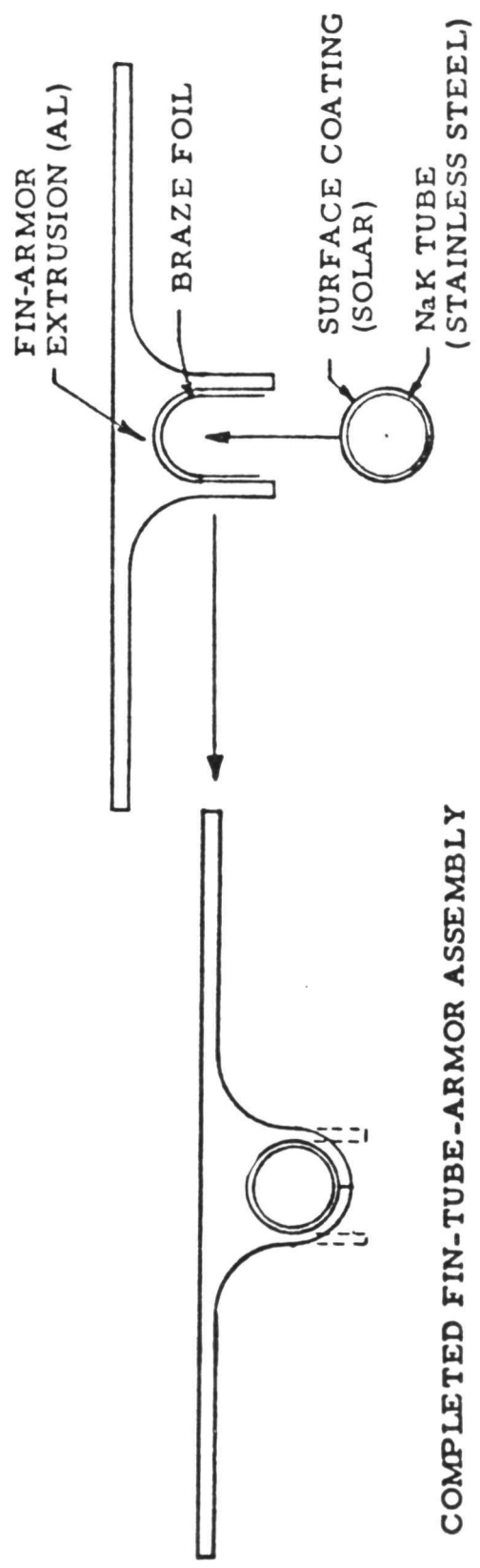
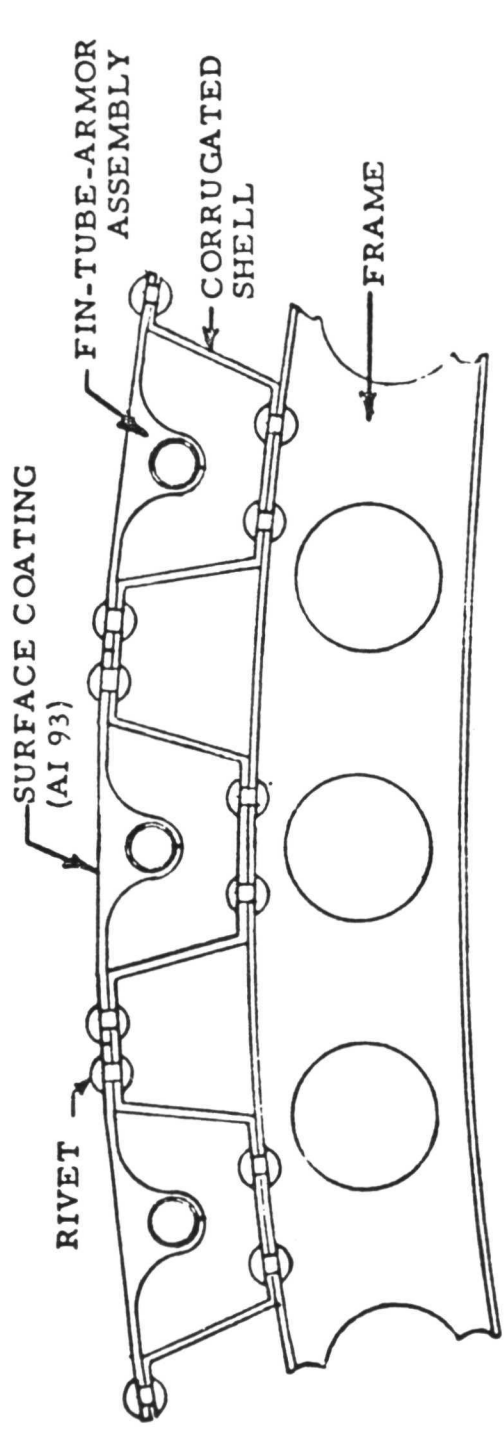


Figure 17. Radiator/Structure Design



A seamless stainless steel coolant tube is bonded to the hole in each radiator fin extrusion. The coolant tubes are connected in parallel to form a one pass heat rejection system. A stainless steel tubular header distributes the hot coolant to the tubes at the top of the radiator. Coolant passes through the radiator sections where it is collected at a bottom header.

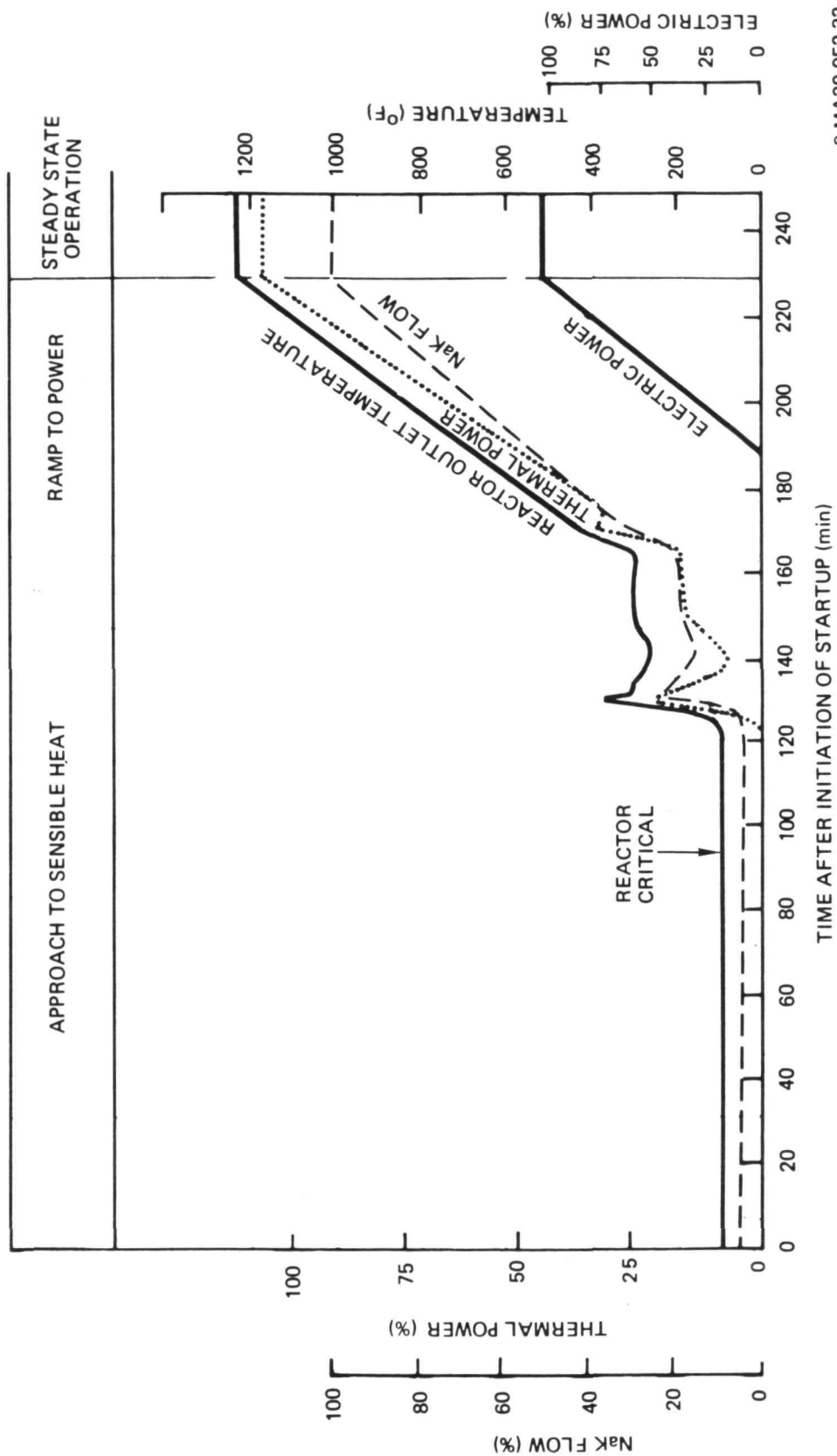
The outside surface of the radiator structure is coated with an emissive coating designated AI93, which was used on the SNAP 10A aluminum radiator. The AI93 utilizes a bi-layer coating consisting of a sub-coat containing a chrome-cobalt-nickel oxide mixture and a top coat containing stannic oxide. Both layers use aluminum phosphate as the binding agent. Between 300 and 700<sup>o</sup>F, the total hemispherical emittance of AI93 is 0.90 and the solar absorptance is 0.30. AI93 has undergone complete qualification in a simulated space environment, and, in addition, has attained in excess of 1000 hrs of successful operation in the space environment at temperatures exceeding 700<sup>o</sup>F.

#### IV. STARTUP AND CONTROL

After the reactor system has achieved a satisfactory orbit or has started its spiral trip to geosynchronous orbit, reactor startup will be initiated. Figure 18 shows a typical startup sequence. A ground command will initiate stepping-in of the control drums or segments. The reactor will reach criticality and the segments will continue to step in. Eventually, the reactor power will start to increase rapidly. However, because the reactor has a negative temperature coefficient (its reactivity decreases with temperature) the transient is self limiting. After going through a period of minor power oscillations, the reactor will linearly ramp to full power. As the reactor power increases, system temperature increases and the TE modules start to generate electricity. The pump modules start powering the EM pumps and the flow rate increases. Reactor power, temperature, NaK flow rate and electrical power all increase to their design levels automatically by simply stepping in the control segments. When design electrical power is reached, stepping of the drums stops. The total time of startup can be reduced by using a faster stepping rate up until the time the reactor is nearly critical. During the first few days, frequent changes in control segment changes must be made to account for short-term changes in the reactor. However, after that, the control segments need only be moved a small amount each week upon command from the ground.

The primary control variable is electrical power, although reactor outlet temperature is also monitored as are other system parameters. Figure 19 illustrates three methods of power control. The first of these is control by reactor outlet temperature changes. This would only be used where long term changes are anticipated and would not be used as load following where frequent power demand changes occur. The second type of control is utilization of a shunt regulator in parallel with the load.

# TYPICAL REACTOR - THERMOELECTRIC SYSTEM STARTUP



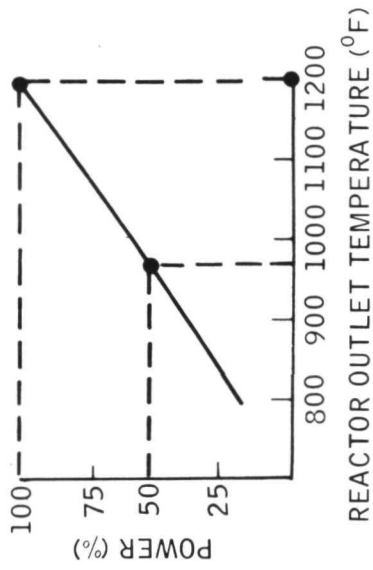
9-MA20-052-32

AI-BD-70-24  
48

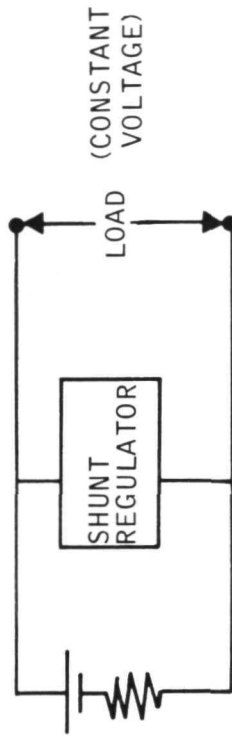
Figure 18

# POWER CONTROL METHODS

- REACTOR OUTLET TEMP VARIATION



- CONSTANT TOTAL ELECTRICAL POWER



- PULSE MODULATED CONTROL

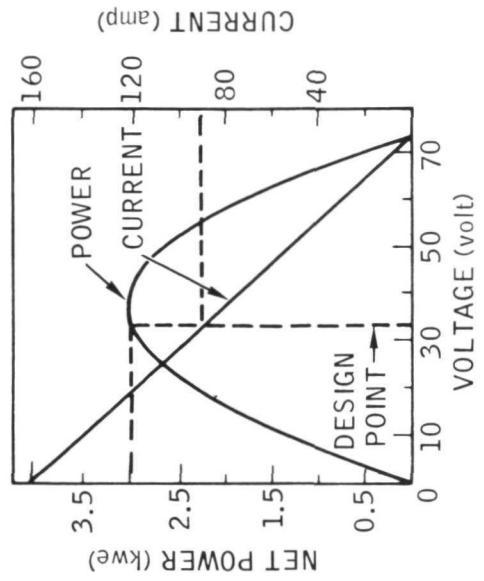
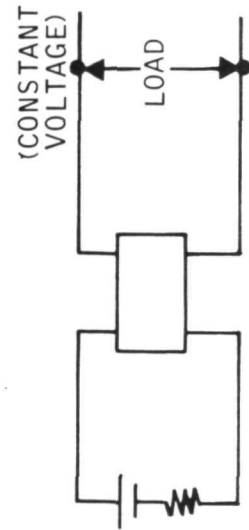


Figure 19

As the load changes, the amount of power dissipated in the regulator changes. The net result is that the thermoelectric converter (denoted as a battery and resistance) sees a constant electrical load. For high power systems where there are large changes in the load, this becomes impractical. For the high power systems, pulse modulated control is used, as shown in the figure. In the example, the normal design power is 3.0 kwe at 33 volts. If the load demand drops to 2.5 kwe, the device automatically changes the converter load voltage to slightly more than 50 volts so that the thermoelectric converter is operating less efficiently and only producing 2.5 kwe. This permits the excess power to be rejected by the system radiator. At the same time, the device also maintains the load voltage constant so that the load receives 2.5 kwe at 33 volts.